On Series Compensation of Open-Winding Permanent Magnet Machines

by

Di Pan

A dissertation submitted in partial fulfillment of

the requirement for the degree of

Doctor of Philosophy

(Electrical Engineering)

at the

University of Wisconsin – Madison

2012

Date of final oral examination: October 1st, 2012

This dissertation is approved by the following members of the Final Oral Committee:

Thomas A. Lipo, Professor Emeritus, Electrical and Computer Engineering

Thomas M. Jahns, Professor, Electrical and Computer Engineering

Robert D. Lorenz, Professor, Mechanical Engineering

Giri Venkataramanan, Professor, Electrical and Computer Engineering

Yehui Han, Assistant Professor, Electrical and Computer Engineering

Bulent Sarlioglu, Assistant Professor, Electrical and Computer Engineering

Abstract

An open-winding machine drive with two voltage source inverters was originally conceived for high power applications in order to equally split the power into two single inverters to reduce the voltage rating of each converter. Some FACTS devices utilize voltage source inverter to generate reactive power for shunt or series compensation. In this work, the possibility of applying FACTS concepts to smaller single machine systems instead of utility sized power systems is investigated. Specifically, a three-phase voltage source inverter with a DC link capacitor is used to provide controllable reactive power compensation for open-winding PM machines. The concepts of impedance control, power flow control and voltage control by the means of series compensation are considered in different scenarios including both motoring and generating operations.

For motoring operation, it will be demonstrated by simulation and experiment results that the power supply DC voltage of a PM motor drive can be better utilized in both low and high speed regions. By supplying reactive power from the auxiliary inverter, the corner speed of the drive can be postponed to a higher speed. In addition, the CPSR (constant power speed ratio) of the PM motor drive can be improved. A control method for the open-winding PM motor drive is herein proposed and verified. The sizing of the auxiliary inverter based on machine parameters and required CPSR is studied.

For generating operation, a new diode rectifier based wind power topology employing an open-winding PMSG is proposed. Compared to conventional diode rectifier based wind power systems, the cost of the proposed system can be reduced by avoiding a full scale DC/DC converter without sacrificing the capability of controlling

the generated power. The proposed open-winding PMSG wind power system is applicable to both fixed and variable speed wind turbines. In addition, distribution side voltage regulation of an open-winding PM generator in a small CVVF (constant voltage variable frequency) power grid is also considered for generating operation.

The effectiveness of the proposed series compensation scheme has been verified by simulation and experimental studies. It has also been demonstrated that the proposed series compensation by open-winding configuration is a cost effective method compared to the existing compensation methods.

Acknowledgements

Fist of all, I would like to thank my advisor Professor Thomas A. Lipo for his generous support, professional guidance and continuous encouragement through out my graduate study. His profound knowledge and sparkling ideas made every discussion we had enriching. I truly appreciate the freedom and opportunities he provided to work on a variety of different projects which greatly broadened my interests and experiences.

Second, I would like to thank the committee members, Professor Thomas M. Jahns, Professor Robert D. Lorenz, Professor Giri Venkataramanan, Professor Yehui Han and Profesosr Bulent Sarlioglu for the comments and suggestions on the thesis. Moreover, I enjoyed every WEMPEC class I took from them. Being a TA for a couple of WEMPEC classes was a pleasant learning experience as well.

Third, I am indebted to all the other people who helped me through out the thesis work. I would like to thank Ray Marion, Chen-Yen Yu, Yang Wang, Wei Xu and Patel Reddy for helping with the experimental setup. I would like to thank Andrew A. Rockhill for helping me in various aspects through out my study in WEMPEC. I would also like to thank James D. McFarland and Wenying Jiang for the insightful discussions from the perspective of machine design.

Fourth, I would like to thank WEMPEC and Ford Motor Company for providing the financial support for the project. I would also like to thank Dr. Feng Liang and Christopher M. Wolf at Ford Motor Company for providing suggestions on the project.

In addition, I would like to thank the whole WEMPEC family for making my stay in Madison an enjoyable and unforgettable experience. The WEMPEC office staff is always ready to help. I also enjoyed the companion of all my WEMPEC fellow graduate students, especially Larry Juang, Yichao Zhang, Phillip Kollmeyer, Dan Ludois, Justin Reed, Micah Erickson, Kee Ho Shin, Patricio Mendoza Araya, Jin Li, Jae

Suk Lee and Pedro A. Meléndez-Vega. Apart from many of the inspiring discussions on electric machine, power electronic, control theory, I will also remember the enjoyable moments we had together.

Finally, I would like to thank my family for their love and long term support. Without them, I would not have had the courage to start this long term journey.

Table of Contents

List of Figures

List of Tables

Nomenclature

Symbol	Definition
A	turbine surface area
C_{com}	compensation DC bus capacitance
C_p	wind power coefficient
E	back-emf
f_b	base frequency
f_r	rated frequency
$i_0,\ i_d,\ i_q$	machine current in rotor reference frame
$i_a,\ i_b,\ i_c$	machine phase current
i_{Ccom}	compensation DC bus current
I_{ch}	characteristic current
I_{chv}	virtual characteristic current
i_{dc}	main DC bus current
I_{dmaxT},I_{qmaxT}	d and q-axis current for maximum torque at certain speed
$i_{dref},\ i_d^*,\ i_{qref},\ i_q^*$	d and q-axis current reference
i_k	kth harmonic of current waveform
I_r	rated current
$I_s,\ i_s$	machine current vector
$f_0,\ f_d,\ f_q$	variables in rotor reference frame
$f_a,\ f_b,\ f_c$	phase variable
J	rotational moment of inertia
L_{com}	compensation inductance
L_{comopt}	optimal compensation inductance
$L_d,\ L_q$	d and q-axis inductance

$L_{deff},\ L_{qeff}$	d and q-axis effective inductance
L_{lk}	stator leakage inductance
$m_{a1},\ m_{b1},\ m_{c1}$	INV1 modulation index
$m_{a2},\ m_{b2},\ m_{c2}$	INV2 modulation index
$m_{d1},\ m_{q1}$	INV1 modulation index in rotor reference frame
$m_{d2},\ m_{q2}$	INV2 modulation index in rotor reference frame
n_r	rated speed in rpm
P	number of poles
P_{airgap}	air gap power
P_g	generator power
P_{load}	load power
P_{mech}	mechanical input power of wind turbine
P_s	machine power
P_{sr}	machine rated power
P_{wind}	power in the wind
Q_s	machine reactive power
R_{blade}	blade radius
r_{com}	compensation resistance
R_{load}	load resistance
r_s	stator resistance
T_e	airgap torque
T_{er}	rated torque
$T_m,\ T_l$	load torque
$v0,\ v_d,\ v_q$	machine voltage in rotor reference frame
$v_{d1}^{*},\ v_{q1}^{*}$	INV1 voltage reference in rotor reference frame
$v_{d2}^{*},\ v_{q2}^{*}$	INV2 voltage reference in rotor reference frame
$v_{di}^{*},\ v_{qi}^{*}$	voltage reference in current synchronous reference frame

$v_a,\ v_b,\ v_c$	machine phase voltage
$v_{a1},\ v_{b1},\ v_{c1}$	INV1 voltage reference
$v_{a2},\ v_{b2},\ v_{c2}$	INV2 voltage reference
V_{com}	compensation voltage vector
v_{Ccom}	compensation DC bus capacitor voltage
V_{dc}	main DC bus voltage
V_g	generator distribution side voltage
V_{max}	maximum available voltage
V_{om}	approximate maximum available voltage
V_r	rated voltage
V_{r1}	INV1 rated voltage
V_{rect}	rectifier AC side voltage
V_{rect1}	rectifier AC side fundamental voltage
$V_{rectrms}$	rectifier AC side rms voltage
V_s	machine voltage vector
V_t	terminal voltage vector
v_{wind}	wind speed
X_{com}	compensation reactance
$X_d,\ X_q$	d and q-axis reactance
X_s	synchronous reactance of non-salient synchronous machine
Z_{com}	compensation impedance
β, γ	internal power factor angle
δ	power angle, between back-emf and machine voltage
θ_i	current angle
θ_{ir}	current angle in rotor reference frame
θ_{rf}	reference frame angle

θ_{INV1}	INV1 voltage angle
λ	tip speed ratio
λ_m	permanent magnetic flux linkage
$\lambda_d,\ \lambda_q$	flux in rotor reference frame
ρ	density of air
ω_b	base speed
ω_c	corner speed
ω_r	rotor speed in elec rad/s
ω_{rm}	rotor speed in mech rad/s

Abbreviations

AC	alternating current
ANPC	active-neutral-point-clamped converter
DC	direct current
DFIG	doubly fed induction generator
DVR	dynamic voltage restorer
CSC	current source converter
CSI	current source inverter
CVCF	constant voltage constant frequency
CVVF	constant voltage variable frequency
GaA	gallium arsenide
GB	gear box
GTO	gate turn-off thyristor
FACTS	flexible alternating current transmission systems
IGBT	insulated-gate bipolar transistor
IM	induction machine
IPM	interior permanent magnet machine

MERS	magnetic energy recovery switch
MOSFET	metal-oxide-semiconductor field-effect transistor
MPPT	maximum power point tracking
MTPA	maximum torque per ampere
PM	permanent magnet
PMSG	permanent magnet synchronous generator
PMSM	permanent magnet synchronous machine
PWM	pulse width modulation
SCIG	squirrel cage induction generator
SEIG	self-excited induction generator
SiC	silicon carbide
SPM	surface permanent magnet machine
SRM	switch reluctance machine
SSSC	static synchronous series compensator
STATCOM	static synchronous compensator
SVC	static var compensator
SVPWM	space vector PWM
TCR	thyristor controlled reactor
TCSC	thyristor controlled series compensator
THD	total harmonics distortion
TSC	thyristor switched capacitor
UPFC	unified power flow controller
VSC	voltage source converter
VSI	voltage source inverter

Introduction

I.1 Project Overview

This research is to investigate the applications of reactive power compensation of open-winding permanent magnet synchronous machines (PMSM) by using a series connected voltage source inverter (VSI).

PMSM are seeing increasing use in various applications including electrical hybrid vehicles, renewable energy, more electric aircraft because of their high efficiency and power density. Due to their intrinsic properties, PM machines, either as motors or generators, are often equipped with a fully rated power electronics converters to supply or extract real and reactive power.

Today most AC machines are three-phase Y-connected. The neutral point is left floating to eliminate the path for zero sequence current. In contrast, the three-phase windings of an open-winding machine do not have a connected neutral point inside the machine. Instead, all six leads are brought out to the machine terminal. Traditionally, open-winding machines are used with dual voltage source inverters as an alternative to conventional three-level inverter in very high power AC drives. The power of the motor is divided equally for the two inverters to reduce the size of each single inverter. In this work, a VSI with a floating capacitor connected to one set of the three-phase terminals is used as a reactive power source to compensate for open-winding permanent magnet machines.

The function and control method of the proposed compensation inverter is similar to the existing series compensation devices in the flexible alternating current transmission system (FACTS). In power systems, reactive power can be injected to the

grid to change the voltage and/or power flow in the fashion of shunt or series compensation. The FACTS devices utilize power electronics technologies to realize such functionalities. The FACTS concept of controlling the system by reactive power injection is adapted in smaller single electric machine systems in this research.

As a series compensation method, its capabilities to control impedance, power flow and voltage will be studied and demonstrated for three distinct applications.

A series compensated open-winding PM motor drive is proposed. The motor and compensation inverter together can be considered as a variable impedance machine. The operating space of the motor can be extended when the inverter is powered from a fixed voltage supply. For power flow control, a wind power generation system is proposed. The compensation inverter is used to improve the generator utilization and reduce the cost of the overall system. For voltage control, a small constant voltage variable frequency (CVVF) AC distribution system is proposed. The load voltage can be controlled using the series connected compensation inverter.

Although an interior permanent magnet machine (IPM) is used for investigation in this work, the proposed compensation method and topology is applicable to non-salient surface permanent magnet (SPM) machines or synchronous reluctance machines as well.

I.2 Organization of Report

This document has six chapters. Chapter 1 reviews the state of the art that is related to this research. The history of AC machine drives and power electronics is briefly reviewed. As the origin of open-winding machine drives, high power AC drives are studied. Previous literature on the open-winding machine drives is studied extensively. The other major related area, flexible alternating current transmission systems (FACTS)

and the application of FACTS type of devices in smaller systems are reviewed as well.

Chapter 2 presents the concept of series compensation of open-winding PM machine drives and the mathematical of the open-winding drive system. This chapter develops the foundation for the latter chapters. Series compensation of open-winding machines by PWM voltage source inverter with either DC voltage source or capacitor is discussed in detail. The dynamic model of open-winding machine in rotor reference frame with zero sequence circuit is given. The overall model including the machine and inverters is presented.

Chapter 3 presents a new open-winding PM motor drive. A voltage source inverter with a floating capacitor is used to provide the reactive power required by the motor. At low speed, the compensation inverter can be controlled as a capacitor so that the main inverter operates under unity power factor. The onset of flux weakening can be postponed to a higher speed. At high speed, the compensation inverter is controlled as an inductor to extend the constant power region of a PM machine. In both cases, the utilization of limited DC bus voltage can be improved. The operating space of the drive can be extended considerably. The sizing of the auxiliary inverter and applicability of the proposed topology to other motors is discussed. Simulation and experiment results are given to show the validity of the topology and control method.

Chapter 4 proposed a wind power generation system utilizing an open-winding PM generator. A diode bridge rectifier and a series connected VSI are used to extract power from the generator. System overall cost can be reduced comparing to a conventional fully sized active rectifier because a fractional sized active converter is employed. The generator underutilization issue in diode rectifier based system can also be solved by the proposed topology. The sizing of the compensation inverter is studied. The capabilities of the proposed topology to operate with both fixed and variable speed turbines are verified by computer simulation and experiment.

Chapter 5 demonstrates the voltage control capability of the proposed

open-winding compensation scheme. A PM generator based small CVVF AC distribution system for vehicular application is proposed. The voltage amplitude at the distribution side can be controlled to be constant while the generator speed and load condition varies. The proposed topology is compared with its shunt compensation dual in detail. The impact of generator selection on dimensioning of the compensation inverter is discussed. Simulation and experiment results are given at the end.

Chapter 6 summarizes the key conclusions and contributions. Suggested future works are listed as well.

Chapter 1

State of the Art Review

This chapter presents a state of the art review of the areas that are related to this work. Section 1.1 is a brief broad introduction of adjustable speed AC drives including some historical perspectives. Section 1.2 reviews the area that the open-winding machine drives are originated from, namely high power machine drives. Section 1.3 presents a detailed review on open-winding machine drives research in the existing literature. Section 1.4 and 1.5 introduce the FACTS and some previous applications of FACTS concepts in smaller systems.

1.1. Adjustable Speed AC Drives

For more than a century, electric machine drives have served us to enhance the productivity of the industry and improve the quality of our lives [1-8]. It has been estimated that 65% of the generated electric power is consumed by electric drives [1]. AC machines, particularly, are now used everywhere. To give a few examples, large induction and synchronous machine drives are used in industry facility to power fans, pumps and all kinds of different machinery. Smaller AC drives can be found at our homes in air conditioners, washing machines, computer hard disk drives, etc.

1.1.1. AC Machines in Adjustable Speed Drives [1-8]

There are three major types of machines that are commonly used with adjustable

AC drives: induction machines (IM or asynchronous machines), synchronous machines and switched reluctance machine (SRM).

Squirrel cage type induction machines have been around for more than 150 years. The rotor of a squirrel cage induction machine is constructed with conductive bars (copper or aluminum). The rotor bars are shorted together at the end of the bars. Therefore, induction machines are very rugged and robust.

Synchronous machines are another major type of AC machines. Synchronous machines include wound field synchronous machines, permanent magnet machines and synchronous reluctance machines. Would field synchronous machines can be further categorized as salient pole and round rotor according to the shape of rotor. Permanent magnet (PM) synchronous machines are becoming more and more popular in low to medium power level due to their higher efficiency and power density. Like induction machines, synchronous reluctance machines do not have excitation on the rotor. But synchronous reluctance machines do not "slip" like induction machines. The torque is created due to the saliency on the rotor.

Switched reluctance machines are not traditional multiphase AC machines. The SRM is not excited from balanced multiphase sinusoidal voltage. A power electronics converter and absolute position sensor are usually required in SRM drive. SRM drives can be found in high speed applications because it is robust and it usually has low losses in the rotor. In addition, there is no high back-emf like for PM machines in SRM. SRM is also a good candidate for applications like mining equipment which often work under environment of high temperature and conductive dust.

1.1.2. Early Drives

Prior to the 1950's, applications that required accurate speed or position control were domain of DC motor drives because of the ease of control due to their roughly

linear relationship between armature current and produced torque. However, continual efforts were constantly spent on the development of adjustable AC drives because of the disadvantages of DC machine such as more frequent maintenance, larger size and lower reliability [3].

The evolution of adjustable speed AC drives can be dated back to the beginning of the 20th century. Before the introduction of thyristor, electromechanical AC drives dominated the industry AC drives in the first half of the century. Electromechanical AC drives such as Krämer systems and Scherbius systems for wound rotor induction machines were used for decades [2]. However, many fundamentals of electronic AC adjustable speed drive were developed in early 1900's after the invention of various triggered-arc switches like thyratrons and ignitrons. These concepts include phase control, natural commutation, forced commutation, dc-to-ac inversion, cycloconversion and many others that are still with us today [2]. But due to their high cost and vulnerability, those ancestors of modern AC drives were never widely used in the industry.

1.1.3. Current Source Inverter

In 1957, thyristor, also known as silicon controlled rectifier, was commercialized by General Electric, marking the beginning of modern solid state power electronics era [2]. Simple thyristor based phase control and line commutated rectifier were well accepted as AC-DC front end of AC drive. Thyristor bridges are the most popular type of current source inverters (CSI) [3]. An inductor is placed between the rectifier and the inverter to smooth the DC current. CSI is usually used to drive large AC machines. When driving synchronous machines using thyristor based CSI, load commutation is possible by proper advance triggering. Extra forced commutation circuits are required to drive induction machines. The CSI is naturally good for power conversion that

requires regeneration. Electric power can be fed back to the grid simply by varying the firing angle of the switches. The disadvantages of a CSI are apparent. To name a few: lower order harmonics are generated on both machine side and grid side; it has a bulky DC link inductor, and produces large voltage spikes. Nowadays, PWM type of CSI is commercially available. Self turn-off devices are usually used in this type of CSI. For this type of CSI, AC filter capacitors are often required at the output of the inverter.

1.1.4. Voltage Source Inverter

Self turn-off devices became available in late 1970's and early 1980's. Major devices like gate turn-off thyristor (GTO), power metal–oxide–semiconductor field-effect transistor (MOSFET) and insulated-gate bipolar transistor (IGBT) were introduced during that time period. Voltage source inverters (VSI) became possible which brought a major change in power electronics and electric drives. The VSI is the dual of the CSI. A DC capacitor is used in the DC link as the energy storage element to "stiffer" the DC voltage seen by the inverter and to handle the transient current due to switching events [4]. Power MOSFET is the dominant device in low voltage adjustable AC drives nowadays. It usually can switch at higher frequency than IGBT and GTO. The IGBT is probably the most popular power electronics device in industrial AC drives. It can be found in most industrial AC drives of voltage levels ranging from 120 V to several kV. It has higher voltage blocking capability than MOSFET. Switching frequency is between MOSFET and GTO. A GTO is mostly used in very high voltage and high power level drives. The switching frequency of GTO based drive is often below 1 kHz. There are new types of devices being developed and some of them are becoming commercially available in small amount. Gallium arsenide (GaA) and silicon carbide (SiC) devices can operate at higher temperature. As a result, higher switching frequency is possible because the junction is able to handle the extra heat generated by

increased switching events in the same time period. SiC devices are also able to block higher voltage in their off state. Diamond also has great potential as good material for power electronics device [4]. It can be predicted that electric drives performance will be improved once those new devices become widely available.

1.1.5. Matrix Converter

Matrix converters use an array of bidirectional solid state devices and converter directly between arbitrary voltage sources. With proper control, matrix converters can be DC/DC, DC/AC, AC/DC, AC/AC converters. The most popular application is the matrix converter motor drives, driving three-phase AC motor from three-phase AC source. Ideally, matrix converters have numerous benefits such as no energy storage link (capacitor or inductor), controllable input power factor, and regenerating capability. However, because matrix converters use more power electronics switches (often the most expensive parts in a converter) than other drive topologies, there are few commercialized AC drives based on a matrix converter. In addition, the complexity of control and reliability issues also inhibits its adoption in industry. Complicated commutation technology is usually required to make sure there is no short circuit at input side or open circuit at output side [5]. The size of three filter capacitors required at the input of the converter is often not much smaller than a DC bus capacitor in VSI. There are several topologies proposed to reduce the number of active switches in matrix converter [6]. But in those topologies, some of the features like regenerating capability are no longer available. Although matrix converters have been under research constantly, but matrix converters can not compete with VSI or CSI in industry up till now.

1.2. High Power Drives

The size of electronic drives is usually limited by the rating of available switching devices. Traditionally, CSI is popular in high power electric drives. Although the capability of power electronics devices has been improved dramatically during the past few decades, it is still difficult to directly extent normal six-switch two-level VSI topology into high power application. There are two common trends in high power AC drives: using multilevel voltage source converter on three phase machines and employing higher phase order machines with multiple inverters.

1.2.1. Multilevel Drives

Multilevel converter is a more common way to handle high power [9,10]. Inverters with rating in MW range are usually powered from medium voltage grid (several kV) to reduce the current requirement and the losses. Up till now, it is still difficult to use single device to block such high voltage. Although GTO has very high voltage blocking capability, the limited switching frequency introduces high harmonics pollution to the power grid. Multilevel converter includes an array of devices and capacitors at different voltage levels. By proper switching, output voltage waveform is of more than two levels [9]. Diode clamped multilevel converter, flying capacitor clamped multilevel converter and cascaded H-bridge multilevel converter are the three most popular types of multilevel converters.

The cascaded H-bridge topology utilizes single-phase H-bridge inverters with isolated DC source connected in series [11]. Different number of cells can be used in each phase. With a high number of cells, the output voltage will contain very low harmonics. If the windings of the secondary of input transformers are properly phase shifted, the input power factor can be very close to unity even with diode rectifier is used for each cell. The cost and size are the major disadvantages of the cascaded

H-bridge topology.

In [12], Peng discussed about a generalized multilevel converter with self balancing capability. Wang and Li also pointed out that many multilevel converter topologies with reduced number of switches or capacitors (including diode-clamped and flying-capacitor topology) can be derived from the generalized topology [10]. Several active-neutral-point-clamped (ANPC) multilevel converter topologies have been reported as well [13,14]. Commercial five-level ANPC based medium voltage drives are already available on the market [15].

The advantages of multilevel converter include reduced voltage rating on each device, better voltage waveforms, lower differential mode (dv/dt) and common mode voltage and higher effective switching frequency. The disadvantages are apparent as well. The control complexity and higher possibility of failure are the major ones. Many modulation algorithms have been proposed for multilevel converters including carrier based modulation, space vector modulation for different purposes [11,16,17]. Capacitor voltage balancing, harmonics elimination and other purpose can be achieved using redundant switching states of the converter. Reference [18] compares several of the existing multilevel converter modulation techniques.

As mentioned above, the possibility of failure in multilevel converters are higher than two-level converters due to the increased parts count. The failure mode analysis, fault protection and post-fault operation of multilevel converters have been investigated by various researchers [19, 20]. Extra switching devices and other parts are usually required for protection and post-fault operation.

At the moment, the advantages of multilevel converters are still over its disadvantages in very high power applications. Before more advanced devices become widely available, multilevel converters will continue to serve the industry as a very attractive option for high power AC drive.

1.2.2. Multiphase Drives

Multiphase is another trend in high power AC adjustable speed drives. Since adjustable AC drives are mostly based on power electronics nowadays, the number of phases of AC machines is no longer limited to the available number of phases of the electrical grid. In high power applications, it is possible to reduce the per phase converter rating by employing machines with higher phase order [21]. Five-phase, six-phase (also known as split-phase or dual three-phase machines), seven-phase and nine-phase are the most popular choices among multiphase machines. Khan and et al. compare the different types of multiphase machines from the point of view of machines themselves with an emphasis on three and six-phase machines [22]. It is suggested in the paper that the benefits of multiphase machine are sensitive to the voltage supply angle of the two set of stator windings and 30 degrees phase shift is optimal for six phase machines.

There is a significant number of publications on modeling and control of multiphase machines since 1980s. Lipo published a d-q model for a six phase induction machine [23]. Later, Zhao and Lipo proposed a space vector PWM method based on vector space decomposition method [24]. The original six-dimensional vector space was mapped into three two-dimensional orthogonal subspaces. In the transformation, there are a fundamental subspace (like the d-q plane in three-phase machines), a new type of zero sequence subspace which rotates but does not create electromechanical torque and finally the regular zero sequence harmonics. The authors later extended this work to modeling and control of induction machine under structural unbalance [25]. Rockhill and Lipo applied the theory to nine-phase generalized n-phase synchronous machines [26]. In three-phase machines, third harmonics do not create any average torque. Lyra and Lipo investigated improvement of torque density by injecting third harmonics into a six-phase induction machine [86]. Control methods like direct torque

control [27] and independent field-oriented control [28] of six-phase machines have also been reported. Yazdani and et al. proposed a space vector classification algorithm for six-phase machine drives to fully utilize the inverter [29]. There is also research on driving more than one multiphase machines using single inverter supply [30].

In addition to lower per phase converter rating, multiphase AC drives usually have better fault tolerance capability. As a result, multiphase drives are also popular in applications like aerospace, automotive and electric ship propulsion, where both power and fault tolerant capabilities are of concern. Jahns investigated the improvement of reliability in solid-state AC drives by means of multiple independent phase-drive units [31]. Ouyang investigated a modular five-phase PM machine with fault tolerant capability [32].

In the near future, three-phase machine will continue to dominate industry in most applications due to its historical popularity and wide availability. However, multiphase AC drives will become more popular in more specialized areas.

1.3. Open-Winding Machine Drives

Y connection is the most common connection method in three-phase machines. The advantages of Y-connection over delta-connection such as lower cost and absence of circulating current path were discussed long time ago [33]. Therefore, most AC machines presently on the market are Y connected although delta-connected transformers are sometimes used in power systems. Before the invention of power electronics drive, star-delta starters were used to limit the starting surge current in induction machines and relief the stress on the grid [34]. As shown in Fig. 1.1, the machine has three independent windings. By external switches, it can be configured as either star (Y) or delta connected. Essentially, the machine is an open-winding machine

[35]. A three-phase open-winding machine has three independent windings and six leads.

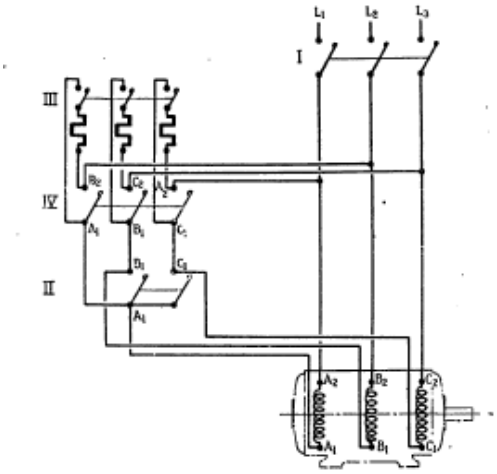

Fig. 1.1 Star-delta starter for induction machine [34]

Stemmler and Guggenbach proposed several high-power open-winding drives based on two or three-level VSI in 1993 [36]. It is the earliest publication that is found on an actual open-winding drive. Two possible configurations were discussed: two inverters with common DC bus or isolated DC bus (Fig. 1.2). For the common DC bus topology, there is a zero sequence current path in the circuit. Therefore, zero sequence choke was used when two inverters shared common DC bus. It was also pointed out that the voltage of each inverter did not have to be the same. In addition, inverters of more voltage levels could be used on either side of the motor to obtain better voltage waveforms.

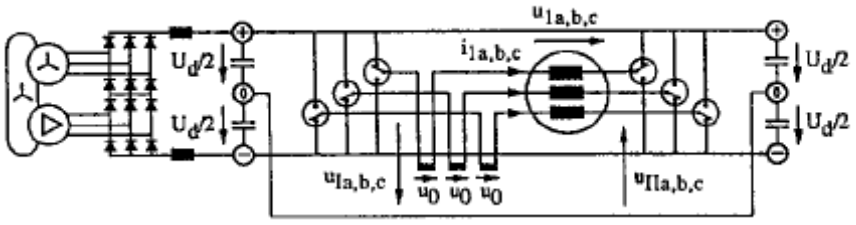

(a) Open-winding drive with common DC bus

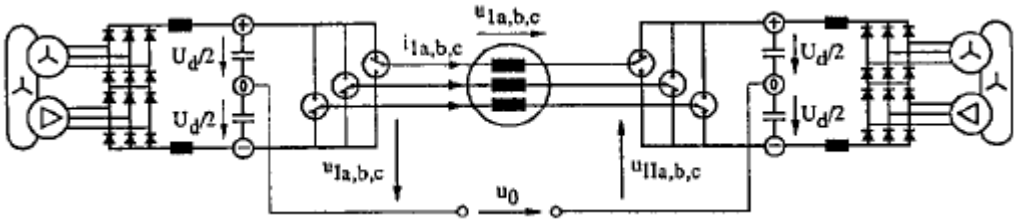

(b) Open-winding drive with isolated DC bus

Fig. 1.2 Open-winding machine drive configuration for high power application [36]

Since then, there has been some constant research efforts spent on the modulation technique of open-winding drives. Shivakumar and et al. proposed a space vector PWM control method for open-winding induction machine with isolated DC bus. Two 2-level inverters results in 64 switching states. As shown in Fig. 1.3, the hexagon voltage vector space was divided into 24 triangular sectors and a look-up table was used to generate the switching sequence [37]. Shiny and Baiju proposed a SVPWM algorithm without sector identification to reduce the PWM computational time [38].

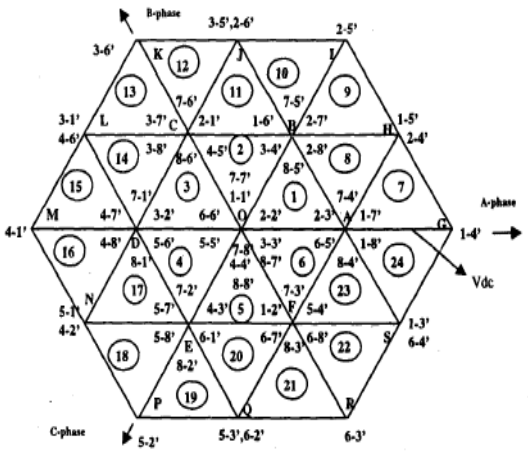

Fig. 1.3 Space vector modulation of open-winding machine drive [37]

Somasekhar and et al. investigated the effect of zero-vector placement in an open-winding induction motor drive. By proper placing the zero-vector in each individual inverter, zero sequence voltage in machine windings could be enforced to zero in a sampling period average sense. The disadvantage of this algorithm was that there was a 15% percent DC bus voltage underutilization [39].

Instead of minimizing zero sequence voltage in machine windings, Sivakumar and et al. proposed a method to eliminate the zero sequence current paths in the machine itself. The machine windings were broken into two spatially apart Y-connected sets as shown in Fig. 1.4. The modified induction machine was similar to a six-phase machine [40]. But the two set of windings did not have a phase shift like regular split-phase induction machine. In the results shown in [40], there was significant ripple in current waveform, which may due to the low impedance of differential mode current path between the two sets of windings similar to that in split-phase induction machines.

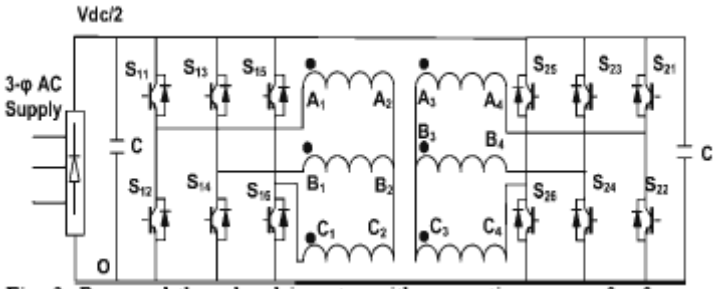

Fig. 1.4 Modified open-winding machine [40]

Open-winding drive is essentially a multilevel converter. In [41], it was shown that open-winding drive was similar to three single-phase H-bridge converters driving independent windings. When common DC bus is used, the voltage waveform of an open-winding motor drive is identical to that of a six-leg bridge converter. Compared to regular diode clamped or flying capacitor 3-level inverters, the open-winding dual inverter drive has lower parts count. Moreover, the control will be easier in the dual inverter open-winding motor drive.

Grandi and et al. presented a PWM technique to regulate the load sharing between the isolated DC buses in an open-winding induction machine drive. A power sharing ratio k was defined and the amplitude of voltage command of each inverter was assigned based on the ratio [42].

Open-winding drives are also receiving attention in hybrid vehicle applications recently. Rossi and et al. proposed a series hybrid powertrain based open-winding configuration. An open-winding PM generator was coupled with internal combustion engine. The generated power was split into two isolated DC buses through individual converters. Two regular three-phase PM machine drives were used to drive two individual shafts [43].

Welchko proposed an open-winding inverter drive system with isolated DC bus for combined propulsion and energy management functions for hybrid vehicles with an energy storage element. One of the DC bus is connected to an energy storage element,

for instance a battery. Regenerative energy during braking could be stored in the battery and be used later when needed. Three control methods were mentioned: unity power factor control, voltage quadrature control and optimum inverter untilization control [44].

Kwak and Sul proposed a flux weakening control method for open-winding SPM machine. Current reference modification and over modulation in flux weakening region were discussed. The power flow through each inverter could be controlled independently. A separate set of diode rectifier and an isolation transformer are used for the second inverter. It was claimed the torque capability can be extended by 15% at the top speed under the same current limit [45].

Kwak and Sul also proposed a grid connected open-winding SPM based distributed generation system. Unlike conventional open-winding drive, only one inverter is used with an open-winding SPM machine. The other set of the three-phase terminals is connected to the load (and/or grid). There are multiple renewable energy sources in the system including wind, solar, fuel cell and etc. All energy sources in the distributed generation system are connected to a shared DC bus. The open-winding SPM is not only used as a generator, but also as an interface between the DC power from other local energy sources and the grid. The power from the DC bus and engine generator set can be controlled simultaneously by only one inverter [46].

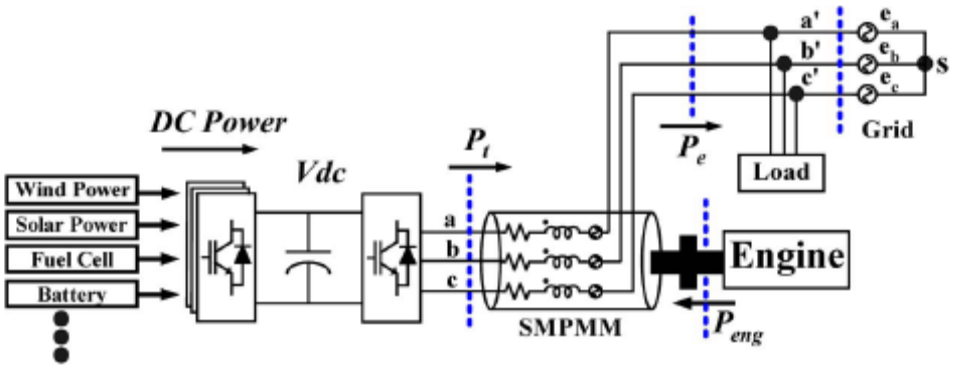

Fig. 1.5 Open-winding SPM machine based grid connected distributed generation system [46]

1.4. FACTS

The flexible alternating current transmission systems (FACTS) devices are solid state power electronics based devices that are used to dynamically control the power flow, voltage, impedance and/or phase angle in the power grid. With the help of FACTS devices, the existing grid can be better utilized, transmission line reliability can be improved, dynamic and transient grid stability can be improved, quality of electricity supply can be enhanced [47].

The static var compensator (SVC) is a shunt type FACTS device. Its function is similar to traditional fixed shunt capacitor bank in power systems. But with the help of modern power electronics devices, SVC is faster and continuously variable over a specified capacitive and inductive range. The thyristor switched capacitor (TSC) and the thyristor controlled reactor (TCR) with fixed capacitor are two thyristor based SVC devices. Those devices still require reactive elements of similar rating as traditional fixed capacitor banks. The static synchronous compensator (STATCOM) or static synchronous condenser (STATCON) is a voltage source converter based shunt compensation device. The STATCOM operates in a way that is similar to a rotating synchronous condenser. By controlling injected current in quadrature with voltage at

the point of coupling, the amount of reactive compensation can be adjusted. Compared to thyristor based SVC devices, the STATCOM has faster response and only use one DC capacitor. Nevertheless, filters or coupling transformer are usually needed. Fig. 1.6 gave some examples of the SVC [48].

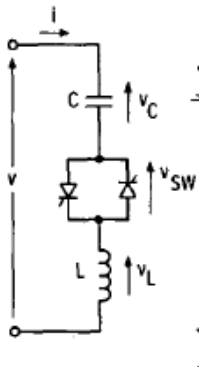

(a) TSC

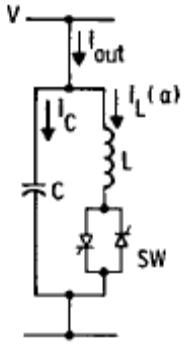

(b) TCR with fixed capacitor

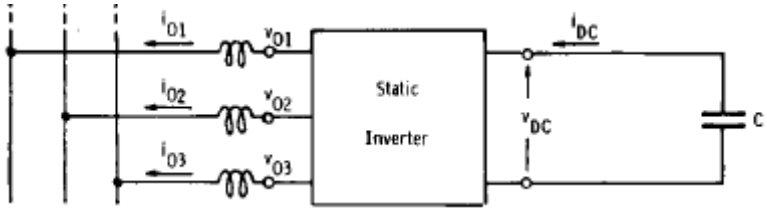

(c) STATCOM

Fig. 1.6 Examples of SVC devices [48]

Thyristor controlled series compensator (TCSC) is a line impedance control device. Topologically, it is the same as TCR in parallel with fixed capacitor type SVC. It includes a back-to-back pair of thyristors, an inductor in series with the thyristors and a capacitor in parallel with inductor and thyristors. As shown in Fig.1.7, the capacitor provides fixed capacitance in series with the transmission line. By controlling the firing angle of the thyristor pair, the average reactive compensation seen by the line can be continuously varied. As a result, the total impedance of the TCSC is controllable. Since TCSC uses thyristors, the compensation can only be adjusted in an average sense [49].

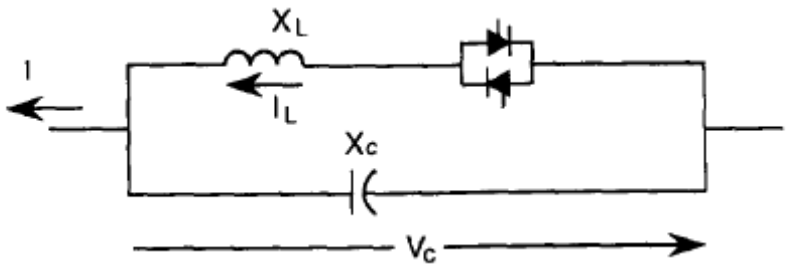

Fig. 1.7 TCSC [49]

A more advanced series compensation FACTS device is the static synchronous series compensator (SSSC). As a dual of the STATCOM, the SSSC is a VSC based device. It can provide the same range of capacitive and inductive compensation. Power flow is controlled by varying the equivalent impedance between two buses in power grid. Series capacitors may cause sub-synchronous resonance in the grid [50]. The SSSC, in contrast, is immune to the sub-synchronous resonance. If equipped with an active power source or sink, the SSSC can even be used to damp oscillations in the grid. A block diagram of SSSC is shown in Fig.1.8. [51]

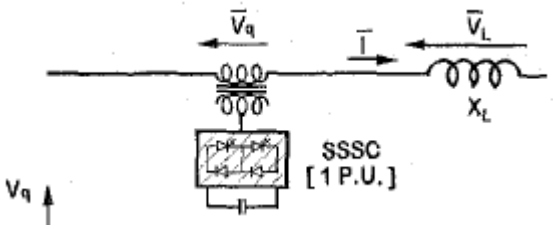

Fig. 1.8 SSSC [51]

The dynamic voltage restorer (DVR) is a means of mitigating voltage sag in power systems. It is a series compensation device using VSC with coupling transformer similar to the SSSC. Wang and Venkataramanan proposed a DVR using cascaded H-bridge multilevel converter [52]. Kim and Sul used an open-winding transformer with a six-leg converter to implement a DVR. A command feedforward and state

feedback combined control method is proposed by the authors [53].

The magnetic energy recovery switch (MERS) is an emerging series type of FACTS device. The MERS is a single-phase H-bridge with a DC capacitor. Under proper control, the MERS acts as a variable capacitor. Power electronic switches in the MERS only switch at the fundamental to minimize the switching losses. The waveform of the MERS is very good since there is not much harmonics introduced by the switching events. Unlike the SSSC, the MERS is inserted directly in line. Coupling transformer is therefore not required. However, the MERS requires more power electronic switches than the SSSC. Also, the total capacitance of all three phases will be larger compared to the one DC capacitor in the SSSC because MERS is a single-phase type of device. Fig. 1.9 shows the topology of MERS [54].

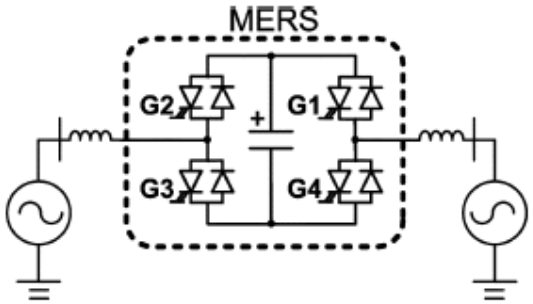

Fig. 1.9 MERS [54]

The unified power flow controller (UPFC) consists of two back-to-back converters with a DC link in between. The two converters are like the STATCOM and the SSSC with their DC bus tied together. The UPFC can provide independent shunt and/or series compensation. The real power flow through UPFC can be controlled. The UPFC is a very powerful real and reactive power flow controller and is able to control voltage, impedance and angle at the same time. Fig. 1.10 shows a block diagram of UPFC [55].

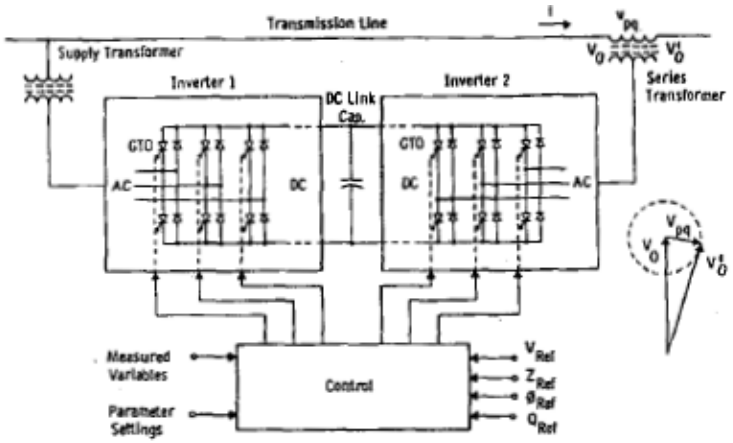

Fig. 1.10 UPFC [55]

Except for the major FACTS devices mentioned above, there are some other devices. Phase shifter is uses a quadrature phase voltage to change the phase of bus voltage [56]. Ξ-controller is a series compensator using direct AC/AC conversion [57]. Γ-controller is an AC link UPFC type of device [58].

To sum up, shunt compensation type of FACTS devices is good at controlling voltage and reactive power in the grid. Series compensation is better for line impedance and power flow control. UPFC type of devices have all the benefits of both shunt and series compensation. Table. 1.1 is a comparison of functions of three major types of FACTS devices.

Table 1.1 FACTS devices comparison

control capabilities	shunt compensation	series compensation	UPFC
bus Voltage	*	-	*
VAR flow	*	-	*
power flow	-	*	*
impedance control	-	*	*
inject voltage	-	*	*
phase angle	-	*	*

1.5. Application of FACTS Type of Devices in Smaller Scale Systems

FACTS devices are traditionally proposed for power grid scale applications. However, similar ideas have been used in smaller systems as well.

1.5.1. Generator Voltage regulation

Self-excited induction generators (SEIG) are often used in rural or remote areas. Traditionally, a large enough capacitor is connected to the machine terminal to supply enough leading reactive power to balance the lagging reactive power required by the magnetization induction generator. Hunt investigated steady state operation of SEIG under line excitation, AC capacitors and electronic excitation via voltage source inverter. The electronic excitation is basically a small scale STATCOM [59].

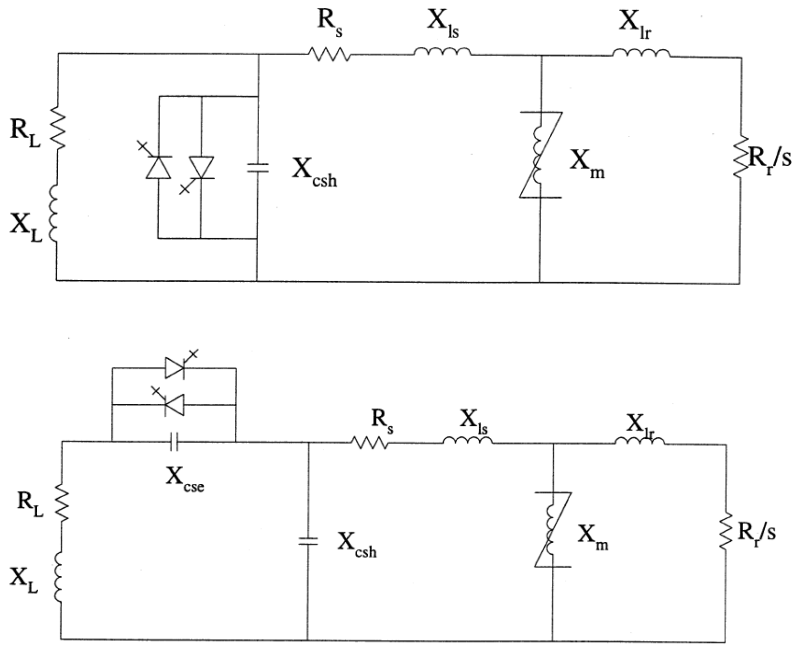

Fig. 1.11 Two SEIG with a continuously controlled capacitor topologies [60]

In his PhD dissertation, Al-Saffar used continuously controlled capacitors to

regulate the voltage of a SEIG system. As shown in Fig.1.11, an anti-parallel pair of self turn-off switches is connected in parallel with an AC capacitor. The continuously controlled capacitor is similar to a TSC or a MERS. But unlike TSC which use thyristor in series with AC capacitors, self turn-off switches are used in parallel with the capacitor. Compared to MERS, two instead of four switches are used for each phase by the controlled capacitor. However, DC capacitors can not be used in the switched capacitors [60].

For three-phase SEIG, Muljadi took a different compensation approach. Fig.1.12 shows Muljadi's method. An open-winding induction machine was used. A series compensation method by VSI and battery was proposed. The author discussed the concept of equivalent impedance and used admittance diagram to obtain proper compensation value. This is the earliest publication found on the series compensation using open-winding machine configuration [61,62].

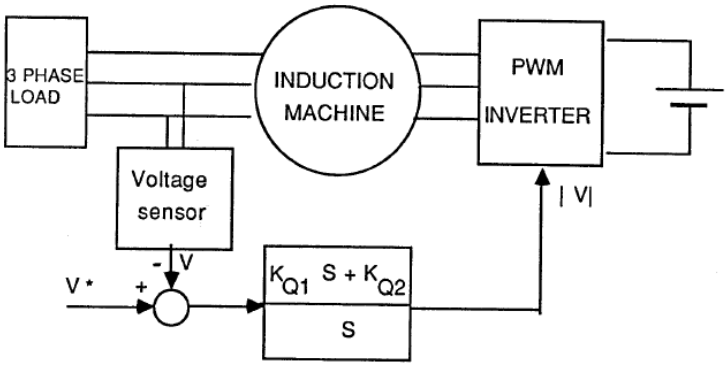

Fig. 1.12 Series compensated PWM inverter with battery supply applied to an isolated induction generator [61]

Naidu and Waters proposed an induction machine based generating system with a diode rectifier and a PWM inverter for automotive application. All real power went through the diode rectifier into the battery. Although there is no AC load in the system,

the system operated in a way that is similar to the STATCOM-based SEIG. An auxiliary PWM MOSFET VSI was used to injecting reactive power into the machine. The output DC voltage of diode rectifier was controlled in a way similar to that in a SEIG system [63].

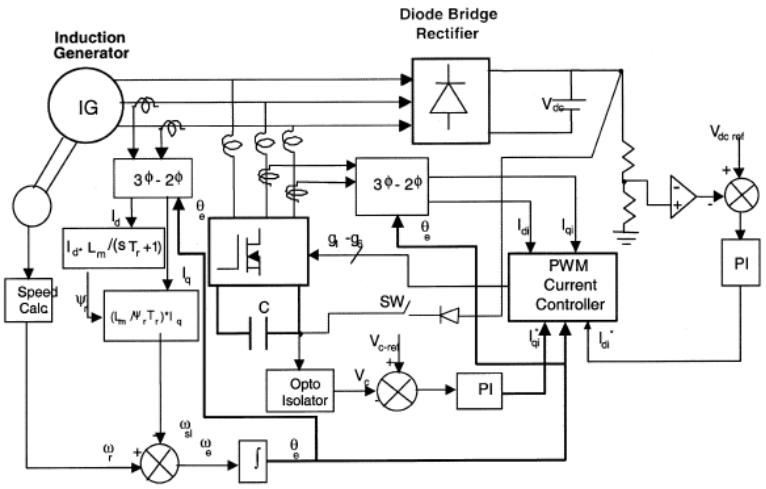

Fig. 1.13 Induction machine based generating system for automotive application [63]

Huggett and Kalman patented a generating system using a PM machine and the shunt AC regulator. The regulator was basically a VSI reactive power source. The amplitude of the voltage is regulated by injecting reactive power into the generator. It is similar to SEIG but a PM machine is used instead of induction machine. The diagram is shown in Fig.1.14 [64].

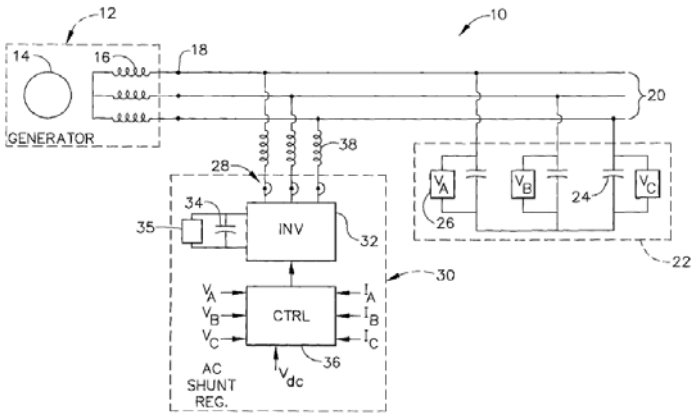

Fig. 1.14 Generating system using PM machine and shunt AC regulator [64]

Nishida and et al. proposed a similar system for automotive application. Instead of only having AC load at the generator terminal, the system also included a nonlinear diode rectifier. The shunt connected VSI was used for both regulating AC voltage and as an active power filter for harmonics generated by diode rectifier. A deadbeat current controller is used in the system [65].

Recently, Clements proposed to use the PM machine generating system invented by Hugget and Kalman in vehicular applications. The author found that the size of power converter could be reduced significantly if IPM generators of proper saliency and characteristic current value. A control method based on modulation index magnitude and angle with respect to rotor angle was proposed to improve system performance. Mitigation of failure mode was considered by proper selection of generator characteristic current [66].

1.5.2. Motor Drive Systems

Muljadi and et al. applied the same continuously controlled capacitor used by Al-Saffar to a single-phase induction motor. AC capacitor is often used to help starting single-phase induction machines. Sometimes another capacitor is used to improve motor efficiency during normal operation. The controllable capacitor is connected in

series with the auxiliary winding of a single-phase induction machine. The capacitance is controlled to be different during starting and normal operation [67].

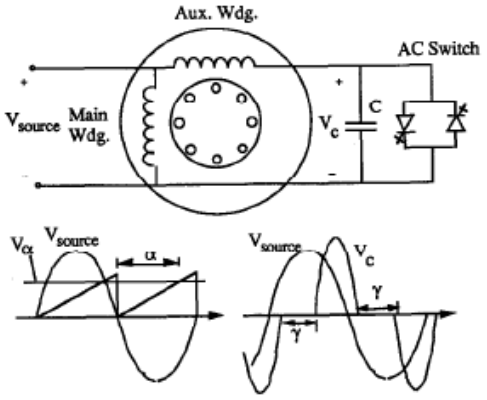

Fig. 1.15 Single-phase induction machine with controlled capacitor [67]

Muljadi and Lipo also investigated the application of series compensation of an open-winding induction machine in the motoring region. But a split-phase induction machine instead of open-winding (used in SEIG application) is used. The main set of windings is connected to the power line. A VSI with a DC capacitor is connected to the second set of the windings to supply reactive power required. The machine with compensator together only extracts real power from the grid (unity power factor at the point of coupling) [68].

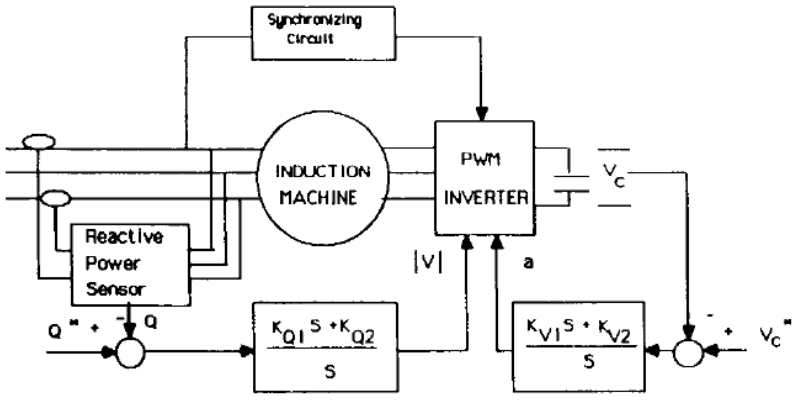

Fig. 1.16 VSI compensation for split-phase induction machine [68]

1.5.3. Renewable Energy Systems

Ahmed and et al. proposed a SEIG for wind generation system employing a diode rectifier. The TSC is used as reactive source. The output DC voltage of the diode rectifier can be controlled by varying the firing angle of the TSC [69].

Kimura et al. replaced the TSC with a voltage source converter. The VSC is used to set excitation frequency of induction machine in order to ensure a negative slip. As shown in Fig.1.17, VSC DC bus is directly connected to main DC bus [70].

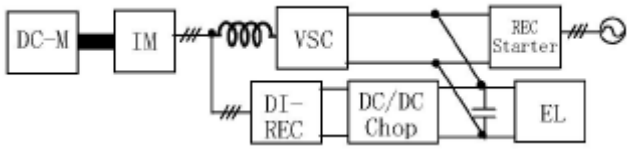

Fig. 1.17 VSC compensated diode rectifier wind generation system [70]

To improve the generator utilization in a diode rectifier based PM machine wind power generation system, Singer and Hoffman used the SSSC to compensate for the voltage drop on the synchronous reactance under loaded condition. It was verified by simulation and experiment that the output power of the generator can be increased [71]. In [72], a passive filter was added to reduce the harmonic content generated by the nonlinear diode rectifier.

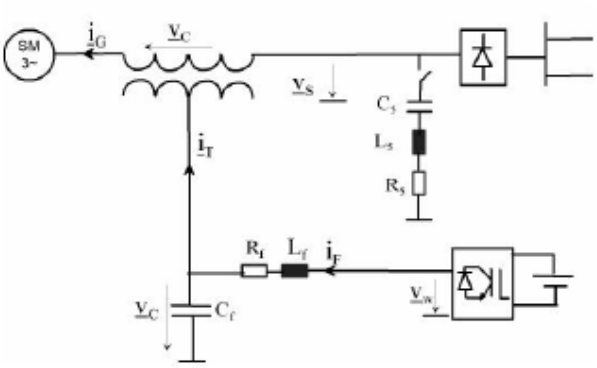

Fig. 1.18 Diode rectifier based PM machine wind power generation system with SSSC [72]

Takaku and et al. realized the same compensation as that of Singer and Hoffman by using the MERS. The switching frequency of the devices in the MERS is the fundamental frequency. The author claimed a significant losses reduction compared to an active PWM rectifier [73]. Wiik investigated the control of the same topology. A control method with rotor position sensor eliminated was proposed. A look-up table is used to generate the gate signal for the MERS [74].

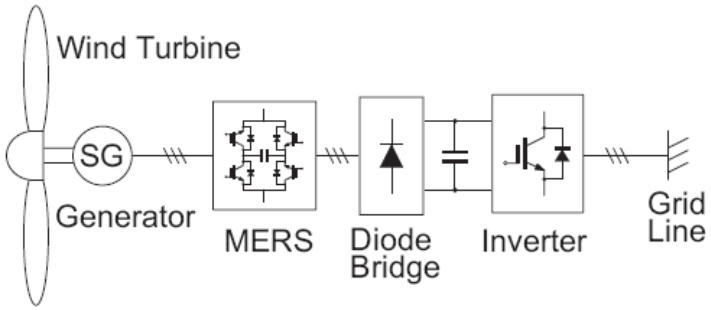

Fig. 1.19 Wind power conversion system using MERS [73]

Grabic and et al. proposed an open-winding PM machine based wind power generation system. The auxiliary series converter is sized 20% of the rated generated power. The function of the series converter is to provide active damping of the generator in case of input power and/or grid disturbances. The design is aiming at fixed

speed wind turbine, but more efficient PM generator was used instead of induction generator [75]. The author did not use the converter to compensate for reactive power.

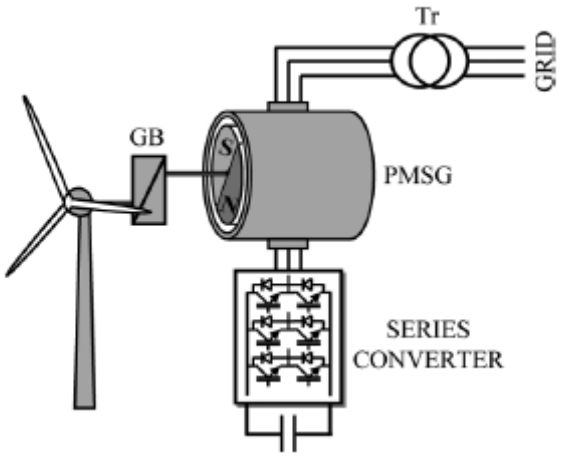

Fig. 1.20 Open-winding PM machine based wind power generation system

1.6. Summary

The areas that are closely related to this work are reviewed in this chapter. The key findings are listed here:

Open-winding machine drive evolved initially as a high power AC machine drive. From the terminal point of view, open-winding machine drive is similar to a six phase machine drive but it is essentially a multilevel machine drive.

Although there is a significant amount of researches found on open-winding machine drives, most of them are about control and modulation technique assuming power coming from both inverters. There is concept presented before mentioning partition of real and reactive power in open-winding drive. However, a separate set of isolation transformer and diode rectifier have to be used. There is no literature found on series compensation on PM machines by an open-winding configuration.

Two FACTS types of concepts have been adapted for smaller single machine systems. For wind power systems using diode rectifier for the power conversion, conventional series compensation devices have been used to improve the generator utilization.

In small CVVF distribution systems, the voltage can be regulated by injecting reactive power. Shunt compensation has been used before. However, the series dual has not been investigated.

Chapter 2

Series Compensation and Open-Winding Machine Drive Modeling

This chapter introduces the concept of using a voltage source inverter directly connected to the PM motor for reactive power compensation. The shared basic theory of the later chapters is presented. The dynamic models of the open-winding PM machines and the overall system are developed in this chapter as well.

2.1. Series Compensation of Open-Winding Machine by a Voltage Source Inverter

2.1.1. Series Compensation Basics

Series compensation is a well established technology that is commonly used in the power systems. The benefits of using series compensation include increased power transferability, limits of load-dependent voltage drops, improved system stability, etc. Often, series compensation is implemented by insertion of reactive elements or power electronics converter based devices in series with the circuit.

A very simple example is shown in Fig. 2.1. Consider a circuit shown in the left side of Fig. 2.1 (a), an AC voltage source is connected to a RL circuit. To increase the power at the load resistor, a capacitor can be inserted in the circuit to counteract the voltage drop on the inductor. By varying the capacitance, the power of the load resistor can be changed. In addition, the voltage on the resistor is changed at the same time.

Similarly, for the circuit shown in Fig. 2.1 (b), a variable inductor can be connected in series with a RC load to control the power and/or voltage at the resistor.

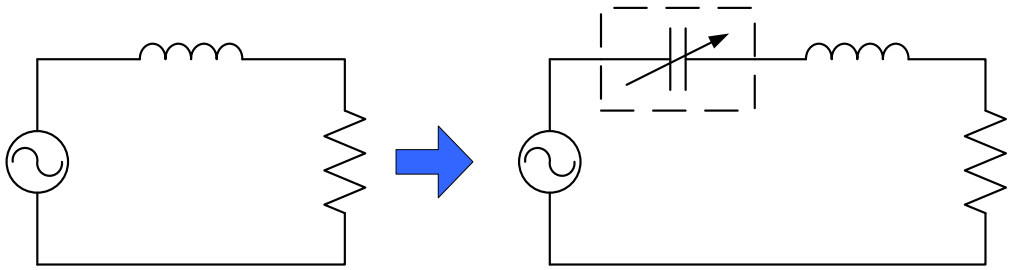

(a) Capacitive Compensation

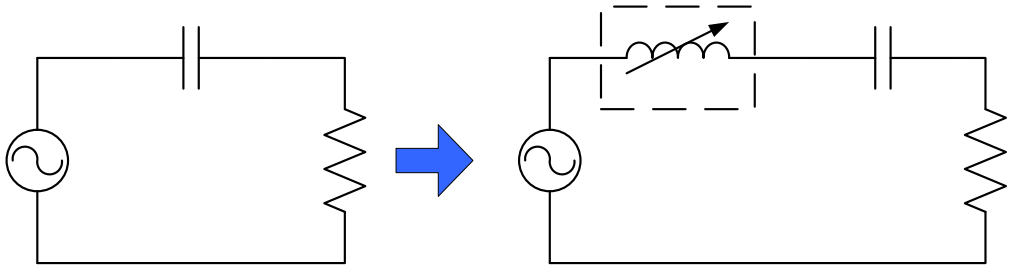

(b) Inductive compensation

Fig. 2.1 Basics of series compensation

Consider an open-winding machine with a series connected single VSI as shown in Fig.2.2. The VSI is connected to one set of the three-phase terminal *a'b'c'*. It can be controlled to insert an AC voltage in series of the machine according to the current in machine windings. The VSI would perform as a compensation device similar to the SSSC in FACTS. Compared to the conventional SSSC, VSI with an open-winding machine does not require a bulky and pricy coupling transformer. Moreover, the machine itself has a reasonably high inductance. Therefore, there is normally no requirement for inductive filters. Like in many FACTS devices, a floating capacitor connected to the DC bus of the inverter is sufficient for the purpose of reactive power compensation. However, when the DC bus of the VSI is connected to an energy source and/or sink, real power compensation is possible. The three basic operating modes of the compensation inverter are introduced in the following sections.

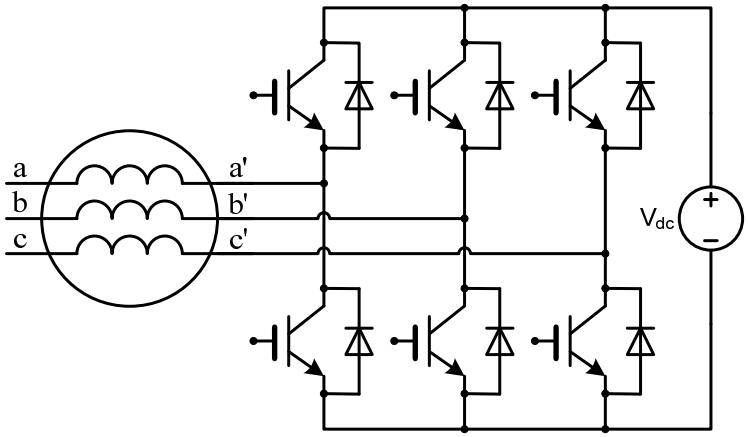

Fig. 2.2 VSI series compensated open-winding machine

2.1.2. Voltage Mode

Fig.2.3 (a) shows the VSI series compensation concept in the fashion of equivalent circuit. V_{com} is the compensation voltage. V_S is actual voltage applied on machine terminals. V_t is the terminal voltage at the other set of three-phase terminals (*abc*) of the machine.

Fig.2.3 (b) is a vector diagram illustrating the same concept. A circle centered at the tip of V_S with a radius of maximum compensation voltage is shown in the figure. All possible V_t vectors lie within or on the circle. If machine voltage V_S is given, the VSI can be controlled to obtain desired terminal voltage V_t. Similarly, a circle of machine voltage V_S can be drawn if V_t and the maximum amplitude of V_{com} are given. Fig.2.3 (c) gives possible V_S vector when V_t is known. When V_t is fixed or at its limit, V_{com} is an additional handle that can be used to shape the actual voltage applied to the machine terminal.

The relation between the three voltage vectors is simply:

$$\tilde{V}_t = \tilde{V}_S + \tilde{V}_{com} \qquad (2.1)$$

The compensation in the voltage mode assumes the compensation inverter is capably of supplying or sinking both real and reactive power.

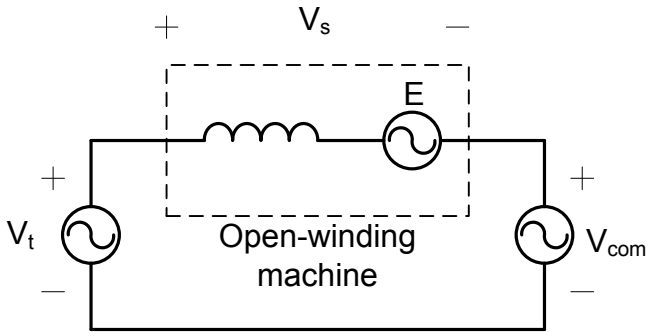

(a) Equivalent circuit type diagram

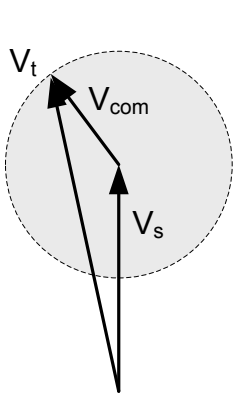

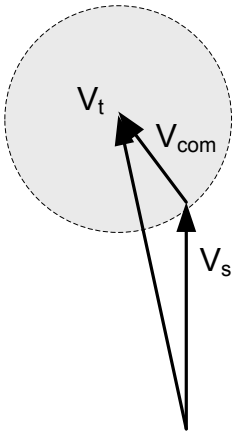

(b) Possible V_t vector given V_S (c) Possible V_S vector given V_t

Fig. 2.3 VSI series compensation concept, voltage mode

2.1.3. Power Mode

In stead of compensating for machine terminal voltage, the power in the machine can be addressed directly. This is a typical compensation method in the power grid application. In Fig. 2.3 (a), define the internal power factor angle δ as the angle from back-emf E to terminal voltage V_t. Assuming the compensation is purely reactive and ignoring the machine resistance, the current vector angle is always one half of internal

power factor angle. Therefore, the power of a non-salient machine can be calculated as:

$$P_S = \frac{V_t E}{X_S} sin(\delta) + \frac{V_t V_{com}}{X_S} cos(\frac{\delta}{2}) \quad (2.2)$$

From (2.2), the angle between terminal voltage and back-emf is near constant, the machine power is approximately in a linear relationship with the machine power at a given speed and terminal voltage. This result indicates that the machine power can be easily changed by using the compensation inverter to inject reactive power.

2.1.4. Impedance Mode

Fig.2.4 is the vector diagrams of four fundamental possible relationships between the applied compensation voltage and machine current vectors. I_S is the current vector in machine winding. The applied voltage is defined as compensation voltage V_{com}. The equivalent impedance of the VSI is of different forms in the four cases:

(a) When V_{com} is lagging the current by 90 degrees, the VSI is equivalently a capacitor;

(b) When V_{com} is leading the current by 90 degrees, the VSI is equivalently an inductor;

(c) When V_{com} is controlled to be in phase of the current, the VSI is equivalently a resistor. In this case, the VSI is sinking real power;

(d) When V_{com} is controlled to be 180 degree from the machine current, the VSI is equivalently a negative resistor. In this case, real power flows out of the DC link. It is similar to the rotor equivalent circuit of an induction machine, when the slip is negative.

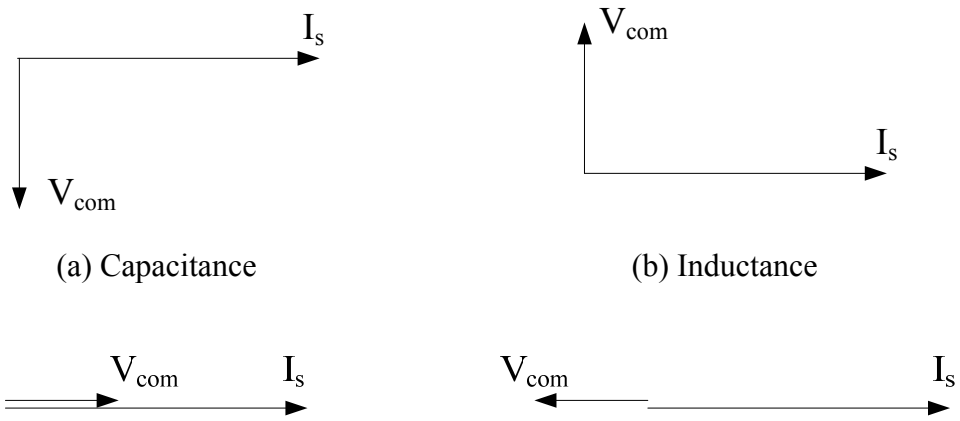

(a) Capacitance (b) Inductance

(c) Resistance (d) Negative resistance

Fig. 2.4 Variable impedance

In practice, the VSI can be controlled as complex impedance with both real and reactive parts. The voltage command can be directly calculated from desired compensation impedance and measured current as:

$$\tilde{V}_{com} = \tilde{Z}_{com}\tilde{I}_S = (r_{com} + jX_{com})\tilde{I}_S \quad (2.3)$$

Where

$\tilde{Z}_{com}$ is complex compensation impedance

r_{com} is real part of compensation impedance, reflecting real power flow

X_{com} is imaginary part of compensation impedance, reflecting reactive power flow

The equivalent impedance of the machine seen from the *abc* set of three-phase terminal can be changed by controlling the compensation inverter at different compensation impedances. However, the compensation voltage V_{com} is limited by the available voltage and the voltage rating of the inverter in practice. Therefore, the compensation impedance cannot remain constant when the voltage limit of compensation VSI is reached. The absolute value of compensation impedance is going to drop hyperbolically if current keeps increasing after the voltage limit of the inverter. Fig.2.5 illustrates the relationship between compensation voltage, impedance and

current.

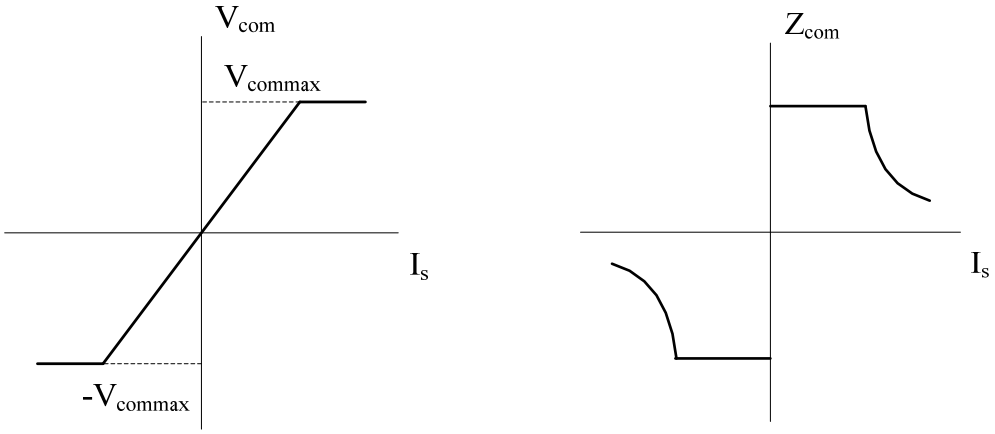

(a) Compensation voltage vs. current (b) Compensation impedance vs. current

Fig. 2.5 Compensation voltage command

In impedance mode, the d- and q-axis equivalent circuits of the machine are given in Fig.2.6. The 0-axis model is not drawn because there is no zero sequence current paths in a VSI compensated open-winding machine drive. The DC bus of compensation inverter is electrically isolated from the other three terminals of the machine. The machine and VSI together can be considered as a variable impedance machine.

Fig.2.7 shows an example for an open-winding IPM machine when compensation impedance is inductive and positively resistive. The machine resistance is ignored here for ease of analysis. V_S is machine voltage vector. V_t is terminal voltage of VSI compensated open-winding machine. X_d and X_q are machine's impedance in the d- and q-axis.

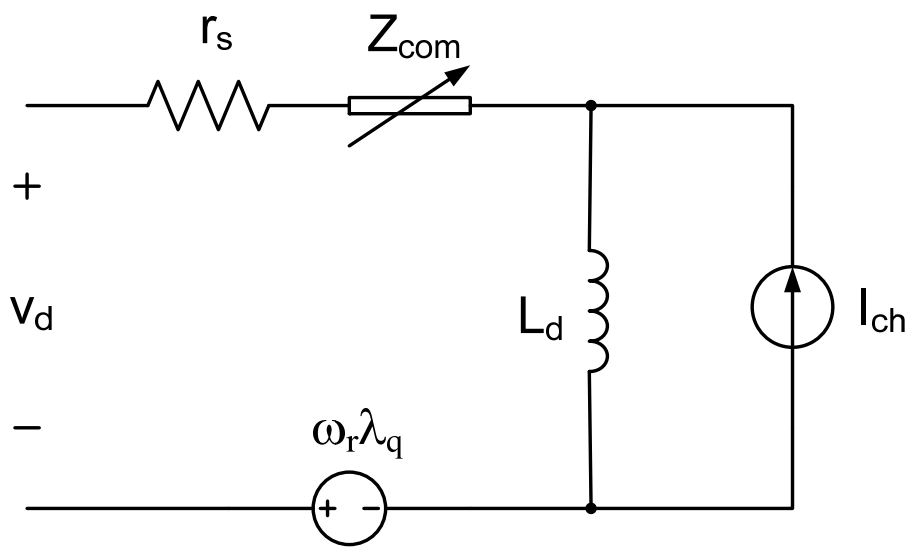

(a) d-axis voltage model with compensation

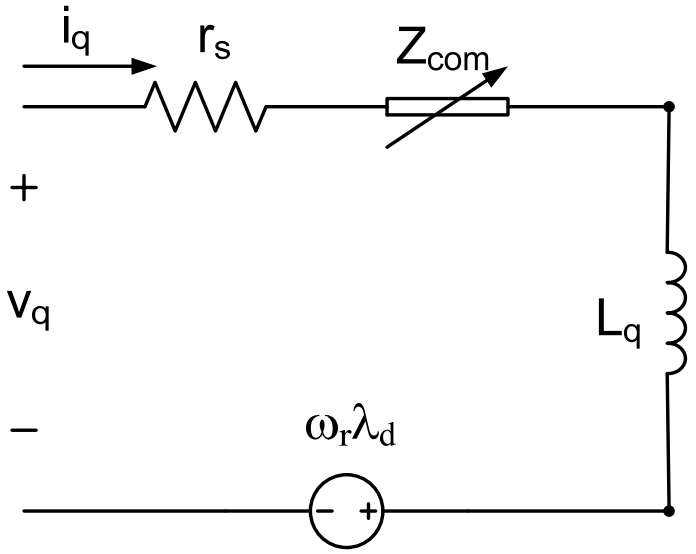

(b) q-axis voltage model with compensation

Fig. 2.6 VSI compensated open-winding PM machine equivalent circuit

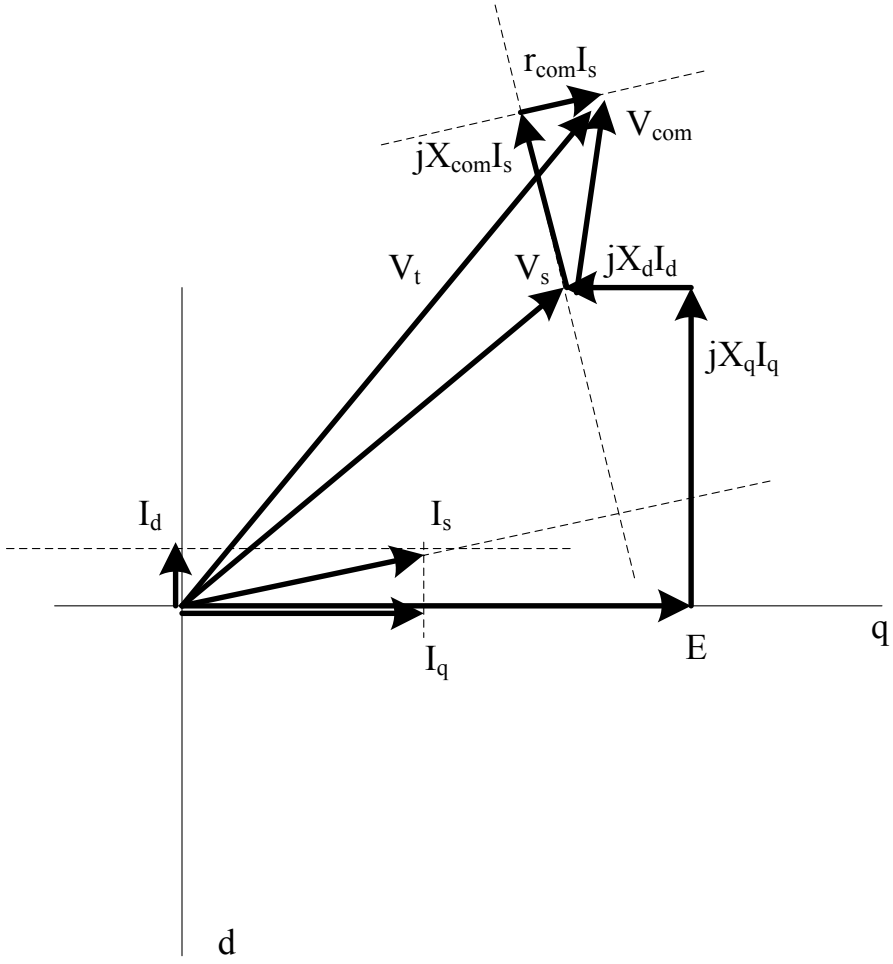

Fig. 2.7 Example of impedance mode compensation

2.1.5. Compensation with VSI and DC Capacitor

If only reactive power is required for compensation, a DC capacitor can be used at the DC bus of the compensation VSI. The circuit can be draw as shown in Fig. 2.8. To keep compensation DC bus voltage constant, V_{com} vector should always be in quadrature with machine current vector. In the impedance mode, the VSI now can be only controlled as either an inductor or a capacitor. It should be pointed out that the inverter has symmetric capability in inductive and capacitive compensation. Therefore, a 1 per unit VA inverter has a compensation range of 2 per unit var capability.

If compensation voltage V_{com} has a component in phase with the stator current,

compensation DC bus voltage will go higher. In contrast, a component that is 180 degrees out of phase with the stator current will decrease the compensation DC bus voltage. Therefore, by controlling the component of the injected voltage that is in phase with stator current, compensation DC bus voltage can be adjusted at will.

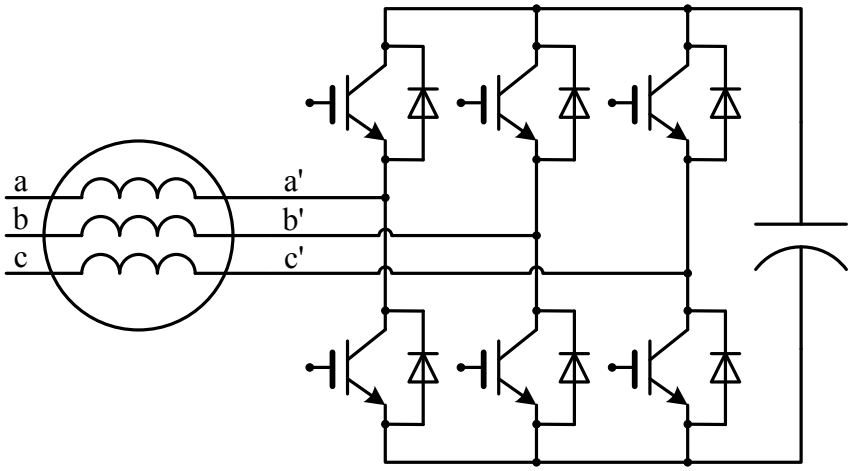

Fig. 2.8 VSI and DC capacitor compensation

2.2. Development of System Model

A dynamic model of the open-winding PM machine and inverter system is developed in this section for the study in later chapters.

2.2.1. Phase Voltage of Open-Winding Machine Drive

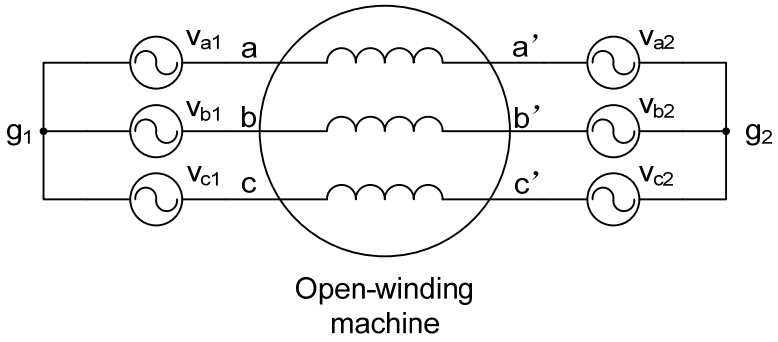

Fig. 2.9 Open-winding machine phase voltage

The instantaneous phase voltage of the open-winding machine drive has to be derived first for the study of VSI operation. Unlike a conventional three-phase Y-connected AC machine, an open-winding machine can be excited by two sets of three-phase voltages. Fig.2.9 shows an open-winding machine with two sets of excitation voltages. V_{x1} and V_{x2} are per phase excitation voltage ($x = a, b$ *or* c) of each set. Instantaneous and averaged machine excitation voltages are derived below. The machine phase voltage of open-winding topology can be calculated as:

$$v_a = v_{ag1} - v_{a'g2} + v_{g1} - v_{g2} \tag{2.4}$$

$$v_b = v_{bg1} - v_{b'g2} + v_{g1} - v_{g2} \tag{2.5}$$

$$v_c = v_{cg1} - v_{c'g2} + v_{g1} - v_{g2} \tag{2.6}$$

Here v_{g1} and v_{g2} are the ground point voltage of the two sets of excitation voltage with respect to arbitrary reference point. Also v_{ag1} is electrical potential between machine terminal a and point g_1 and $v_{a'g2}$ is electrical potential between machine terminal a' and g_2. If the ground point of the two sets of excitation voltage is connected, the machine phase voltage will simply be:

$$v_a = v_{ag1} - v_{a'g2} \tag{2.7}$$

$$v_b = v_{bg1} - v_{b'g2} \tag{2.8}$$

$$v_c = v_{cg1} - v_{c'g2} \tag{2.9}$$

However, when the two grounds are isolated, the phase voltage must be calculated differently. Assume the machine is symmetric:

$$v_a + v_b + v_c = 0 \tag{2.10}$$

Substitute (2.7)~(2.9) into (2.10), we have:

$$v_{g1} - v_{g2} = -\frac{1}{3}(v_{ag1} + v_{bg1} + v_{cg1} - v_{a'g2} - v_{b'g2} - v_{c'g2}) \tag{2.11}$$

Therefore, the instantaneous phase voltage can be calculated as:

$$v_a = \frac{2}{3}(v_{ag1} - v_{a'g2}) - \frac{1}{3}(v_{bg1} - v_{b'g2}) - \frac{1}{3}(v_{cg1} - v_{c'g2}) \tag{2.12}$$

$$v_b = \frac{2}{3}(v_{bg1} - v_{b'g2}) - \frac{1}{3}(v_{cg1} - v_{c'g2}) - \frac{1}{3}(v_{ag1} - v_{a'g2}) \tag{2.13}$$

$$v_c = \frac{2}{3}(v_{cg1} - v_{c'g2}) - \frac{1}{3}(v_{ag1} - v_{a'g2}) - \frac{1}{3}(v_{bg1} - v_{b'g2}) \tag{2.14}$$

When PWM inverters are used to drive an open-winding machine, the instantaneous phase voltage will be different for isolated DC bus and common DC bus configurations. For common DC bus open-winding drive, the phase voltage is a 3-level PWM waveform. The zero sequence impedance of AC machines are usually low, zero sequence voltage will result in large current in the machine windings since there is a low impedance zero sequence current path in common DC bus open-winding machine drives. When the two DC bus are isolated, the phase voltage of an open-winding machine drive will be the same as regular three-level inverter.

On average, each inverter must be balanced:

$$v_{ag1} + v_{bg1} + v_{cg1} = 0 \tag{2.15}$$

$$v_{a'g2} + v_{b'g2} + v_{c'g2} = 0 \tag{2.16}$$

The potential between two reference points is zero on average even when the two grounds are isolated:

$$v_{g1} - v_{g2} = -\frac{1}{3}(v_{ag1} + v_{bg1} + v_{cg1} - v_{a'g2} - v_{b'g2} - v_{c'g2}) = 0 \tag{2.17}$$

Average phase voltage model can be write as:

$$v_a = (v_{ag1} - v_{a'g2}) - \frac{1}{3}(v_{ag1} - v_{a'g2}) - \frac{1}{3}(v_{bg1} - v_{b'g2}) - \frac{1}{3}(v_{cg1} - v_{c'g2})$$

$$= v_{ag1} - v_{a'g2}$$

$$= v_{a1} - v_{a2} \quad (2.18)$$

$$v_b = v_{b1} - v_{b2} \quad (2.19)$$

$$v_c = v_{c1} - v_{c2} \quad (2.20)$$

In a synchronous dq0 reference frame:

$$v_d = \frac{2}{3}\left[v_a \sin(\theta_r) + v_b \sin(\theta_r - \frac{2}{3}\pi) + v_c \sin(\theta_r + \frac{2}{3}\pi)\right] \quad (2.21)$$

$$v_q = \frac{2}{3}\left[v_a \cos(\theta_r) + v_b \cos(\theta_r - \frac{2}{3}\pi) + v_c \cos(\theta_r + \frac{2}{3}\pi)\right] \quad (2.22)$$

$$v_0 = \frac{1}{3}[v_a + v_b + v_c] \quad (2.23)$$

Substitute (2.18)~(2.20) into (2.21)~(2.23):

$$v_d = \frac{2}{3}\left[(v_{a1} - v_{a2})\sin(\theta_r) + (v_{b1} - v_{b2})\sin(\theta_r - \frac{2}{3}\pi) + (v_{c1} - v_{c2})\sin(\theta_r + \frac{2}{3}\pi)\right] \quad (2.24)$$

$$v_q = \frac{2}{3}\left[(v_{a1} - v_{a2})\cos(\theta_r) + (v_{b1} - v_{b2})\cos(\theta_r - \frac{2}{3}\pi) + (v_{c1} - v_{c2})\cos(\theta_r + \frac{2}{3}\pi)\right] \quad (2.25)$$

$$v_0 = \frac{1}{3}[(v_{a1} - v_{a2}) + (v_{b1} - v_{b2}) + (v_{c1} - v_{c2})] \quad (2.26)$$

The dq0 voltage on the machine is equal to the vector sum of two sets of excitation voltage in dq0 frame:

$$v_d = v_{d1} - v_{d2} \quad (2.27)$$

$$v_q = v_{q1} - v_{q2} \quad (2.28)$$

$$v_0 = v_{01} - v_{02} \quad (2.29)$$

2.2.2. Open-Winding PM Machine Model

Synchronous machines are easier to model and control in a synchronous reference frame, where the machine currents are DC values in steady state. The reference frame

used has the d-axis aligned with the rotor flux and is often referred as the rotor reference frame. The angle used in reference transformation is the rotor position angle θ_r in elec rad/s. It is defined that $\theta_r = 0$ when the q-axis is aligned with phase *a*.

Conventional mathematical model of a PM machine in synchronous *dq0* reference frame is given below in (2.30) – (2.35). To keep it general, an IPM machine model is given. If an SPM machine is considered, the only change is to set d and q-axis inductance equal. The zero sequence model is added in addition to conventional Y-connected PM machine model.

$$v_d = (r_s + pL_d)i_d - \omega_r L_q i_q \tag{2.30}$$

$$v_q = (r_s + pL_q)i_q + \omega_r L_d i_d + \omega_r \lambda_m \tag{2.31}$$

$$v_0 = r_s i_0 + pL_{lk} i_0 \tag{2.32}$$

$$T_e = \frac{3P}{4}\left[\lambda_m i_q + (L_d - L_q) i_d i_q\right] \tag{2.33}$$

$$Jp\omega_{rm} = T_e - T_m \tag{2.34}$$

$$\omega_{rm} = \omega_r \frac{2}{P} \tag{2.35}$$

Where

p is the derivative operator with respect to time $\frac{d}{dt}$

r_s is the stator resistance

L_{lk} is the stator leakage inductance

L_d is the d-axis inductance including both d-axis magnetizing inductance L_{md} and stator leakage inductance L_{lk}

L_q is the q-axis inductance including both q-axis magnetizing inductance L_{mq} and stator leakage inductance L_{lk}

λ_m is the flux linkage due to permanent magnet

P is the number of poles

ω_{rm} is the shaft speed n mech rad/s

ω_r is the shaft speed in elec rad/s

Fig.2.10 is a block diagram of PM machine model in Laplace domain.

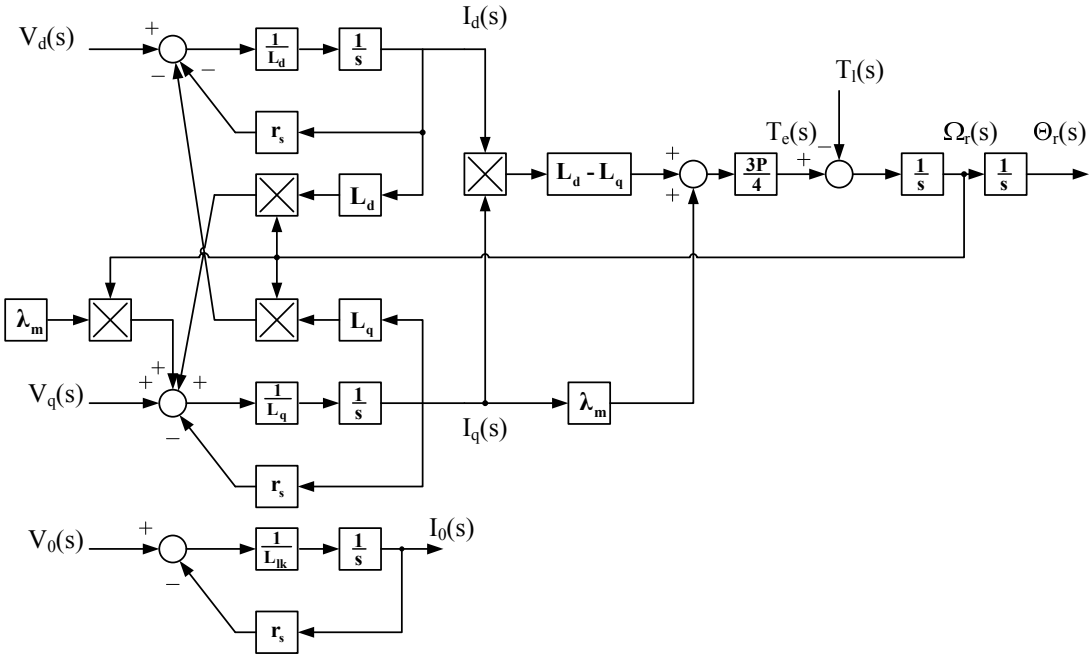

Fig. 2.10 PM machine model block diagram

The model presented above is an ideal machine model. Some limitations of the model are listed here. First, core losses are ignored in the model. Second, the machine parameters are constant. Saturation effect in the machine is not considered. Skin effect is ignored. The change of permanent magnet materials due to temperature change is ignored. Third, the mechanical model only includes the inertia. Mechanical losses due to friction and windage are ignored.

Characteristic current is defined as permanent magnet flux linkage over d-axis inductance. As will be discussed in later chapter, characteristic current is a very important parameter for PM machines.

$$I_{ch} = \frac{\lambda_m}{L_d} \tag{2.36}$$

Substitute characteristic current definition into (2.31), PM machine's electrical model can be rewritten as:

$$v_d = (r_s + pL_d)i_d - \omega_r L_q i_q \quad (2.37)$$

$$v_q = (r_s + pL_q)i_q + \omega_r L_d(i_d + I_{ch}) \quad (2.38)$$

$$v_0 = r_s i_0 + pL_{ls} i_0 \quad (2.39)$$

Define flux linkage in d and q-axis as:

$$\lambda_d = L_d i_d + \lambda_m \quad (2.40)$$

$$\lambda_q = L_q i_q \quad (2.41)$$

Machine equivalent circuit in dq0 reference frame can be drawn as in Fig.2.1.

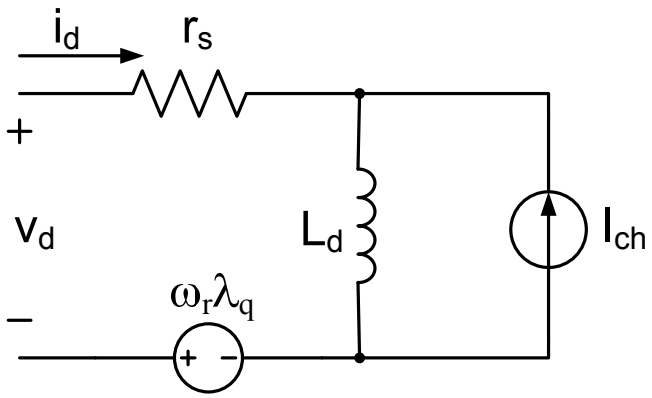

(a) d-axis voltage model

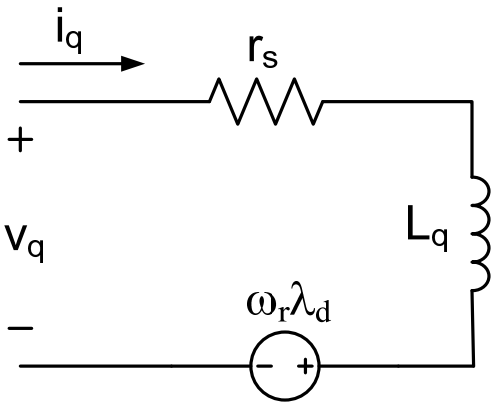

(b) q-axis voltage model

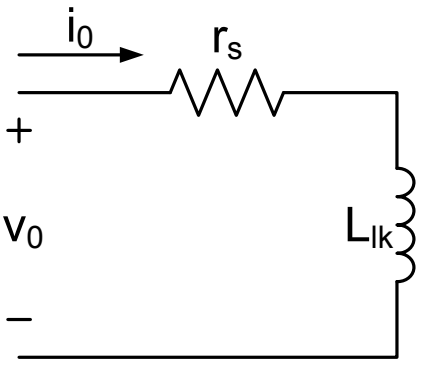

(c) 0-axis voltage model

Fig. 2.11 Equivalent circuit of PM machine

2.2.3. Inverter Model

This section gives the model of a dual VSI open-winding drive with single DC power supply. The topology is shown in Fig.2.12. The VSI compensated open-winding machine is driven by another VSI with a DC voltage source. Each inverter is a standard 2-level VSI. The power supply side VSI is denoted as INV1 and the compensation VSI is denoted as INV2.

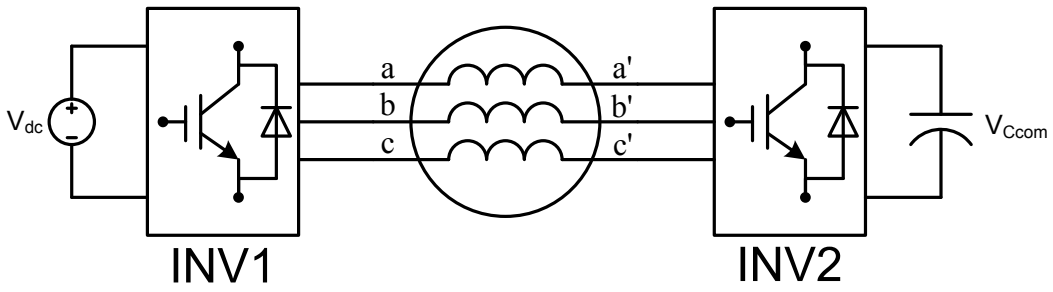

Fig. 2.12 Dual VSI open-winding drive with single power supply

In the stationary reference *abc* reference frame:

INV1:

$$v_{a1} = m_{a1} V_{dc} \quad (2.42)$$

$$v_{b1} = m_{b1} V_{dc} \quad (2.43)$$

$$v_{c1} = m_{c1} V_{dc} \quad (2.44)$$

INV2:

$$v_{a2} = m_{a2} v_{Ccom} \quad (2.45)$$

$$v_{b2} = m_{b2} v_{Ccom} \quad (2.46)$$

$$v_{c2} = m_{c2} v_{Ccom} \quad (2.47)$$

Where

m_{a1}, m_{b1}, m_{c1} are modulation functions of INV1 in the *abc* frame;

m_{a2}, m_{b2}, m_{c2} are modulation functions of INV2 in the *abc* frame;

Substitute in the reference frame transformation:

INV1:

$$v_{d1} = m_{d1} V_{dc} \tag{2.48}$$

$$v_{q1} = m_{q1} V_{dc} \tag{2.49}$$

INV2:

$$v_{d2} = m_{d2} v_{Ccom} \tag{2.50}$$

$$v_{q2} = m_{q2} v_{Ccom} \tag{2.51}$$

Because the two DC buses are isolated, there is no zero sequence current path in the drive system. Therefore, the zero sequence model of the machine is ignored in the transformation. The modulation function in the d-q plane is directly obtained from the *abc* frame modulation function using reference transformation equations.

DC current at each DC bus can be calculated from the machine current and modulation function by:

$$i_{dc} = m_{a1} i_a + m_{b1} i_b + m_{c1} i_c \tag{2.52}$$

$$i_{Ccom} = m_{a2} i_a + m_{b2} i_b + m_{c2} i_c \tag{2.53}$$

In the synchronous reference frame:

$$i_{dc} = \frac{3}{2}\left(m_{d1} i_d + m_{q1} i_q\right) \tag{2.54}$$

$$i_{Ccom} = \frac{3}{2}\left(m_{d2} i_d + m_{q2} i_q\right) \tag{2.55}$$

For the compensation DC capacitor:

$$C_{com}\, p v_{Ccom} = i_{Ccom} = \frac{3}{2}\left(m_{d1} i_d + m_{q1} i_q\right) \tag{2.56}$$

2.2.4. Overall Model

The block diagram of VSI compensated open-winding machine (machine and INV2 only) is shown in Fig.2.13. The whole block diagram of the dual inverter system is shown in Fig.2.14.

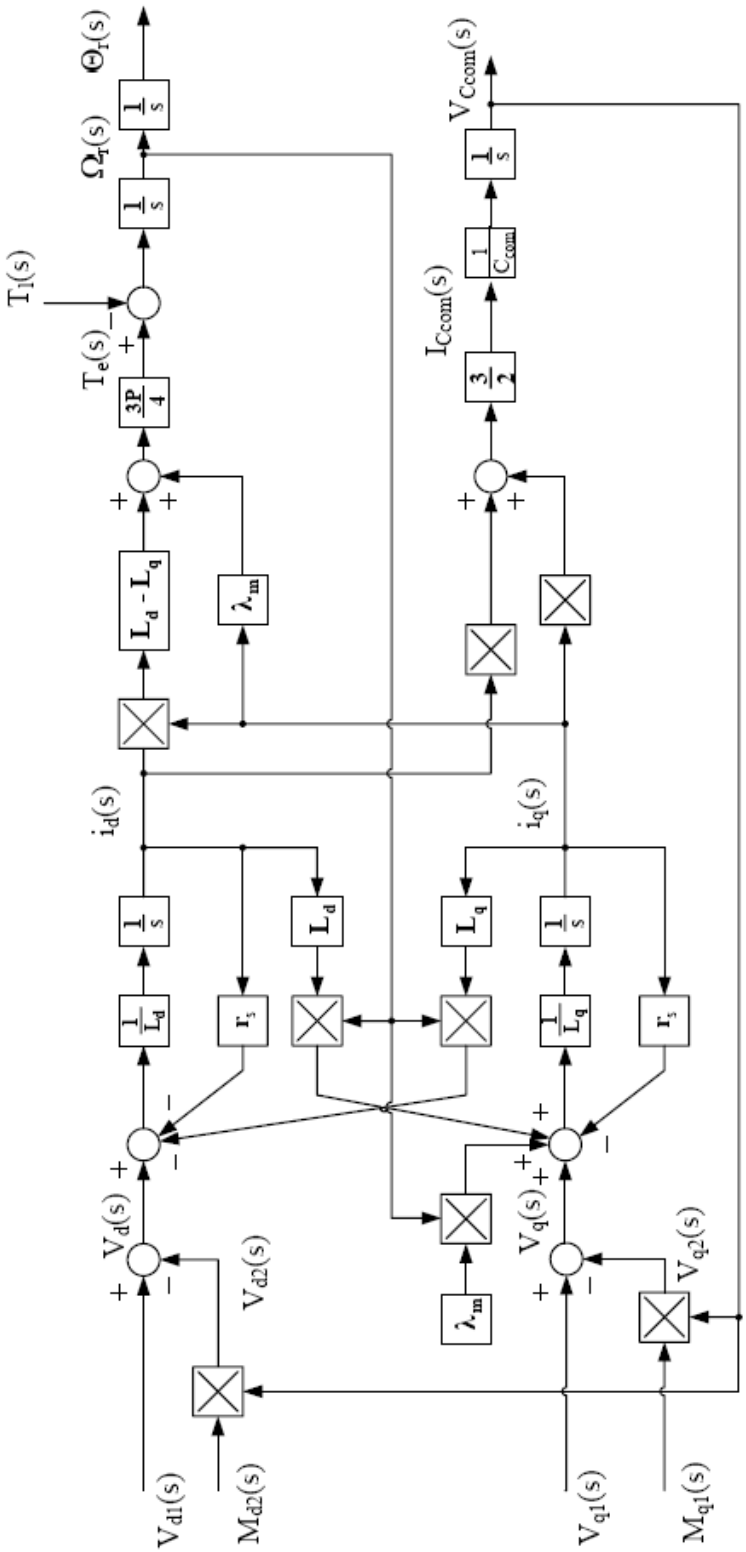

Fig. 2.13 Block diagram of an open-winding IPM machine model

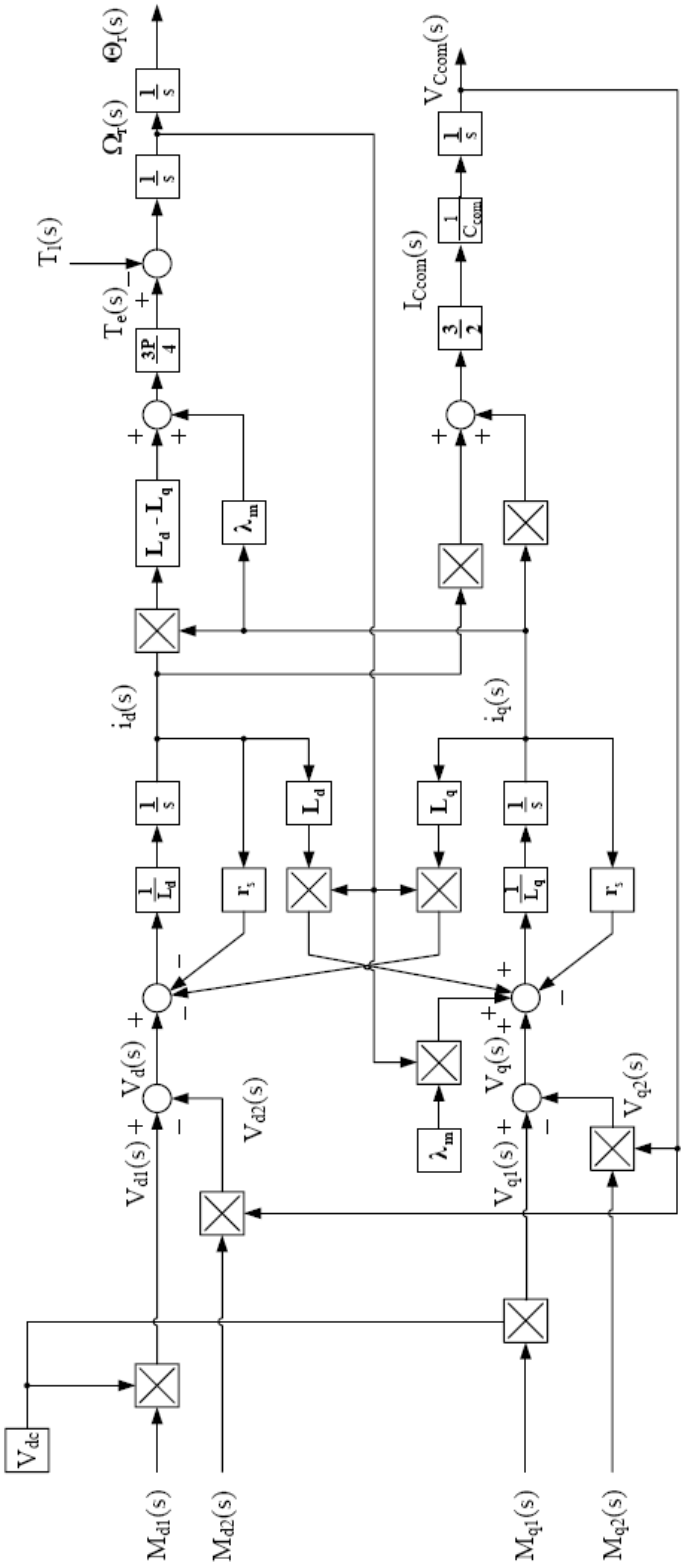

Fig. 2.14 Dual inverter open-winding IPM machine drive with single power supply block diagram

2.3. Summary

The concept of series compensation of PM machines by using open-winding configuration that will be used through out this work was presented in this chapter. Three different operating modes were introduced. An ideal system model was developed for the study in the later chapters.

Chapter 3

Extending the Operating Region of an Open-Winding PM Motor by Series Compensation

3.1. Introduction

Permanent magnet synchronous machines (PMSM) are being adopted in many applications. They are very popular in the fields like servo drives and traction drives due to their high efficiency and torque density. There are two major types of PM machines, surface permanent magnet (SPM) machines and interior or buried permanent magnet (IPM) machines, categorized by how the magnets are mounted on the rotor. Often, SPM machines have equal inductance in the direct and quadrature axis while most IPM machines show a saliency ratio in the two inductances.

The wide application of PM motors is also indebted to the advance of power electronics inverters. Most PM machines are equipped with an electronic drive for operation due to their intrinsic property. Below the base speed, PM machines are usually controlled to follow its maximum torque per ampere (MTPA) curve in order to minimize the copper losses inside the motor. The MTPA curve of a SPM motor is simply the q-axis. To utilize the reluctance torque, the motor current must be leading the back-emf on MTPA curve (negative i_d) for most IPM machines [76,77].

Above the base speed, flux weakening algorithms are often needed to prevent the current regulator from saturation due to the increased back-emf. Traditionally, IPM motors are more preferable for flux weakening operation. Schiferl and Lipo

investigated the effect of inverter capability and machine parameters on power capability of IPM motors [78]. Jahns proposed a method to identify the onset of current regulator saturation and modify current command vector in the flux weakening region of IPM machines [79]. Various alternative flux weakening methods are proposed by other authors as well. Morimoto and et al. further divided the operation region of IPM drives into three regions. High performance current regulator with decoupling was also proposed by the authors [80,81]. Kim and Sul proposed to directly use the voltage command to identify the onset of current regulator saturation in order to reduce the machine parameter dependency [82]. In summary, there are two basic types of flux weakening control strategy, feedforward style and feedback style. The feedforward style uses the machine parameters to calculate the current command based on voltage and current limits. The implementation of this method is easy and straightforward. Also, the transient performance is superior. The feedback approach uses the output of the current regulator (voltage commands) as a feedback to modify the current vector command. The feedback approach for the flux weakening controller is less sensitive to machine parameters accuracy. However, the dynamic performance of the feedback style flux weakening is not as good as the feedforward style.

SPM motors are traditionally not considered as good candidates for flux weakening operation due to their low inductance [83]. External inductor can be connected in series with the motor to extend the flux weakening region of an SPM motor drive. An alternative is to properly design the machine therefore it has increased leakage inductance [84]. Lawler and et al. proposed a dual-mode inverter control method, employing back-to-back thyristors in series with the VSI to extend the constant power speed range [85]. EL-Refaie and et al. showed that the series back-to-back thyristors were fundamentally equivalent to inductance while also introducing significant current harmonic distortion [86].

In this chapter, a VSI is used to mimic the inductors in series with the motor to

expand the operating space of an IPM motor in the flux weakening region. In this case the harmonic distortion is minimal. A new open-winding motor drive configuration and its control method are proposed. As shown in Fig. 3.1, INV1 is connected to a DC voltage source and INV2 is connected to a floating capacitor. The floating capacitor will charge from the main DC bus when needed. There is no extra pre-charge circuit or procedure required. The floating capacitor voltage can be controlled to be either higher or lower than the source voltage by INV2. This configuration can also be considered as a special condition in the conventional isolated dual inverter open-winding motor drive when one of the power sources is not able to deliver real power to the motor. When INV2 is controlled as a compensation device, the function of INV2 is similar to that of the SSSC used in FACTS (Flexible AC Transmission Systems) [51]. It is used to provide reactive power to the motor and to change the equivalent impedance seen by INV1. As will be shown in the later sections, by providing reactive power to the motor from INV2, the power capability of the motor can be considerably improved at high speed. When powered from the same supply voltage, the drive will be able to operate the motor under study at a higher maximum speed. The size of the inverter and the applicability of the proposed system to other motors will be discussed as well.

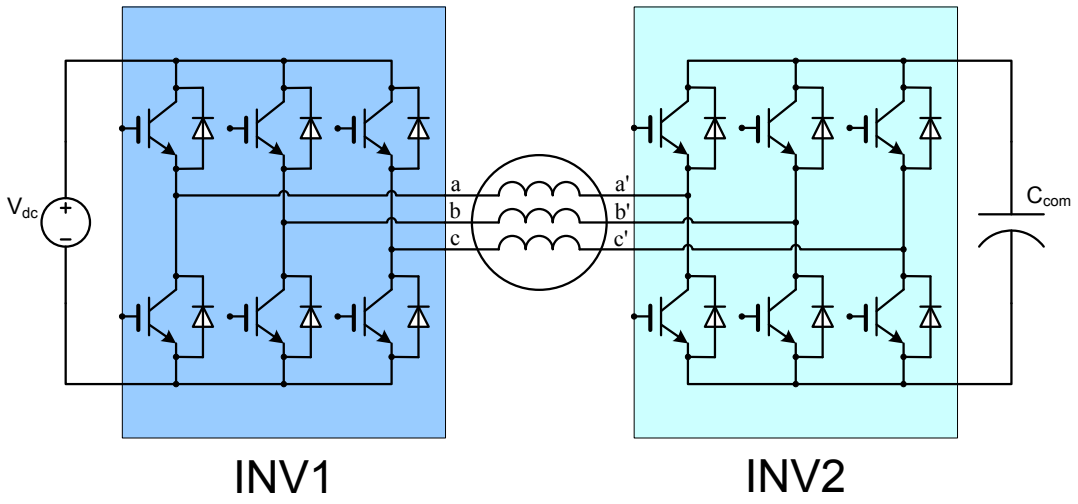

Fig. 3.1 Series Compensated open-winding PM machine drive

3.2. Operating Principle

Field oriented controllers (FOC) are widely used in PMSM drives. In this control algorithm, the three-phase current is transformed into the rotor reference frame. Two orthogonal components i_d and i_q are separately controlled by two current regulators. Below the base speed, the motor is generally controlled to follow the MTPA curve to minimize the copper losses in the motor. For a given current amplitude I_S, neglecting resistance, the MTPA condition can be obtained by using (3.1~3.3) below.

$$\beta = asin\left(\frac{\lambda_m - \sqrt{8I_S^2(L_d - L_q)^2 + \lambda_m^2}}{4I_S(L_d - L_q)}\right) \tag{3.1}$$

$$i_d = -I_S sin(\beta) \tag{3.2}$$

$$i_q = I_S cos(\beta) \tag{3.3}$$

The internal power factor angle β in the equations above is defined the angle from q-axis to the current vector as shown in Fig. 9.

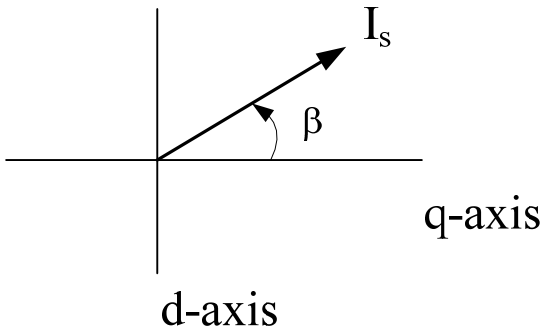

Fig. 3.2 Internal power factor angle

The terminal voltage of the motor can be calculated using the mathematical model of the motor presented in Chapter 2. The base speed is defined as the speed at which the terminal voltage of the motor equals to the maximum available voltage from the inverter under MTPA operation.

Above the base speed, flux weakening algorithms are used to prevent the current regulator from saturation due to the increased back-emf. The motor is operated within the current and voltage limits of the drive. The current and voltage limits of an ideal lossless machine can be expressed as:

$$I_{max}^2 = i_d^2 + i_q^2 \tag{3.4}$$

$$V_{max}^2 = (-\omega_r L_d i_d)^2 + (\omega_r L_q i_q + \omega_r \lambda_m)^2 \tag{3.5}$$

On the plane of rotor reference frame current vector, the current limit is a circle and the voltage limit is a set of ellipses that shrink as the speed increases. Each ellipse corresponds to the voltage limit at a certain speed. The center of the voltage limits ellipsis is located on the negative d-axis. The distance from the center to the origin of the plane is equal to the characteristic current which is defined as:

$$I_{ch} = \frac{\lambda_m}{L_d} \tag{3.6}$$

An example of the current limit circle and voltage limit ellipsis is shown in Fig. 3.3. The parameters used are from a lab scale IPMSM.

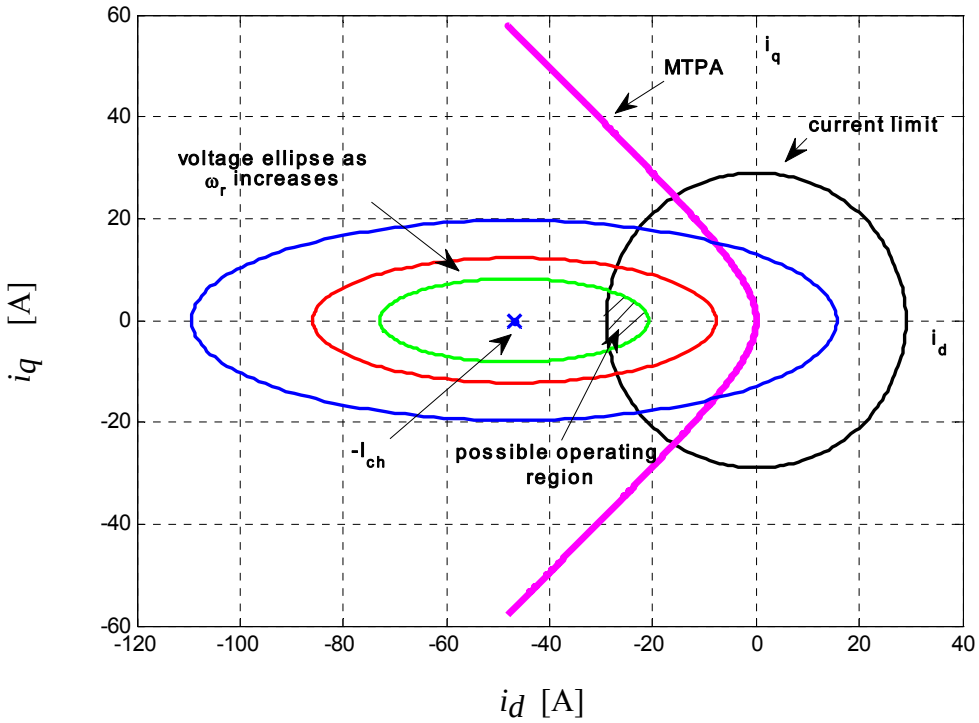

Fig. 3.3 IPM operating limit on d-q current plane

The characteristic current I_{ch} is a very important parameter in determining the power capability of a PM machine in flux weakening operation. There are three distinct cases of the power capability of PM motors in flux weakening region differentiated by the relationship between characteristic current I_{ch} and rated current I_r.

(1) $I_{ch} > I_r$: PM machine has a finite maximum speed limit;

(2) $I_{ch} = I_r$: the constant power region of PM machine is theoretically infinite;

(3) $I_{ch} < I_r$: PM machine is able to deliver reduced power at high speed, but there is no maximum speed limit.

In the proposed system, INV2 can be controlled as a three-phase inductor in series with the motor to extend the CPSR of the motor beyond base speed. Assuming pure inductive compensation is used, the equivalent impedance seen by INV1 is changed. The voltage limit equation can be modified to the form:

$$\left(i_d + \frac{\lambda_m}{L_d + L_{com}}\right)^2 + \left(\frac{L_q + L_{com}}{L_d + L_{com}}\right)^2 i_q^2 = \frac{V_{max}^2}{(L_d+L_{com})^2 \omega_r^2} \frac{1}{} \tag{3.7}$$

On the rotor dq current vector plane, the center of the voltage limit ellipsis is moved towards the origin with inductive compensation. The shapes of the ellipses change slightly as well due to the change of the virtual saliency ratio. Ideally, the optimal compensation inductance for infinite CPSR will result in the center of the voltage limit eclipses located on the edge of the current limit circle. The optimal compensation inductance is calculated via

$$L_{opt} = \frac{\lambda_m}{I_r} - L_d \tag{3.8}$$

The modified voltage limit eclipses (solid) are shown in Fig. 11 with the original voltage limit ellipsis (dotted) and the current limit circle. The easiest method to control INV2 will be directly emulating a three-phase inductor by injecting a voltage vector that is leading the machine current vector by 90 degrees.

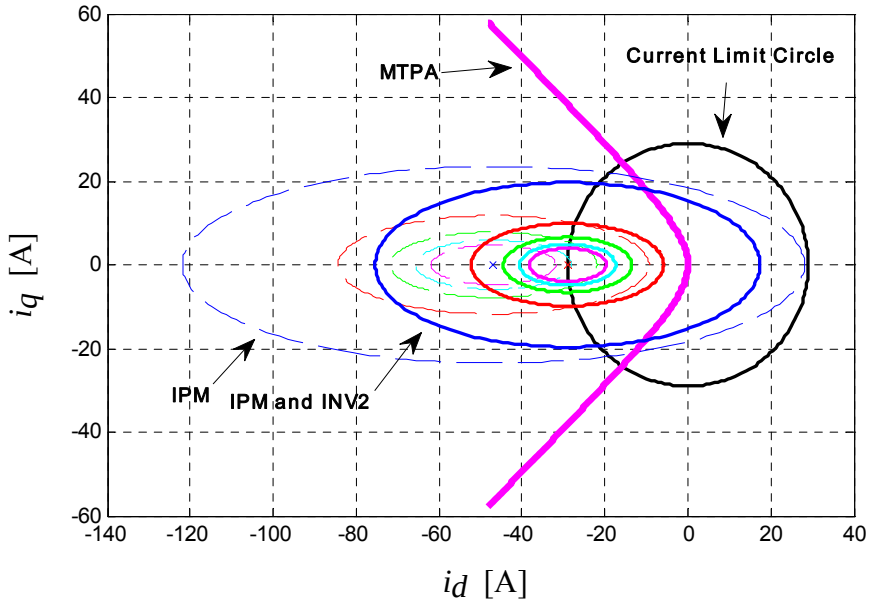

Fig. 3.4 IPM capability curve with compensation

Figs. 3.5 and 3.6 show the torque-speed and power-speed curves under different

compensation inductances. As the compensation inductance varies, the torque-speed curve and power-speed curve will change accordingly. By purely inductive compensation, the ideal CPSR of an open-winding motor drive could be extended to infinity ignoring the voltage limit of INV2. Moreover, the power capability can be improved considerably at high speed. However, if a fixed value, the added inductance would initiate the flux weakening at a lower speed resulting in reduced power capability of the drive around the corner speed. Unlike physical inductors, INV2 can be controlled to be a variable inductance or even be capacitive when needed. By varying the compensation impedance, the drive will be able to operate the motor within the envelope of all power-speed curves shown in Fig. 3.6.

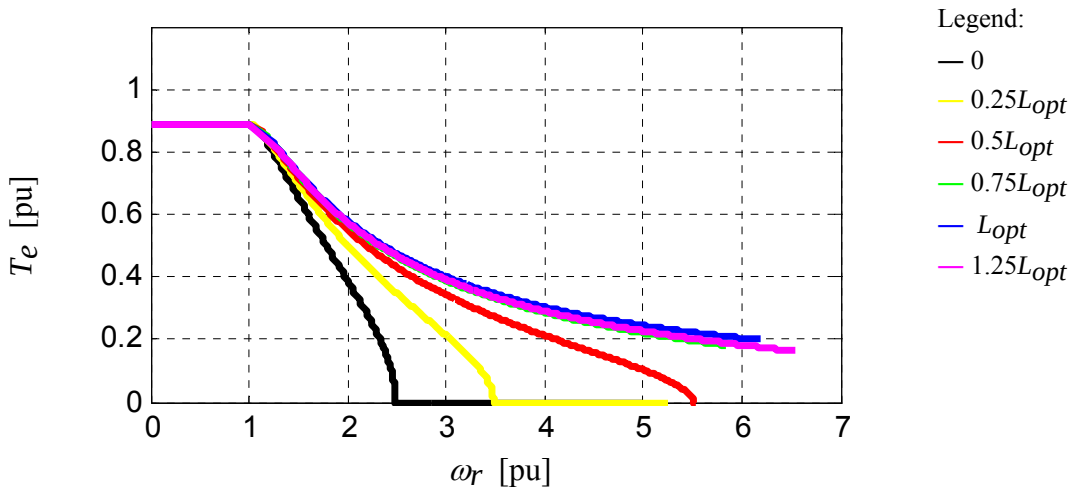

Fig. 3.5 Power- speed curve with different compensation inductances

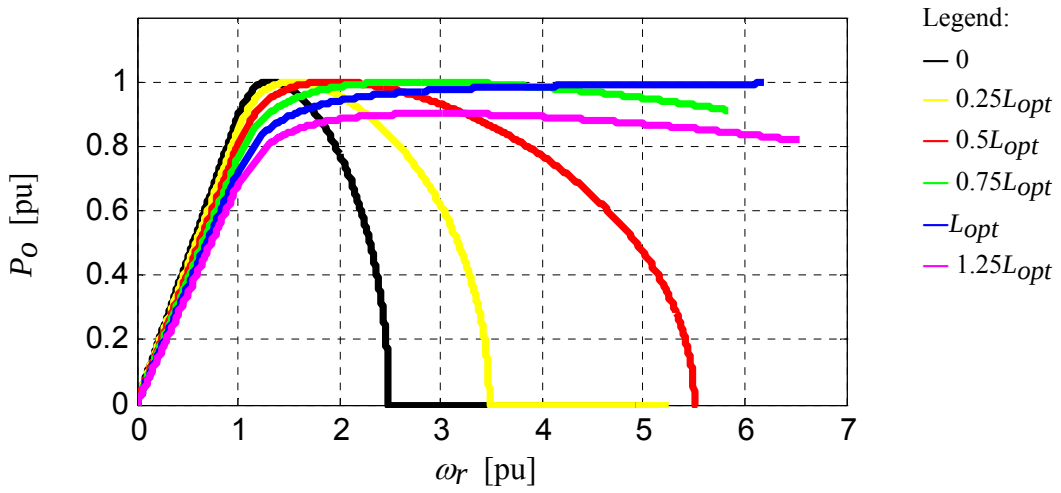

Fig. 3.6 Torque-speed curve with different compensation inductances

3.3. Inverter Sizing Consideration

3.3.1. Reactive Power Requirement

In the proposed system, INV2 only supplies reactive power to the motor. Therefore, the amount of reactive power required by the motor determines the size of INV2. In general, PM motors have very good power factor. However, depending on the specific machine parameters and ratings, the power factor of a PM motor could become worse at certain operating conditions. Ignoring the losses in the machine, the power factor is only determined by the current vector. The power factor of an ideal lossless machine can be calculated as:

$$pf = \frac{\lambda_m cos(\beta) - \frac{1}{2} I_s^2 sin(2\beta)(L_d - L_q)}{\sqrt{(L_q I_s cos(\beta))^2 + (L_d I_s sin(\beta) + \lambda_m)^2}} \tag{3.9}$$

The power factor contour for the motor under study is plotted in Fig. 3.7 with the MTPA curve. It can be seen that the power factor is around 0.8 at the intersection of MTPA curve and current limit circle. As the current vector swings towards the negative d-axis on the current limit circle, the power factor initially increases. However, it starts to decrease rapidly as the vector gets close to the d-axis.

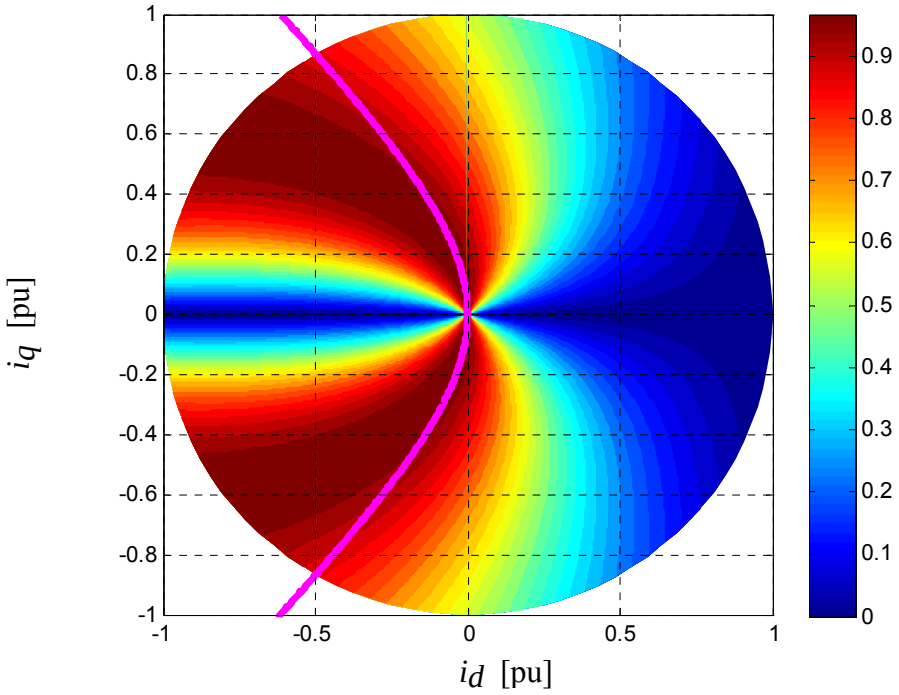

Fig. 3.7 Power factor contour of a lab scale IPM motor

The real and imaginary components of the motor under study are compared in Fig. 3.8. The imaginary component goes from positive to negative as the current vector swings towards the negative d-axis. It indicates the power factor of the motor changes from lagging to leading. This is expected because the characteristic current of the motor is relatively high. A similar phenomenon can be observed if the motor is replaced by an over excited wound field synchronous motor.

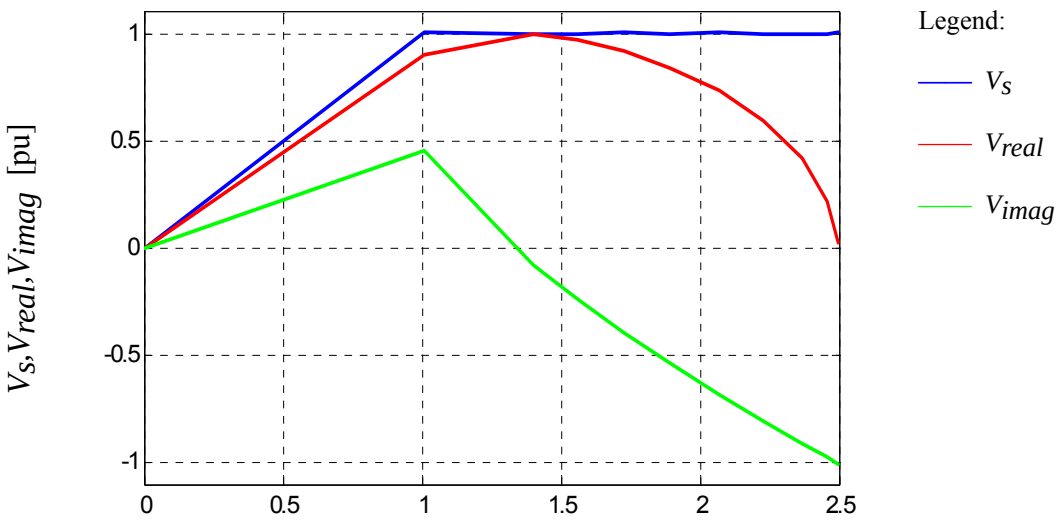

Fig. 3.8 Voltage real and imaginary components

The reactive power required by the machine as a function of torque and speed under MTPA and flux weakening operation is shown in Fig. 3.9 and 3.10. It can be concluded that reactive compensation will be able to improve the power capability of the motor around the corner speed and at high speed when there is significant amount of var required by the motor.

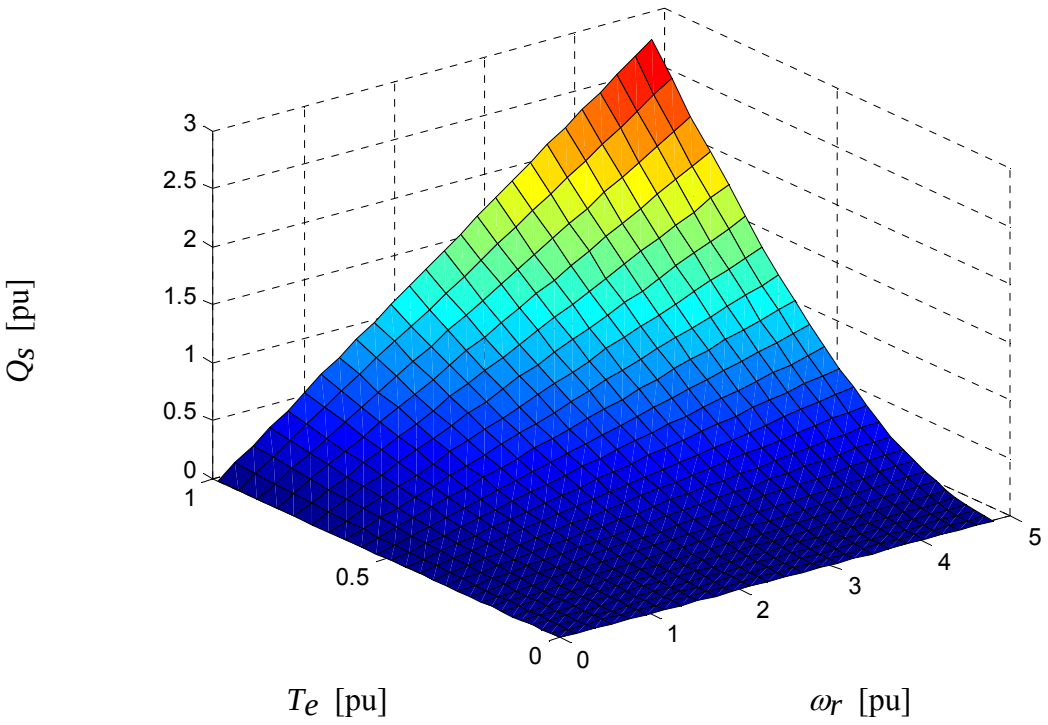

Fig. 3.9 Reactive Power Requirement under MTPA operation

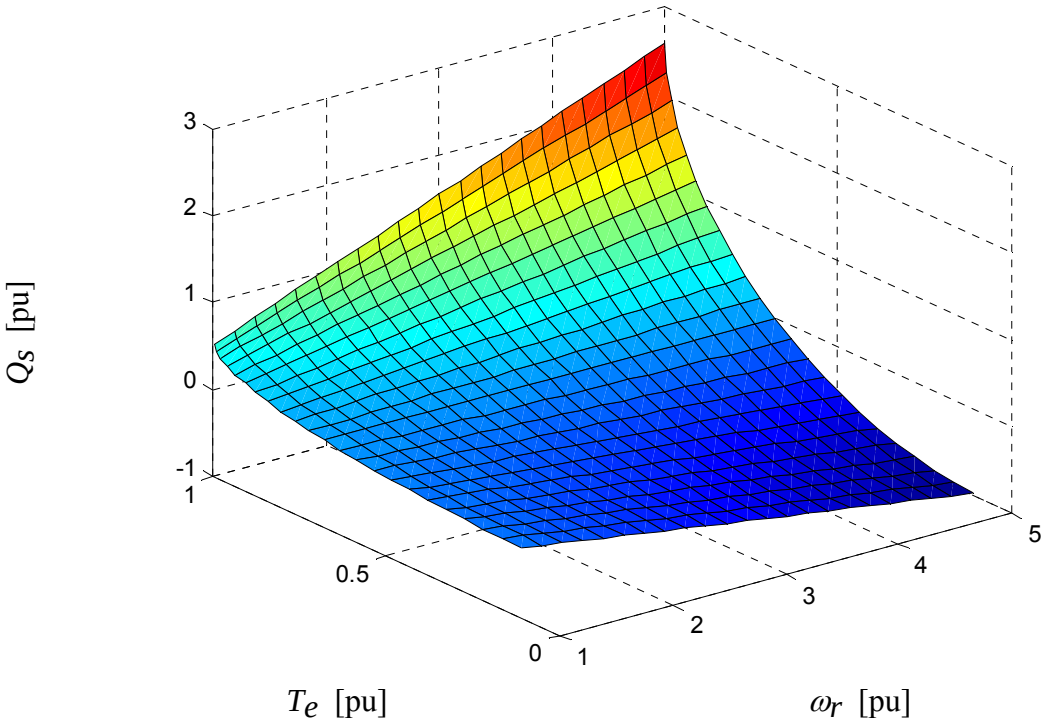

Fig. 3.10 Reactive Power Requirement in flux weakening operation

3.3.2. Power and Torque Capability with Finite Compensation Voltage Limit

Conceptually, the CPSR of a PM motor with large characteristic current would become infinite when INV2 is controlled as inductors in series. In practice however, INV2 would reach its voltage limit as the speed of the rotor increases. Since INV2 is connected in series with the motor, the current rating has to be the same as the main inverter. Nevertheless, the voltage rating of INV2 can be sized differently according to the requirements of applications. Comparisons of the power-speed curves and torque-speed curves when INV2 voltage rating is sized differently are shown in Fig. 3.11 and 3.12. It can be seen that even a small size INV2 will be able to improve the power capability at high speed considerably.

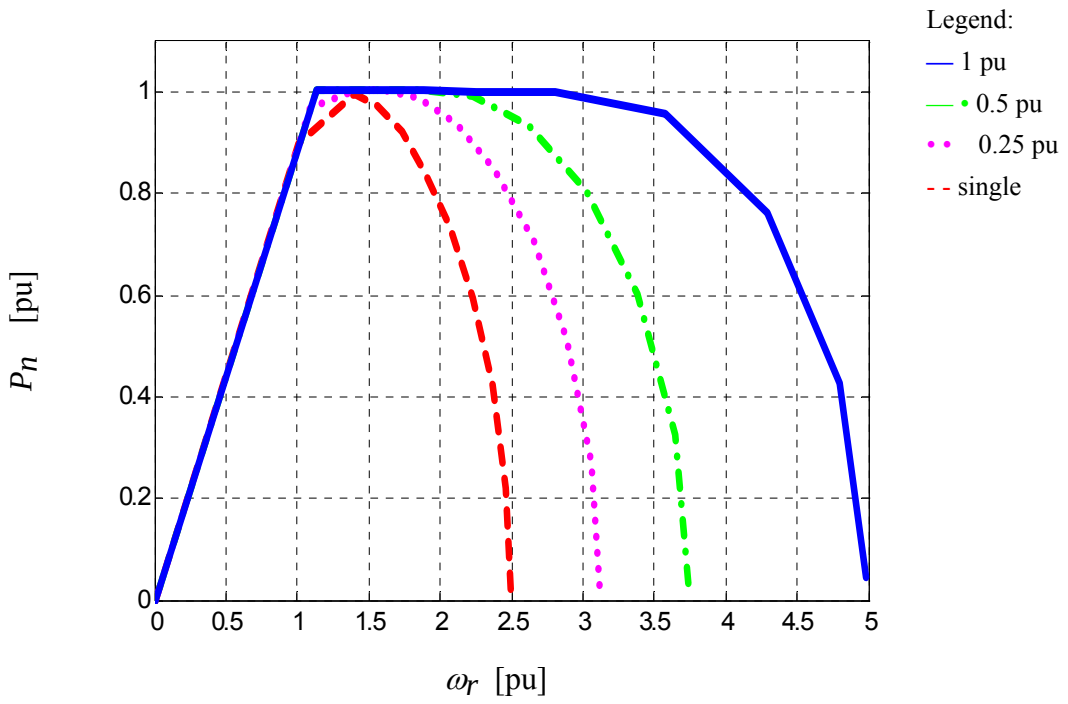

Fig. 3.11 Power-speed curves for different INV2 voltage rating

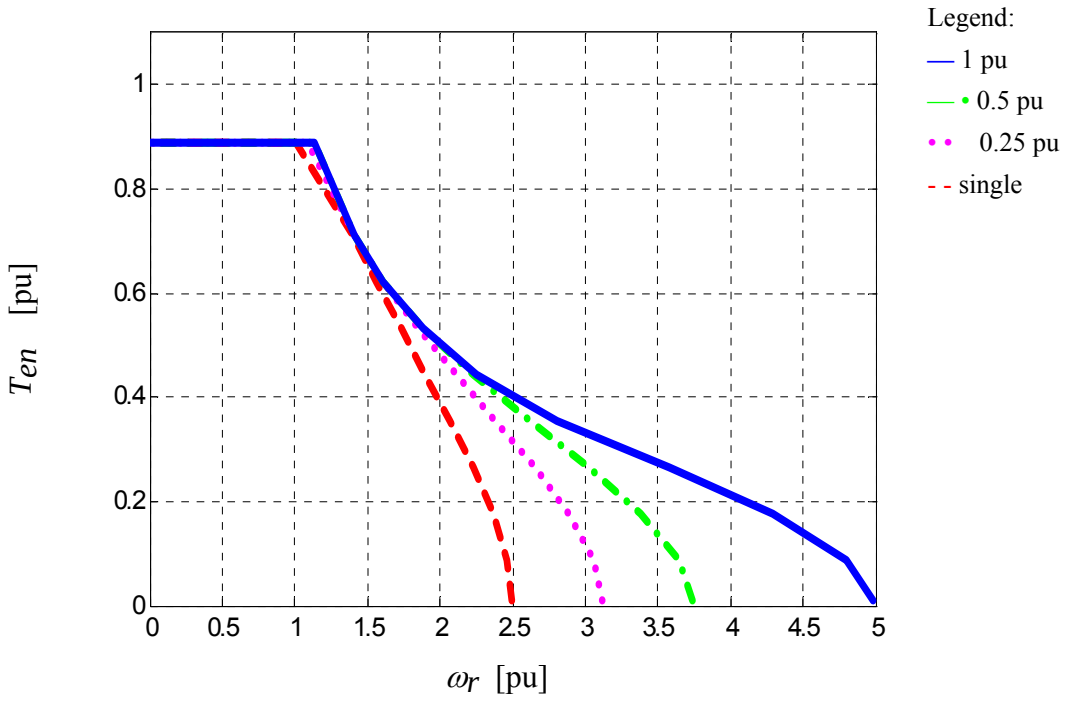

Fig. 3.12 Torque-speed curves for different INV2 voltage rating

3.3.3. Size of Floating Capacitor

The size of the floating capacitor is another important factor when considering the overall cost of the proposed system. Like in most switching converters, the capacitance can be determined by the desired voltage ripple, peak motor current and capacitor parameters like capacitance and equivalent series resistance (ESR). In practice, the ripple current rms value may play a more important role in sizing the floating capacitor. Simulation can be carried out to determine the ripple current rms value and the results can be used to predict the life time of the capacitor. The capacitor can be selected according to the requirement of the applications.

3.3.4. Comparison with Other Topologies

It has been shown that the proposed dual inverter open-winding motor drive is capable of expanding the operating space of PM motors for a given source voltage.

However, the number of power electronics switches doubles in this drive topology compared to a conventional 2-level inverter, which will lead to significant cost increase. If the source voltage can be raised when the motor needs higher voltage to operate at higher speed, the proposed open-winding drive will have few major benefits over a single inverter drive. When the source voltage is fixed, a more conventional method is to use a bidirectional DC/DC boost converter to raise the DC bus voltage for the inverter as shown in Fig. 3.13.

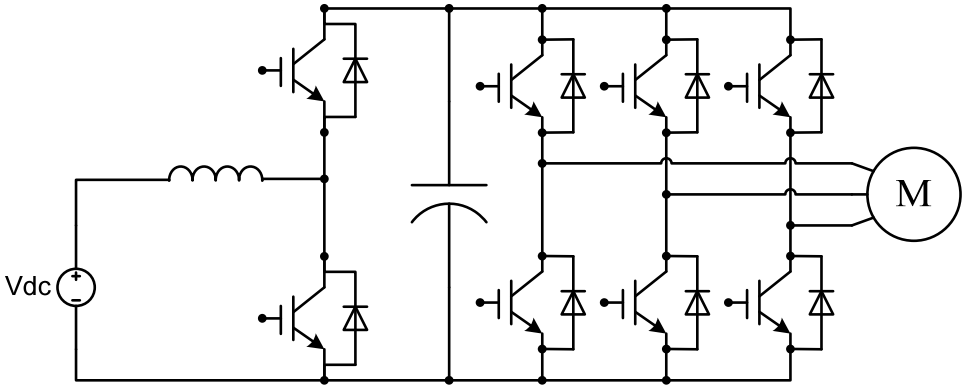

Fig. 3.13 Single inverter with a DC/DC boost converter for higher available voltage

To evaluate the advantages and disadvantages of the proposed topology, it is compared with three more conventional drive topologies. The maximum speed is assumed to be twice of the original motor drive in the comparison. The comparison includes:

Drv1: Proposed series compensated open-winding PM motor drive

Drv2: Open-winding PM motor drive with two isolated voltage sources

Drv3: 2-level inverter drive with a DC/DC boost converter

Drv4: 2-level inverter drive with doubled supply voltage

To allow the same peak voltage amplitude to be applied to the motor terminals, the rating of INV2 in the open-winding dual inverter drive is set equal to the rating of INV1. The boost ratio of the DC/DC converter is set to 2.

First, the torque-speed curves of four drives are compared in Fig. 3.14. For comparison, the green curve represents a 2-level inverter directly powered from a 1 per unit voltage power supply. With a DC/DC boost converter added to the system, the motor will not only be able to operate at a higher maximum speed, the real power capability is improved as well. It can be seen from Fig. 3.15 that all four drives have the same improvement in the maximum speed limit. However, the boost converter topology is able to deliver full torque at 2 per unit rotor speed. The CPSR of the drive is the same as the single inverter drive, but the corner speed is postponed to 2 per unit speed with the DC/DC boost converter. It is worth to note that if two isolated power supplies are available, the dual inverter open-winding drive would have the same power and torque capability as the boost converter topology. For the proposed topology with a floating capacitor connected to INV2, the improvement of torque capability around corner speed is not very apparent for the machine under study because it has a high power factor at this operating point. After all, INV2 is only able to provide reactive power to the motor. However, as the speed increases and the motor goes into flux weakening region, the torque capability can be improved considerably compared to the single inverter drive power from 1 per unit voltage power supply. The CPSR of the drive is increased compared to the single inverter drive.

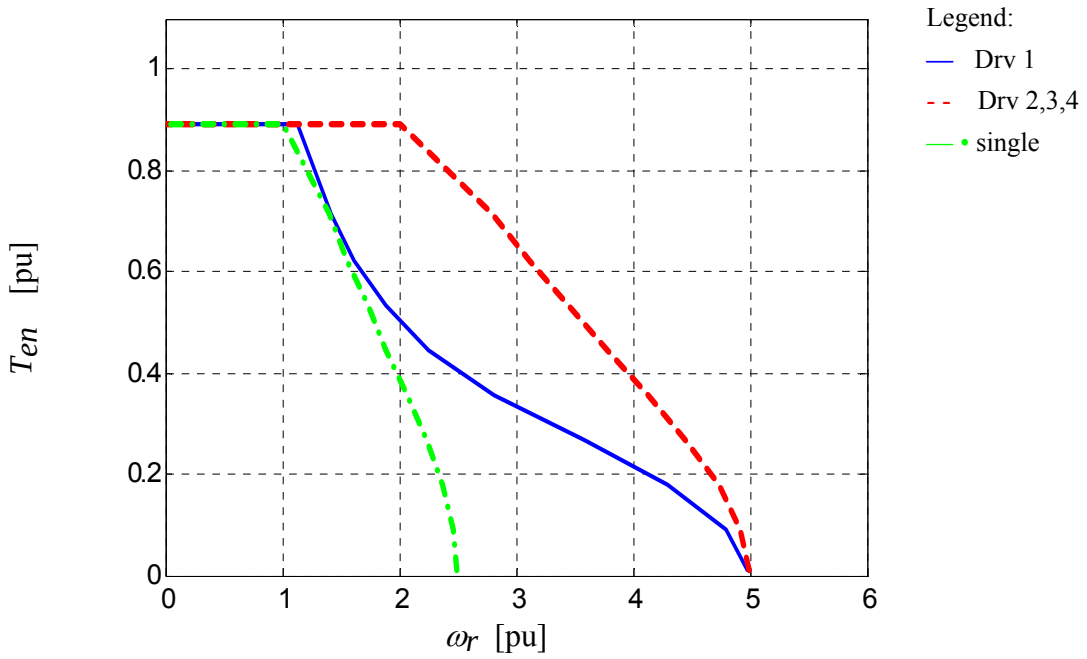

Fig. 3.14 Torque-speed curves comparison of different drives

The benefits of adding a DC/DC boost converter are apparent. The torque capability is greatly enhanced and only two extra power electronics devices are used. However, the total rating of the power electronics switches is higher than that of the proposed open-winding dual inverter drive. The voltage rating of the inverter itself is doubled when the DC bus voltage doubles. The same voltage rating is required for the power electronics switches in the DC/DC boost converter. Meanwhile, the switches in the boost converter have to be sized according to the low voltage side high current. The total active power switch rating will exceed the active power switch rating of the proposed dual inverter open-winding drive.

Another comparison is carried out when the maximum speed requirement varies. The total converter active switch ratings of the four drive topologies at different required maximum speed are compared in Fig. 3.15. In can be concluded the total active converter rating difference between the topology using DC/DC boost converter and other topologies will be more significant as the required maximum speed goes up. The increased boost ratio of DC/DC converter is the major factor leading to this result.

Although Drv2 and Drv4 have the same power capability as Drv3, there is no extra DC/DC converter required. As a result, the total active power electronics device rating will be much lower.

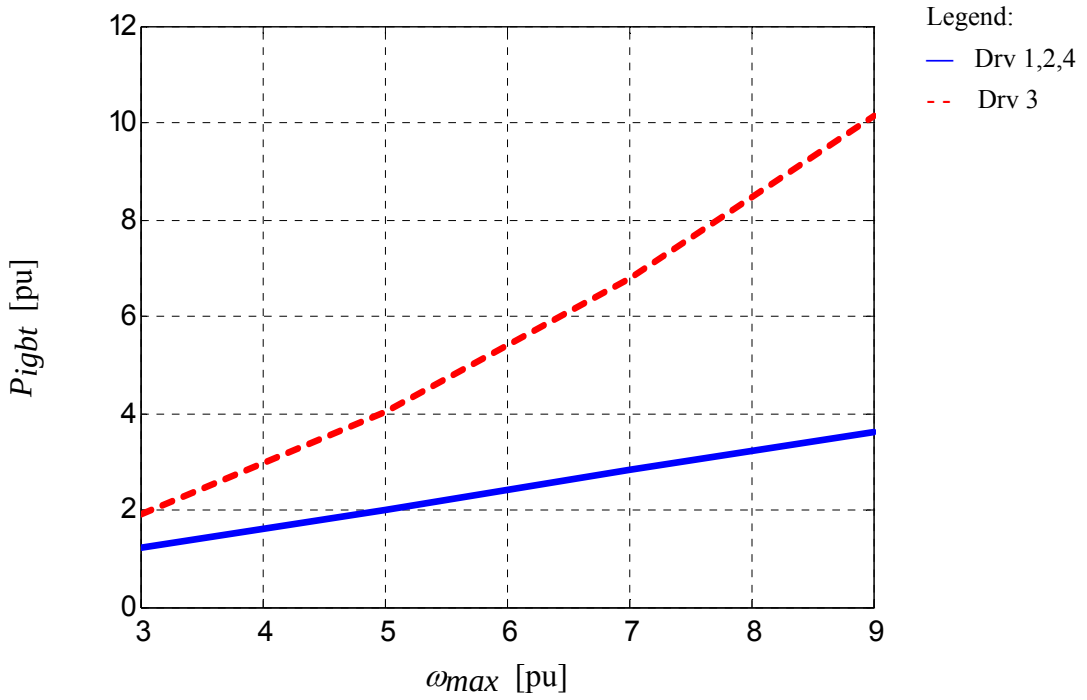

Fig. 3.15 IGBT total rating comparison between the proposed open-winding dual inverter drive and single inverter with DC/DC boost converter

Compared with Drv4, the most apparent advantage of Drv2 is the capability of multilevel operation. Not only the effective switching frequency can be doubled, the voltage slope during switching events (dv/dt) is also reduced. As a result, the noise in the control system could potentially be reduced. Stress on the insulation of machine windings can also be reduced as well.

In Drv1, the floating capacitor voltage could be controlled to zero when the motor terminal voltage is lower than the limit imposed by the power supply voltage. Similarly, in Drv3, the boost ratio can be reduced at low speed when the power supply voltage is sufficient. In both cases, the converter switching losses can be reduced below the rated speed. However, Drv2 and Drv 4 do not have this flexibility. It is clear that the

conduction losses can not be avoided.

An inductor is needed for the DC/DC boost converter in Drv3. Drv1 is able to increase the motor terminal voltage without a DC/DC boost converter and therefore eliminate the bulky inductor. Instead, an additional capacitor that has the same ripple current capability as the main inverter capacitor is needed in Drv1. However, considering the stored energy in capacitor is in proportion to the square of capacitor voltage, the total amount of stored energy in Drv1 is only half of that in Drv3 without even taking into account of the stored energy in the inductor.

The comparison of the four drive topologies are given in Table. 3.1.

Table 3.1 Comparison of the proposed topology to more conventional topologies

Parameters	Drv 1	Drv 2	Drv 3	Drv 4
Max Motor Voltage	2 pu	2 pu	2 pu	2 pu
Source Voltage in Total	1 pu	2 pu	1 pu	2 pu
Max Device Voltage	1 pu	1 pu	2 pu	2 pu
No. of Switches	12	12	8	6
Maximum Motor Power	1 pu	2 pu	2 pu	2 pu
Inverter KVA Rating	2 pu	2 pu	4 pu	2 pu
Extra Inductor	No	No	Yes	No
Stored Energy in Capacitor	2 pu	2 pu	4 pu	4 pu
CPSR	expanded	same	same	same
Onset of Flux Weakening	< 1.414 pu	2 pu	2 pu	2 pu
Output Voltage	3-level	3-level	2-level	2-level
Voltage Slope, dv/dt	1 pu	1 pu	2 pu	2 pu
Reduce Switching losses	yes	no	yes	no

3.3.5. Applicability to Other Motors

It is obvious that the reactive power requirement will be different for different machines. It would be beneficial to use normalized machine parameters to obtain more insight into the reactive power requirement and size of the auxiliary inverter INV2 [87]. Saliency ratio ξ and normalized PM flux linkage λ_{mn} are used as the per-unitized

parameters to represent different designs of motors. The PM flux linkage is normalized to the flux linkage amplitude at the rated current under MTPA excitation. A normalized machine parameter plane can be formed using the normalized PM flux linkage λ_{mn} as the horizontal axis and saliency ratio ξ as the vertical axis. Each point on the normalized machine parameter plane represents a certain set of designs regardless the actual power ratings. SPM motors have no saliency and therefore are located on the horizontal line of saliency ratio of 1. Synchronous reluctance motors will have a higher saliency ratio but zero PM flux linkage. Synchronous reluctance motors are located on the vertical axis of the machine parameter plane. When the machine does not have any saliency ($\xi = 1$) or permanent magnet flux linkage ($\lambda_{mn} = 0$), it is not able to deliver any torque or power. In the per-unitized system, the rated voltage and current are both 1 per unit.

When powered from a 2-level inverter, the power/torque-speed curves for the motors on the normalized parameters are shown in the Fig. 3.16. A speed range up to 10 per unit is used for all plots. In general, the designs in the upper right part of the plane have characteristic current higher than 1. As a result, machine designs located in this part of the parameter plane will have a maximum speed limit. For the machines located in the lower left part of the parameter plane, the characteristic current values are lower than the rated current. These machines will not have a maximum speed limit. However, the power capabilities of these machines will decrease as the speed increases. The power factors of the machines in the lower left part of the plane are lower at high speed. An apparent example will be a synchronous reluctance motor which is known for poor power factor. If the design is carefully done so that the machine is located on the boundary of the two parts of the plane mentioned above, the machine would have optimal flux weakening capability.

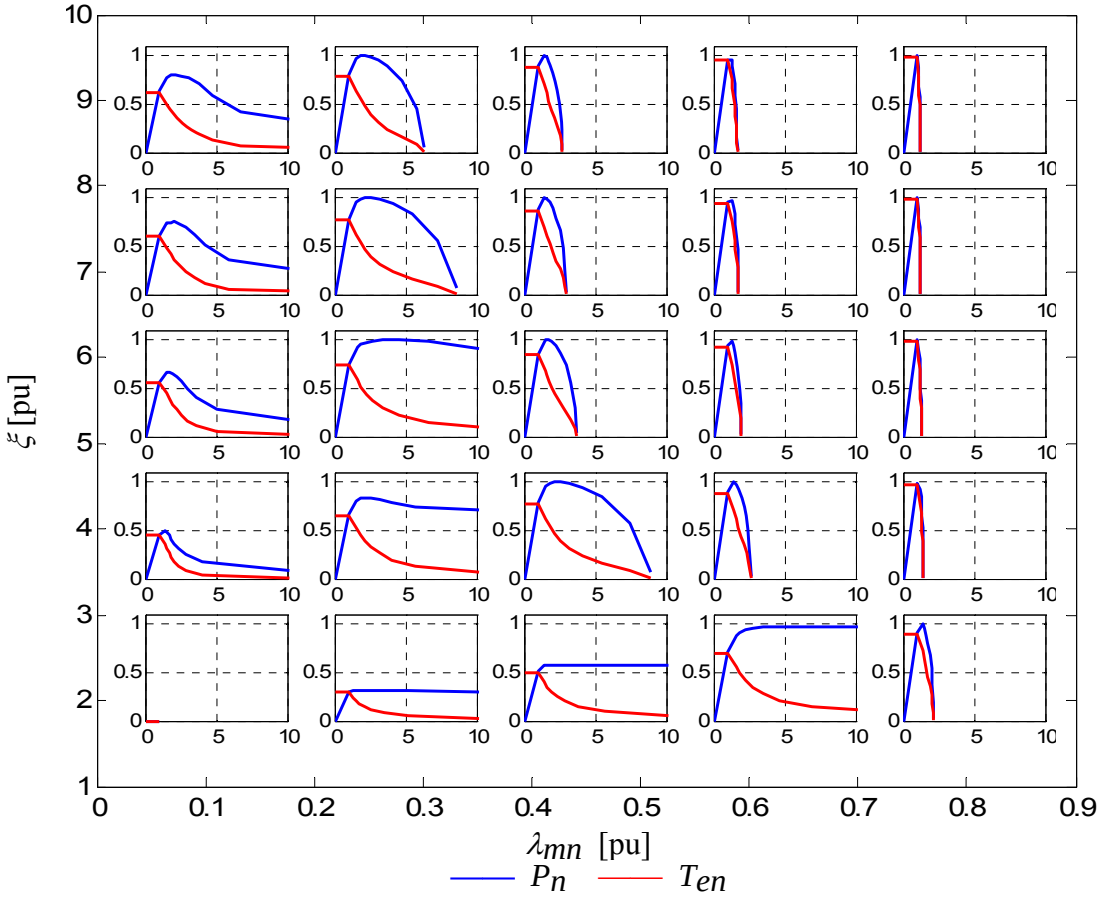

Fig. 3.16 Power speed curve of different machines on the normalized machine parameter plane, driven by single inverter drive

In Fig. 3.17, the machines on the parameter plane are driven by the proposed open-winding dual inverter drive. INV2 is assumed to have the same rating as the main inverter INV1. In all cases, the power and torque capability of the machines are improved. For the machines of poor flux weakening capabilities when driven by a single inverter drive (in the upper right part of the parameter plane), the maximum speed is greatly improved. In this situation, the auxiliary inverter INV2 is controlled as a three-phase inductor. For the motors that are already good for flux weakening operation (lower left part of the parameter plane), the improvement is mostly around the corner speed (1 per unit speed). Rated torque can be achieved beyond rated speed. INV2 is controlled as a three-phase capacitor in this situation. The start of flux weakening is postponed to a higher speed. It should be noted that, the transition from

capacitive to inductive compensation is automatically handled by the controller.

In some applications, the required CPSR is not as high as 10. The INV2 can be then sized accordingly to reduce the total system cost. Fig. 3.18 shows the power and torque capability of the machines when the voltage rating of INV2 is reduced to half of the voltage rating of the main inverter INV1. As can be predicted, the improvements are not as much as that when a fully rated INV2 is employed. Nevertheless, the cost of the inverters can be reduced if the performance meets the application requirement.

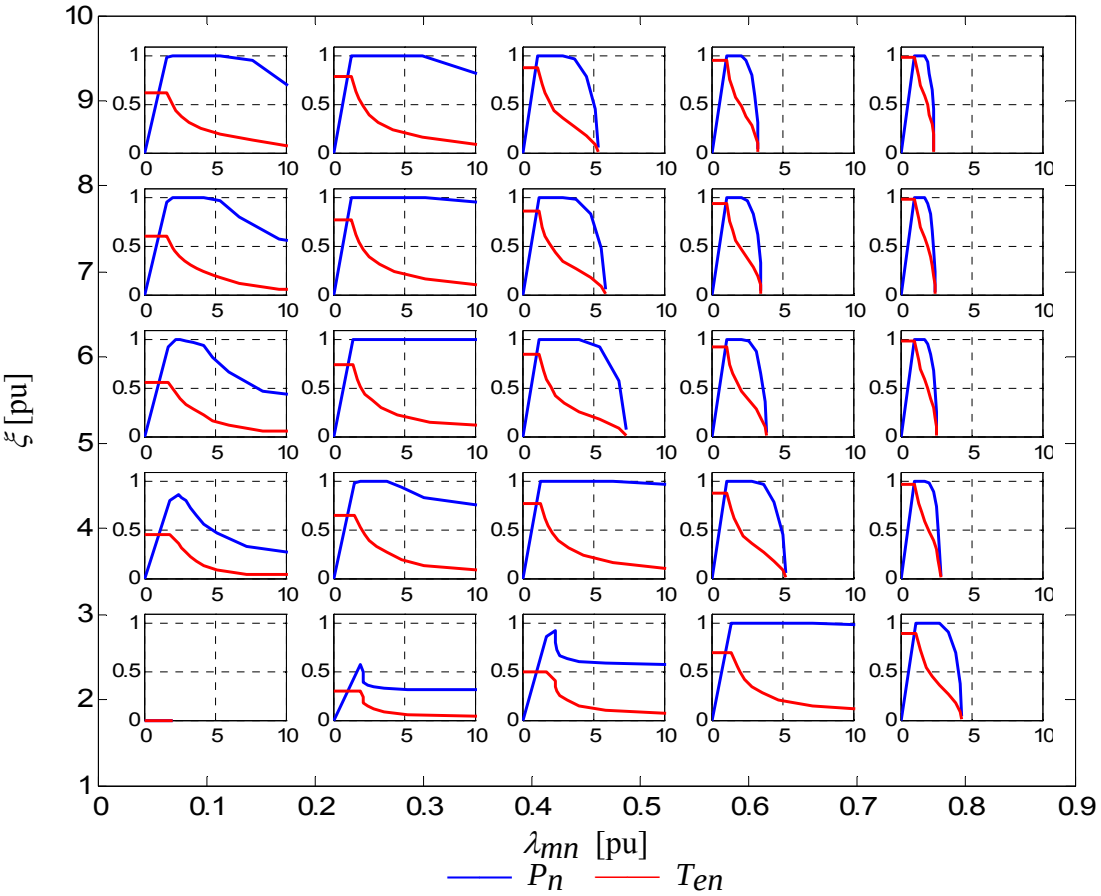

Fig. 3.17 Power speed curve of different machines on the normalized machine parameter plane, driven by open-winding dual inverter drive, INV2 has the same rating as INV1

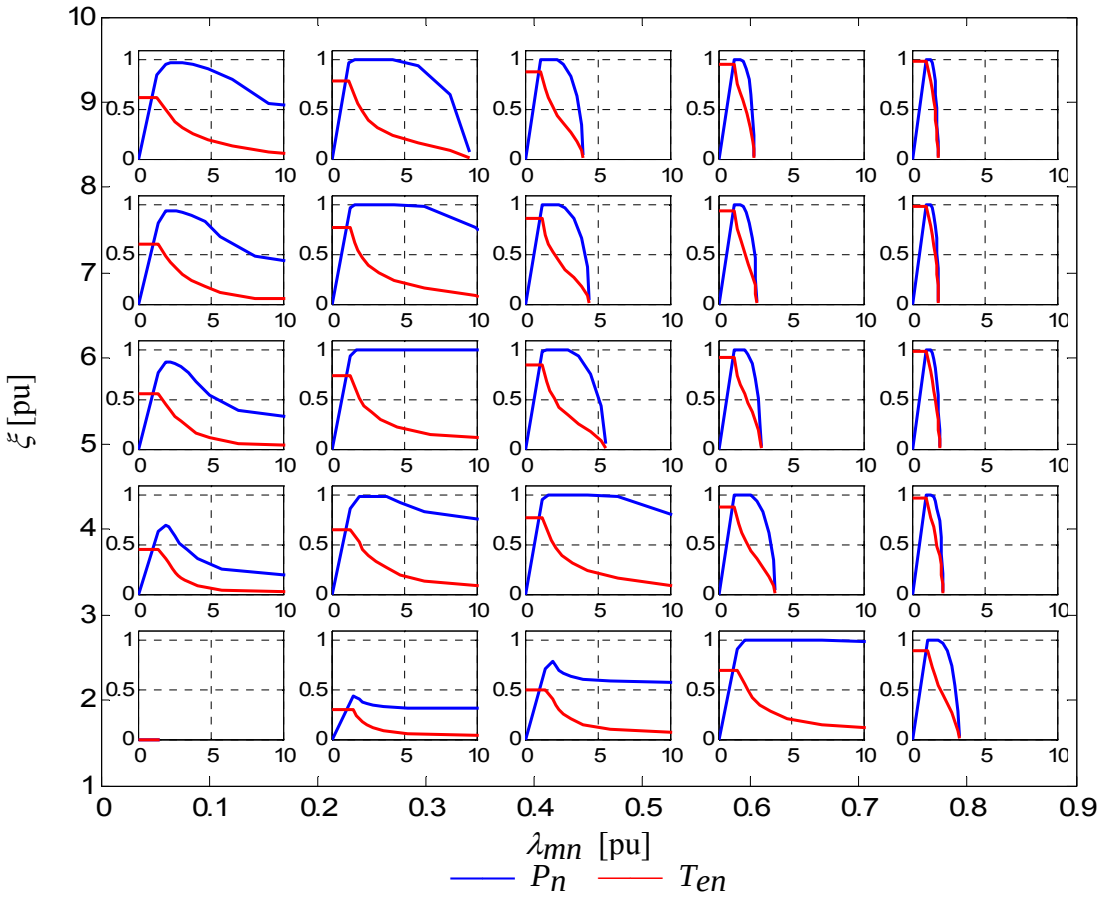

Fig. 3.18 Power speed curve of different machines on the machine parameter plane, driven by open-winding dual inverter drive, INV2 has half of the voltage rating of INV1

In addition to investigating the machines on the parameter plane, several machines were selected as examples for a more detailed study. The selected example machines are Toyota's 07 Camry motor, a 30 kw SPM motor that is optimized for torque density, a 60 kw permanent magnet assisted synchronous reluctance motor and a high saliency ratio synchronous reluctance motor. Without further complicating the problem, constant parameters and a lossless model are used in all cases. The machine parameters for the case study are given in Table. 3.2.

Table 3.2 Parameters for case study machines

Case	Description	λ_{mn} [pu]	ξ [pu]
I	07 Camry motor	0.504	2.85
II	SPM high torque density	0.95	1
III	PMASynRM	0.244	2.72
IV	SynRM	0	10

Case I: 07 Camry Motor

The 07 Camry motor is a high power/torque density IPM motor that has a characteristic current slightly higher than 1 per unit (parameters estimated for continuous operation). The power/torque-speed curve, motor voltage with its real and imaginary components and the power factor on the boundary of power-speed curve are shown in Fig. 3.19. The flux weakening capability of this motor is very good. The theoretical absolute maximum speed is higher than 10 per unit. The power factor remains good up to 6~7 per unit speed. Beyond the corner speed, the current starts to advance in phase and the motor changes from lagging to leading power factor. It can be seen that the imaginary part of the motor voltage becomes dominant at higher speed. It is expected that the motor will have better power capability around corner speed and at speed higher than 5 per unit if extra reactive voltage is available.

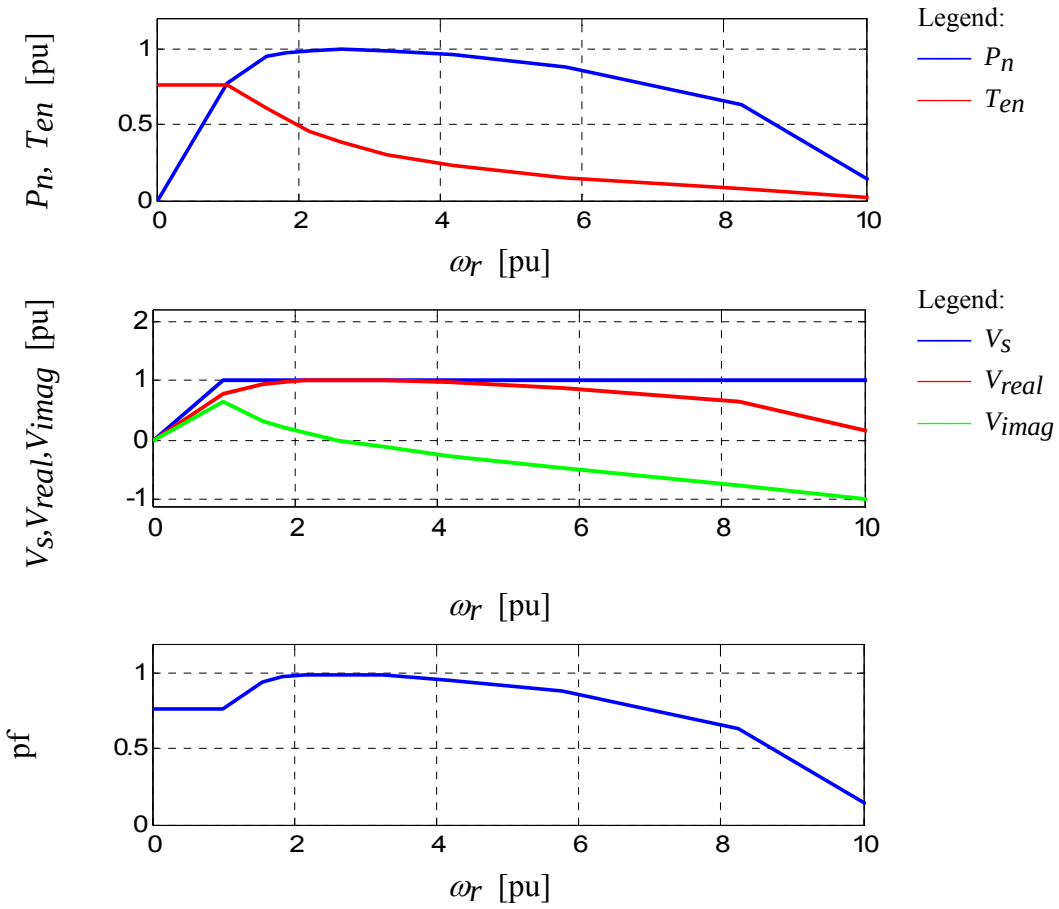

Fig. 3.19 Case study, 07 Camry motor single inverter drive

Fig. 3.20 shows the same curves when the 07 Camry motor is driven by the proposed dual inverter open-winding motor drive. In addition, the amplitude of voltage delivered by INV1 and INV2 are given as well. INV1 voltage is kept at 1 per unit beyond the corner speed. The power capability remains very good even at 10 per unit speed. The corner speed is postponed compared to that shown in Fig. 3.19. INV2 is not used to its full capability across the entire operating range considered. It can be concluded that for some motor designs, a smaller sized INV2 can be used to fulfill the application requirements.

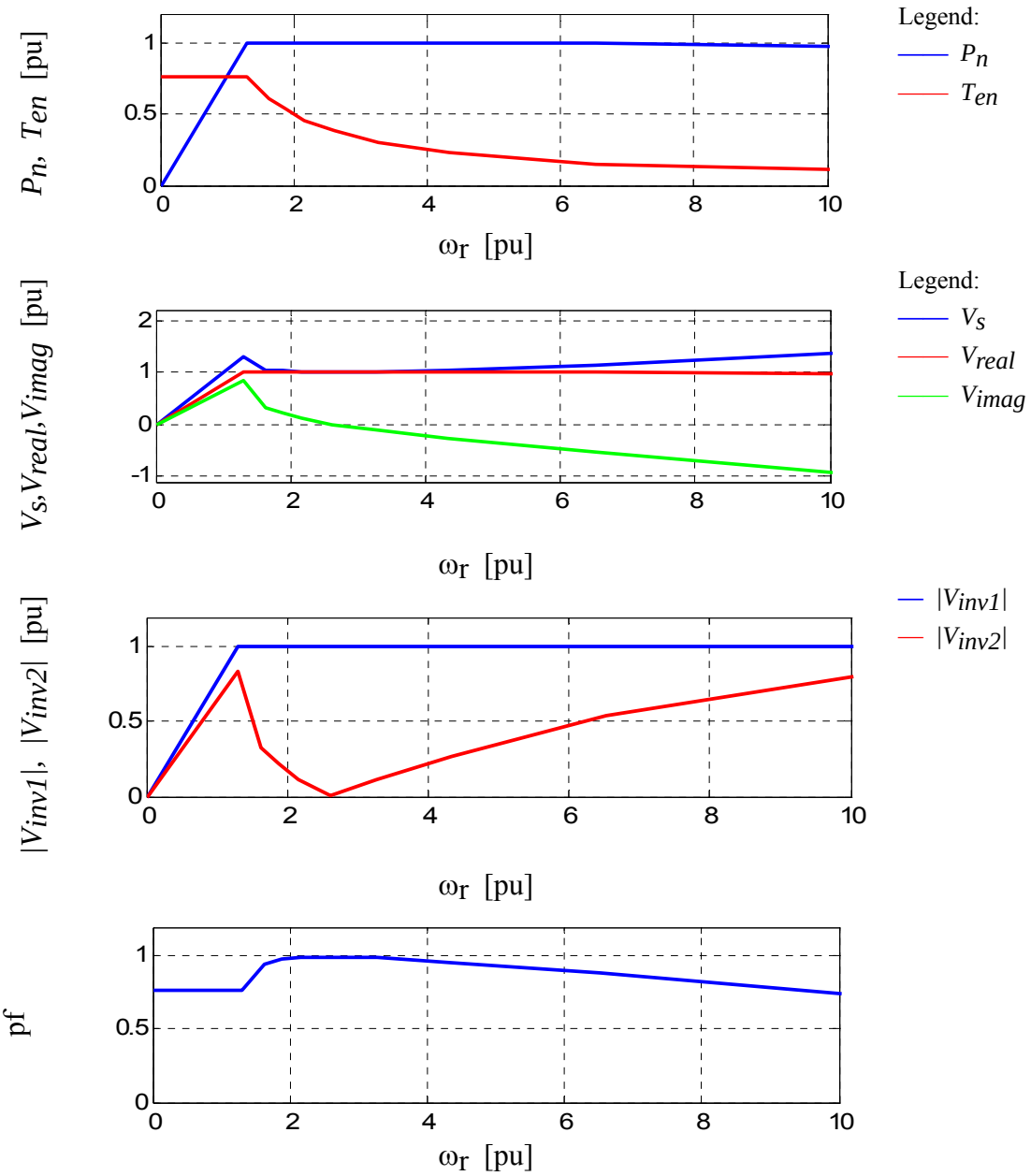

Fig. 3.20 Case study, 07 Camry motor dual inverter open-winding drive

Case II: SPM Optimized for Torque Density

For the high torque density SPM motor under study, the normalized permanent magnet flux linkage is very high, meaning the back-emf is the dominant part of the motor voltage under rated condition. The power factor of this motor is very high below the corner speed because of the small inductance. Nevertheless, the low inductance of

the motor leads to a high characteristic current and poor flux weakening capability beyond the corner speed. From Fig. 3.21, the theoretical maximum speed is only about 1.5 per unit. To keep the motor terminal voltage within the limit, the power factor deteriorates quickly once the speed exceeds the rated speed.

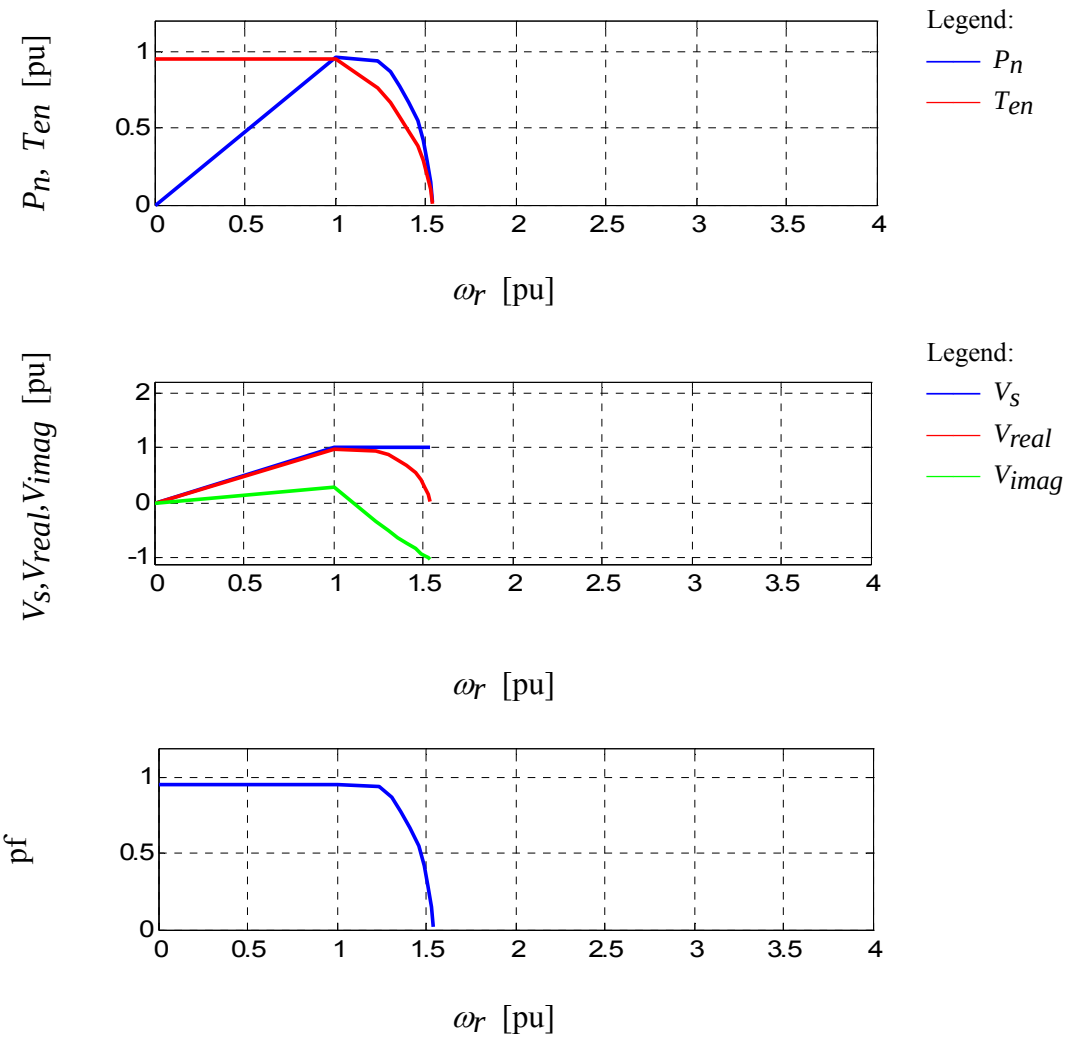

Fig. 3.21 Case study, SPM motor optimized for torque density single inverter drive

From Fig. 3.22, the maximum speed of the motor can be doubled when the proposed dual inverter open-winding drive topology is used. The improvement of the power capability is significant. The voltage component needed to accomplish this improvement is purely reactive. INV2 is used to its maximum voltage capability at the

maximum speed.

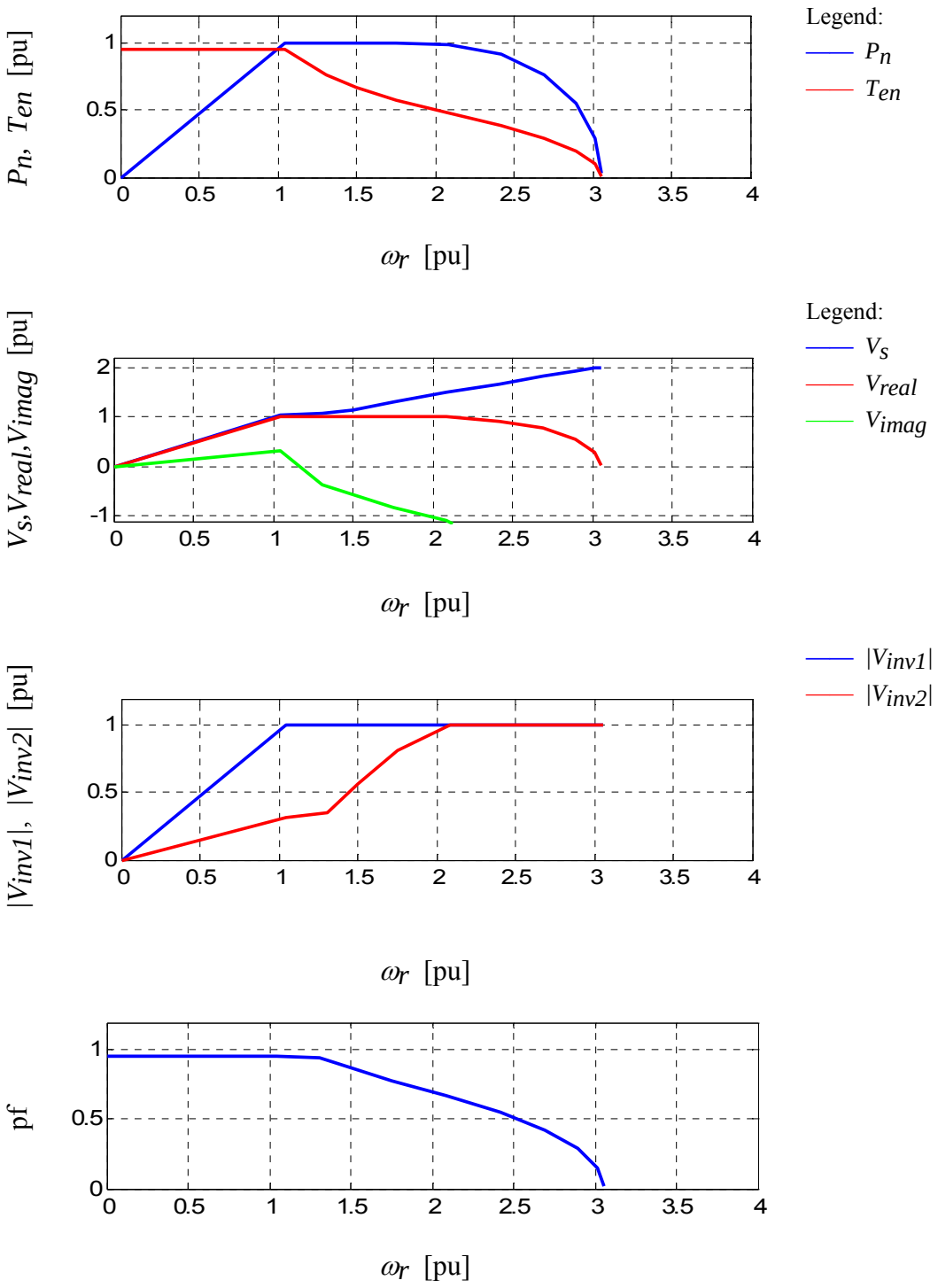

Fig. 3.22 Case study, SPM optimized for torque density dual inverter open-winding drive

Case III: PM Assisted Synchronous Reluctance Motor

PM assisted synchronous reluctance motors are now being considered as one of the promising alternatives to high power/torque density but more expensive Neodymium based PM motors. This kind of machines often has a relatively high saliency ratio. Magnets of lower price are used to improve the power density and power factor of the motor. However, due to the difficulty of mounting magnets in a radially laminated rotor, the saliency ratio is often limited compared to some other synchronous reluctance motors. As shown in Fig. 3.23, the power factor of the motor is quite poor below the rated speed even with the assistance of the ferrite magnets. The inverter VA rating has to be over sized for this type of motor when compared to the SPM motor shown in Case II due to the requirement of more reactive power. As the motor enters the flux weakening region, the power factor starts to improve as the speed increases. However, the power capability will decrease slightly as the speed increases because the motor has a characteristic current smaller than 1 per unit.

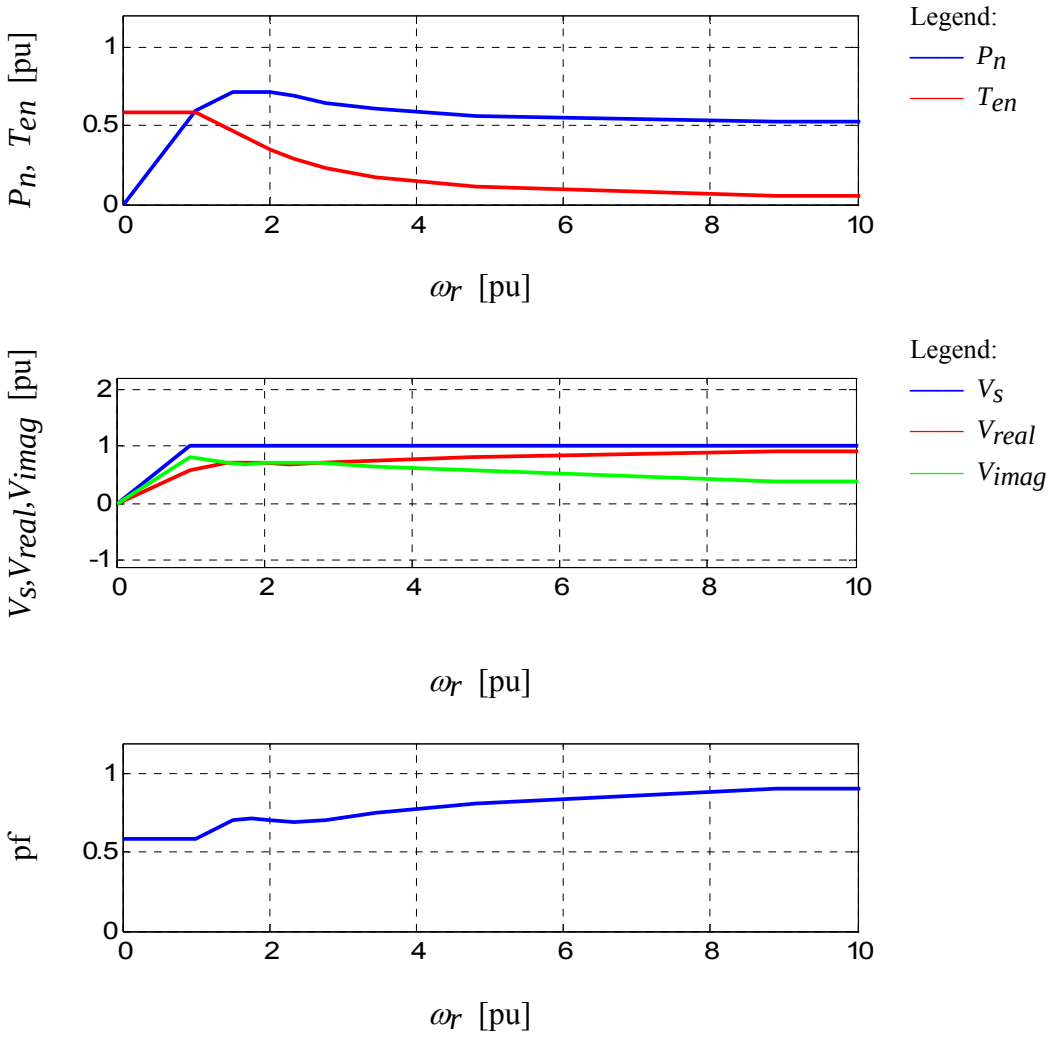

Fig. 3.23 Case study, PM assisted synchronous reluctance motor single inverter drive

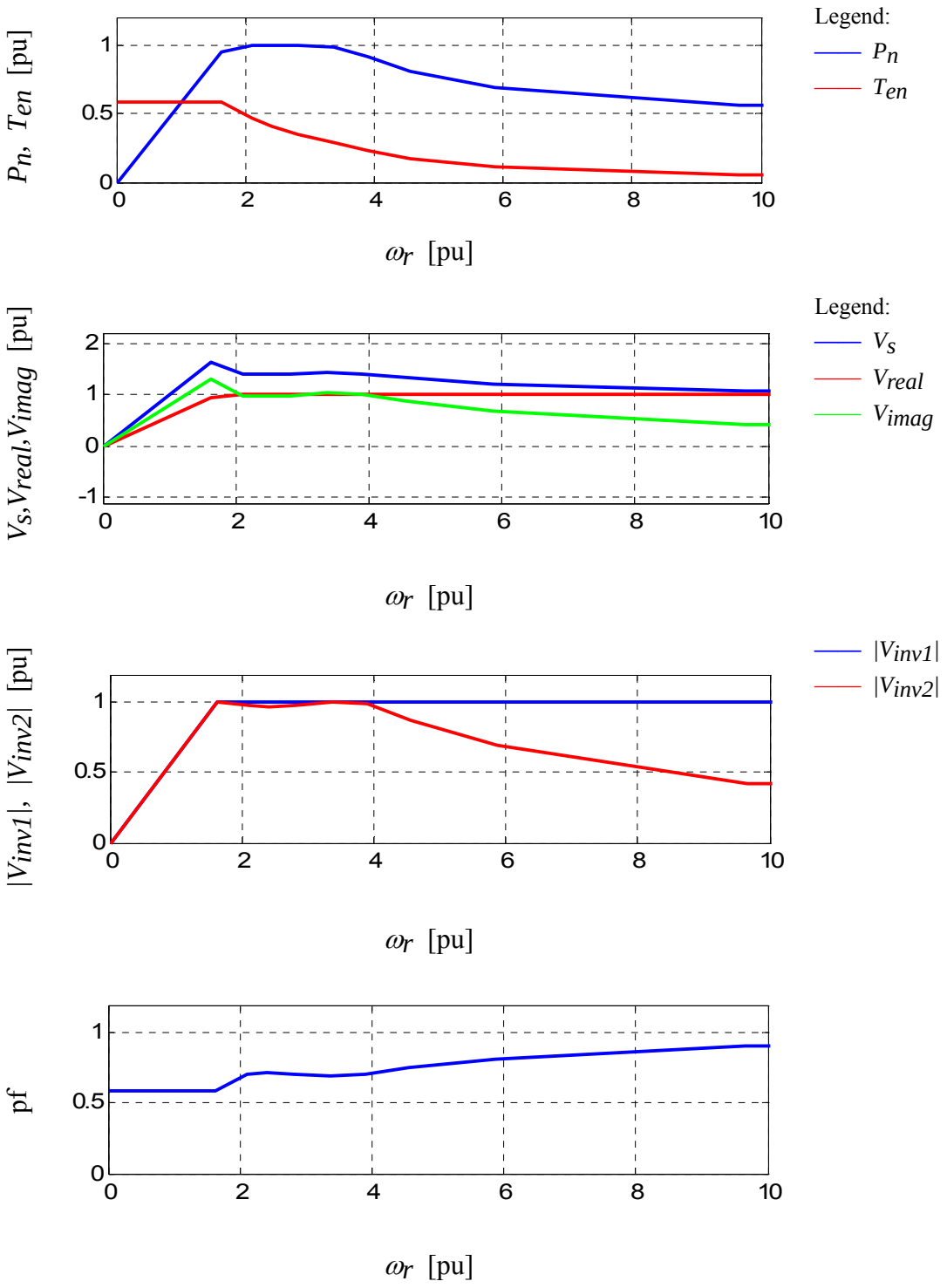

Fig. 3.24 Case study, PM assisted synchronous reluctance motor dual inverter open-winding drive

Fig. 3.24 shows the power/torque-speed curve prediction along with the motor voltage components when the PM assisted synchronous reluctance motor is driven by the proposed series compensated open-winding motor drive. The corner speed is postponed to a value that is very close to 2 per unit. For this particular motor, the power/torque capability improvement is very similar to the case when a DC/DC boost converter is used. However, the total converter rating will be much smaller for the open-winding motor drive. PM assisted synchronous reluctance motor is potentially a very good target application of the proposed open-winding motor drive topology. It is also worth to note that INV2 is not utilized to its full capability at high speeds because the requirement of reactive power decreases as the motor goes deeply into flux weakening.

Case IV: High Saliency Ratio Synchronous Reluctance Motor

In this case, a high saliency pure synchronous reluctance motor is investigated. When radially laminated rotor is used, it is claimed that a saliency ratio as high as 10 can be achieved. Since the characteristic current is zero for this type of motor, the center of the voltage limit ellipses is located at the origin on the current vector plane. As expected, there will not be a theoretical maximum speed limit for this motor. Similar to the PM assisted synchronous reluctance motor discussed in Case III, the power factor is very low below the corner speed as shown in Fig. 3.25. Without the assistance from the permanent magnets, the power factor remains poor for this motor even in high speed region. The reactive part of the voltage exceeds the real part at some operating points.

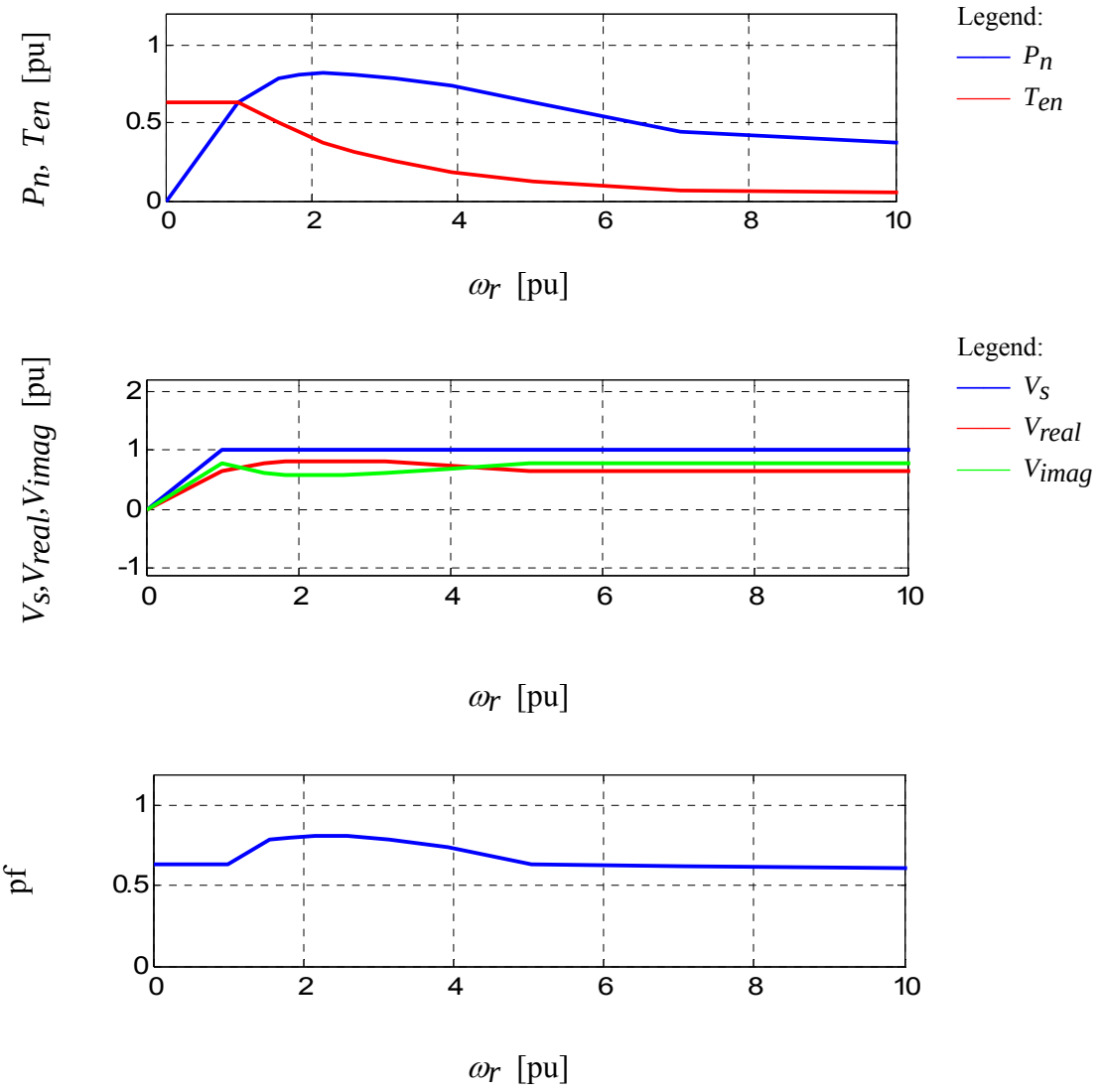

Fig. 3.25 Case study, high saliency ratio synchronous reluctance motor single inverter drive

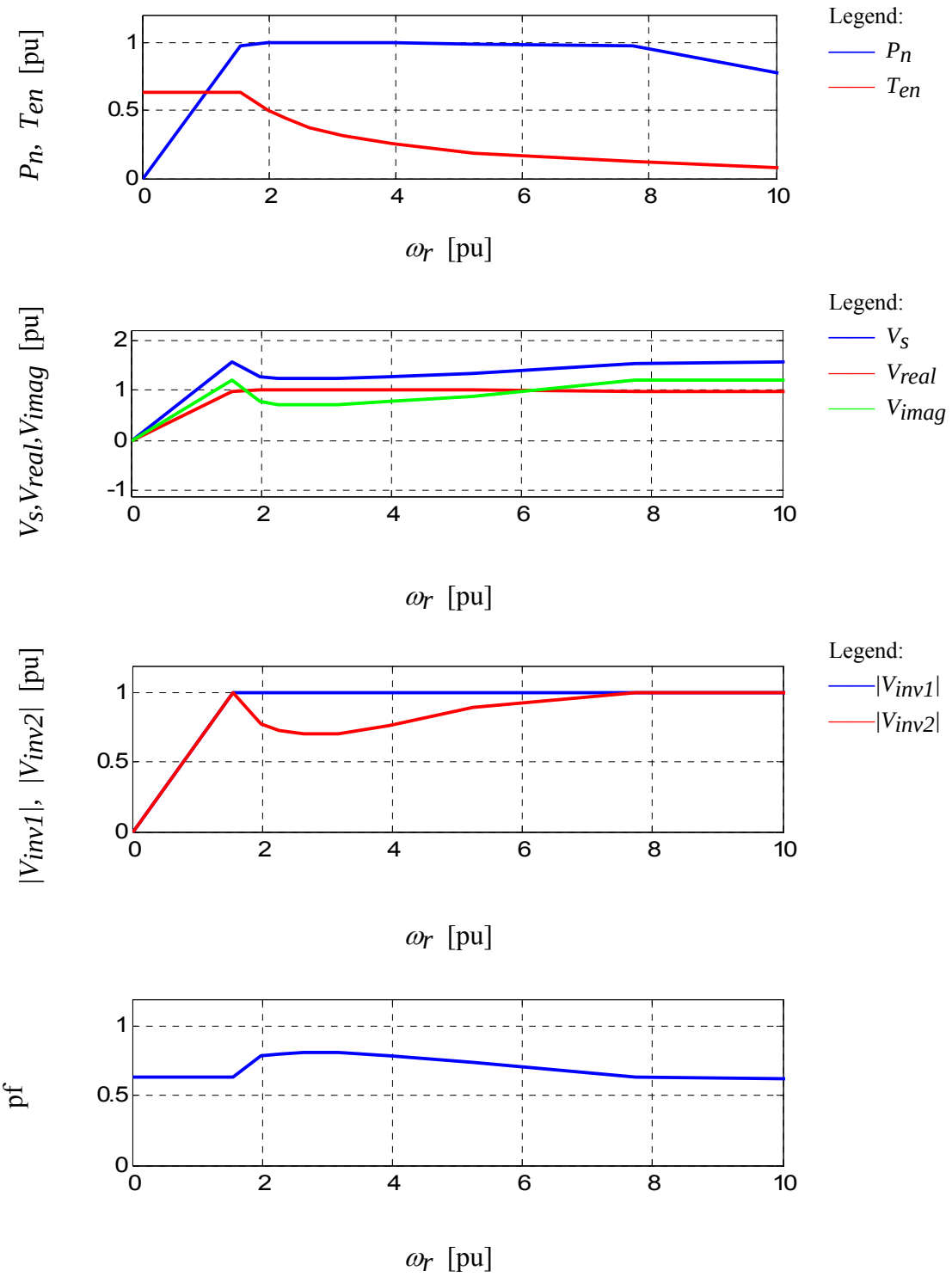

Fig. 3.26 Case study, high saliency ratio synchronous reluctance motor dual inverter open-winding drive

With the compensation inverter, the power/torque capability analysis results are shown in Fig. 3.26. Same as in the previous case, the power capability can be significantly improved with the dual inverter arrangement. The improvement is almost as good as adding an extra DC/DC boost converter. Different from the PM assisted synchronous reluctance motor in Case III, INV2 will be fully utilized at high speed because of the poor factor in this case. Synchronous reluctance motor is another promising application of the proposed topology.

In all the cases investigated, the proposed dual inverter open-winding machine drive is able to improve the power/torque capability of various motors under a fixed voltage source. For machines that are not well designed for high CPSR, the proposed topology is able increase the maximum speed limited significantly. For machines that already have good flux weakening capability, the major improvement is the capability to operate the motor at rated torque beyond rated speed. The motors between the two situations will benefit from both posted start of flux weakening and improved CPSR.

3.4. Impact on Excitation Voltage

It has been mentioned previously that the open-winding motor drive is essentially a multilevel inverter drive. Unlike a conventional three-phase Y-connected AC machine, an open-winding machine can be excited by two sets of three-phase voltages. The resulting machine terminal voltage is the vector sum of the two applied voltage vectors. Traditionally, the two sets of voltage are equal and balanced with a 180 degree phase shift as shown in the vector diagram in Fig. 3.27 (a). When INV2 is used for the purpose of reactive power compensation, the motor terminal voltage is likely to be different from INV1 voltage in most situations. An example of vector diagram is shown in Fig. 3.27 (b).

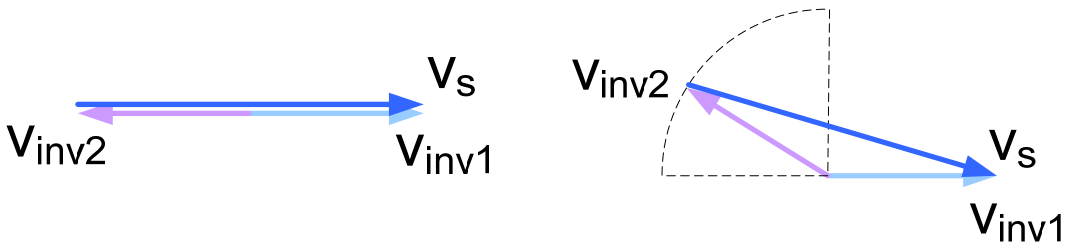

(a) Conventional open-winding motor drive

(b) Open-winding motor drive with INV2 for compensation

Fig. 3.27 Open-winding motor drive voltage vector

When PWM inverters are used to drive an open-winding machine, the instantaneous phase voltage will be different for isolated DC bus and common DC bus configurations. Three-level voltage is applied to the phase winding when the two inverters share a common DC bus. In the isolated DC bus configuration, the line-to-line voltage of the machine is a three-level voltage. Fig.3.28 is a comparison of the instantaneous phase voltage waveform of several different drive configurations.

Fig. 3.28 (a) is the phase voltage of a common single 2-level inverter drive. Fig. 3.28 (b) shows the phase voltage waveform for a common DC bus open-winding machine drive. For common DC bus open-winding machine drive, the phase voltage is a 3-level PWM waveform. When the two VSIs share a common DC bus, the zero sequence current is able to circulate through the common DC bus. Moreover, the zero sequence impedance of AC machines is usually very low. As a result, a small zero sequence voltage will result in large zero sequence current in the machine windings in an open-winding drive with common DC bus. Fig.3.28 (c) is the machine phase voltage PWM waveform for an isolated DC bus open-winding machine drive when the voltage commands of the two inverters are equal and shifted by 180 degrees. The waveform is the same as any conventional 3-level converters. Fig. 3.28 (d) is the phase voltage PWM waveform for the isolated DC bus open-winding drive when the voltage commands of the two inverters are equal and shifted by 90 degrees. This situation can be observed when INV1 is only delivery real power to the motor.

For the isolated DC bus open-winding motor drive, the switching frequency is virtually doubled when the two voltage commands are shifted by 180 degrees because the motor terminal voltage waveform is the same as other three-level inverters. Fig. 3.29 gives an example of the phase voltage harmonic content comparison between a Y-connected motor with a 2-level inverter and an open-winding motor drive with an isolated inverter. The phase shift between the voltage commands of the two inverters are set to 180 and 90 degrees. Sine-triangle PWM is used for the analysis. The modulation index is set to 1 and the switching frequency is set to 30 times of the fundamental frequency in both cases. It is apparent from the spectrum that the harmonics at the switching frequency and its odd multiples do not exist for the open-winding motor drive when there is a 180 degree phase shift between the two voltage commands. This is one of the major advantages of having two isolated power sources in more conventional dual VSI open-winding motor drive. Therefore, this configuration is used in most of the existing literature for an open-winding motor drive.

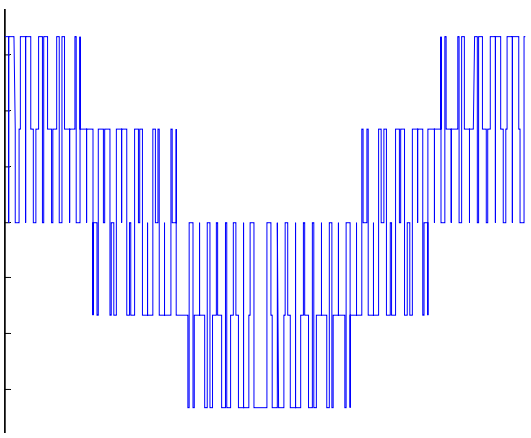

(a) Y-connected machine with 2-level inverter

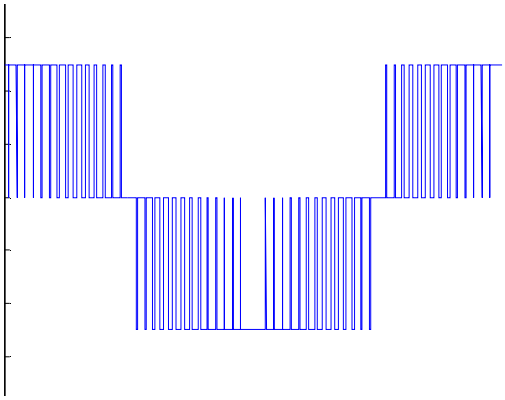

(b) Open-winding machine with common DC bus inverters

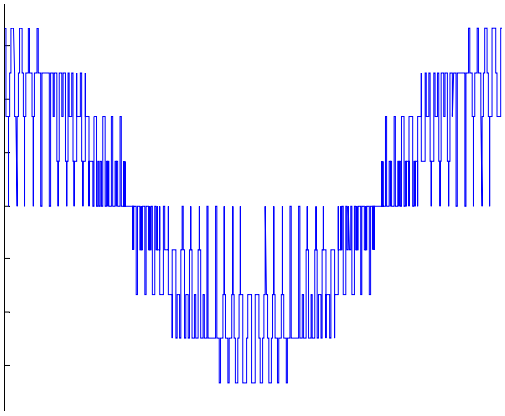

(c) Open-winding motor drive with isolated DC bus, 180 phase shift

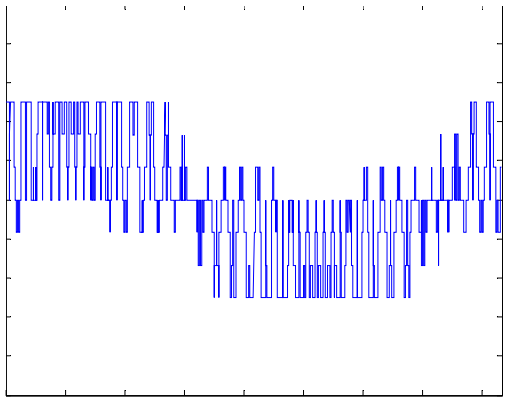

(d) Open-winding motor drive with isolated DC bus, 90 degree phase shift

Fig. 3.28 Phase voltage waveform comparison of different drives

However, if INV2 is required to deliver only reactive power to the motor, the voltage commands of the two VSI would often not be 180 degrees apart. Assuming INV1 is only providing real power and INV2 is providing reactive power to the motor, there would be a 90 degree phase shift between the two voltage command vectors. The spectrum of the phase voltage when the phase shift is 90 degree is given in Fig. 3.29 (c). The modulation indices used are again set to 1. The carrier signals of the two inverters are the same. Different from the situation when the phase shift between the two voltage command vectors are 180 degrees apart, harmonics around the switching frequency and

its odd multiples appear in the spectrum.

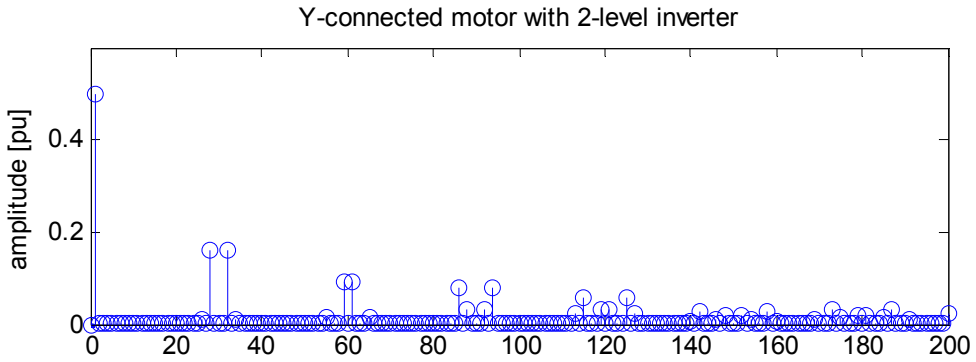

(a) Y-connected motor with 2-level inverter

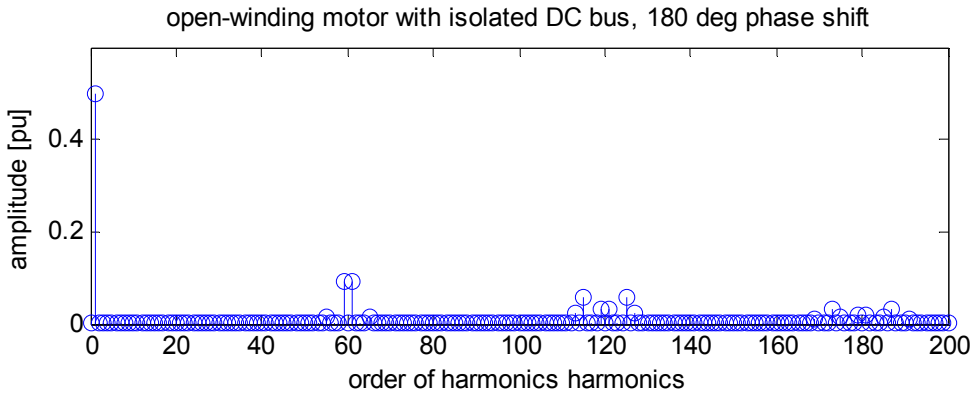

(b) open-winding motor drive with isolated DC bus, 180 degree phase shift

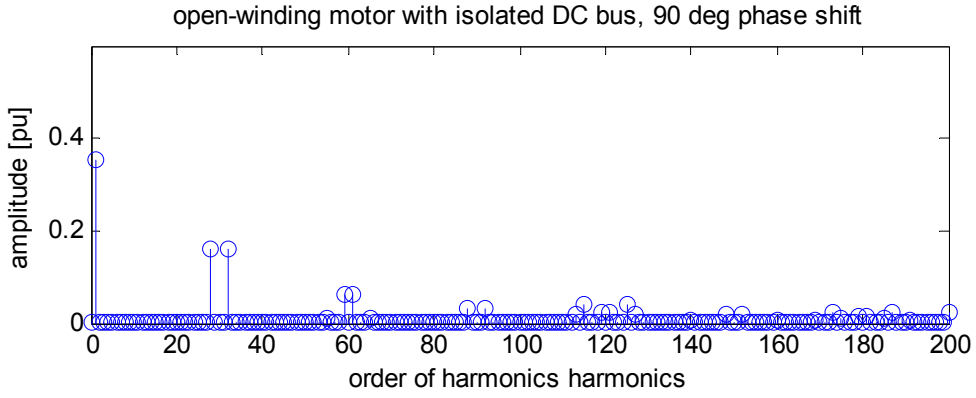

(c) open-winding motor drive with isolated DC bus, 90 degree phase shift

Fig. 3.29 Phase voltage harmonics comparison between Y-connected motor with 2-level inverter and open-winding motor drive with isolated DC bus

A natural solution to reduce the harmonics when the voltage commands of the two VSIs are shifted is to shift the phase of carrier signal of INV2 at the same time. The spectrum of the phase voltage waveform when the carrier frequency is shifted is given in Fig. 3.30. It is apparent that the harmonics of phase voltage can be reduced significantly. However, it is difficult to dynamically change the phase angle of carrier signal when the voltage command phase shift is changing during normal operation. Therefore, the carrier signals are set to be the same in later studies.

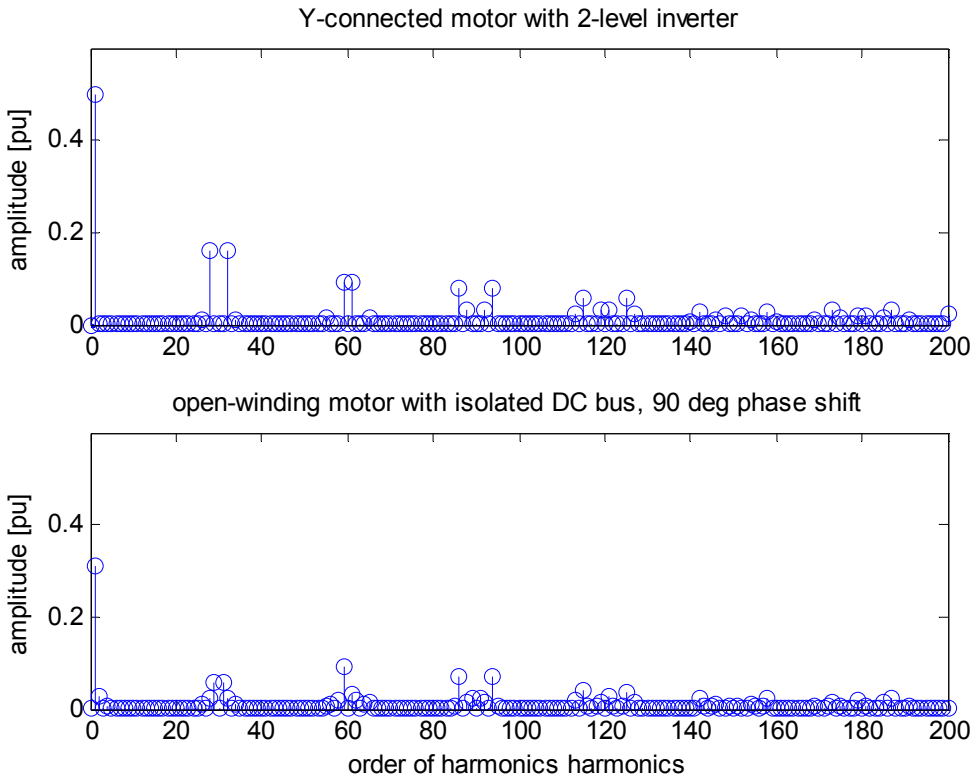

Fig. 3.30 Spectrum of the open-winding machine drive phase voltage when the voltage command from the two VSIs are shifted by 90 degrees, carriers are shifted by 90 degrees as well

With INV1 providing part of the reactive power required by the motor, the phase shift between the two voltage commands will be from 90 to 180 degrees (the sign of compensation voltage will be different for capacitive and inductive compensation, but the harmonic contents will be the same). The harmonic content under these conditions

are studied. Without further complicating the problem, the modulation indices are set to be the same initially. The total harmonic distortion is calculated and plotted against modulation index and phase shift between the voltage commands in Fig. 3.31. It should be noted that only the first 200 harmonics are considered in the computation of THD. The same number of harmonics is used in later analysis.

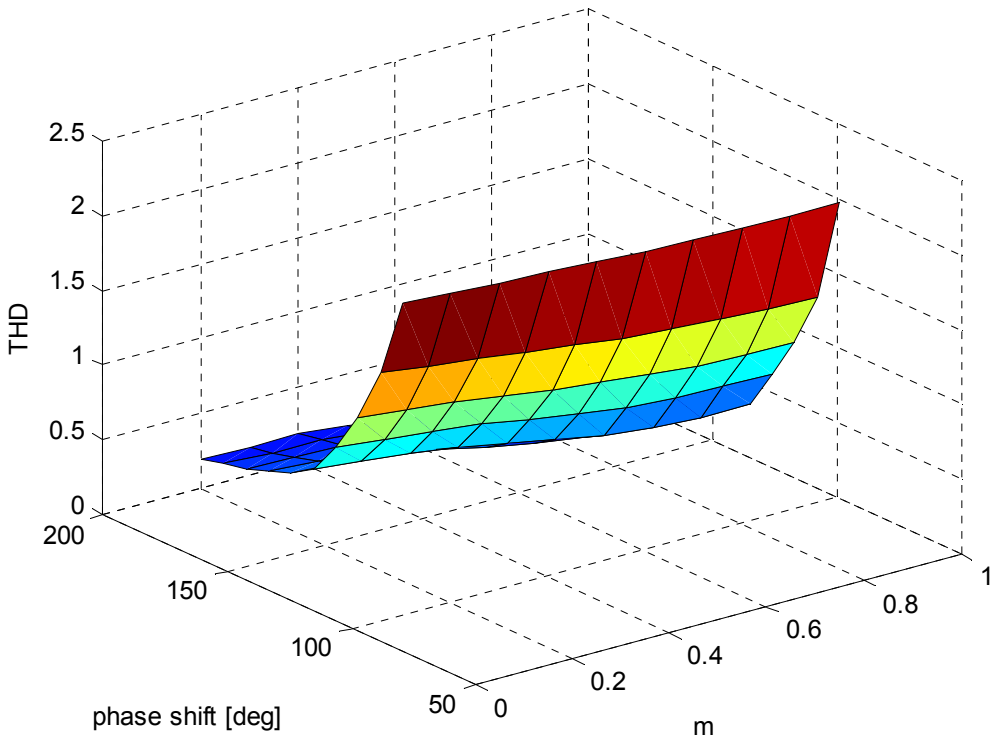

Fig. 3.31 THD of phase voltage of an open-winding motor drive with isolated DC bus, modulation indecis are set the same for the two VSI

Fig. 3.32 shows another case of the THD of the phase voltage waveform when one of the inverter is operated with a fixed modulation index of 1 and the modulation index of the other inverter varies from 0 to 1. The phase shift between the two voltage commands varies from 90 to 180 degrees.

It was found that the THD of the phase voltage in an open-winding motor drive can be either higher or lower compared to a single 2-level inverter depending upon the

modulation indices and the phase shift between the voltage commands of the two inverters. In general, for the same modulation indices, the THD will be higher when the phase shift between the two voltage commands is at 90 degrees.

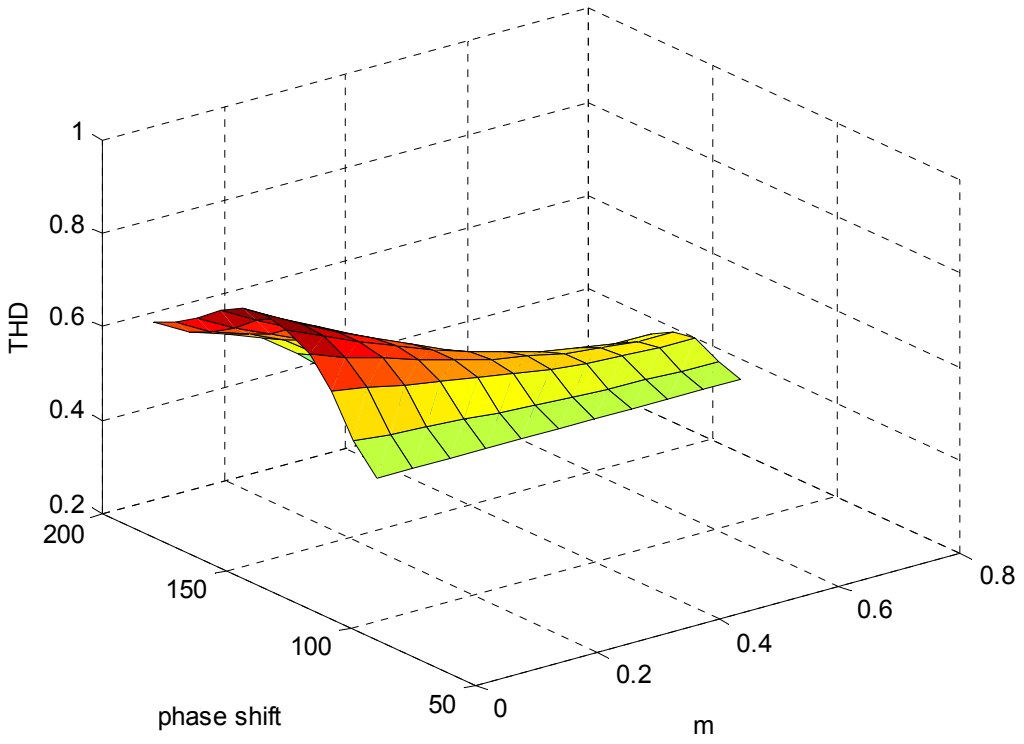

Fig. 3.32 THD of phase voltage of an open-winding motor drive with isolated DC bus, fixed modulation index for one inverter and variable modulation index and phase shift

3.5. Control Method

The proposed open-winding motor drive control method discussed here is based on the widely used field oriented controller. An outer velocity loop has been used to generate the q-axis current for the inner loop. Current references for the d-axis are generated based on the torque command and the MTPA curve.

Two PI regulators in the rotor reference frame are used to control the current in the

d and q-axis. Cross coupling decoupling terms are added to enhance the performance during transient.

As mentioned in previous sections, INV2 is only able to supply reactive power to the motor. All the real power has to be supplied from INV1. Therefore, the voltage command vector from the current regulator is decomposed into real and imaginary components. INV2 is controlled to provide the reactive part of the voltage command vector up to its voltage limit. This part of INV2 voltage command only contains reactive component. INV1 provides the remaining part of the voltage required by the motor. The voltage command of INV1 may contain both real and imaginary components.

Ideally, if INV2 is only supplying reactive power, the voltage of the DC capacitor will be constant. However, in reality, there are some losses associated with the switching of the inverter, the ESR of the floating capacitor and etc. As a result, to keep the INV2 DC bus capacitor voltage constant, a small amount of real power has to be supplied to INV2 to compensate for the losses. A PI regulator is therefore used to regulate the floating capacitor voltage. The output of the controller is the real component of INV2 voltage command. To reduce the switching losses, the reference of the floating capacitor voltage can be set to zero when the voltage required by the motor is low. In the simulation and experiment, the reference is set to the nominal value once the motor current exceeds a threshold value. However, potentially, the floating capacitor voltage reference could be varied dynamically according to the requirement of the motor to minimize the losses.

The voltage command is distributed between the two inverters by (3.4) and (3.5). Sine-triangle PWM with 3^{rd} harmonics injection is used in this project. Before the voltage commands are transformed into the abc reference frame, the linear modulation limit of 1.15 is applied.

$$v_{inv1}^{*} = \left\{ |v_{dq}^{*}|\cos(g - b) + j\left[|v_{dq}^{*}|\sin(g - b) - \mathrm{sgn}(\sin(g - b))\, \min\left(\left| |v_{dq}^{*}|\sin(g - b) \right|, v2max \right) \right] \right\} \tag{3.10}$$

$$v_{inv2}^{*} = \left[v_{real2} + j\, \mathrm{sgn}(\sin(g - b)) \min\left(\left| |v_{dq}^{*}|\sin(g - b) \right|, v2max \right) \right] T^{-1}(q_r - b) \tag{3.11}$$

The quantities δ and β are the voltage and current phase angles with respect to the q-axis. The matrix T is the reference frame transformation.

A feedback style flux weakening controller is employed to prevent the current regulators from saturating. The amplitude of INV1 voltage command is used as the control variable for the outer voltage loop. This allows maximum voltage utilization and higher voltage to be applied to the motor terminals.

The block diagram of the controller is shown in Fig. 3.33.

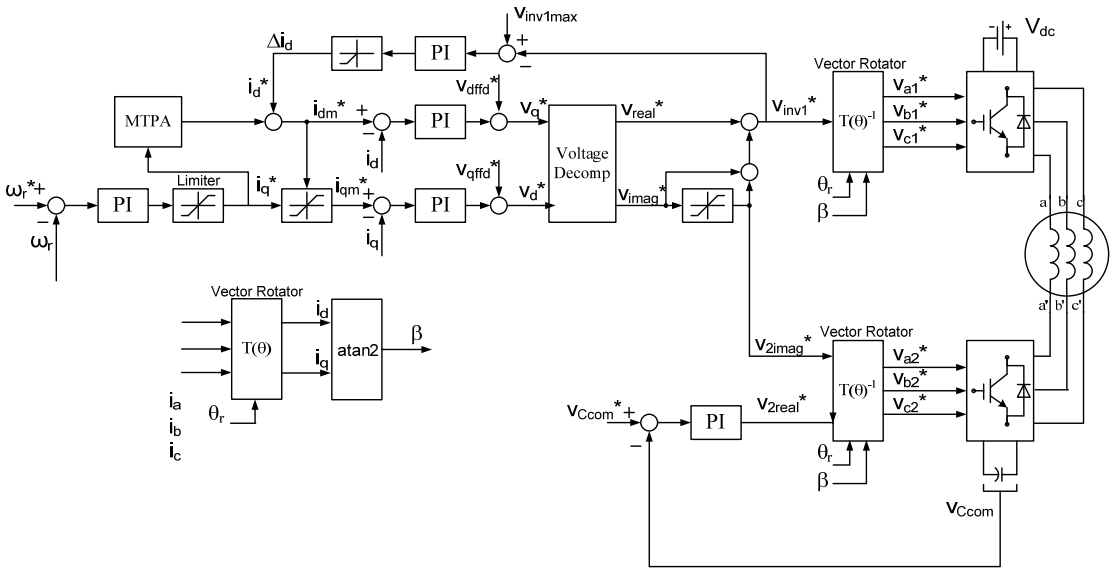

Fig. 3.33 Block diagram of open-winding PM motor drive control method

3.6. Simulation Study

The proposed system was simulated using the parameters of a lab scale IPM machine. The parameters of the motor and inverters are given in Table. 3.3. It should be pointed out that due to the mechanical limit of the experimental setup, the rated current of the motor is decreased so that the maximum speed limit is at a safe level for experimental verification.

Table 3. 3 Motor and drive parameters

Symbol	Parameters	Value
r_s	stator resistance	0.315 Ohm
L_d	d-axis inductance	16 mH
L_q	q-axis inductance	51 mH
λ_m	permanent flux linkage	0.75 wb
P	number of poles	4
I_r	rated peak current	21.6 A
V_{dc}	DC bus voltage	200 V
V_{dc2}	floating capacitor voltage	200 V
C_{com}	Floating capacitor capacitance	800 μF
f_s	switching frequency	8 kHz

The inverter phase voltage references are plotted with the motor current of the same phase in steady state in Fig. 3.34. Two operating conditions in steady state are shown. Low speed loaded operation is shown in Fig. 3.34 (a). INV1 voltage reference is in phase with current, indicating that INV1 is only supplying real power to the motor. INV2 voltage reference is lagging the current by 90 degrees. Therefore, INV2 is acting as a three-phase capacitor in this case. In Fig. 3.34 (b), the motor is operated at high speed with no applied load torque. The motor is operated at a leading power factor in this situation. INV2 is controlled as a three-phase inductor.

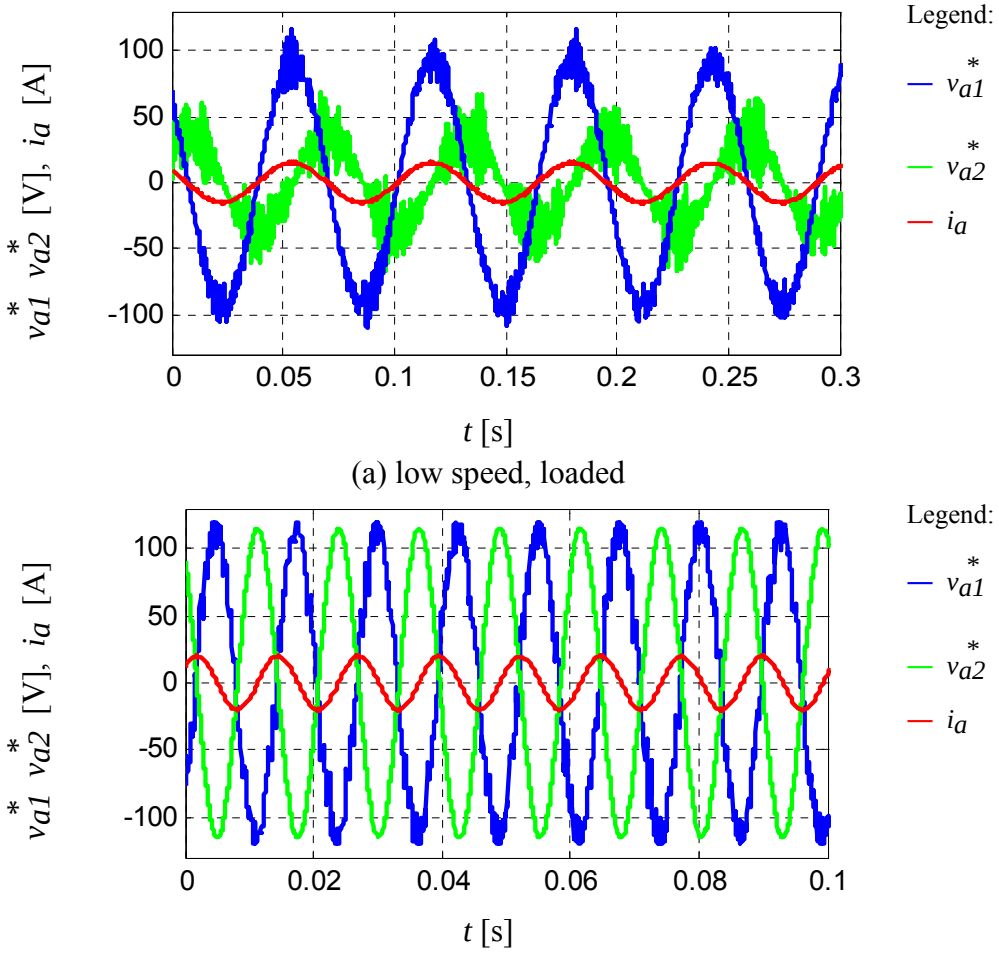

(a) low speed, loaded

(b) high speed, no load

Fig. 3.34 Simulated nverter voltage references and motor current

Acceleration under no load is simulated and the results are shown in Fig. 35. Fig. 3.35 (a) shows the speed of the motor. The velocity reference is ramped up. The motor accelerates until the inverters reach the voltage limit. The amplitude of INV1 voltage reference is shown in Fig. 3.35 (b). The amplitude is controlled within its limit to prevent the current regulator from saturation. The floating capacitor is charged during the transient as shown in Fig. 3.35 (c). It can be seen that the capacitor can be charged smoothly without any pre-charge circuit or special procedure. The voltage reference of INV1 has some transients when the capacitor is charged. This is because INV1 sees a

large resistance during the charge of the floating capacitor.

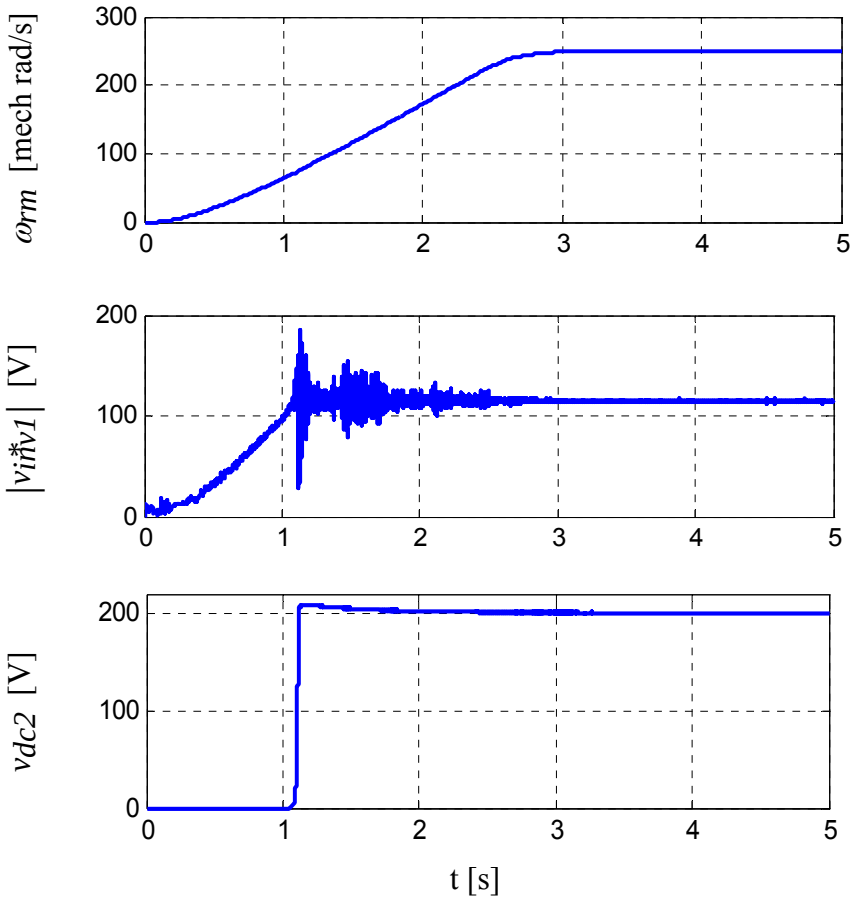

Fig. 3.35. Simulated transient during acceleration

3.7. Experimental Results

The transient during acceleration is shown in Fig. 3.36. It is shown that the flux weakening controller is able to keep the amplitude of INV1 voltage reference within its limit.

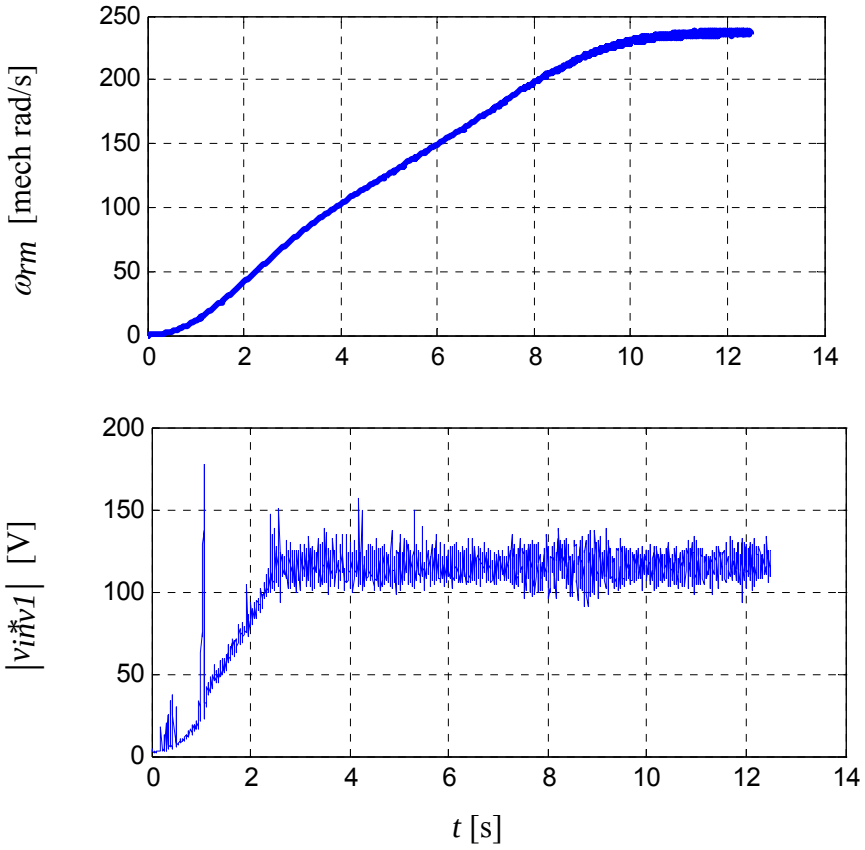

Fig. 3.36 Measured transient during acceleration

The floating capacitor is controlled to be charged during normal operation. Fig. 3.37 shows the transient during a load change. The capacitor is charged only when the current exceeds a threshold value. The waveform shown is the filtered voltage recorded using the DSP. A minimum value of 10 volts is set to prevent division by zero when the inverter is not powered. Also, the floating capacitor voltage can be controlled very well during a load change. Fig. 3.38 and 3.39 shows the floating capacitor voltage during load step up and down. The voltage shown is the unfiltered sampled data. The harsh spike should be the noise instead of actual voltage spike on the capacitor.

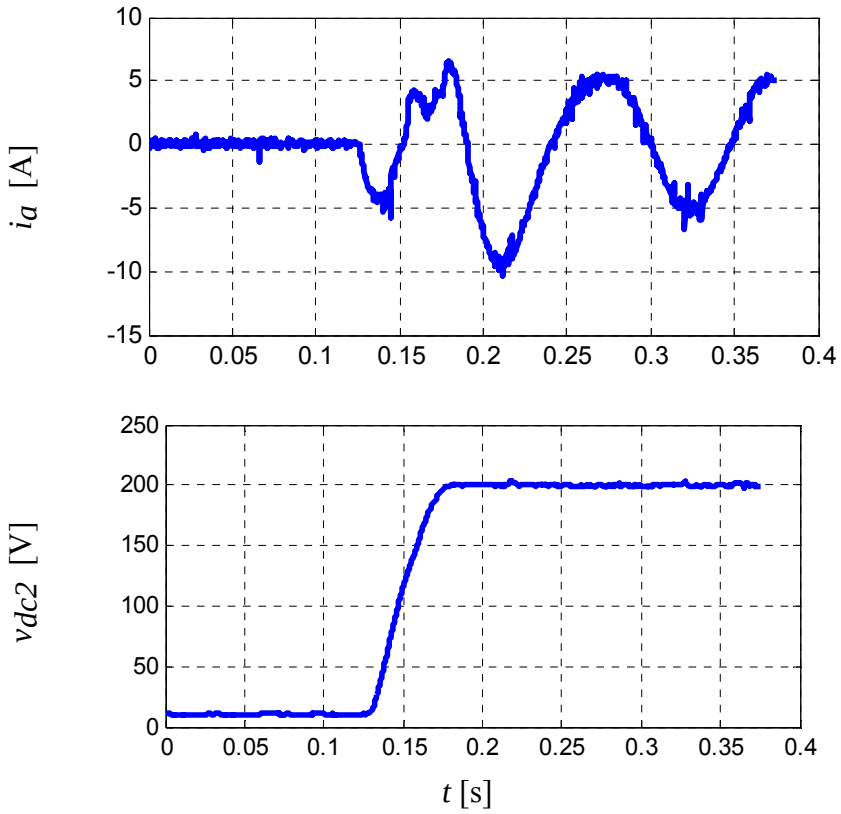

Fig. 3.37 Measured charge of floating capacitor during transient

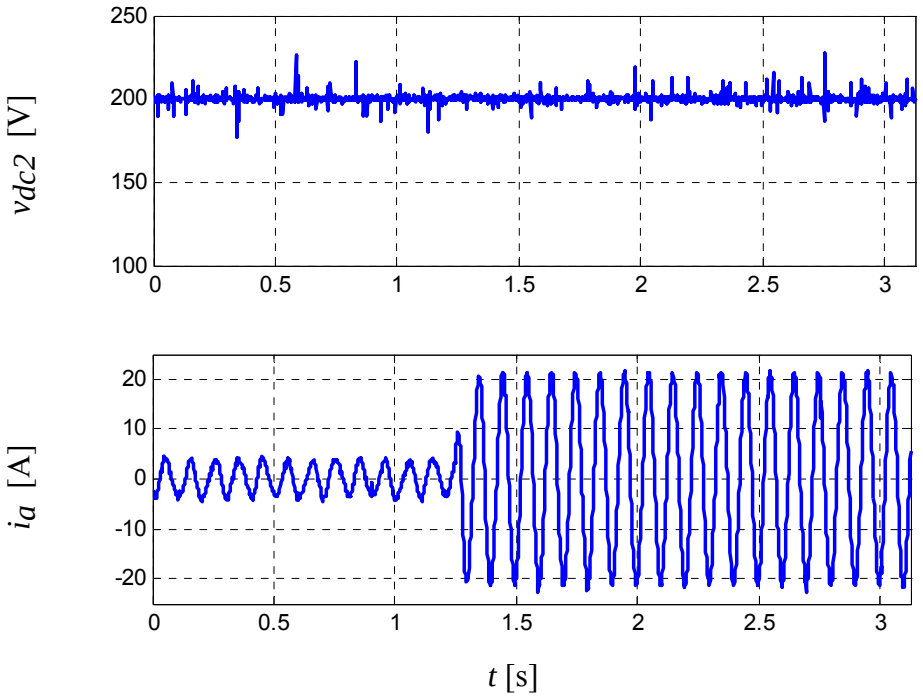

Fig. 3.38 Floating capacitor voltage control during transient with increase in load

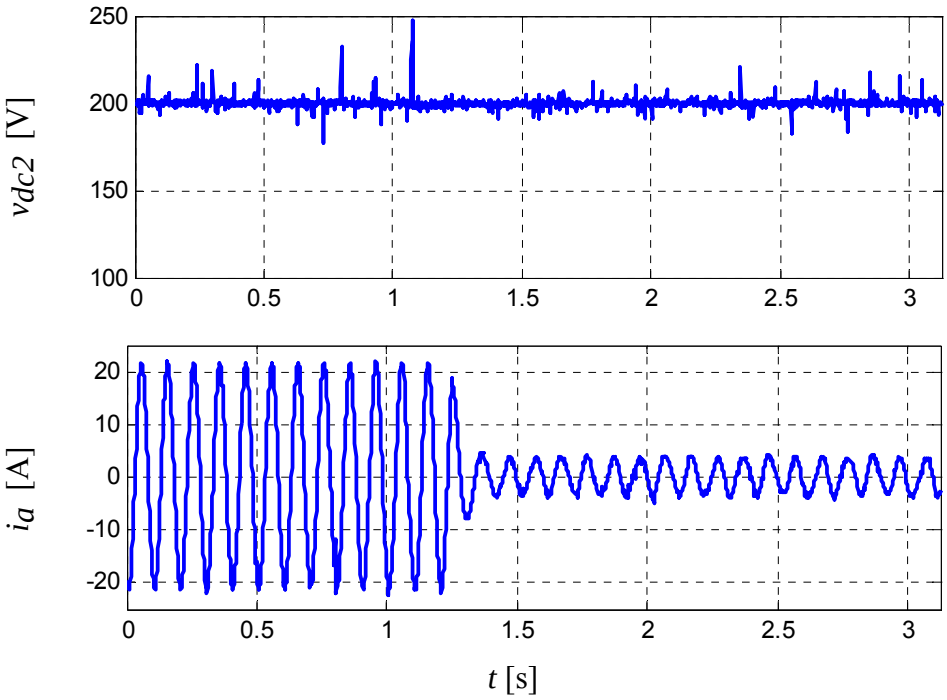

Fig. 3.39 Floating capacitor voltage control during transient, sudden decrease in load

The power-speed and torque-speed curves, when INV2 is sized differently, have been obtained by experiment as well. Each of the point on the curves is a steady state operating point. The results are compared with the single 2-level inverter drive in Figs. 3.40 and 3.41. The theoretical calculation shown in previous section is also plotted for comparison. As predicted, the power capability of the motor is improved considerably in the high speed region. In the theoretical prediction, an ideal model was used. Therefore, the nonlinear effect like saturation was not taken into account. Moreover, the iron losses and mechanical losses were ignored. These are the major factors that contribute to the difference between the experimental results and the theoretical prediction.

The transient responses during acceleration are also compared for different sizes of INV2. The motor accelerates until the drives reach their limits. Fig. 3.42 provides the comparison. The results show that the maximum speed is about twice compared to the single 2-level inverter drive when INV2 is sized to be 1 per unit.

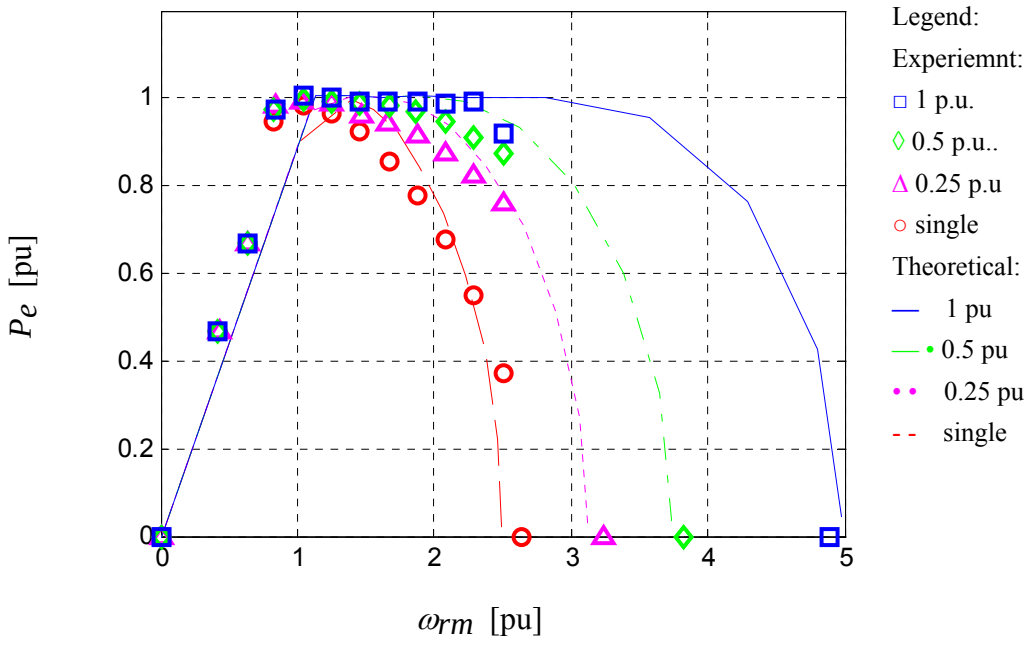

Fig. 3.40 Measured power-speed curve for different INV2 ratings

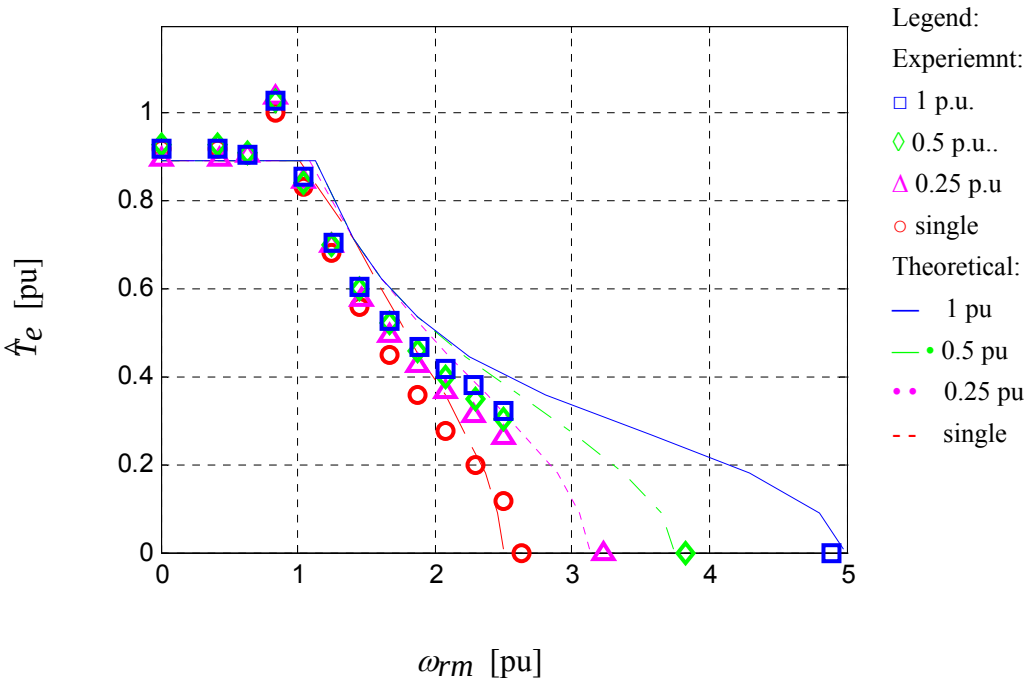

Fig. 3.41 Measured torque-speed curve for different INV2 ratings

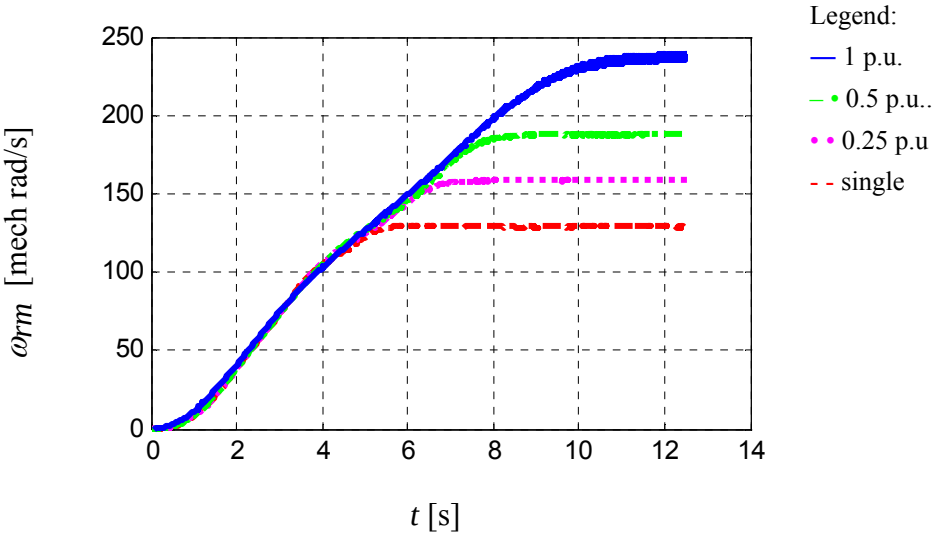

Fig. 3.42 Comparison of measured ramp speed response in experiment

3.8. Summary

In this chapter, a dual inverter open-winding IPM machine drive is proposed. The auxiliary inverter was used to supply only reactive power to the machine. The DC bus of the auxiliary inverter is simply a floating capacitor. By series compensation, the operating space of the motor can be expanded when power is obtained from a fixed voltage power supply. The sizing of the auxiliary inverter has been discussed. The applicability of the proposed method to other PMSM was also discussed. The impact on excitation voltage of using the proposed topology was presented. The proposed drive and control method has been verified both by simulation and experimental studies.

Chapter 4

Series Compensated Open-Winding PM Generator Wind Power System

4.1. Introduction

For the past few decades, renewable energy has been important supplement to traditional energy source such as coal and natural gas. Among all the renewable energy sources, wind is the most accepted. By the end of 2009, the world wide installed capability is 159.2 gigawatts [88]. In the U.S., 10,010 megawatts of generating capacity was installed in 2009, representing 30% of all U.S. electricity generation capacity addition of the year [89,90].

An open-winding PM machine based wind power generation system is proposed in this chapter. A series connected VSI is used to control the generator power and improve the generator utilization when a diode rectifier is used with PM generator. Both constant speed and variable speed operation are considered. The proposed topology is able to improve the generator utilization and reduce the total cost of the system. In addition, the proposed wind power system shows the potential of maximum power point tracking (MPPT) in variable speed operation.

4.1.1. Common Wind Technologies

Before introducing the proposed series compensated wind power system, common wind power technologies are briefly reviewed in this section [91,92]. The first

successful commercial wind generation system is the constant speed squirrel cage induction generator (SCIG, also known as the Danish concept). Today, they are still a very large portion of the total wind power installed capability. The generator is connected to the gird through a transformer. Stall control or pitch control are usually used with gear box to keep the rotor shaft speed nearly constant. As shown in Fig.4.1 (a), a soft starter is used to reduce inrush current when the generator is connected to the grid. AC capacitors are often used to supply the reactive power required by the induction generator. Capacitor banks are switched in and out for different operating points. The advantages of this topology include low cost and robustness of generator. However, there is no control of the generator, leading to poor wind power capture and low generator utilization.

Would rotor induction machine with variable resistor shown in Fig.4.1 (b) is similar to the fixed speed SCIG. However, there are external variable resistors connected to the rotor circuit. By varying the resistance in rotor circuit, the speed of the shaft can be controlled in a small range to improve wind power harvest, usually 10% above the synchronous speed. Soft starter and local var support are still needed in this type of wind power systems.

Doubly fed induction generator (DFIG) is the most popular wind power topology at the moment. Fig.4.1 (c) shows the DFIG topology. Instead of connecting resistor to the rotor circuit, a back-to-back AC/DC/AC converter is employed. The size of the converter is only about 30% of the system rated power. By controlling the frequency in the rotor circuit, the turbine is able to run at both sub-synchronous and super-synchronous speed. Typically, the rotor speed is allowed to vary in the range of -40% to 30% of synchronous speed. By adding a fractional sized converter, real and reactive power can be individually controlled. There is no requirement of external soft starter or capacitor banks. However, DFIG requires slip rings to transfer power and/or reactive power to the rotor circuit, which reduces the reliability of the overall system.

Wind generation systems with full rated power converters are becoming more popular in recent years. Fig.4.1 (d) shows a wind power system with full rated active power converter. SCIG, wound field synchronous generators, PM synchronous generators can all be used with a full rated power converter. The turbine speed is allowed to vary in a wide range. The shaft speed can be controlled according to the wind speed for optimal wind power capture. Real and reactive power supply to the grid can be individually controlled. Direct drive becomes possible by employing high pole number generators which could potentially eliminate the high cost gear box and improve the reliability of the overall system. In addition, less maintenance is required for such a system compared to a DFIG system. The only disadvantage is the high cost associated with the full rating power electronic converters. It can be predicted that this type of wind power system will become more popular due to its advantages in the future.

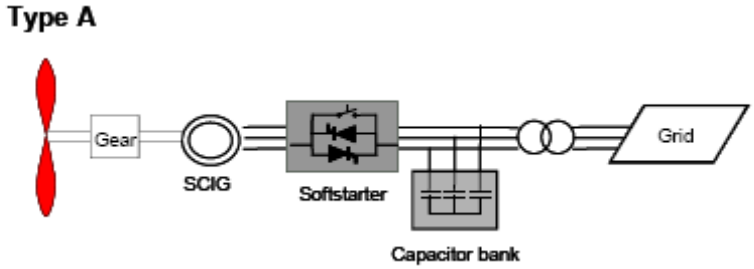

(a) Fixed speed SCIG

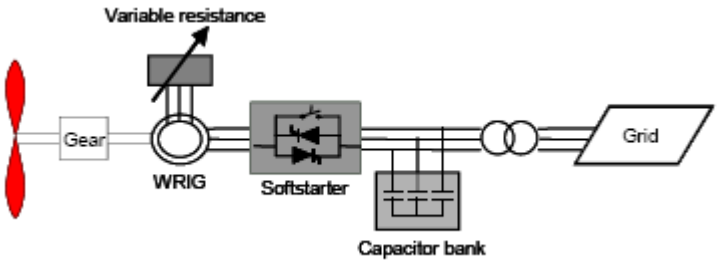

(b) Variable speed wound rotor induction generator with variable resistor

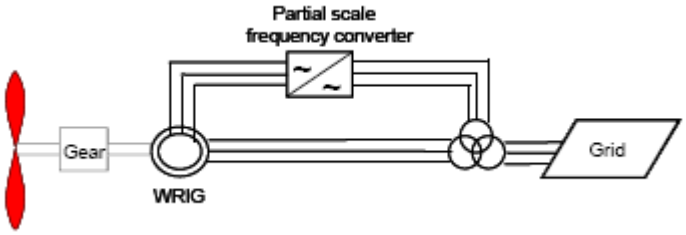

(c) DFIG

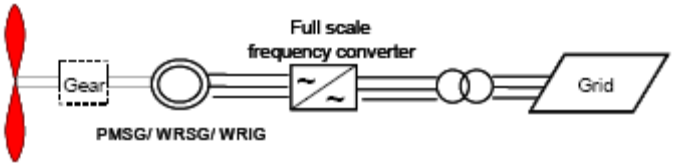

(d) Variable speed, full rated power converter

Fig. 4.1 Common wind power system topologies [90]

4.1.2. Generator under Utilization in Diode Rectifier Wind Power System

Synchronous machine wind power system based on diode rectifier is a low cost alternative to the fully controlled PWM rectifier. However, this type of system has not

seen wide applications in practice. One of the main reasons is that the generator usually delivers less than rated power under rated excitation in such a system.

The voltage drop on synchronous reactance increases as the load current increases. When a diode rectifier is used for the power conversion, the generator will see underutilization. It is convenient to first consider a non salient round rotor synchronous generator or a SPM generator with a diode rectifier. The generator current is in phase with the terminal voltage V_S (180 electrical degrees out of phase by motor convention) ignoring the small amount of reactive power the diode bridge needs for commutation. A phasor diagram can be draw as shown in Fig.4.2. The resistance of the generator is ignored. Since the displacement power factor is close to unity for the diode rectifier, the generator voltage vector will be perpendicular to the voltage drop on the synchronous reactance. Therefore, the generator excitation voltage and the voltage drop on the synchronous reactance have to intersect on the semicircle shown on the phasor diagram when the generator operates at a constant rotor speed. The generator current can be controlled by adjusting the DC side voltage of the diode rectifier when the system is equipped with a DC chopper. However, the generator power does not always increase when the generator current increases. The range of power adjustment is limited. Moreover, the generator current will always lags the generator back-emf. The generator will not be able to deliver rated power at rated current and voltage. In other words, some reactive power is required for the machine to generate rated power at the rated excitation. In wind power systems, the generators are installed in the towers high above the ground. The power density of the generator is a very important factor that determines the cost of construction and installation. Generator underutilization is certainly undesirable for this reason.

Another major factor that stops people using diode rectifier with a DC/DC chopper for wind power is that although there is only one active power electronics switch shown in the schematic, the DC/DC boost converter has to handle the full rated power. In

addition, a high power inductor may be required if the machine inductance is not large enough. Such an inductor will significantly increase the weight and cost of the system.

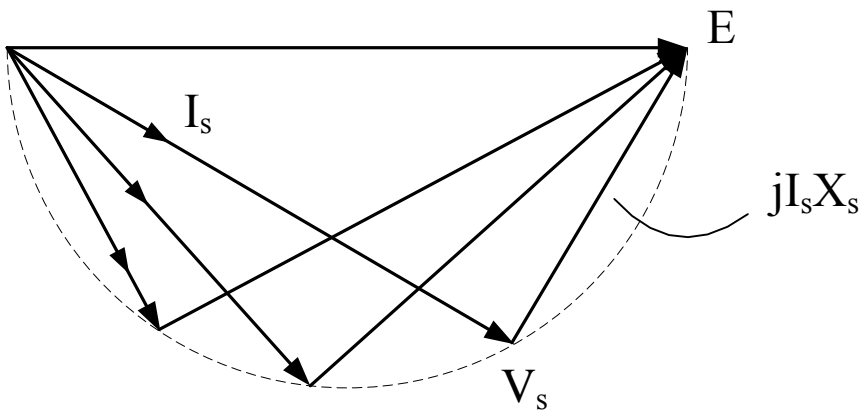

Fig. 4.2 Phasor diagram for wind power system with diode rectifier and DC chopper

4.2. Proposed Topology

An open-winding PM machine based wind power generation system is proposed in this chapter to overcome some of the disadvantages of the conventional diode rectifier based wind power system.

The topology proposed in this chapter is shown in Figure. 4.3. An open-winding PMSG is used with an uncontrolled diode rectifier and an auxiliary fractional sized compensating VSI. The generated real power is rectified by the diode bridge. The auxiliary inverter is used for both generator control and generator utilization improvement. The DC side of the auxiliary VSI is connected to a floating capacitor. A separate PWM VSI is used as the grid side inverter to regulate the main DC bus voltage. Gearbox can be used to increase the generator speed for higher generator power density.

Like the SSSC, the auxiliary inverter is a series compensation device. It can be controlled as a variable three-phase impedance. If the injected voltage is leading the generator current by 90 degrees, the inverter is effectively a three-phase inductor. On

the contrary, the inverter is effectively a three-phase capacitor if the injected voltage is lagging the current by 90 degrees. The DC bus of the auxiliary inverter is simply a DC capacitor with no connection to a power source. The compensation DC bus voltage can be controlled by the inverter. When the injected voltage has a component that is in phase with the current, the compensation DC bus voltage will be increased. In contrast, the compensation DC bus voltage is reduced when there is a component that is 180 degrees away from the current. This component can be considered as resistance or negative resistance from the circuit point of view. If energy storage is desired, the energy storage element can be attached to the DC bus of the auxiliary inverter so that the auxiliary inverter is also used as an interface to the energy storage. There is no requirement for a separate DC/DC converter and the voltage of the energy storage can be different from the main DC bus.

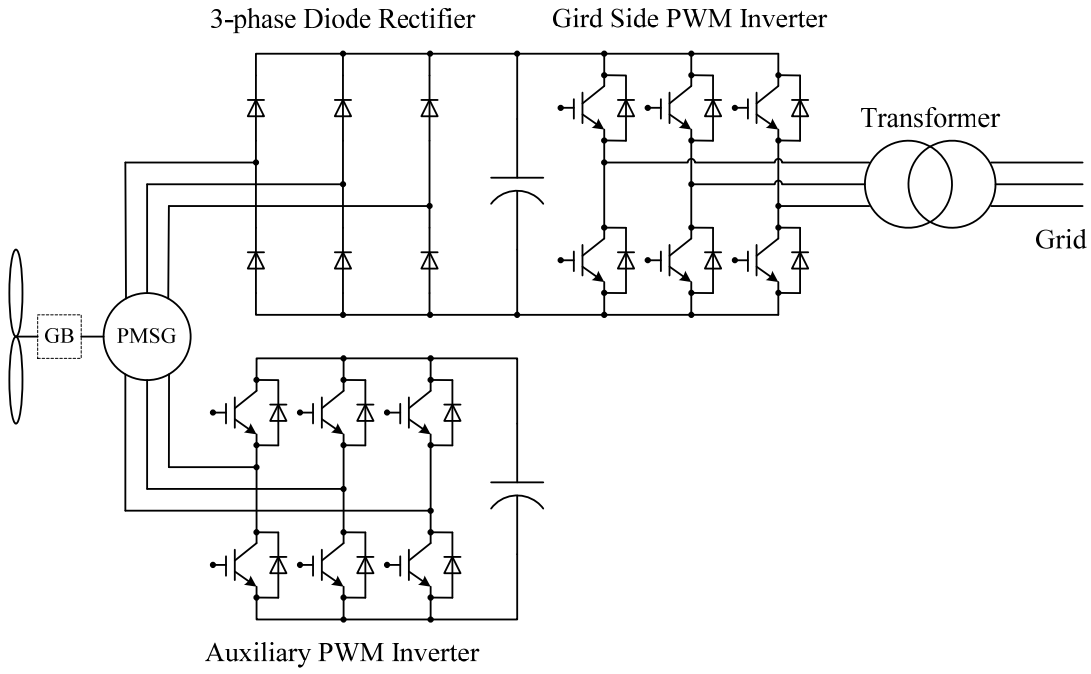

Fig. 4.3 Proposed open-winding PM wind generation system

4.3. Operation Principle

The basic operation principle is discussed in this section. It is convenient to first explain the operating principle by using a simple non-salient generator, for instance a surface permanent magnet (SPM) generator. A single-line diagram is shown in Fig. 4.4. E, V_{rect}, V_{com} are generator back-emf, rectifier voltage and compensation VSI voltage. The AC side voltage of the diode rectifier V_{rect} is equal to the vector sum of the generator voltage V_S and the compensation voltage V_{com}.

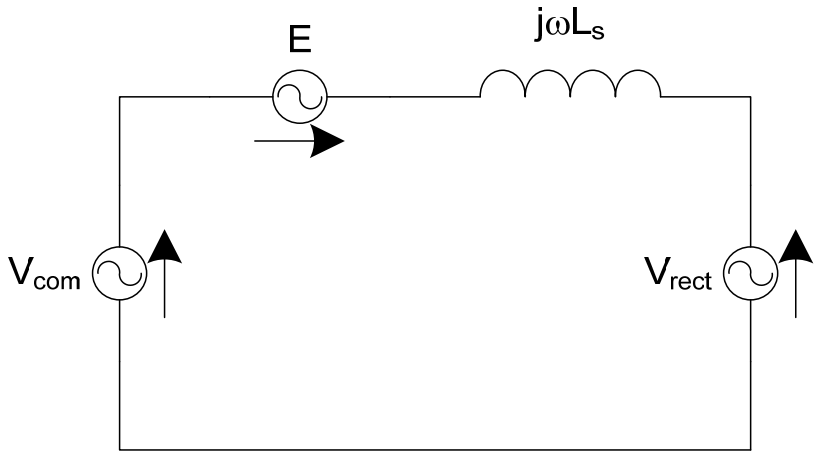

Fig. 4.4 Single line diagram of the proposed system with a non salient generator

Assuming the compensation is purely reactive and ignoring the generator resistance, the power flow into the rectifier can be calculated as:

$$P_S = \frac{3V_{rect}E}{X_S}\sin(\delta) + \frac{3V_{rect}V_{com}}{X_X}\cos(\frac{\delta}{2}) \quad (4.1)$$

Where δ is the power angle defined as from the back-emf E to the rectifier voltage V_{rect}. The generated power can be controlled by varying the compensation voltage. If the current is continuous, the rectifier operates at unity displacement power factor, i.e. the current is in phase with the voltage fundamentally. The phasor diagrams of a lossless non-salient generator with and without compensation are shown in Fig. 4.5.

When the compensation voltage completely cancels the voltage drop on the synchronous reactance, the generator operates on its MTPA curve. When the compensation is capacitive, the generator power is increased and when the compensation is inductive, the generator power is reduced.

For some machines, the synchronous reactance may be very large. It will require a very large converter to compensate for the optimal operation. The compensation voltage can be sized smaller than voltage drop on synchronous reactance. The generator utilization will still be improved although it will not be optimal.

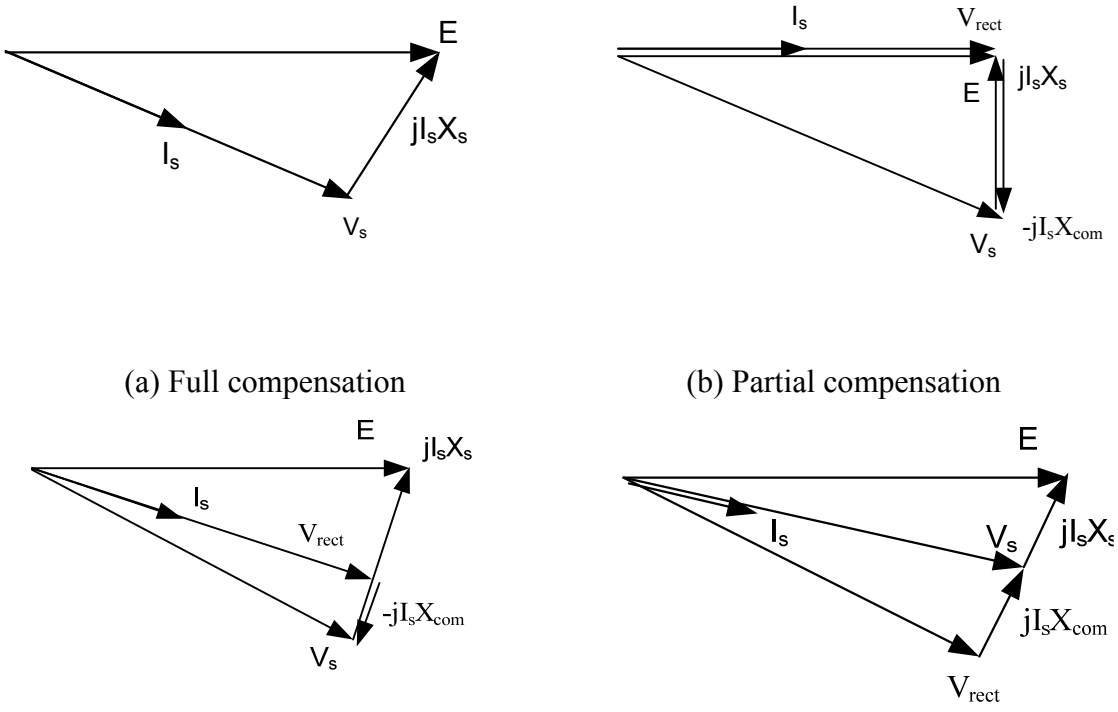

Fig. 4.5 Phasor diagram for capacitive compensation

For a salient IPM generator, it is not possible to construct a simple single line diagram as for a SPM generator. However, the relationship between the compensation voltage and generator power is similar to that of a SPM generator. A phasor diagram

can still be drawn for a salient-pole generator. Fig. 4.6 shows the phasor diagram for an IPM generator in the proposed system. In both salient and non-salient generator cases, the compensation voltage vector is perpendicular to the current vector to ensure pure reactive compensation.

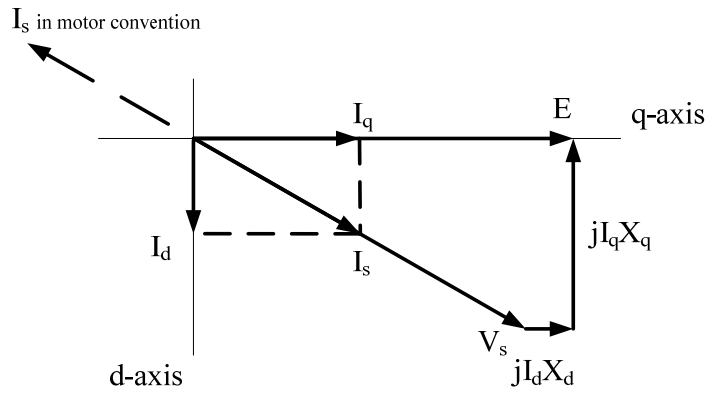

(a) No compensation

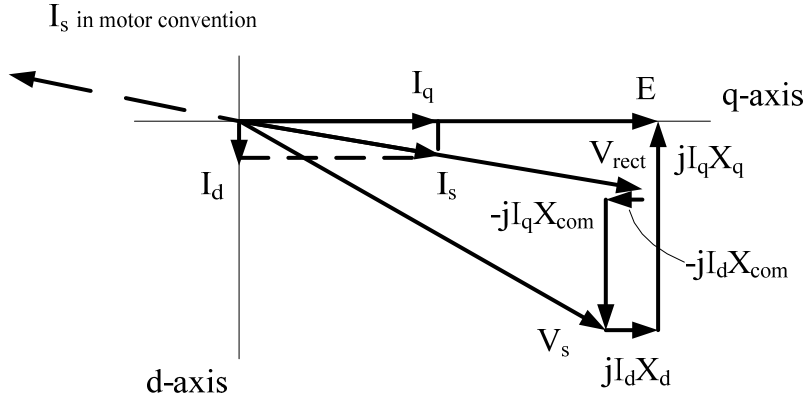

(b) Capacitive compensation

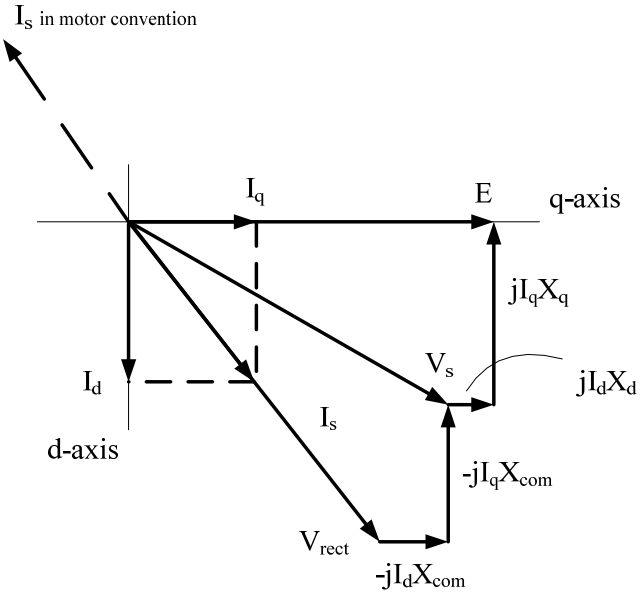

(c) Inductive compensation

Fig. 4.6 Phasor diagram for IPM in proposed wind power system

4.4. Inverter Sizing

4.4.1. Var Requirement for the Lab Scale Generator

In the proposed wind power generation system, the compensation inverter only supplies reactive power to the generator. Therefore, the reactive power needed by the machine determines the size of the PWM inverter. This section investigates the sizing of compensation inverter. Since the inverter is in series with the generator, it will carry rated machine current in the worst case.

Although the proposed system is applicable to both salient and non-salient generators, a lab scale salient IPM generator which is used for later study is considered here. The parameters and ratings of the generator under investigation are listed in Table. 4.1 for reference.

Table 4.1 Machine parameters and ratings

Parameter	Description	Value
P_r	rated power	10 kw
V_r	rated voltage	115 Volts
I_r	rated current	29 Amps
f_r	rated frequency	34.5 Hz
ω_b	base speed	216.8 elec rad/s
r_s	stator resistance	0.315 Ohm
L_d	d-axis inductance	16 mH
L_q	q-axis inductance	51 mH
λ_m	permanent flux linkage	0.75 wb
P	number of poles	4
V_{dc}	main DC bus voltage	200 V
$Vccom$	Compensation DC bus voltage	100 V

The AC side voltage of diode rectifier is difficult to calculate exactly because of the commutation and variance of conduction angle under different operating conditions. An approximation is used here. The three-phase machine currents are assumed to be

continuous. In this case, the generator phase voltage waveform of a diode rectifier for a constant DC bus voltage will look like the one shown in Fig.4.7.

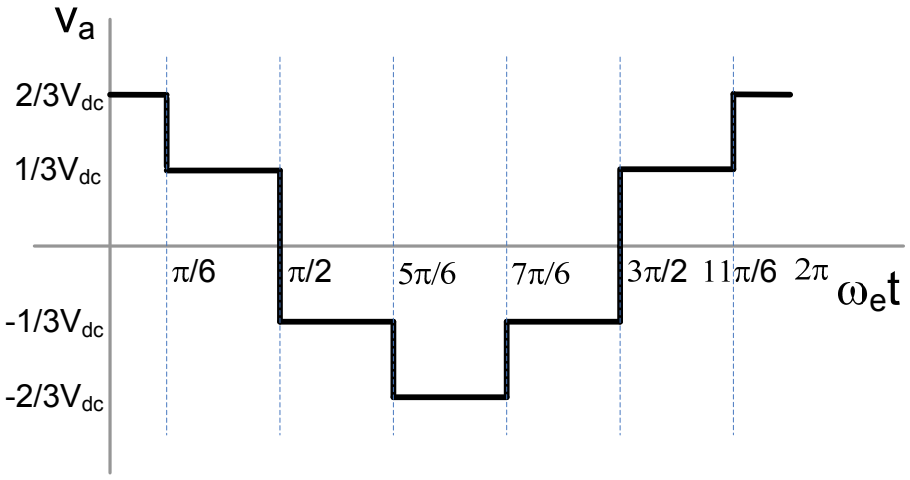

Fig. 4.7 Ideal AC side voltage of diode rectifier

The root-mean-square value can be calculated from the waveform by:

$$V_{rectrms} = \sqrt{\frac{1}{2\pi}\int_{0}^{2\pi} v_a^2(\theta)d\theta} \tag{4.2}$$

The fundamental component can be calculated as:

$$V_{rect1} = \frac{1}{\pi}\int_{-\pi}^{\pi} v_a(\theta)\cos(\theta)d\theta = \frac{2}{\pi}V_{dc} \tag{4.3}$$

Since generated power is concerned, fundamental value is used to approximate rectifier AC side voltage V_{rect} in the calculation. When the current is continuous, the DC bus value determines the rectifier AC side voltage. Based on this assumption, the generated power is estimated for different level of compensation. This assumption is not always true because at low speed, the machine current may not be continuous. However, it is good enough for high speed operation in general. In the steady state, the time derivative terms in (2.1) can be eliminated. Ignoring the losses and assume unity

displacement power factor, (2.1) can be rearranged as (4.4) and (4.5).

$$- V_{rect}\sin(\delta) = - \omega_r L_q i_s \cos(\delta) + V_{com}\cos(\delta) \quad (4.4)$$

$$V_{rect}\cos(\delta) = - \omega_r L_d i_s \sin(\delta) + \omega_r \lambda_m + V_{com}\sin(\delta) \quad (4.5)$$

The power angle and current amplitude can be obtained by solving equations (4.4) and (4.5) numerically. The main DC bus voltage is set to 200 V and the fundamental component of a six step waveform is used as the rectifier voltage. The current and power angle values from numerical calculation are then used to obtain the generator power as a function of compensation voltage. Figure 4.8 shows the curve of generator power versus compensation voltage at different speeds for the 10 kW lab scale IPM generator (ideal lossless model is used). It can be seen from Fig. 4.8 that a compensation voltage of 20 Vpk is sufficient to shape the generated power within a reasonable range. The compensation inverter can be sized to be less than 30% of the rated power to control the power and rotor speed of the generator. It can even be sized smaller if desired. In the situation that the compensation voltage needed to operate the generator on MTPA curve is higher than the available voltage, the inverter can be kept at its highest output voltage, the generator power and utilization can still be improved compared to a diode rectifier only system.

Unlike the systems in the existing literature, the proposed system is capable of reducing generator power in addition to improving the generator power output. When the compensation is inductive, the generated power decreases. This feature enables the proposed system with the capability of maximum power point tracking (MPPT).

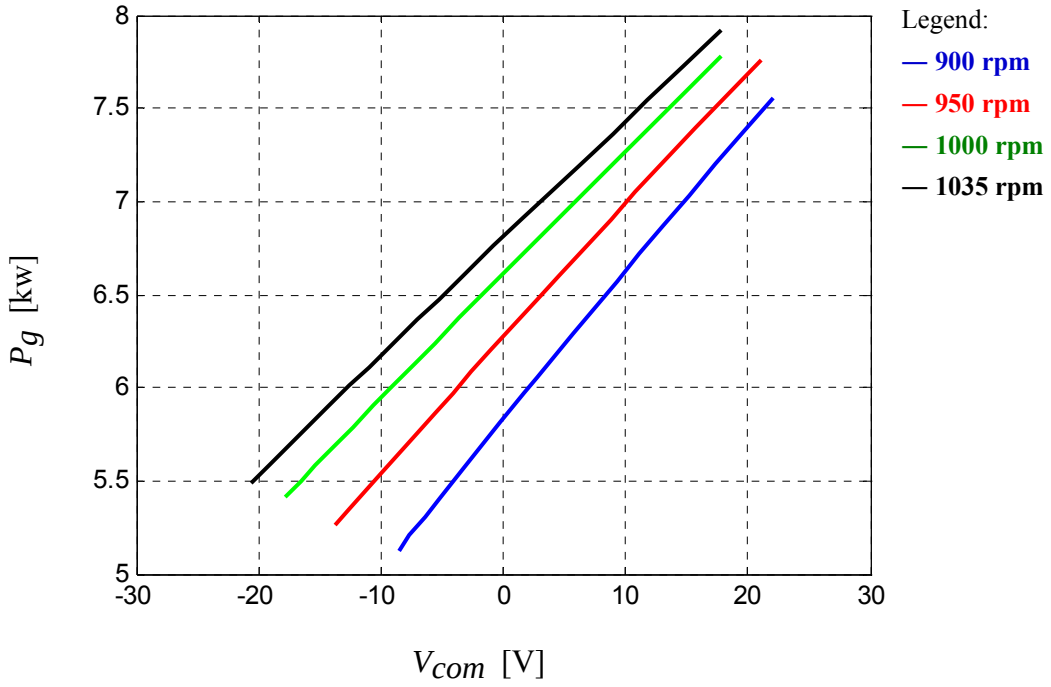

Fig. 4.8 Power vs. compensation voltage plot of proposed system with IPM generator

For a wound field synchronous machine, the inductance can be significant larger than PM generators. As a result, the inverter size will be larger when a wound field synchronous generator is used. However, compared to a fully sized active rectifier that has to handle both active and reactive power, the proposed system still has apparent benefit on converter cost. Moreover, unlike a DC chopper, the compensation inverter does not have to be sized for the worst case. It can be sized according to the condition that the system is mostly operated at. When more var is needed for the MTPA condition, the output of the compensation inverter is kept at its maximum value. The generator power could still be improve although it would not be optimal.

The power versus compensation var of the lab scale generator is plotted in Fig. 4.9 for several different speeds. For the generator used, only a small amount of reactive power would change the real power significantly.

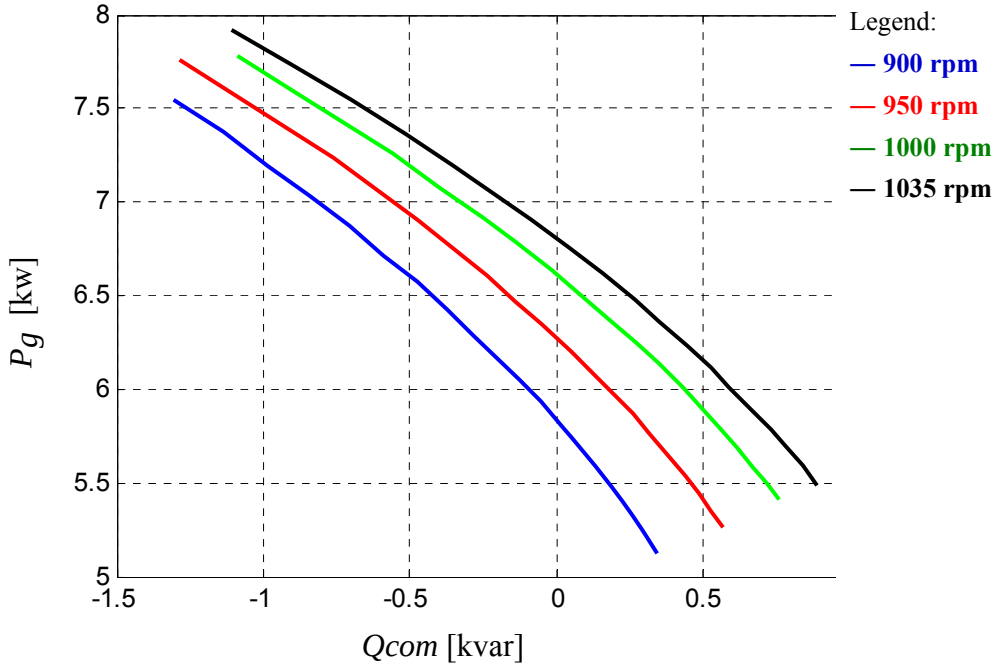

Fig. 4.9 Power vs. compensation var plot of proposed system with IPM generator

4.4.2. Generator Consideration

Although an IPM generator is used in this study, the proposed wind power generation system is applicable to both salient and non salient generators. However, generator parameters will certainly affect the sizing of the auxiliary inverter. In motoring operation, the normalized machine parameter plane is used to study the applicability of the series compensated open-winding PM motor drive in Chapter 3. The maximum available voltage is defined as the rated voltage. Nevertheless, when the generator is not driven by a fully controlled converter, the method could be inconvenient. For example, when the normalized permanent magnet flux linkage is low, the generator terminal voltage will be much smaller than 1 per unit. As a result, the open circuit voltage at rated speed is often defined as the rated voltage in generator convention. To compare the generators, another parameter plane is chosen here. The vertical axis is still the saliency ratio. But the horizontal axis represents the

characteristic current in per unit. The characteristic current is normalized to the rated current of the generator.

When a diode rectifier is used for the power conversion, the displacement power factor at AC side of the rectifier is unity. With a low power factor generator, the voltage rating of the compensation inverter will be very close to a fully controlled active converter, leaving the proposed topology with very little cost benefits. Therefore, a reasonably high power factor is needed for the proposed topology to be economically viable. In the following study, the characteristic current is chosen to vary from 0.8 to 2 per unit. A characteristic current lower than 0.8 pu is considered low for diode rectifier operation here. The saliency ratio varies from 1 to 7. Fundamental component is again assumed for the study.

The peak value of the generator back-emf has to be higher than the main DC bus voltage for diode rectifier to operate. A DC bus voltage that is lower would allow a wider operating range because the diode bridge could start to operate at a lower rotor speed. However, if the voltage is too low, the generator would not be able to deliver rated power at the rated current. The rectifier AC side voltage is chosen to be 0.7 per unit for the following analysis.

The power versus var curve is plotted for a series of generator designs in Fig. 4.10. Three speeds are used here and the power range chosen is roughly from 0.5 to 1 per unit. In the figure, a steeper curve indicates smaller change of reactive power is required to change the same amount of generated power. Negative and positive var represent capacitive and inductive compensation respectively. It can be concluded that the characteristic current has more apparent impact on the slope of the curves than the saliency ratio. In addition, higher saliency ratio tends to move the power-var curve towards the positive direction of the horizontal axis. The two parameters together determine the size of the compensation inverter for a given operating range. To minimize the compensation inverter, it is beneficial to have the compensation var

equally distributed around the vertical axis of the power-var curve for the system to utilize both inductive and capacitive compensation. Meanwhile, the slope of the curves must be steep as well. Another factor that affects the size of the inverter is the distance between the power-var curves at different speed in the horizontal direction. For the same operating speed range, the inverter can be sized smaller if the distances between the power-var curves are shorter in the horizontal direction.

Considering the factors above, a generator that needs a small size compensation inverter will be a design that has a characteristic current between 1 and 1.5 per unit. A saliency ratio about 3 will help decrease the size of the compensation inverter as well. Although generator with a higher saliency ratio would have a steeper slop on the power-var curve, it would need inductive compensation to prevent over current. Moreover, the var different is large for a generator with higher characteristic current.

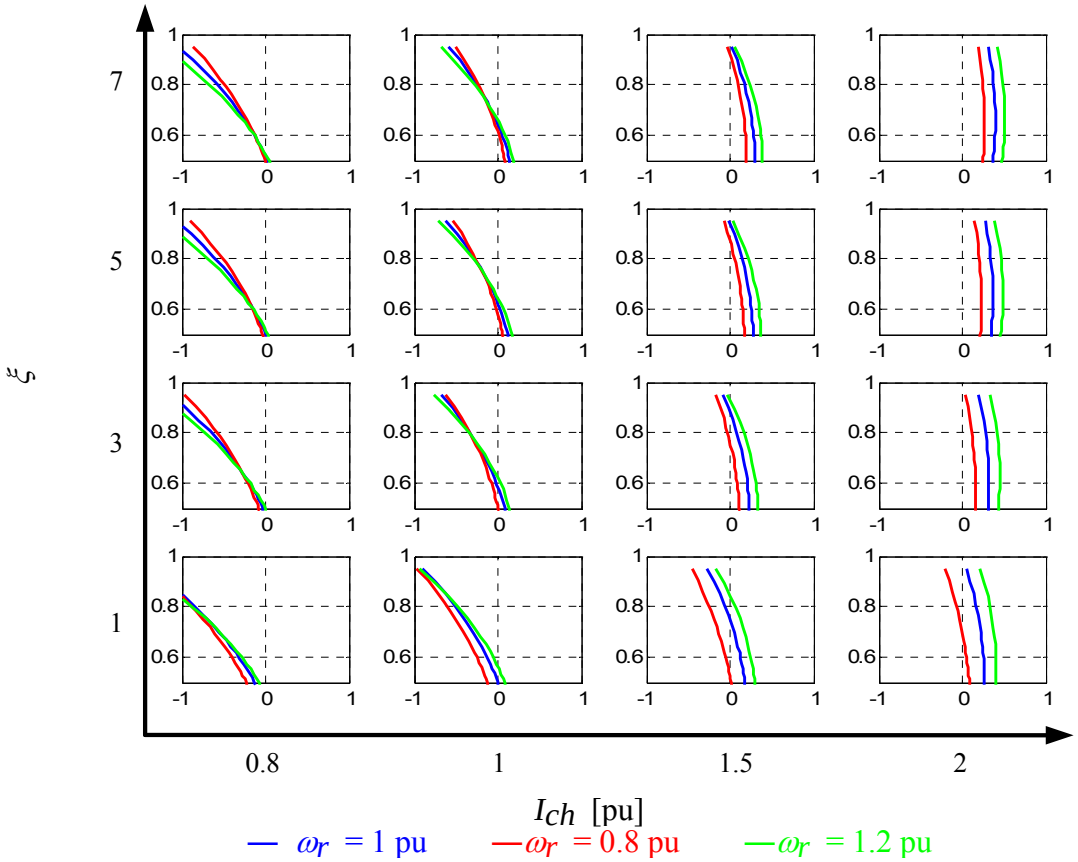

Fig. 4.10 P vs. Q for different generators

The same as the series compensated open-winding motor drive introduced in the Chapter 3, the compensation inverter in the proposed wind power system has to carry the full generator current because it is connected in series of the generator. Therefore, the compensation voltage will determine the size of the inverter. The power versus compensation voltage curves for the various generator designs are plotted in Fig. 4.11. Similar conclusions can be made as from the power-var curves.

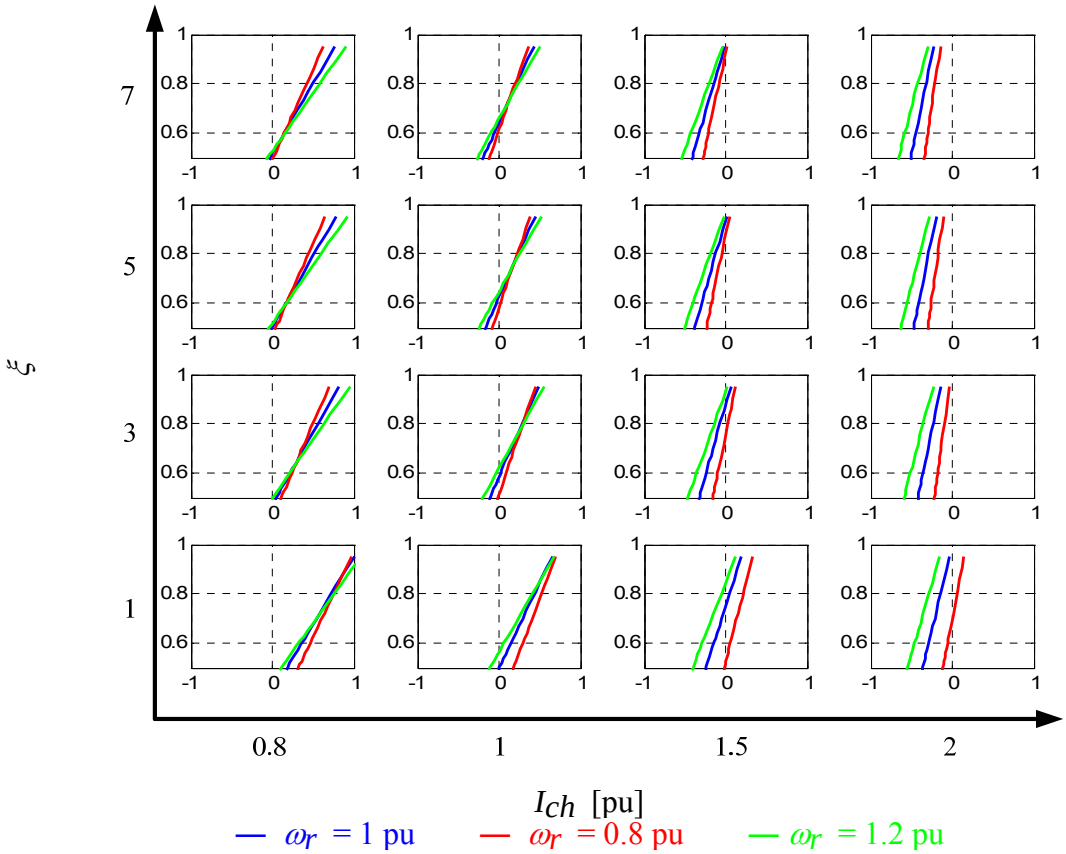

Fig. 4.11 P vs. Q for different generators

4.5. Control Method

The control method of the proposed wind power system is introduced in this section.

In the proposed system, the control of the grid side converter is the same as other topology utilizing standard active front end configurations. A field oriented controller that is synchronized to the grid can be used to control the real and reactive power separately. The controller can receive reactive power command from the grid and support the var required. The DC bus voltage can be controlled using an outer voltage loop to generate the real power command for the inner loop.

At the generator side, the diode rectifier is not controllable. The control of the

generator compensation VSI is discussed in detail here. In the existing literature [71-74], series compensation devices are used to counter the voltage drop on the synchronous reactance of the generator. The series compensation devices are controlled in the impedance mode. When a non salient generator is used with the proposed topology, this control method is certainly applicable. Nevertheless, the method is not directly applicable when a non salient generator is used. Series compensation is commonly used as a scheme for power flow control in the FACTS [51]. The proposed control method employs this concept and uses the estimated generator power as the control variable. This method is suitable for both constant and variable speed turbine systems.

4.5.1. Constant Speed Operation

The proposed system can be used in a constant speed wind power system. Pitch control and gear box could be used to keep the speed of generator rotor approximately constant. This type of wind power system is traditionally equipped with SEIG. As mentioned in the existing literature in Chapter 1, when a PM generator is used with a diode rectifier in such a system, the generator often sees under utilization issue. Some var is required by the generator to deliver rated power at rated excitation. The compensation inverter is controlled to provide the required reactive power to the generator for power improvement under constant speed operation.

As discussed in previous section, the generated power can be shaped by series compensation. With the compensation inverter, more current can be pushed through the diode rectifier without reducing the DC bus voltage. The generator utilization can be improved.

The block diagram of the controller for the proposed system with constant rotor speed is shown in Fig.4.12. The controller of the proposed system has two separate

parts, one controlling the compensation inverter and the other controlling the grid side inverter.

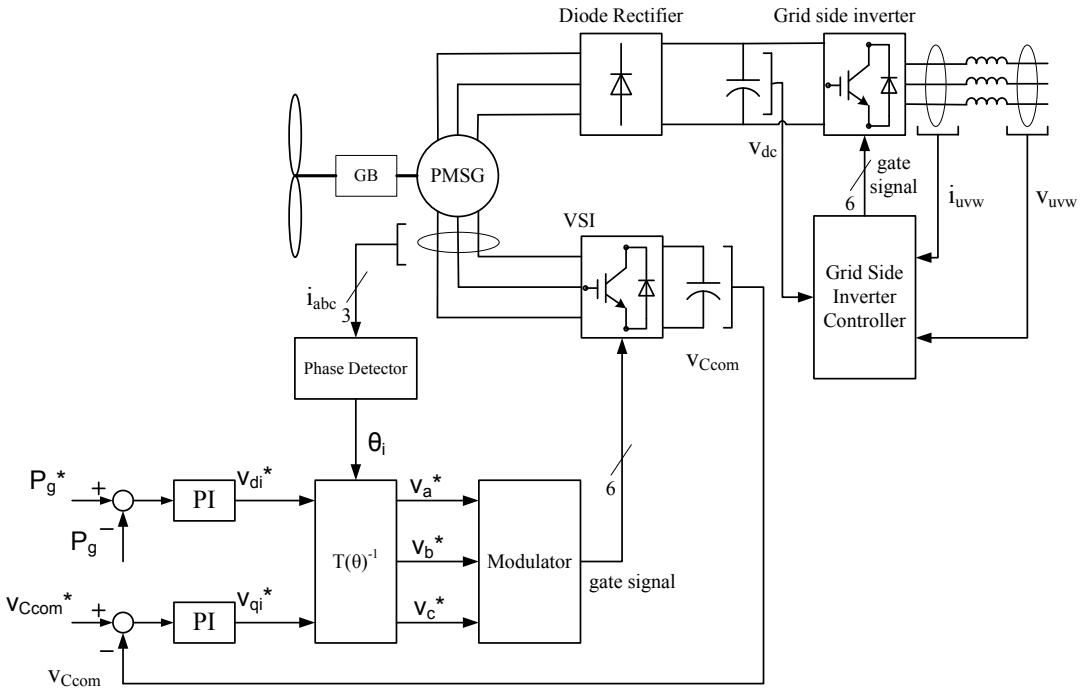

Fig. 4.12 Overall control system of fixed speed turbine

The compensation inverter only compensates for voltage. As a result, there is no current regulator needed. The controller of the compensation VSI is in the synchronous frame that is tied to the generator current, which means the q-axis is aligned with the peak of phase-A current. This reference frame is chosen so that it is easy to control the phase angle of the injected compensation voltage vector with respect to current vector. The two orthogonal components of the compensation inverter voltage vqi, vdi control the real and the reactive power of the compensation VSI. The real components of the VSI voltage vqi is then used to control the floating capacitor voltage. A simple proportional-integral (PI) regulator is used in the capacitor voltage controller. As shown in Fig. 4.8, the reactive compensation voltage has a roughly linear relation with the generator power assuming constant rotor speed and rectifier AC side voltage. Therefore,

another PI regulator is used to control the generator power by varying the reactive component of the VSI voltage.

The generator current can be highly nonlinear due to the diode rectifier. To obtain a smooth current vector angle for compensation VSI control, a current phase locked loop (PLL) can be used as the current phase detector. A PLL in synchronous reference frame is shown in Fig.4.13. The PI regulator forces the output angle to track the peak of phase a. In steady state, the q-axis will align with the peak of phase a current. The PLL is capable of filtering out the error generated due to the current nonlinearity. This property is especially useful when a diode rectifier is used. But there is also potential issue when applying PLL to detect current phase angle. Unlike in the power systems, the amplitude of current is not constant. The PLL gain values that are optimal for heavy load may not be optimal for light load operation. On the contrary, gains that are good for small current will result in degradation in the transient performance. Another advantage of using a current PLL is that the controller does not require any position sensors or complicated position estimation scheme because the control of generator power is only based on current vector angle.

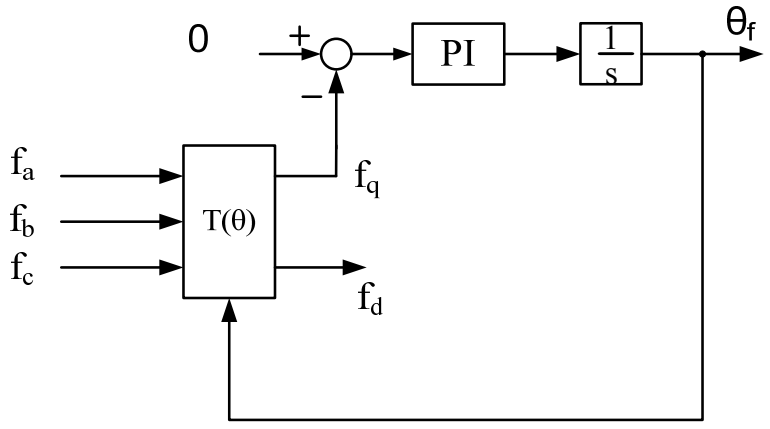

Fig. 4.13 PLL in synchronous reference frame

An alternative method is directly calculating the current phase angle from current

value in rotor reference frame. As shown in Fig.4.14, rotor position sensor is required to transfer the stator phase current into rotor frame. The angle θ_{ir} is the difference between current angular position and rotor position. The rotor position is added to the angle θ_{ir} to obtain current angle. Compared to current PLL, using motor position angle is more accurate. But all the nonlinearity in the current waveform is carried through the calculation. As a result, the calculated current angle will be less smooth than that obtained by a current PLL.

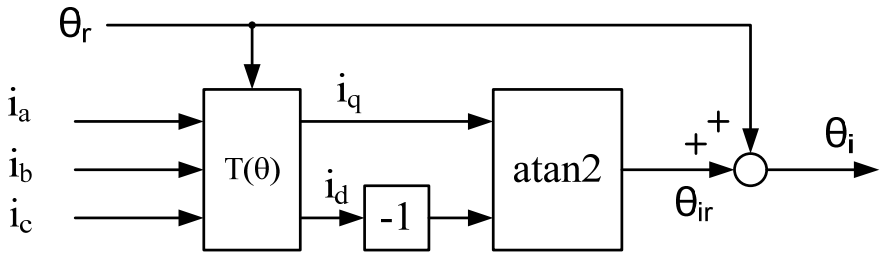

Fig. 4.14 Current phase detection using encoder

The generated power can be obtained by measuring the voltage and current at the main DC bus. However, measuring the power at the main DC bus requires extra current sensors. Instead, the generated power can be estimated from the measured generator current and main DC bus voltage. The assumption made is that the generator current is continuous. The generated power is directly calculated from the measured current and AC side voltage of the diode rectifier.

The voltage command in current d-q reference frame is then transformed back into stationary abc reference frame and sent to a modulator which determines the gate signal of the power electronics switches.

4.5.2. Variable Speed Operation

Compared to constant speed wind power systems, variable speed wind turbines have many advantages. For example, the speed of turbine can vary as the wind speed

and torque change. As a result, the stress on the gear box and other mechanical components can be reduced. Moreover, the power output fluctuation can be reduced. In addition, better wind power harvest is achieved by varying the turbine speed.

The proposed topology is applicable in a variable speed turbine system as well. Compared to the more conventional topologies like the back-to-back PWM VSI or diode rectifier with a DC/DC chopper, the proposed topology is able to operate with PM synchronous generator in a variable speed turbine system equipped with only a fractional sized active converter.

It can be shown that the power of wind passing through a given cross-sectional area is (4.6):

$$P_{wind} = \frac{1}{2} \rho A v_{wind}^{3} \tag{4.6}$$

Where ρ is density of the air, A is the cross section area (πR_{blade}^{2}) and v_{wind} is the wind speed.

The mechanical input power of the turbine can be calculated as:

$$P_{mech} = C_p P_{wind} \tag{4.7}$$

The coefficient C_p is a function of turbine design and tip speed ratio, which can be defined as:

$$\lambda = \frac{\omega_{rm} R_{blade}}{v_{wind}} \tag{4.8}$$

Theoretically, a maximum of about 50% of the wind power can be captured by the wind turbine. A typical power coefficient as a function of tip speed ratio plot is shown in Fig.4.15.

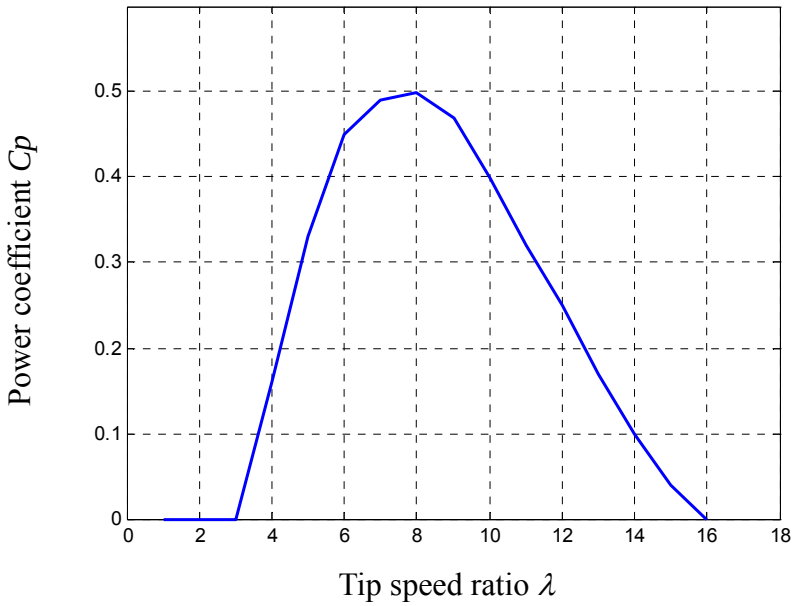

Fig. 4.15 Typical power coefficient vs. tip speed ratio

The maximum power that can be extracted from a wind turbine is loosely in a cubic relationship to the wind speed. In the proposed system, generator power is used as the control variable. The most straightforward method for a variable speed control will be using a look-up table extracted from the turbine design. The power command can be determined using the measured wind speed as shown in Fig. 4.16. MPPT is possible using this method.

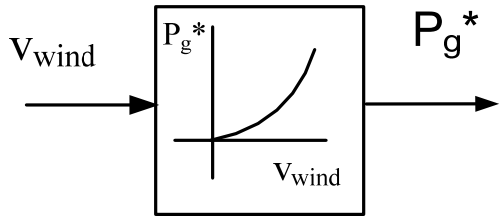

Fig. 4.16 Variable speed operation by look up table

Controlling the turbine speed to match the optimal tip speed ratio is another common way of maximize wind power harvest of a single wind turbine. The turbine speed can be controlled by the rectifier to match the optimal tip speed ratio (TSR). In

the proposed topology, the speed of the generator rotor speed can be controlled by varying the generator power. At a certain speed and torque level, the turbine speed can be increased by decreasing the generator power. In contrast, increasing generator power will decrease the speed. Therefore, an outer speed loop can be added to the constant speed turbine controller. As shown in Fig. 4.17, the speed controller will generate the generator power command that is sent to the inner power loop.

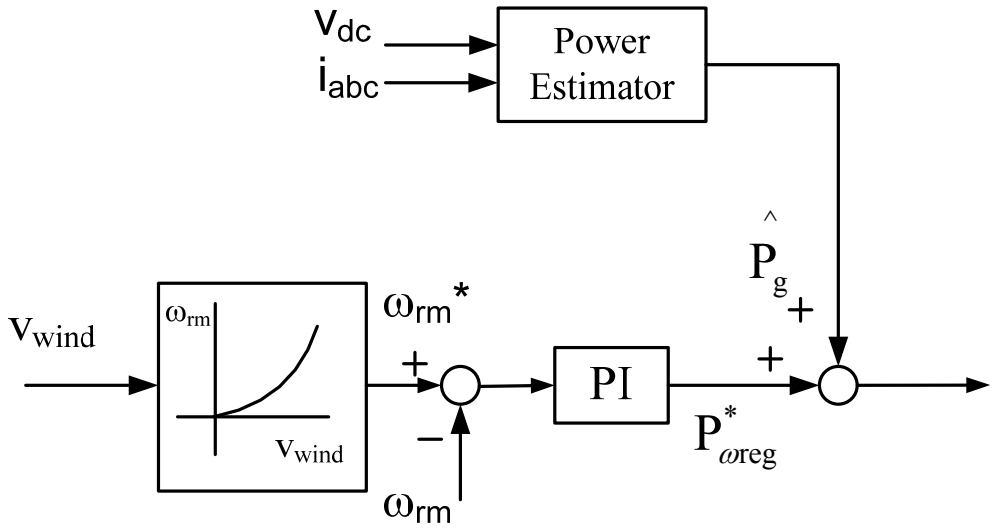

Fig. 4.17 Variable speed operation by Speed Control

The two inner loops are the same as that in a constant speed turbine system. One PI controller controls the compensation DC bus voltage and the other PI controller shapes the generator power. The generator power is again estimated by measured generator current and main DC bus voltage.

It should be noted that the speed controller is not a high performance vector controller. The d and q-axis current cannot be independently controlled by the proposed method. The performance of the proposed controller is not comparable to a full active converter based topology. In addition, the operating speed range is another limitation of the proposed system. The rotor speed has to be high enough for the diode rectifier to

operate. However, wind turbines usually start to operate beyond the cut in speed. With proper design, the proposed wind power system would have a reasonable operating range.

4.6. Simulation Study

The proposed system is simulated with the Matlab/Simulink and PLECS blockset package. The lab scale generator is used in the simulation. The simulation results are presented here.

4.6.1. Constant Speed Operation

For the constant speed operation, the rotor speed is set to its rated value, 108.4 mechanical rad/s. The main DC bus voltage is 200 V. The compensation DC bus voltage is 100 V. The power command is set to 6.5 kw. The phase current waveforms before and after compensation are shown in Fig. 4.18 and Fig. 4.19.

It can be seen from Fig.4.18 that the generator current is not continuous without compensation. The waveform is regular diode rectifier type of waveform. The amplitude is about 10 ampere. As shown in Fig. 4.19, the current can be greatly increased with reactive compensation enabled. The current amplitude increased to about 25 Ampere. Moreover, the current is continuous. Compared to the assumption that the current is continuous, the power improvement is even better than the theoretical prediction.

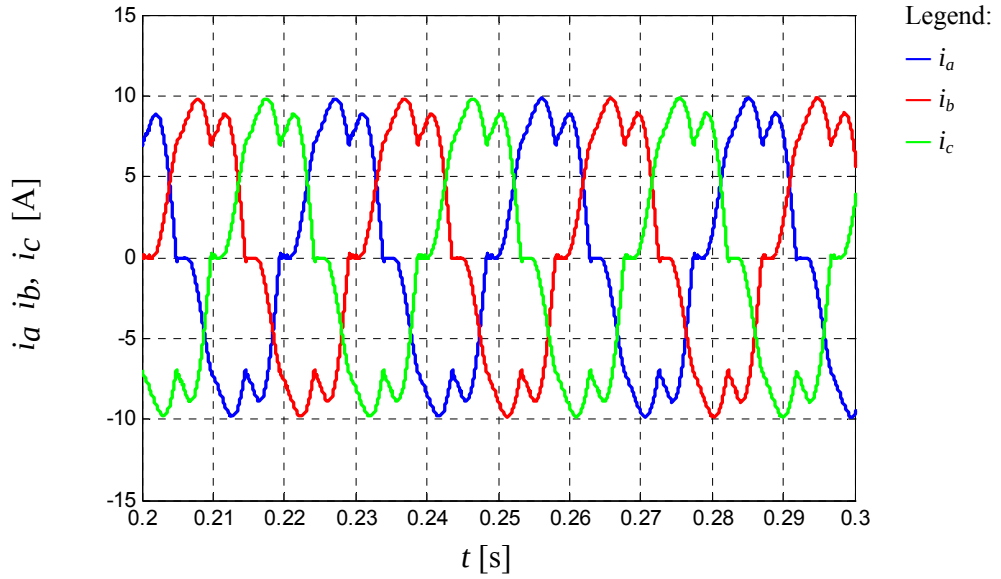

Fig. 4.18 Current waveform without compensation

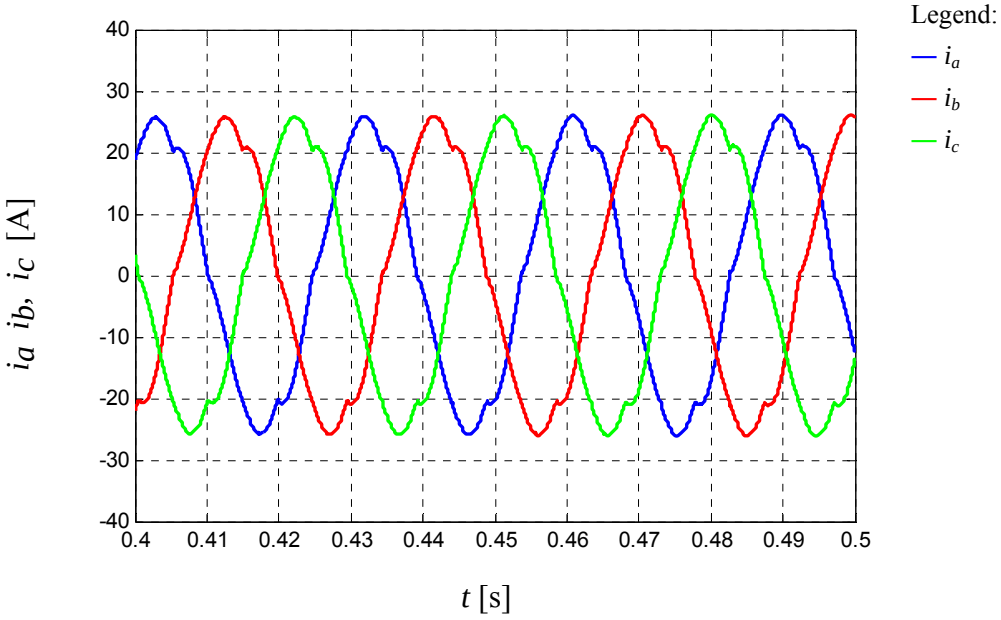

Fig. 4.19 Current waveform without compensation

Fig. 4.20 to 4.22 show the simulation results before and after the compensation controller is enabled. The power control by compensation is enabled at 0.3 second. Fig. 4.20 (a) shows the generator phase current. The current starts to increase after the power controller is enabled. Unlike the wind power system using a diode rectifier and DC/DC boost converter, the current increase actually indicate an improvement in

generated power. Fig. 4.20 (b) is the waveform for compensation voltage command. Same as in theoretical prediction, the compensation voltage required to change generated power is quite low. In steady state, the peak value of compensation voltage is only around 10 Volts. Fig. 4.20 (c) shows the compensation DC bus voltage. The floating capacitor voltage can be controlled at its nominal value during the transient.

Fig. 4.21 (a) and (b) are the waveforms of torque and generator power, respectively. The torque is shown in motor convention. After 0.3 second, both the torque and power increase. The controller is able to keep them nearly constant in steady state. The power generation is improved by reactive power compensation.

Fig. 4.22 shows the current in rotor reference frame. The currents are shown in motor convention. Both d-axis and q-axis currents increase in negative direction after the controller is enabled. The ratio of the two components changes as well, indicating and shift in current vector angle.

The presented simulation results demonstrate that the proposed method is able to improve generated power and generator utilization in a diode rectifier PM generator constant speed wind power system.

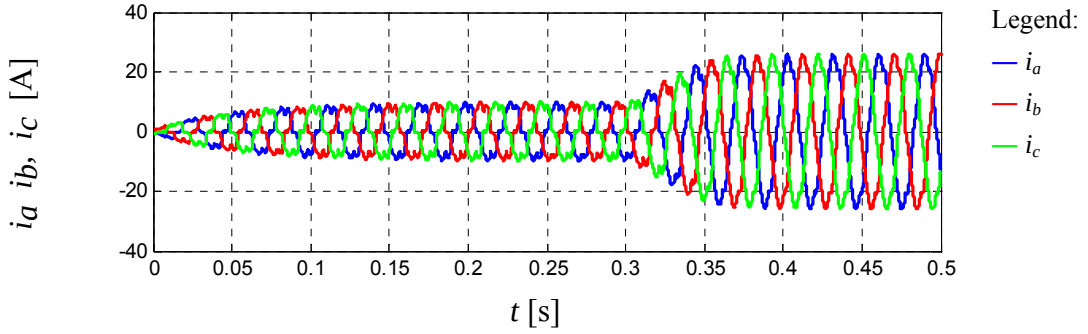

(a) phase current

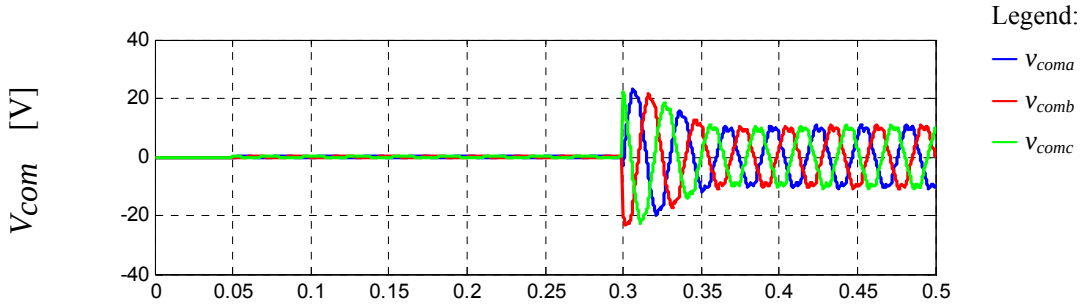

(b) compensation phase voltage

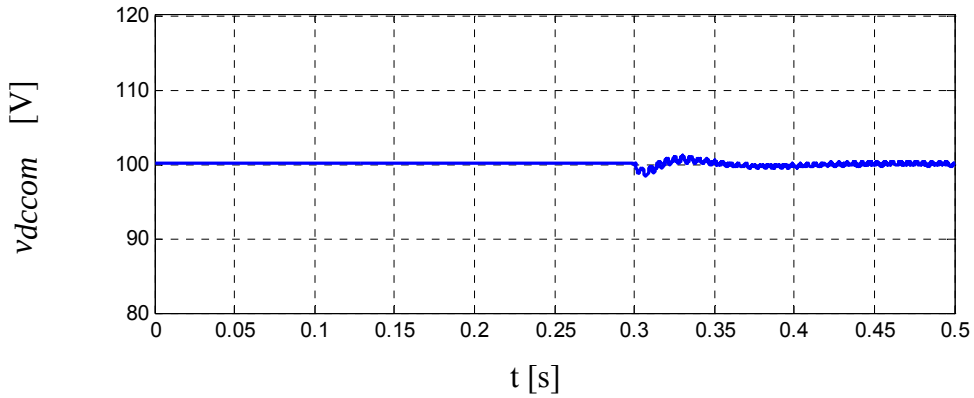

(c) compensation DC bus voltage

Fig. 4.20 Constant speed turbine transient simulation results, current and voltage

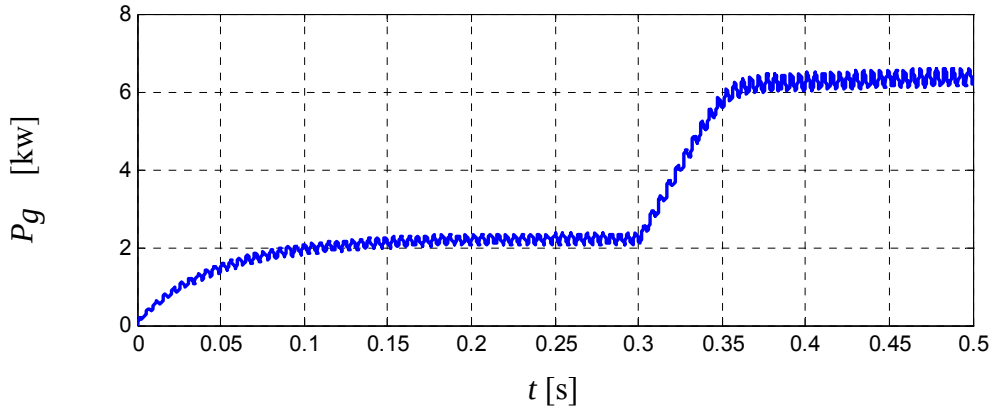

(a) generated power

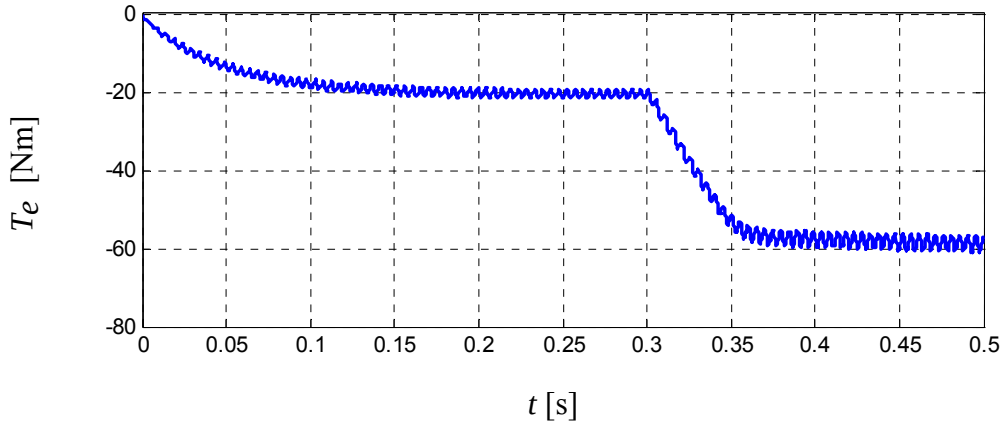

(b) generator torque

Fig. 4.21 Constant speed turbine transient simulation results, power and torque

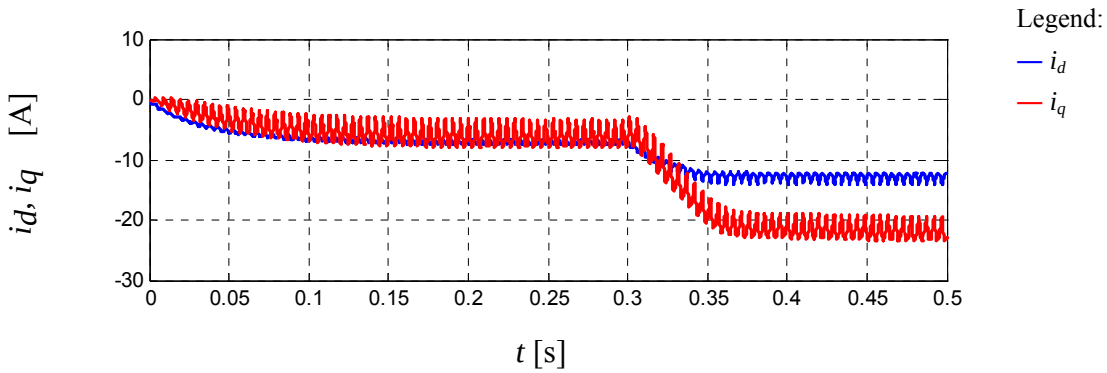

Fig. 4.22 Constant speed turbine transient simulation results, current in rotor reference frame

4.6.2. Variable Speed Operation

The variable speed turbine system is simulated with Matlab/Simulink and PLECS block set package as well. To demonstrate the capability of controlling the rotor speed, a simple constant torque of 40 Nm is applied to the shaft of the generator. The command changes from 120 mechanical rad/s to 100 mechanical rad/s at 0.5 second.

The results are shown in Fig. 4.23. Fig.4.23 (a) shows the rotor speed overlaid with its command. It can be seen the speed is able to loosely follow its command. Considering the controller is not a decoupled vector controller, the performance of the speed regulator is acceptable. Fig. 4.23 (b) is the generator power with its command. Same as in a fixed turbine system, the power controller performance is very good considering it is done by reactive power compensation. The increased power represents the need of energy to change the speed of the turbine. Fig. 4.18 (c) illustrates the generator torque. As expected, the generator torque increases in the negative direction to decelerate the turbine when the commanded speed changes. It returns to the previous value in the new steady state.

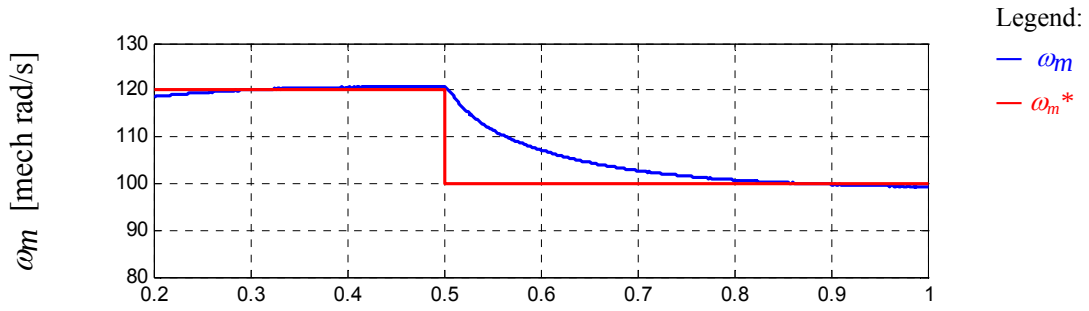

(a) rotor speed

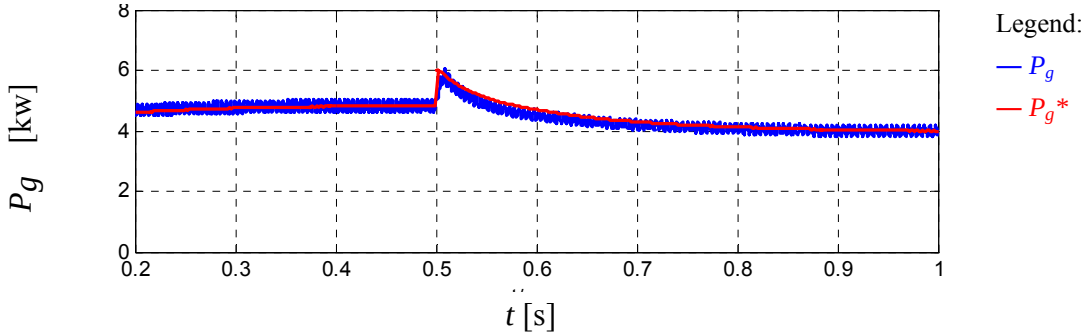

(b) generated power

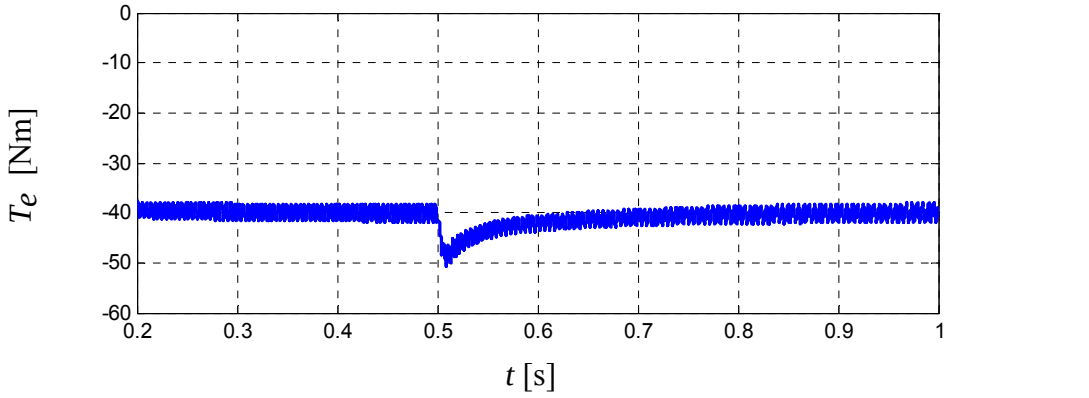

(c) generator torque

Fig. 4.23 Variable speed operation transient simulation results, speed, power and torque

Fig. 4.24 (a) shows the generator phase current during the transient. The amplitude of the current increases immediately after the speed command step is applied. This is due to the desired increased generator torque to slow down the rotor. The amplitude of the current decreases as the speed goes down because the back-emf of the generator also decreases. Fig. 4.24 (b) gives the current waveform in rotor d-q reference frame.

The currents are in motor convention. It is apparent the angle of current vector changes in the two steady states. It worth to point out that the generated power is different for the two cases but the torque is the same. Fig. 4.24 (c) shows the compensation DC bus voltage. The compensation DC bus voltage is well regulated through out the transient.

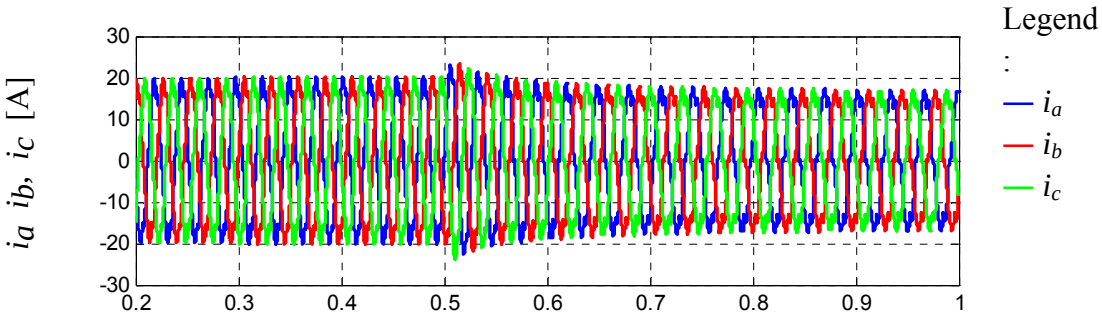

(a) phase current

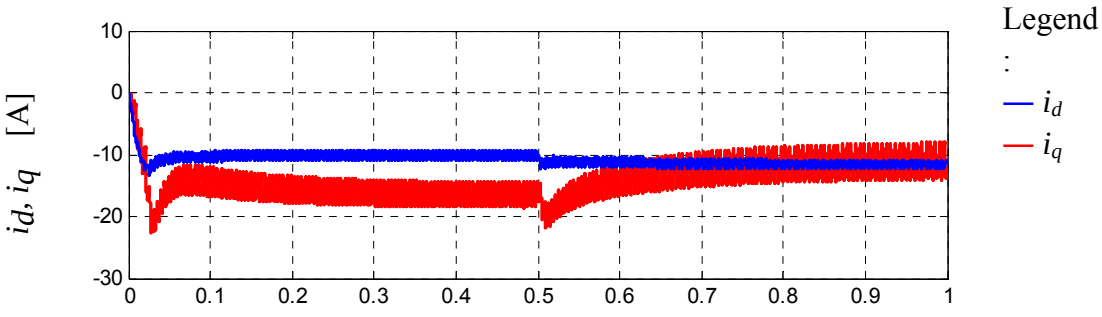

(b) compensation phase voltage

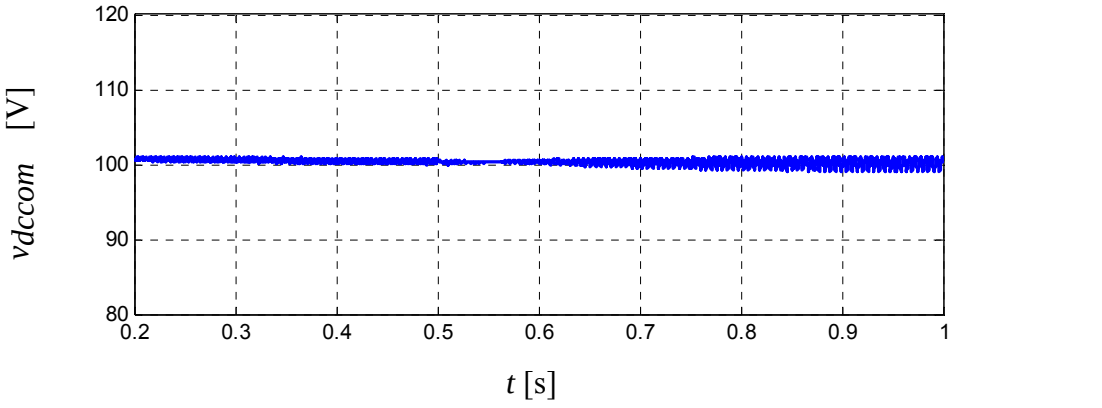

(c) compensation DC bus voltage

Fig. 4.24 Variable speed operation transient simulation results, current and voltage

The simulation results show that the proposed topology is applicable to variable speed wind power system. The proposed control method can control the speed of the turbine with a reduced size active inverter. With the ability to control the speed of the turbine, the topology has the potential capability of MPPT operation.

4.7. Impact on Harmonics

A major concern of diode rectifier based wind power system is the low order harmonics introduced by the nonlinear rectifier. It increases the losses in the generator and also creates torque ripple.

The voltage waveform of the generator is in a six step fashion when a diode rectifier is used. With the compensation inverter, there is a PWM component added to the phase voltage waveform. Examples of the generator phase voltage with and without compensation are compared in Fig. 4.25. The switching frequency is assumed to be 30 times of the fundamental frequency in the example. The compensation DC bus voltage is half of the main DC bus voltage.

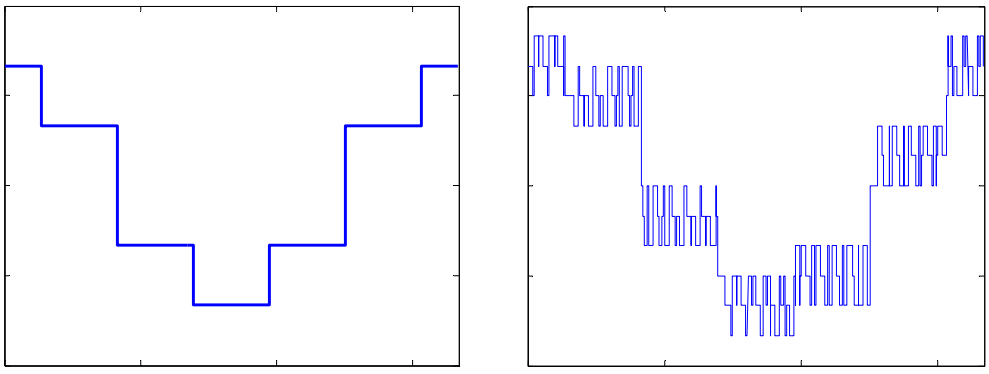

(a) uncompensated voltage waveform (b) compensated voltage waveform

Fig. 4.25 Comparison of phase voltage waveform, floating DC half

The spectrum of the two waveforms is compared in Fig. 4.26. As expected, the harmonics exist in the vicinity of the switching frequency and its multiples.

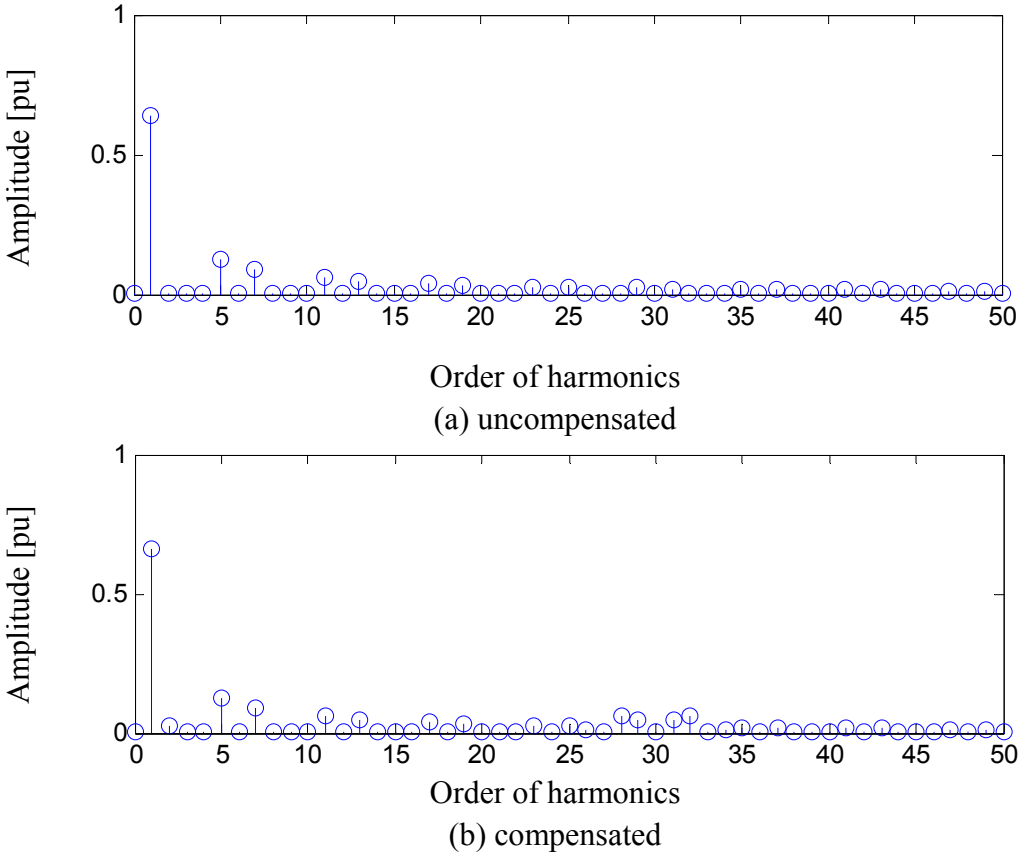

Fig. 4.26 Comparison of Spectrum of uncompensated and compensated generator voltage

Harmonics in current waveform is more important when considering the losses and torque ripple. To investigate the impact of compensation inverter on the current harmonics, the lower order harmonics of phase a current are plotted in Fig.4.27. The waveforms are taken from the simulation results of system with constant speed turbine. Because the current changes from discontinuous to continuous, the 5^{th} and 7^{th} harmonics in fact are improved. The absolute value of 11^{th} and 13^{th} harmonics increased slightly. But considering the increase in fundamental, the ratio of harmonics over fundamental actually decreases.

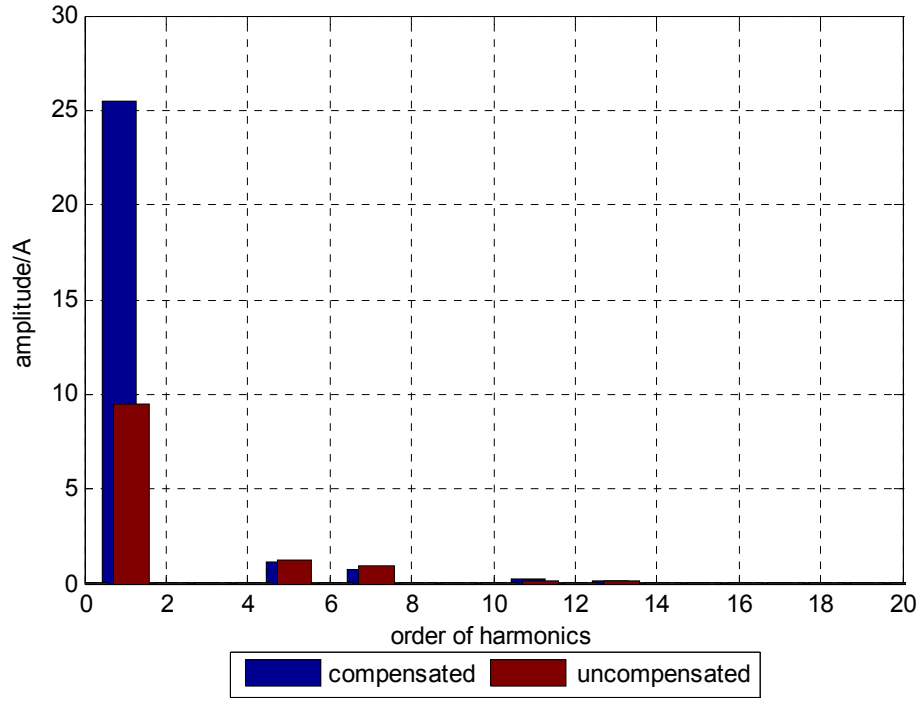

Fig. 4.27 Comparison of current lower order harmonics

The total harmonic distortion (THD) is an important measure of current waveform quality. There are different definitions of THD. The one that is used here is:

$$THD = \frac{\sqrt{\sum_{k=2}^{\infty} i_k^2}}{i_1} \tag{4.9}$$

The THD of the two considered cases are listed in Table.4.2.

Table 4.2 Current THD

Condition	**THD**
Compensated	5.44%
Uncompensated	16.30%

It is apparent if the current changes from discontinuous to continuous, the THD reduces greatly. However, in variable speed application, if the compensation is inductive as the speed needs to be increased, the compensation may result in a worse

discontinuity in current waveform. Nevertheless, there should be less inductive compensation compared to capacitive compensation if the control system is designed to avoid generator underutilization.

All the estimation above is based on the assumption that there is no filter in the system. In practice, filters can be used to reduce the harmonics in the current waveform if desired. But filters bring extra cost and weight to the system.

Based on the analysis above, compensation by auxiliary PWM inverter does not have a negative impact on current harmonics. Most of the time, it tends to improve the current waveform quality by reducing the discontinuity in the waveform.

The reason lower harmonics are not desired in the current is that they generate torque ripple and shorten the lifetime of mechanical parts in the drive train. In wind application, the torque varies greatly due to the change of wind speed. The torque on the shaft is not smooth at all. Therefore, the power train in a wind generation system is more immune to the torque ripple issue compared to other applications.

In addition to waveform quality, current THD can also measure the copper losses in the system. However, the copper loss in the generator due to each current harmonic is proportional to the square of the amplitude. Therefore, a 10% THD leads to only about 1% increase of copper losses compared to pure sinusoidal current.

In short, the current harmonics of the proposed system is not nearly as good as a full PWM rectifier because an uncontrolled diode bridge is used as the main power conversion devices. However, the impact should be bearable in smaller size wind application. Considering the cost reduction in power electronics converter, the proposed topology could be a good alternative to full power rated PWM rectifier.

4.8. Experimental Study

The IPM machine used in the previous Chapters is used for experiment studies. An inverter and a rectifier are built in the lab. For easy verification, a DC chopper and a load resistor is used to control the rectifier DC bus voltage at 200 V.

The power versus compensation voltage curve in steady state is obtained experimentally and plotted in Fig. 4.28. The relationship between power and compensation voltage is not as linear as theoretical prediction shown in Fig. 4.8. The errors at lower speed are quite apparent. However, a similar monotonically increasing trend can be observed. It is worth to mention that the theoretical prediction did not considered the effects like saturation and iron losses. The assumptions that the generator current is continuous and generator voltage is six-step are not accurate in practice, either. Moreover, the main DC bus voltage in the experiment is only control by a DC chopper. As a result, the main DC bus voltage is not as constant as in the theoretical calculation. All of these factors lead to the errors shown in the power versus compensation voltage curve.

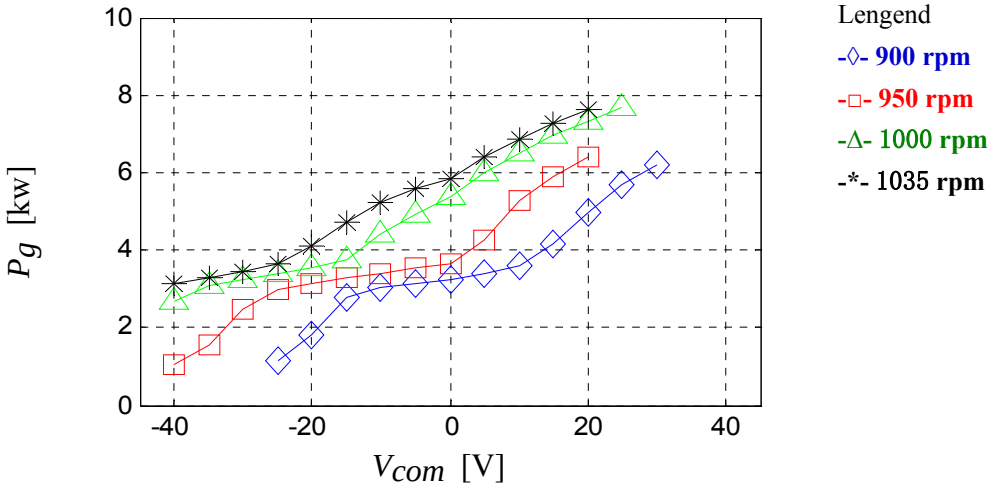

Fig. 4.28 Power vs. compensation voltage plot of proposed system with IPM generator obtained by experiment

The voltage and current waveforms in steady state are shown and compared in Fig. 4.29 and 4.30. The generator speed is kept at 900 rpm by the dynamometer. Fig. 4.29 shows the waveforms for the uncompensated case. The phase voltage is a 6-step waveform. In Fig. 4.30, the compensated phase voltage has a PWM component on top of the 6-step waveform. The power command is 6 kw for the compensated case. The current amplitude is increased compared to the uncompensated case. As a result, the power output of the generator is improved.

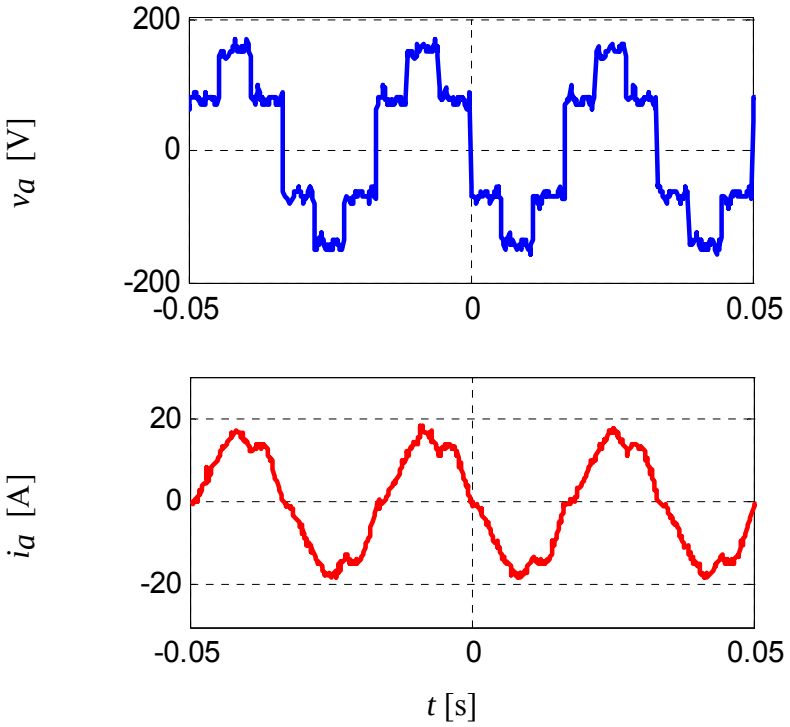

Fig. 4.29 Uncompensated voltage and current

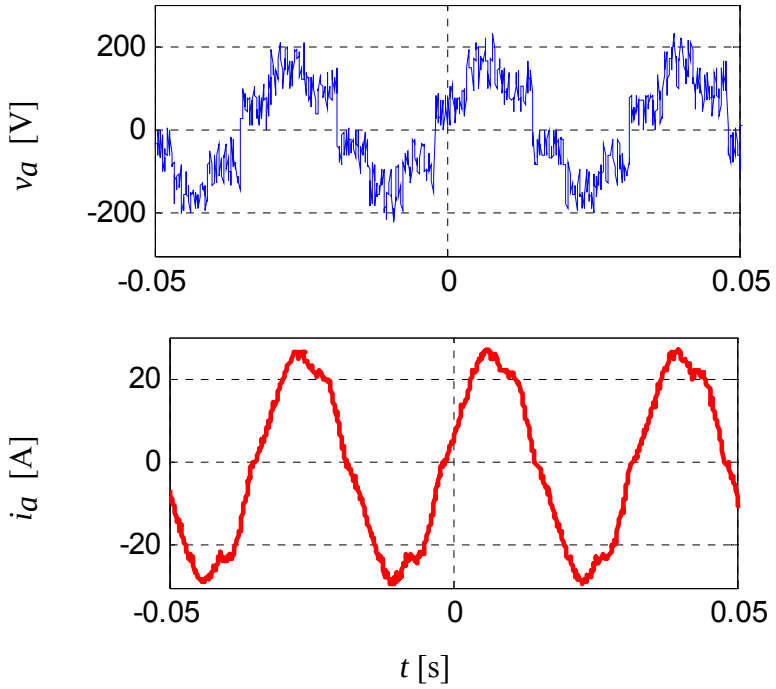

(b) compensated

Fig. 4.30 Compensated voltage and current waveform in steady state

The compensation voltage command and current for phase-A are compared in Fig. 4.31 for capacitive and inductive compensation. For capacitive compensation, the compensation voltage is lagging the current by 90 degrees. In contrast, the compensation voltage is leading the generator current by 90 degrees for inductive compensation. The current amplitude is much lower when inductive compensation is applied. Assuming a constant diode rectifier voltage, the generator power can be reduced.

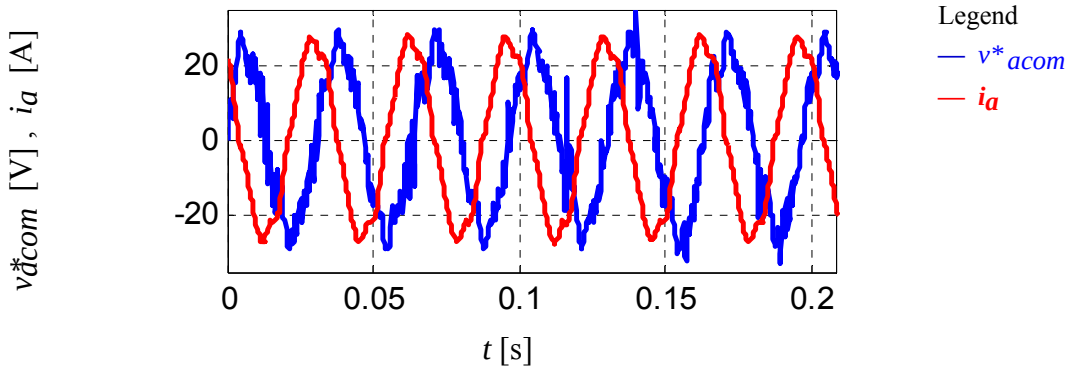

(a) Capacitive compensation

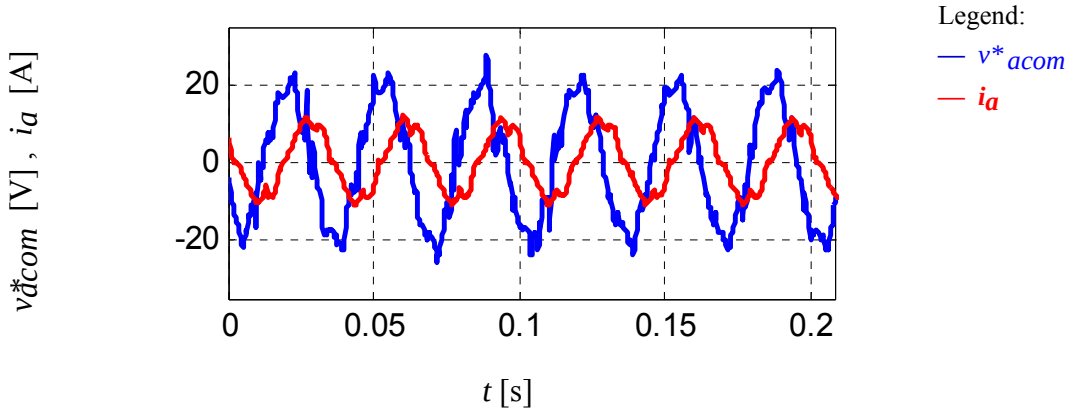

(b) Inductive compensation

Fig. 4.31 compensation voltage vs. generator current, experiment

The transient results before and after the power controller is enabled is shown in Fig. 4.32. The generator is operated at 900 rpm. The power controller is enabled at 1.25 sec. The power output of the generator is regulated to its reference value 6 kw. The compensation DC bus voltage is well regulated during the transient.

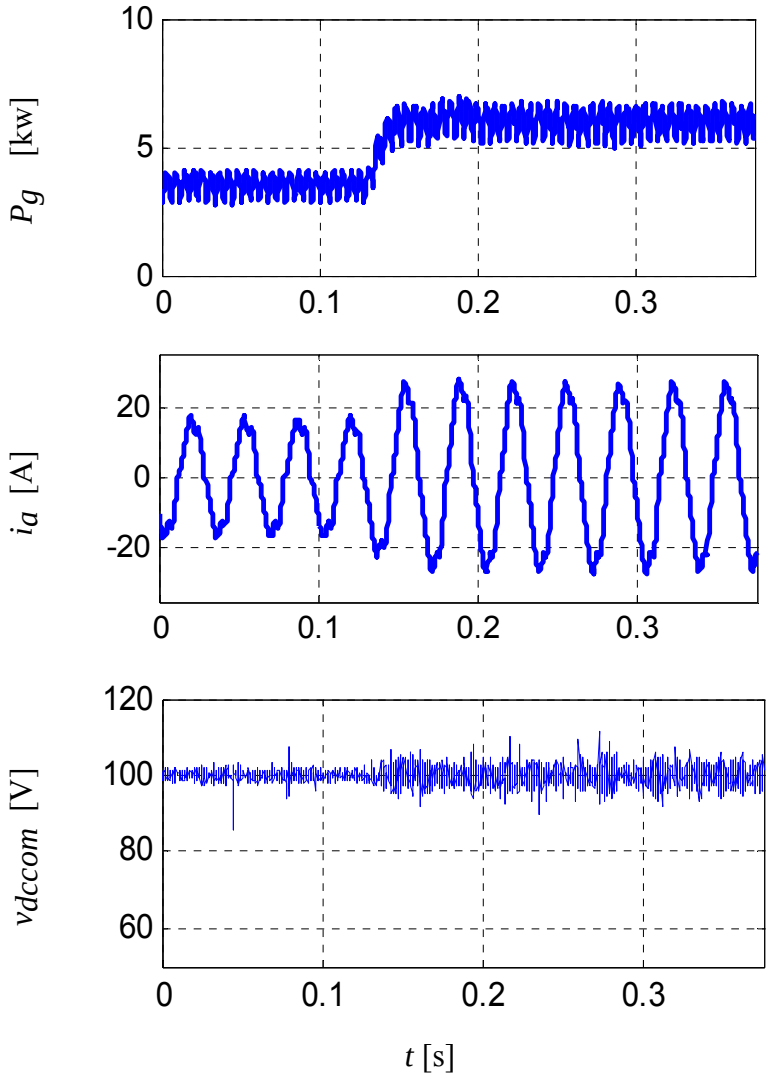

Fig. 4.32 Transient before and after the controller is enabled, experiment

A load step down test is also carried out as well. The results are shown in Fig. 4.33. The power command is changed from 6 kw to 2 kw at 1.25 sec. The generator power is controlled to be less than without compensation. The controller is able to regulate the generator power during the transient. The current amplitude is rapidly reduced. The compensation DC bus voltage is kept at its nominal value throughout the transient test. It is shown that the generator power can be controlled to be both higher and lower than that without any compensation.

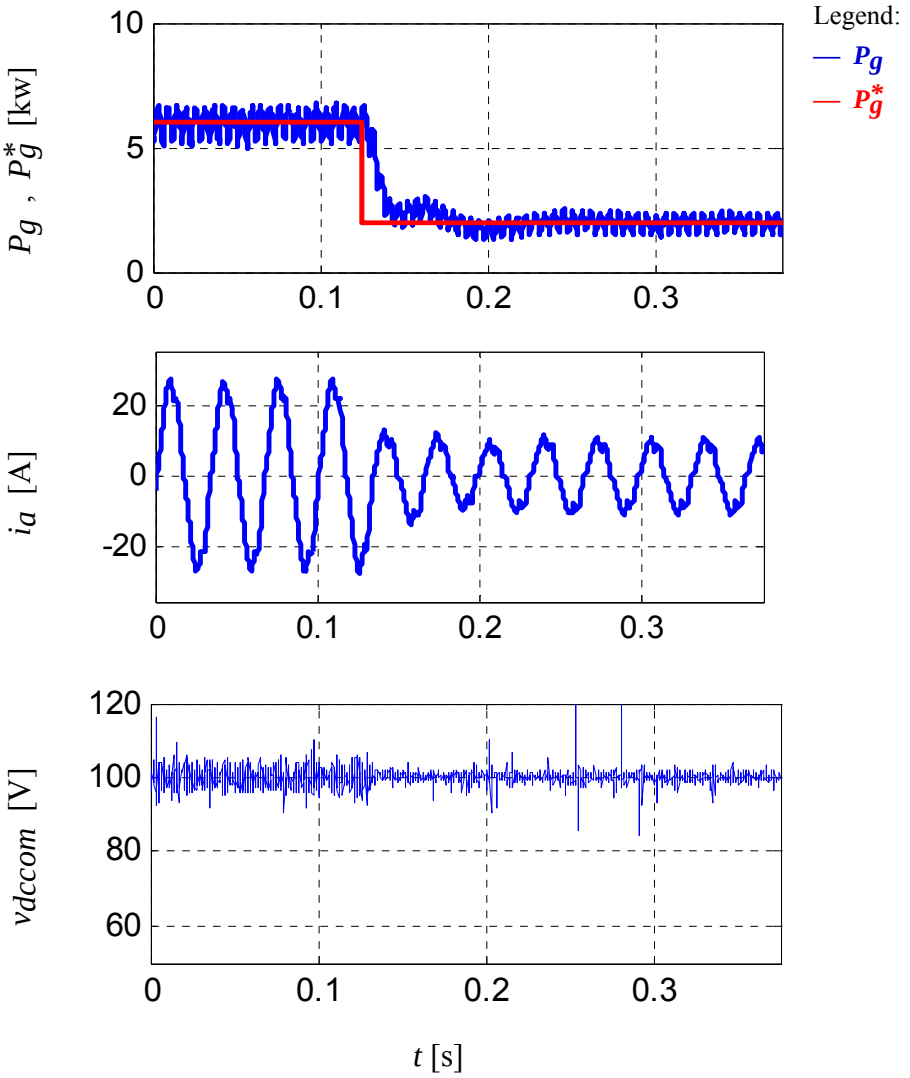

Fig. 4.33 Power step down transient, experiment

4.9. Summary

A PM generator wind power generation topology utilizing open-winding series compensation configuration was proposed in this chapter. The dimension of the auxiliary inverter in total can be considerably smaller compared to a PWM rectifier. The selection of generator to minimize the size of the compensation inverter is discussed. The control methods for both constant and variable speed operation were proposed. In addition, the impact of the current harmonics on the generator is briefly

discussed. The ability of power flow control by series compensation in open-winding PM machine is verified by both simulation and experiment.

Chapter 5

Load Side Voltage Regulation of Open-Winding PM Generator by Series Compensator

5.1. Introduction

In this chapter, the voltage control capability by the proposed series compensation scheme is investigated. A small scale open-winding PM generator based constant voltage variable frequency (CVVF) AC distribution system is investigated as an alternative for existing shunt regulated AC distribution system. The proposed series compensated regulator is compared with its parallel compensated dual. The sizing of the compensation inverter and selection of generator are discussed. A simple control method is proposed and verified by simulation and experiment.

5.1.1. Small Single Generator Power Systems [66]

Small power systems with a single AC generator are often used in remote areas and on vehicles. AC generators are exclusively used in such systems due to reliability and efficiency issues of DC generators. Induction generators are robust and cheap. But their power density is often lower than synchronous generators. Wound field synchronous machine are the most popular choice in aircraft applications. However, the rotor circuit still dissipates an un-neglectable amount of power which reduces the efficiency of the system. Moreover, failures of diodes in the field circuit have been considered as one of the major draw backs. PM generators are light and efficient. However, the terminal

voltage is affected by the rotor speed as well as load condition because the flux linkage due to magnets cannot be adjusted at will. Large power electronic converters are required in such system, either to rectify AC power into DC or regulate the AC voltage amplitude by injecting reactive power into the generator. Several existing configurations of small distribution systems are introduced here.

For small vehicles like automobiles, the loads are mostly DC. In such a system, a central rectifier is often used to convert AC power into DC for distribution. Active rectifier or diode rectifier with a DC/DC converter may be used to regulate the voltage on the DC bus. Small local inverters may be used to drive the AC loads if there is any in the system. The protection of a DC distribution system is generally more difficult than an AC system. The voltage level may be sometimes restricted to lower than 50 Volts for safety reason. As a result, more losses may present in a large distribution system because of the enormous current.

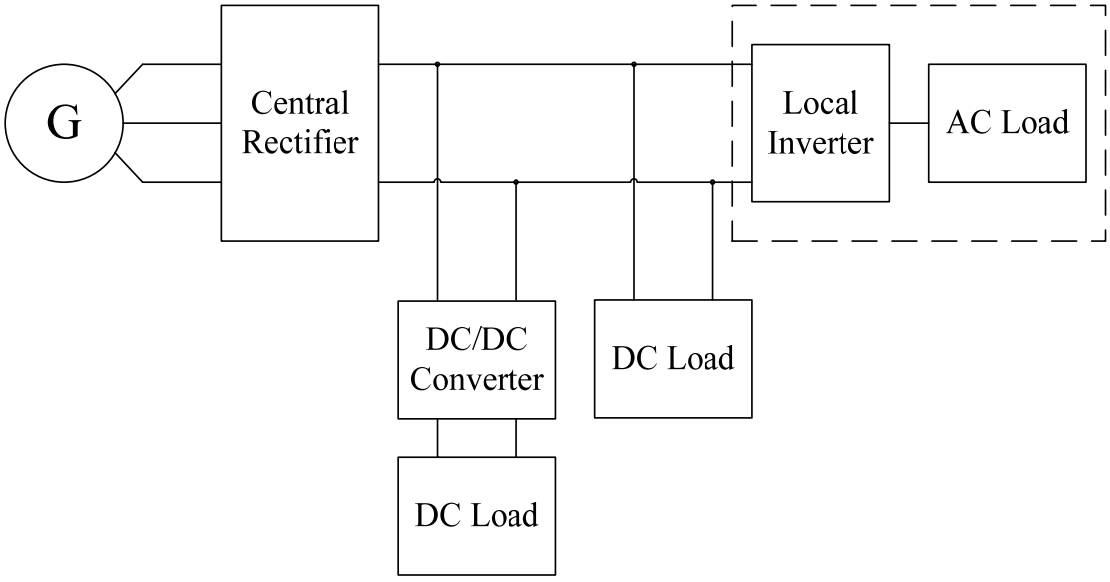

Fig. 5.1 Small DC system

There are some systems where a considerable part of the load are AC loads. A central rectifier and inverter can be used to supply a constant voltage constant

frequency (CVCF) and form an AC transmission system. Many aircraft and ships are examples of this type of system. To reduce the size of reactive components in the system, the distribution frequency is often chosen to be higher than 60 Hz (400 Hz for example). Fig.5.2 shows an example block diagram of this type of configuration.

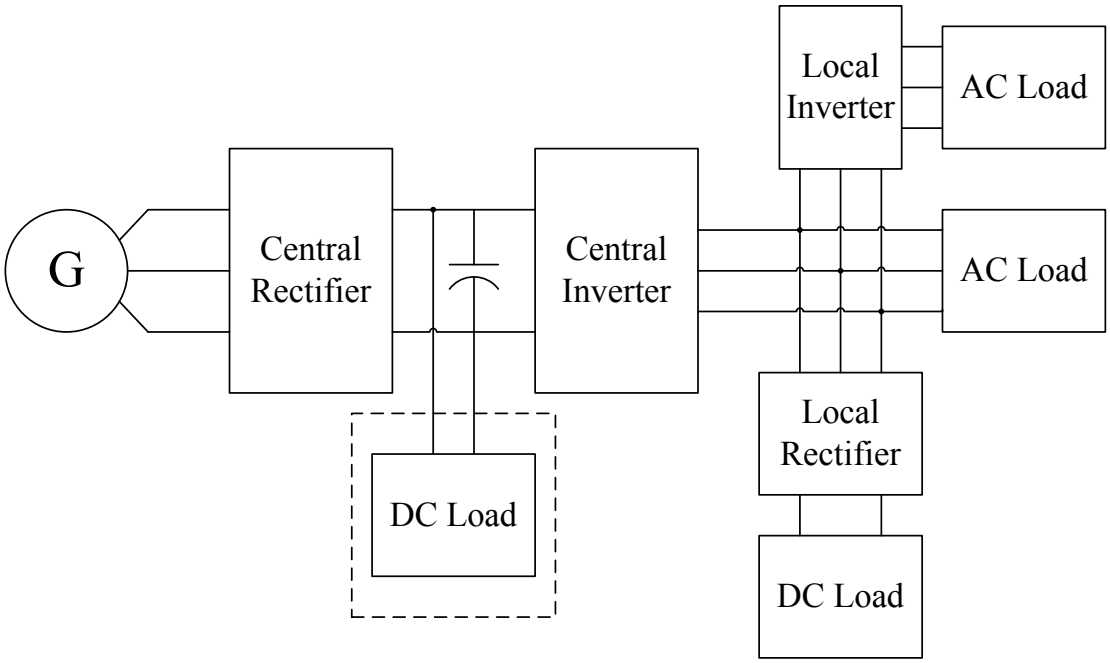

Fig. 5.2 CVCF AC system

Sometimes in an AC distribution system, there are some loads that are relatively frequency insensitive, for example defrosting, anti-icing, lights and power electronics loads in aircraft. If such kind of loads represents a significant part of the overall system, a CVVF AC power system will be a preferred choice. Since the central rectifier and inverter do not exist, the related cost and losses are eliminated. A wound field synchronous generator or PM generator can be used in such a system. When a wound field synchronous generator is used, a separate wound rotor induction machine can be used to provide regulated excitation to the field winding to ensure a constant voltage at the main generator stator side [93]. As an alternative, Fig.5.3 shows a PM generator CVVF distribution system with a shunt regulator. The parallel connected VSI regulates

the AC side voltage amplitude as the load and rotor speed changes. Meanwhile, it can be used as an active rectifier to supply DC load at its DC bus.

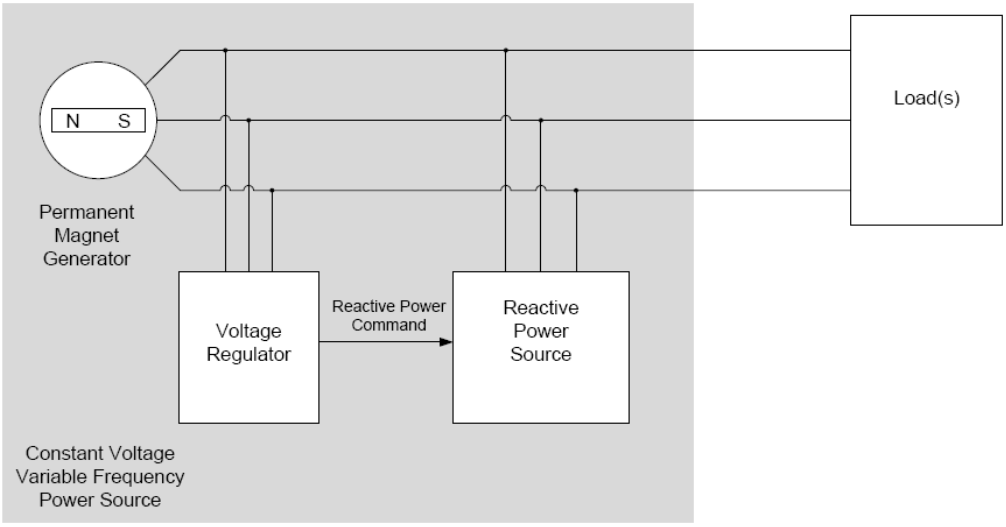

Fig. 5.3 CVVF distribution system with shunt regulator [78]

5.1.2. Proposed Topology

A CVVF AC distribution system configuration similar to the shunt regulated PM generator system is proposed here. Instead of using shunt regulator, a series regulator is employed. The SSSC can be used for the purpose. However, a bulky transformer is required to insert the compensation voltage in series with the generator. Instead, the proposed open-winding compensation method can be used to regulate the voltage of an open-winding PM generator. Fig.5.4 is a block diagram of the proposed CVVF system. Generator inductance is generally large enough to filter out the noise due to switching at the load side. Therefore, no filter is required in the system. The series connected VSI is controlled to inject reactive power to the generator so that the distribution side voltage is kept constant as the load and rotor speed vary. In addition, the compensation inverter can be operated as an active rectifier at the same time. DC load can be attached

to the floating capacitor. However, only a DC capacitor is used at the inverter DC bus. Therefore, the inverter is not able to supply any real power to the AC load.

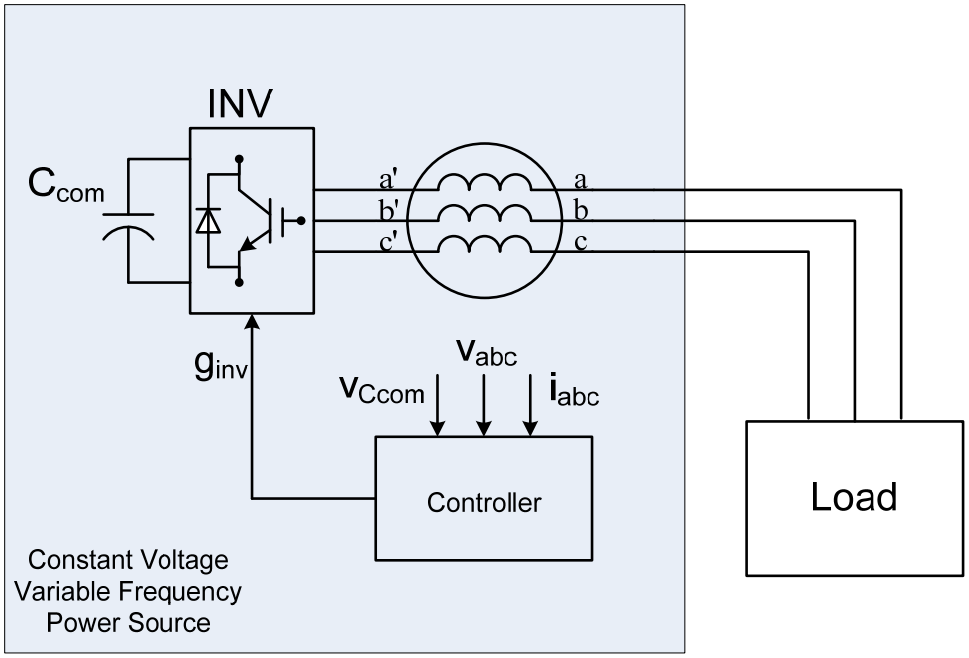

Fig. 5.4 Proposed PM open-winding generator based CVVF distribution system

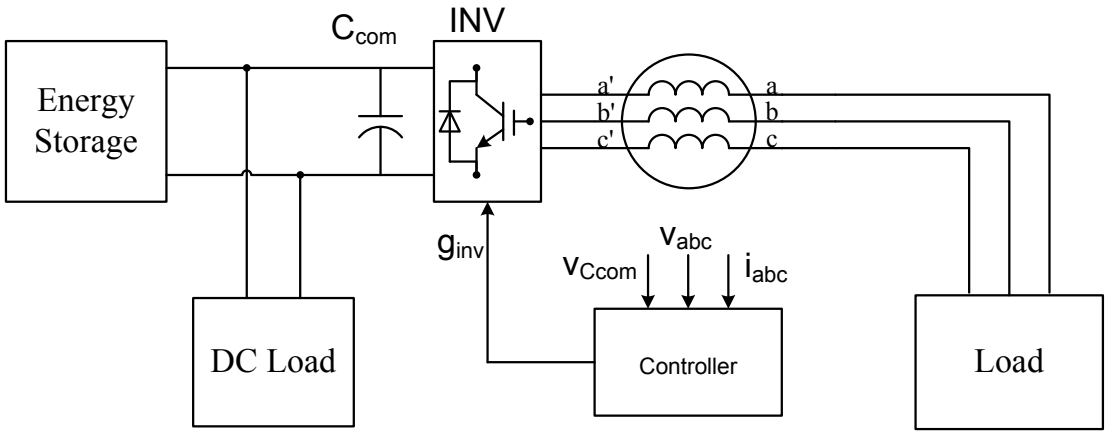

Fig. 5.5 Proposed configuration with energy storage

Fig.5.5 shows a variation of the proposed topology. An energy storage device, for example a battery, is connected to the compensation DC bus. The generator/inverter set is also used as an interface between the AC distribution and energy storage. Moreover,

the inverter is able to supply real power in addition to the generator to the AC load.

5.2. Design Consideration

The same IPM generator used in the previous chapter is used for study. The generator parameters used in machine model are all the same. But the ratings are tailored to this specific application.

Table.5.1 lists the ratings of the proposed series regulated CVVF AC distribution system. The rated voltage is selected the same as the open circuit voltage at lowest speed (0.707 base frequency).

Table 5.1 System Ratings for series regulated CVVF system

Parameter	Symbol	Value
Rated power	P_r	7 kW
Rated voltage	V_r	81.3 Vrms
Rated current	I_r	29 Arms
Rated speed	n_r	1035 rpm
Base frequency	f_b	34.5 Hz
Base radian speed	ω_{rb}	215.8 elec rad/s

5.2.1. Comparison with Shunt Regulated System

As a dual of shunt compensated configuration, series compensated configuration has some similar properties. At the same time, there are many differences between the two configurations. In this section, the two configurations are compared.

First, the compensation variable is different for the two configurations. Series compensation injects reactive power by injecting a voltage that is 90 degrees apart from generator current vector while shunt compensation injects reactive power by inject a current that is 90 degrees away from generator voltage. Therefore, series connected

inverter has the same current rating as the generator but the parallel connected inverter has the same voltage rating as the generator. However, to achieve fast response, the DC bus voltage may be sized significantly higher than the generator voltage [66].

Second, the capability of buck or boost the load voltage is different for the two configurations. With proper chosen machine parameters, the shunt regulator would have similar capability of bucking or boosting the generator voltage. However, the series regulator has limited boosting capability. The distribution side voltage could not be boosted higher than the back-emf of the generator. Fig.5.6 shows the reason in the fashion of a phasor diagram. Taking a resistive load with a non-salient generator as an example, the generator current is in phase with the distribution side voltage. Voltage drop on the synchronous reactance is perpendicular to both generator current and distribution side voltage. When a capacitive compensation is applied, a right triangle is formed by the back-emf E, distribution side voltage V_g and the vector sum of reactance voltage and compensation voltage. In the right triangle, the distribution side voltage is always smaller than the back-emf no matter the compensation is capacitive or inductive.

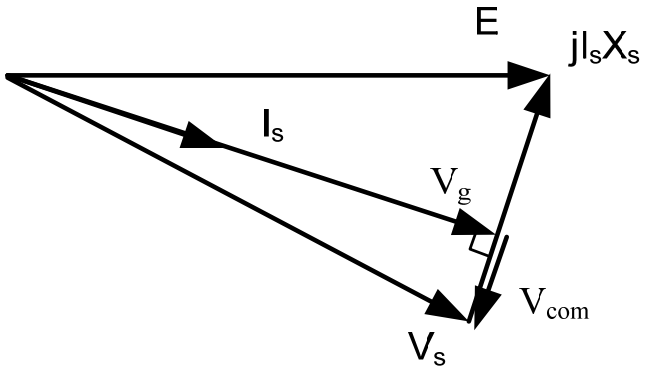

Fig. 5.6 Phasor diagram for non-salient generator

The reason can also be explained from a power balance point of view. The load power is three times the product of the distribution side phase voltage V_g and machine

current I_S for a resistive load:

$$P_{load} = 3V_g I_S \quad (5.1)$$

The MTPA curve of a SPM generator is the q-axis. For the same current amplitude, the maximum air gap power is:

$$P_{airgap} = 3EI_S \quad (5.2)$$

The fact that distribution side voltage is larger than the back-emf leads to the result that $P_{load} > P_{airgap}$ which is clearly not possible for a generator. Therefore, with a SPM generator, the proposed topology is not able to boost the voltage to a value that is larger than the back-emf. For a salient pole generator, the distribution side voltage could be boosted to higher than the back-emf to a limited extent due to the existence of reluctance torque. As a result, the rated voltage of the system can not be selected higher than the generator open circuit voltage at the lowest speed.

Third, the dimension of the generator is sized differently. For the series regulator, the generator needs to be oversized in voltage at high speed due to the fact that the regulator has limited boost capability. In contrast, when a shunt regulator is used, the generator current rating has to be oversized because extra current needs to be injected into the generator in addition to the load current.

Fourth, the fault tolerant capability is different for the two topologies. It has been demonstrated in [66] that the generator can be properly selected so that the system would not see over voltage or current when the inverter shuts down. As a dual, the series regulator is more immune to short circuit fault. During the short circuit fault in the distribution side, the inverter can be controlled as large impedance in series with the generator to reduce the fault current.

Fifth, the shunt regulator is more suitable for unbalanced load. When the load is unbalanced, the STATCOM is capable of reducing the imbalance in the generator current. However, for the proposed series regulated system, any unbalance in the load current will be seen by the generator. Therefore, significant torque ripple will be

generated on the shaft.

5.2.2. Reactive Power Requirement

In the proposed system, the load voltage is regulated by injecting reactive power in series with the generator. The size of the compensation inverter will be determined by the required reactive power for the generator to operate at constant voltage.

In shunt regulated system, the rated voltage is defined as the open circuit voltage at base speed. The operating speed is from 0.707 to 1.414 times base speed. For series compensation, it is has been found that the boost capability is limited. Therefore, the rated voltage has to be redefined. The open circuit voltage at the lowest operating speed is defined as the rated voltage for the system. The generator voltage is oversized as mentioned in the previous section.

For the ease of analysis, pure resistive load is first assumed here. The distribution side voltage can be simply calculated as:

$$V_g = I_S R_{load} \tag{5.3}$$

Given a desired load power level, the load resistance and generator current can be obtained:

$$R_{load} = \frac{3V_g^2}{P_g} \tag{5.4}$$

$$I_S = \frac{P_g}{V_g} \tag{5.5}$$

In steady state, the generator voltage equation in d-q reference frame can be written as:

$$E = - I_S \sin(\delta)\omega_r L_d - V_{com}\sin(\delta) + I_S\cos(\delta)(R_S + R_{load}) \tag{5.6}$$

$$0 = I_S \cos(\delta)\omega_r L_q + V_{com}\cos(\delta) + I_S\sin(\delta)(R_S + R_{load}) \tag{5.7}$$

The equations are in generator convention. Substitute (5.5) into (5.6) and (5.7), the

equations can be solved to obtain the required compensation voltage amplitude and the current angle for the generator to operate at the rated voltage and desired load level. The reactive power that is required for the machine to supplying the power under rated grid side voltage is all provided by the inverter for resistive load. With the compensation voltage, the reactive power can be calculated as:

$$Q = V_{com} I_S \tag{5.8}$$

The power versus reactive power curves at different speeds assuming constant distribution side voltage are plotted in Fig. 5.7. The reactive power requirement is reasonably small for the generator used. Similar to the shunt regulator, if the generator speed is near constant, the reactive power requirement will be very low.

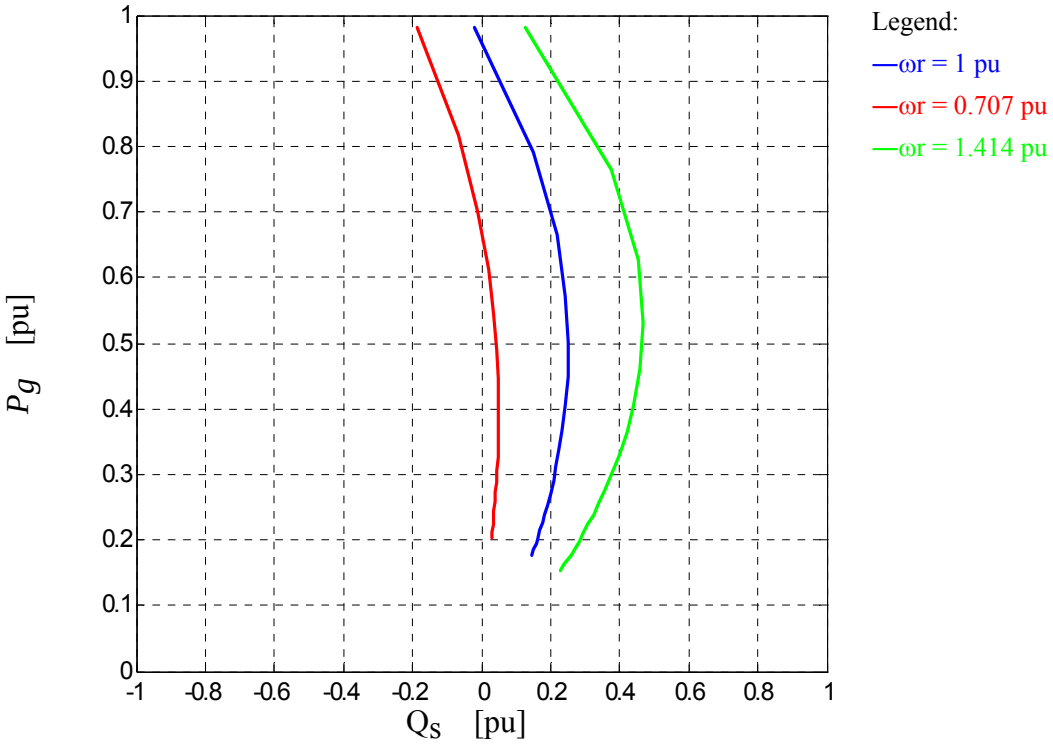

Fig. 5.7 Power vs. Reactive power for constant distribution side voltage

5.2.3. Generator Considerations

Like for the previous application examples, the design of the PM machines will

affect the dimensioning of the compensation inverter. Since generators are considered in this application example, characteristic current and saliency ratio are again used to represent different designs of generator. The power-var curves for a set of different designs are plotted in Fig. 5.8 for resistive load. Similar to a shunt regulated system, a high saliency ratio can reduce the reactive power requirement for the compensation inverter. It is known that a generator with high characteristic current has good self load regulation. At constant speed, the load voltage will vary in a smaller range compared to a generator with smaller characteristic current. It is desired to have a generator with good self load regulation in the system so that the compensation would not change in a large amount when the load varies. The controller bandwidth can also be reduced. However, for a generator with high characteristic current, the reactive power requirement is higher than the ones with a characteristic current near 1 per unit. Moreover, the compensation inverter will be providing inductive compensation most of the time. In contrast, a generator with low characteristic current requires significant amount of capacitive compensation at heavy load. The generator used in the study has a saliency ratio about 3 and a characteristic current slightly higher than 1 per unit. This generator has a good balance of reactive power requirement and natural load regulation.

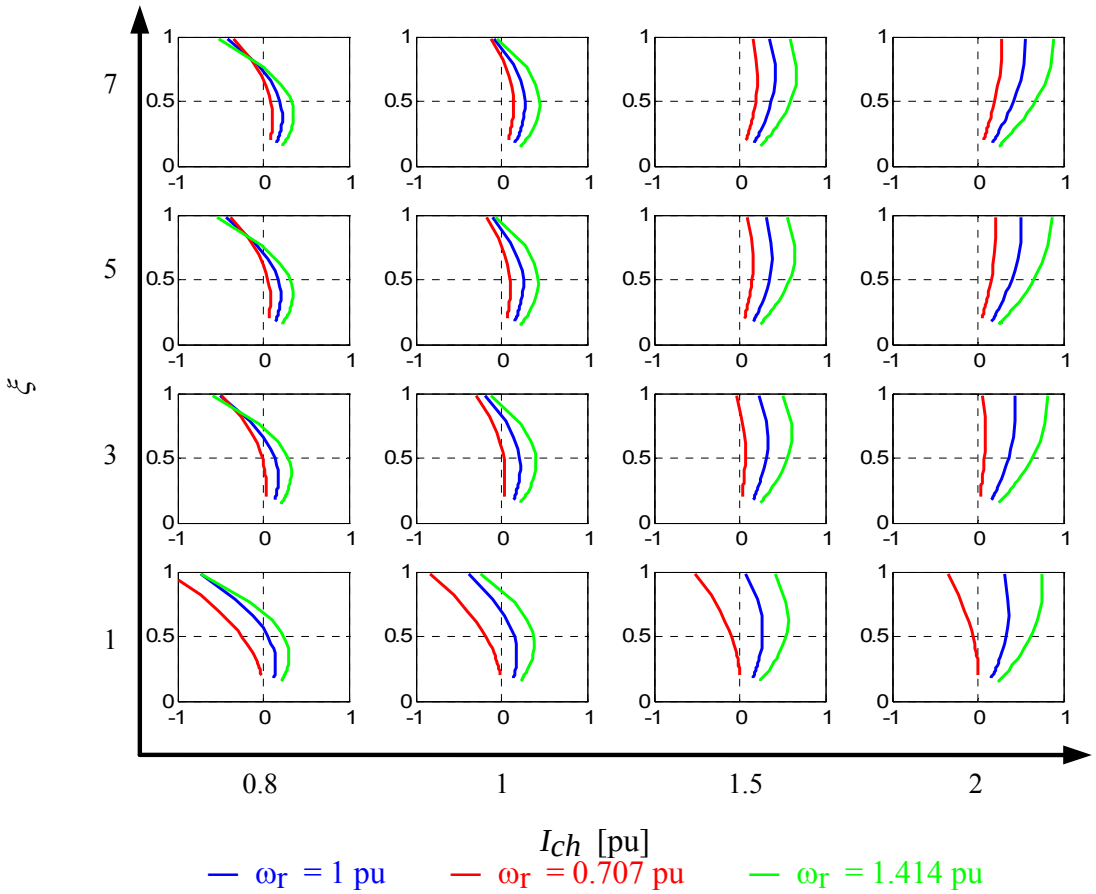

Fig. 5.8 P vs. Qcom under resistive load for different generator types

Fig. 5.9 shows the power versus compensation var curve when the load power factor is 0.8 lagging. It can be expected that more capacitive compensation var is needed due to the increased var demand from the load. The total reactive power requirement for the generator with high saliency ratio and high characteristic current is slightly reduced because the capacitive and inductive compensation required is closer. Instead, for generators with a low characteristic current, the reactive power requirement increases since more capacitive power is required. A generator with characteristic current close to 1 per unit and high saliency ratio is still a good choice for minimizing the VA rating of compensation inverter.

A state of the art IPM generator typically has a saliency ratio of 3 at this time. In the comparisons, such a saliency ratio requires only a small amount of var

compensation. Although increasing saliency ratio is beneficial for reducing the reactive power requirement, increase in saliency ratio larger than 3 does not apparently reduce the var requirement.

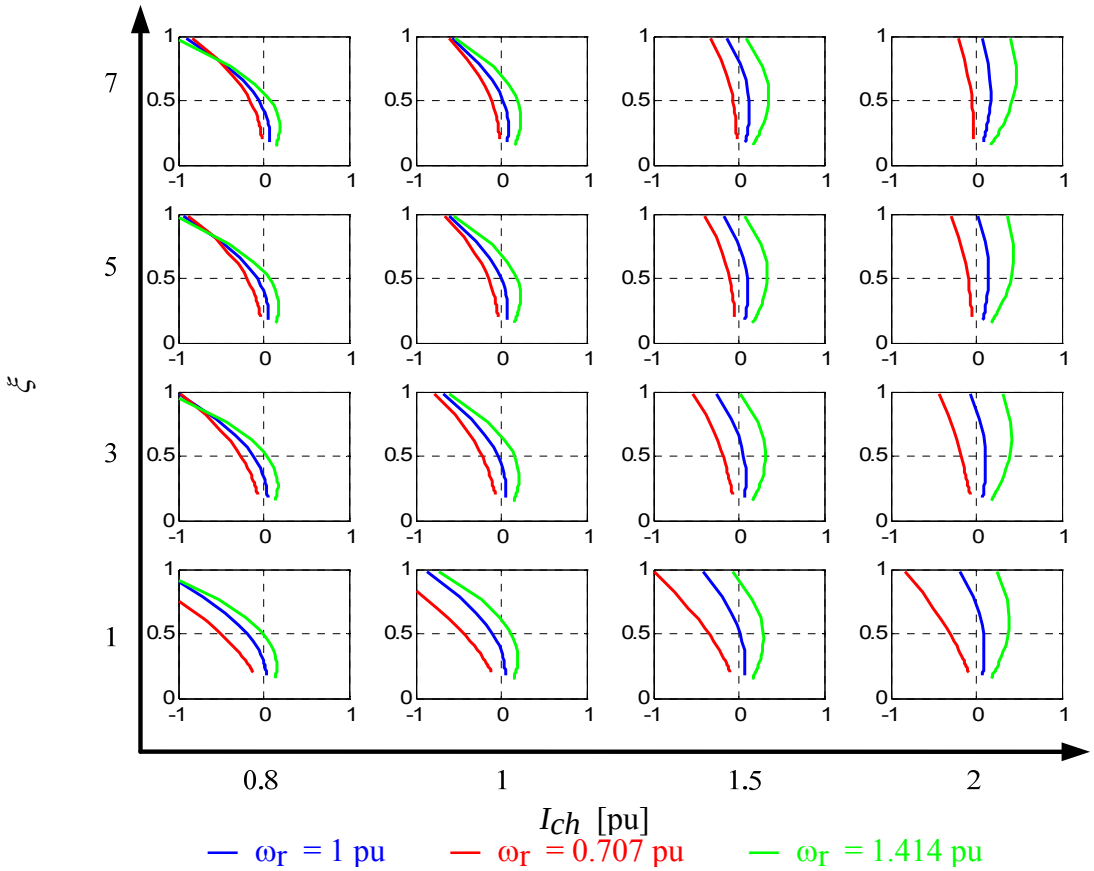

Fig. 5.9 P vs. Qcom under 0.8 pf for different types of generators

5.3. Control Method

The control method of the proposed CVVF series regulator is shown in Fig.5.10. Similar to that of the series compensated wind power system proposed in Chapter 4, this controller is again located in a current synchronous frame. Similarly, the current angle can be either detected with a PLL or a rotor position sensor.

The load side line-to-line voltage is measured and a separate PLL is used to detect the amplitude of the load side voltage. Three-phase balance is assumed in the controller

and only two line-to-line voltage sensors are used. The reason to use a separate PLL instead of using the current phase angle to calculate the voltage amplitude is that dynamics of the PLL can be separately tuned.

It is known capacitive reactive power injection boosts up the distribution side voltage (lower than the back-emf of the generator) and inductive injection bucks down the voltage. A PI regulator is used to control the distribution side voltage. The output of the PI controller is the di-axis injected voltage which is in quadrature with generator current.

The qi-axis voltage component is used to control the floating capacitor voltage. The same as in other applications, a PI regulator is used to generate the real component of the compensation voltage reference.

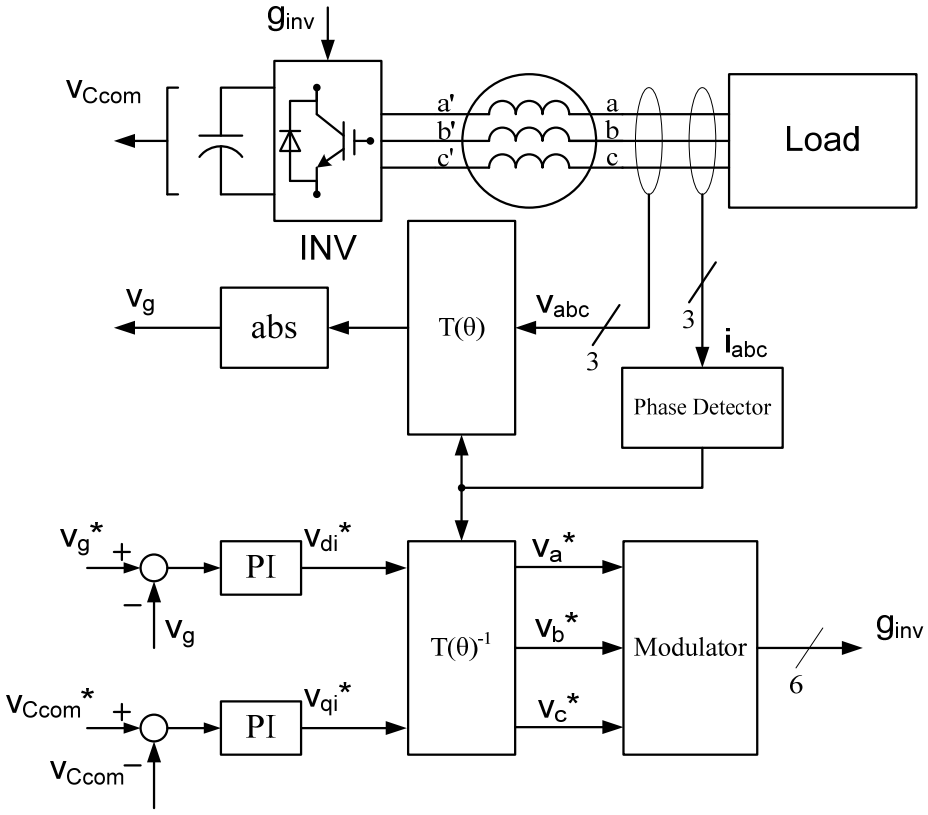

Fig. 5.10 Control of series voltage regulator

5.4. Simulation Results

The proposed system was simulated in Matlab/Simulink and PLECS blocks set and the results are given in this section. The transient performance of the proposed system during a step load change at a variety of different speed and load levels was shown. Since the load is directly in series with the generator, an abrupt load current decrease will result in large voltage spikes in the system because of the generator inductance. To avoid the voltage spike, low cost TRIAC or SCR can be used as an interface between passive loads and generator. Passive load can be smoothly changed to a lower value when the SCRs cease to conduct when the load current drops to a value lower than the holding current. Moreover, SCR gate drive with zero-crossing function can be used so that passive load is switched in only at zero load voltage. Unlike the passive load, the power electronics load in the system can be controlled to only switch in and out at current zero crossing point. Extra switches are not required in this case.

(a) 24.4 Hz

Figs.5.11 to 5.14 are step load transient response at 24.4 Hz, the lowest speed. The load is changed from 28% to 56% in Fig. 5.11 and from 56% to 28% in Fig. 5.12. The transient during the load step up/down in the line-to-line voltage is apparent. However, the voltage is controlled very well in steady state. The DC bus voltage is well regulated as well.

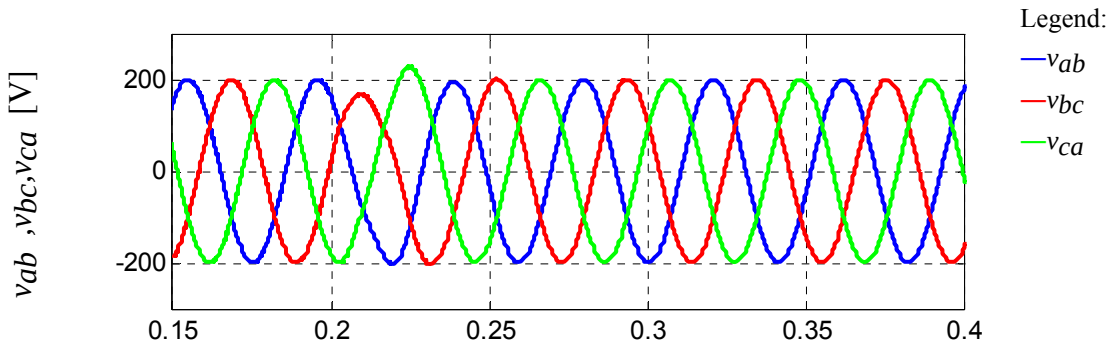

(a) line-to-line voltage

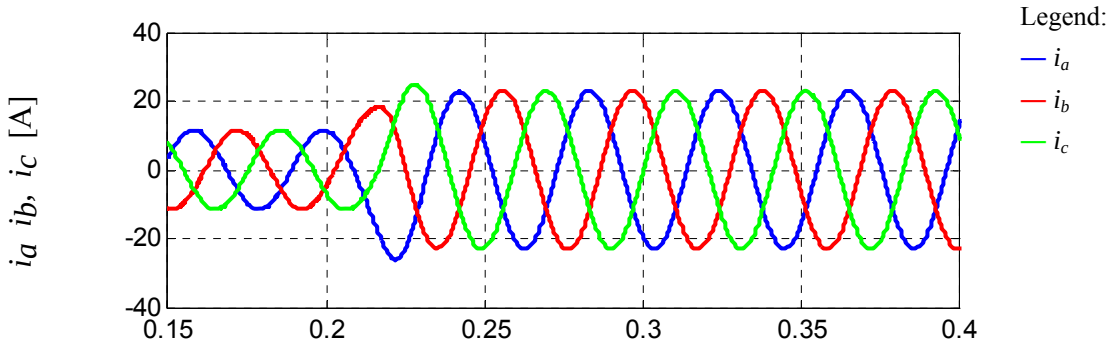

(b) generator current

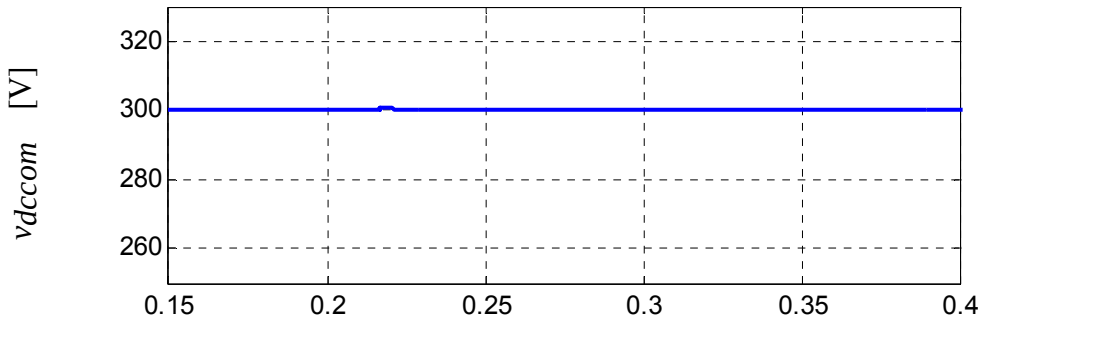

(c) floating capacitor voltage

Fig. 5.11 Series regulated CVVF system, simulation results, 24.4 Hz, 28% to 56%

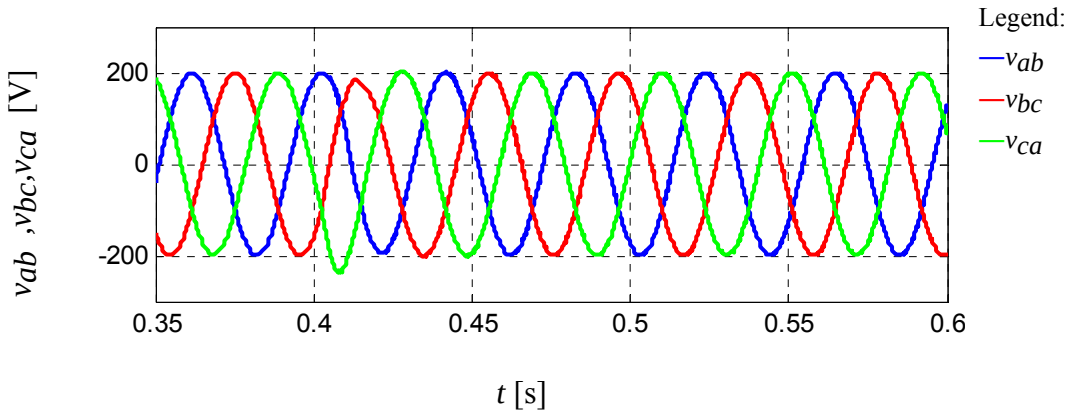

(a) line-to-line voltage

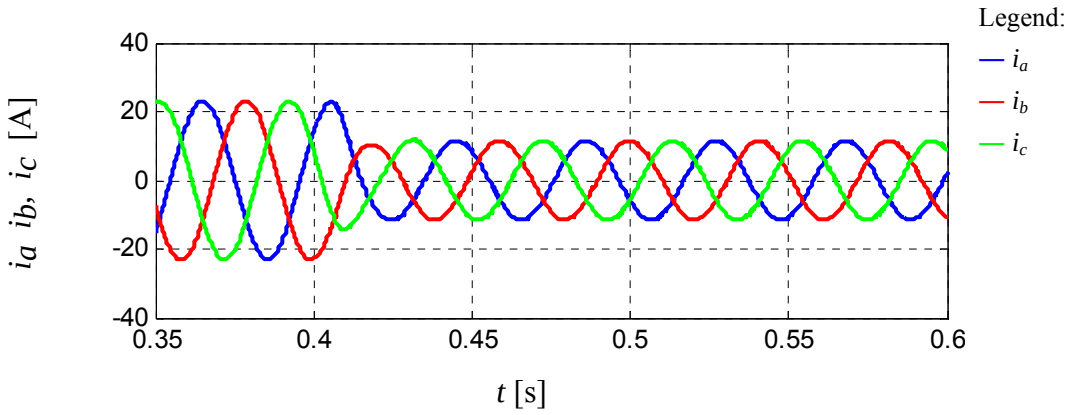

(b) generator current

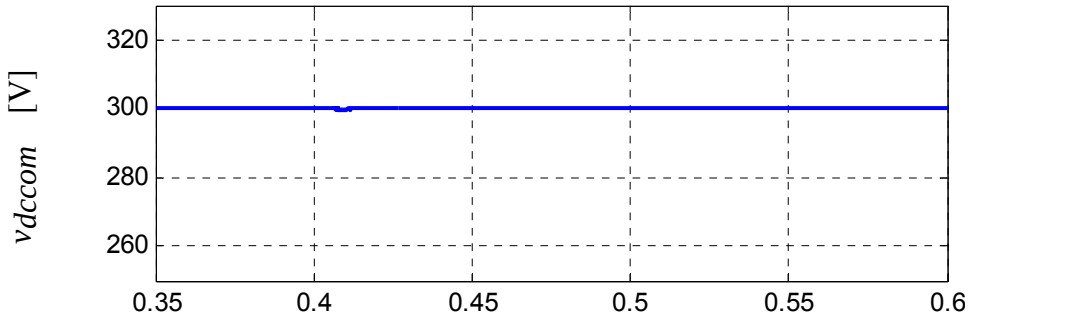

(3) floating capacitor voltage

Fig. 5.12 Series regulated CVVF system, simulation results, 24.4 Hz, 56% to 28%

Fig. 5.15 and 5.16 show a large step load change. The load varies between 28% and 85% in this case. Due to the large inductance of the generator, the voltage change is quite apparent. Again, the controller is able to recover the load voltage to its nominal

value within one cycle. The floating capacitor voltage is well regulated throughout the transient.

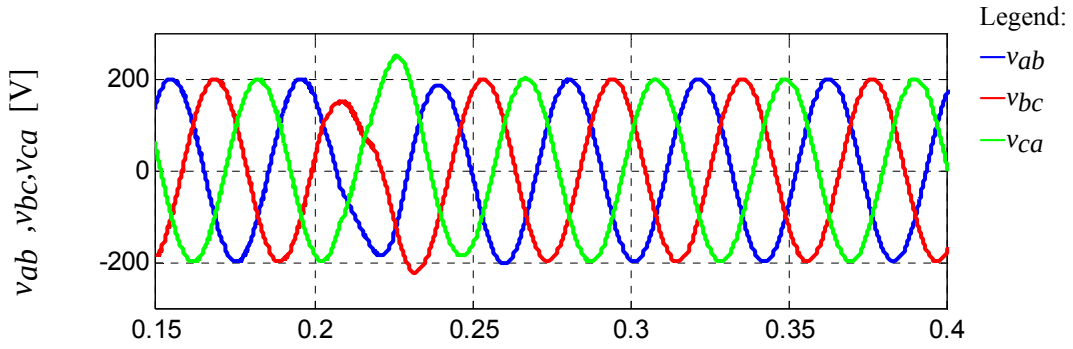

(a) line-to-line voltage

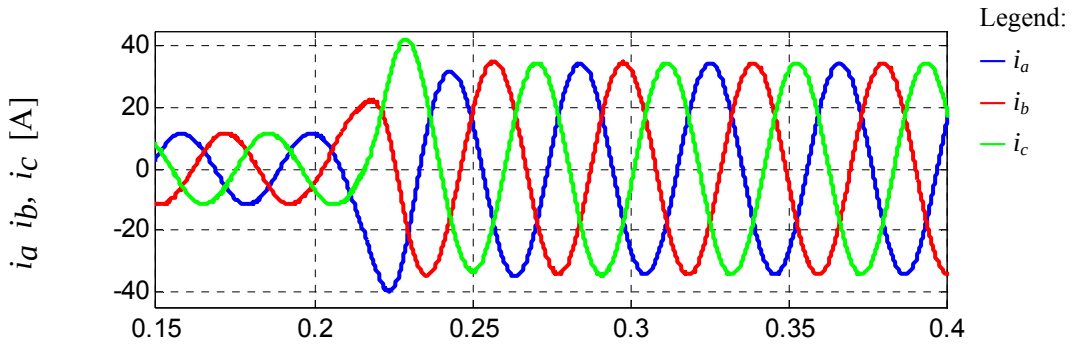

(b) generator current

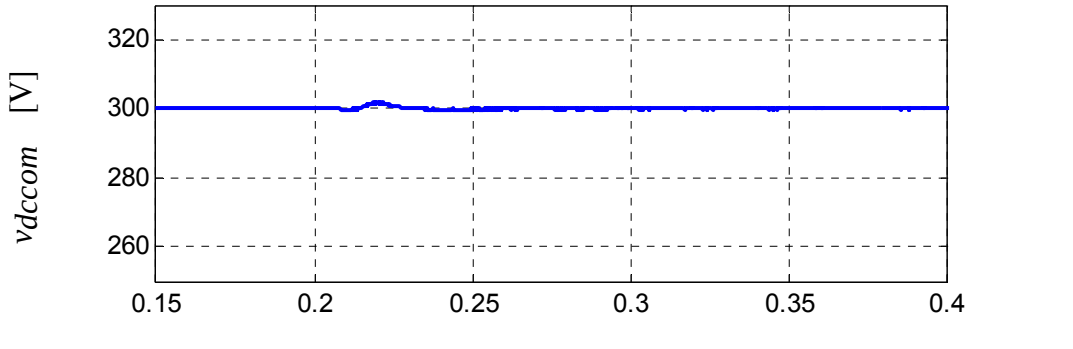

(c) floating capacitor voltage

Fig. 5.13 Series regulated CVVF system, simulation results, 24.4 Hz, 28% to 85%

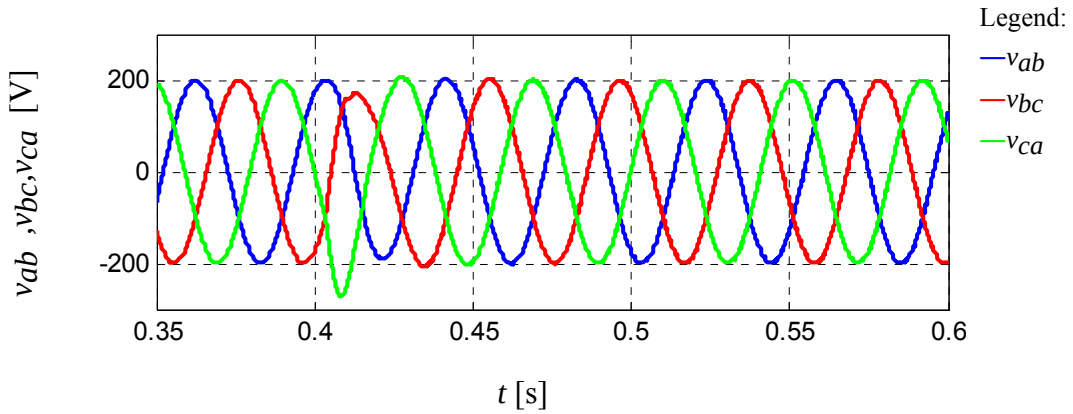

(a) line-to-line voltage

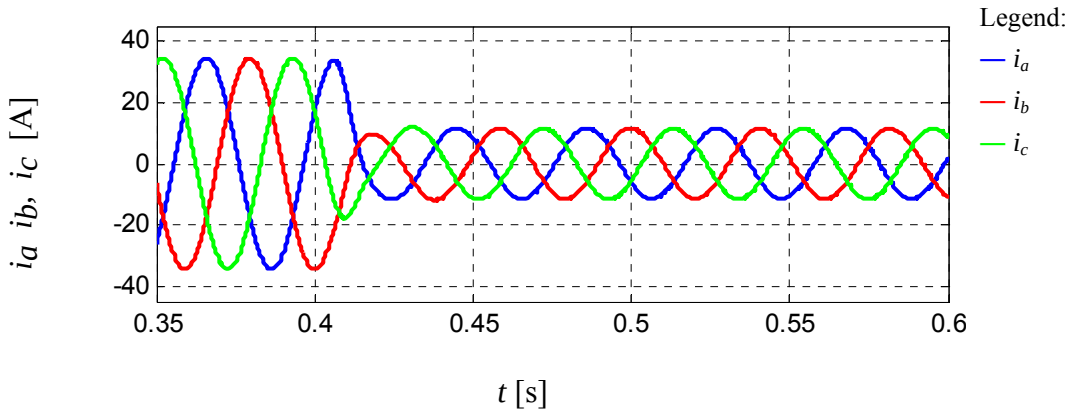

(b) generator current

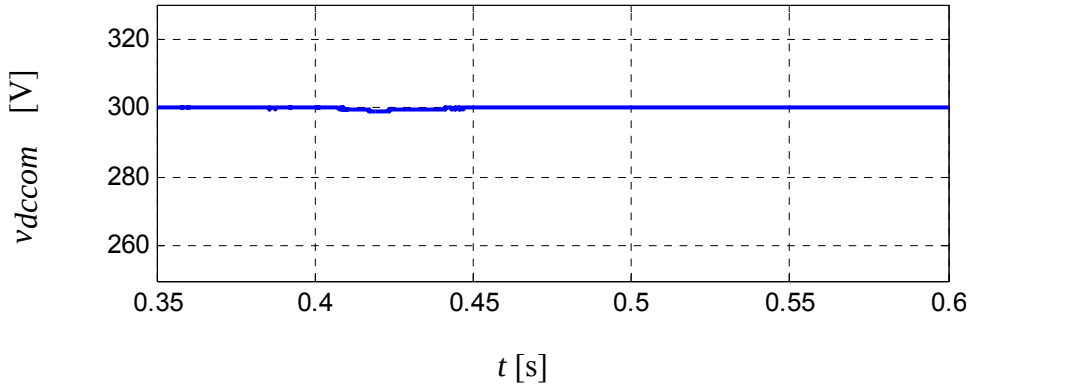

(c) floating capacitor voltage

Fig. 5.14 Series regulated CVVF system, simulation results, 24.4 Hz, 85% to 28%

(2) 34.5 Hz

The same step load changes are simulated at 34.5 Hz. The results are shown in Fig. 15 to 18. As the speed increases, the impedance of the generator increases as well.

Therefore, when the generator current changes for the same amount, the voltage change on the reactance is greater at high speed than low speed. As a result, the transient is more apparent at 34.5 Hz compared to 24.4 Hz.

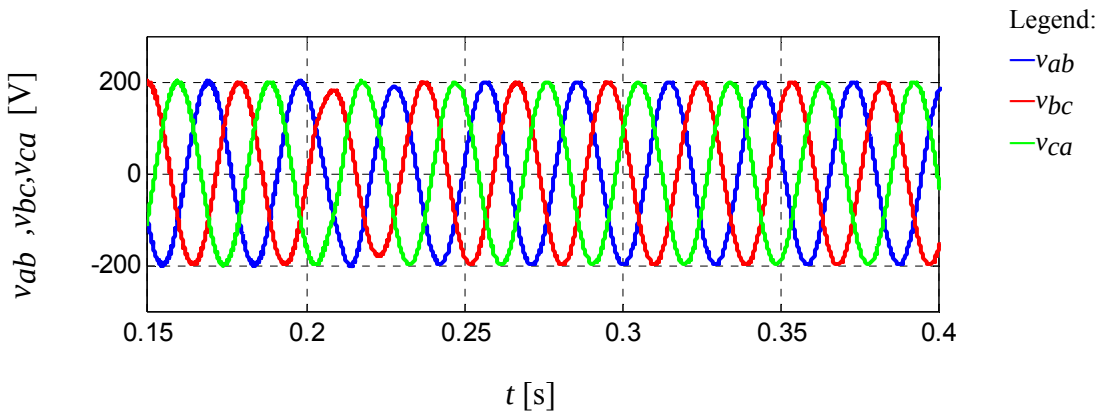

(a) line-to-line voltage

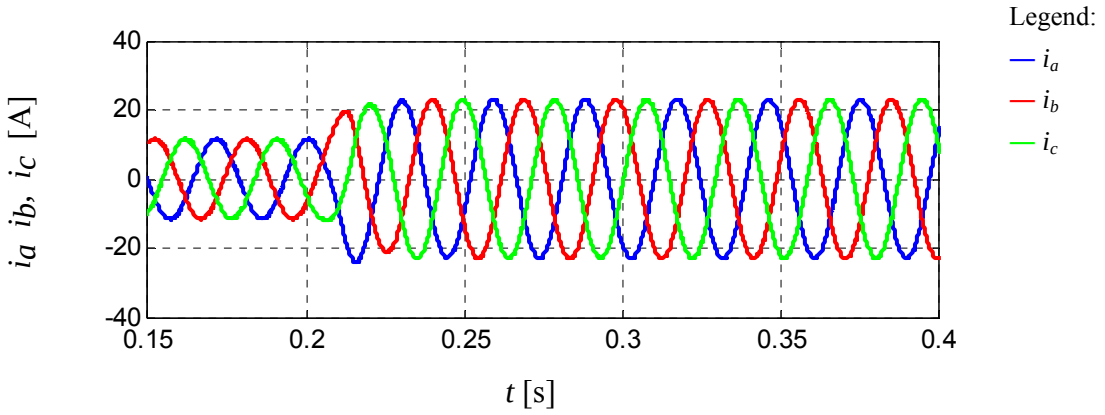

(b) generator current

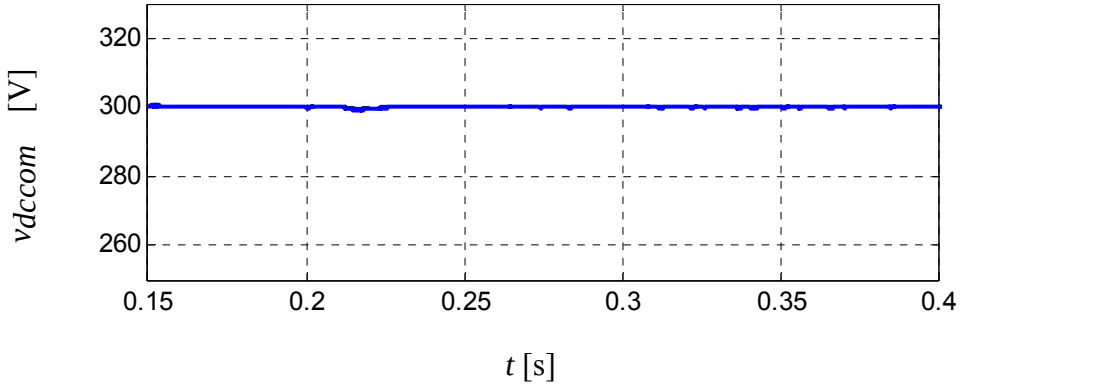

(c) floating capacitor voltage

Fig. 5.15 Series regulated CVVF system, simulation results, 34.5 Hz, 28% to 56%

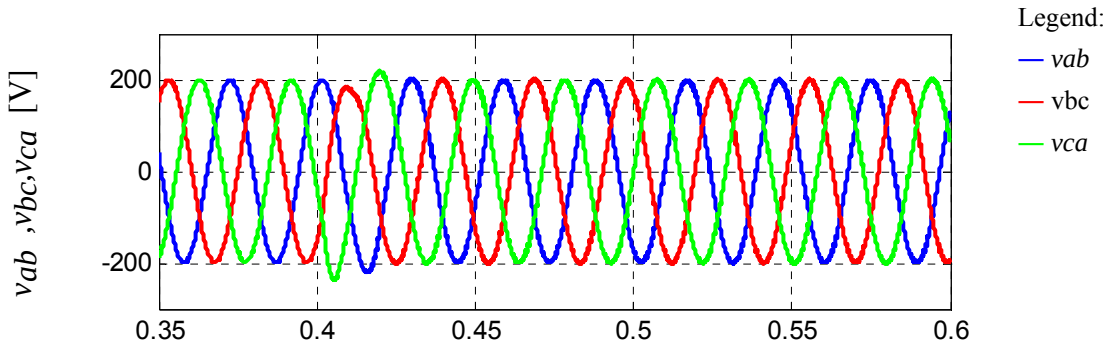

(a) line-to-line voltage

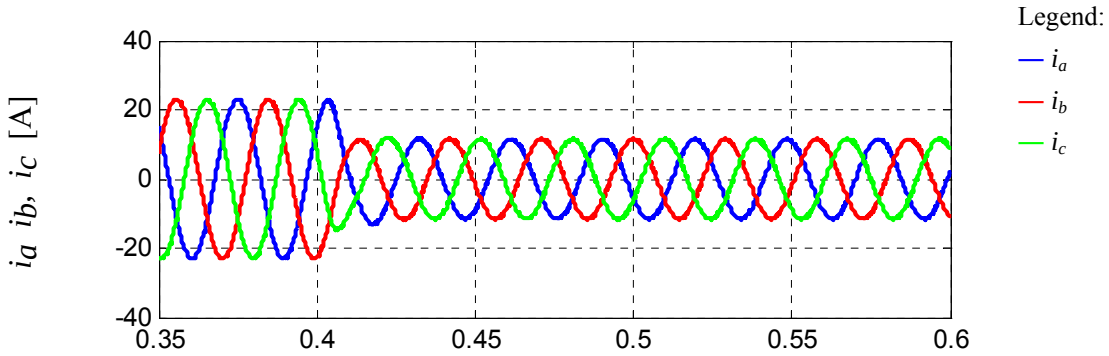

(b) generator current

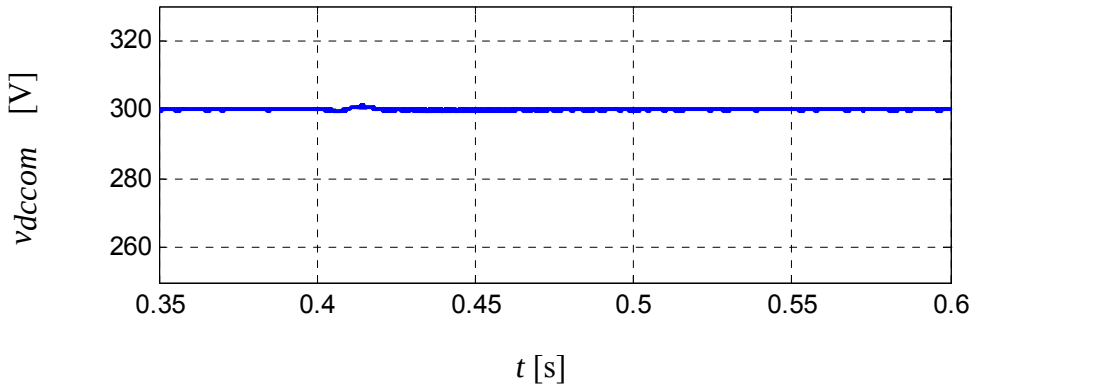

(c) floating capacitor voltage

Fig. 5.16 Series regulated CVVF system, simulation results, 34.5 Hz, 56% to 28%

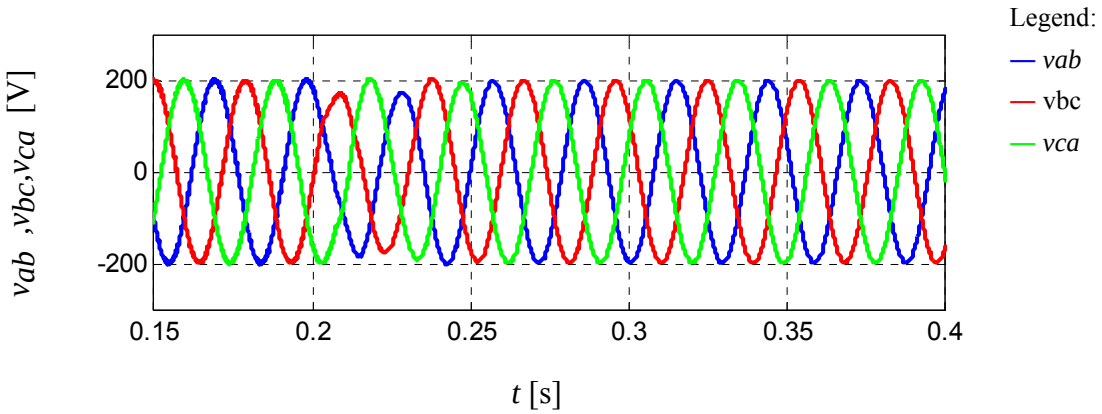

(a) line-to-line voltage

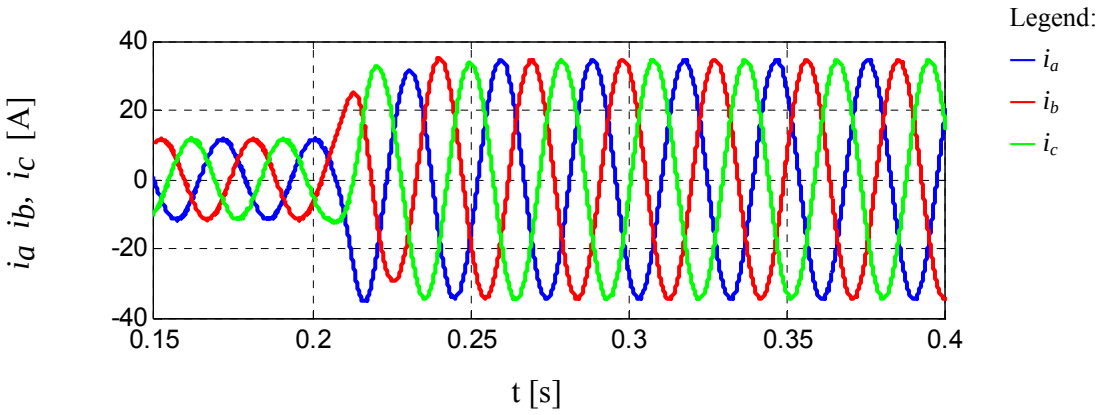

(b) generator current

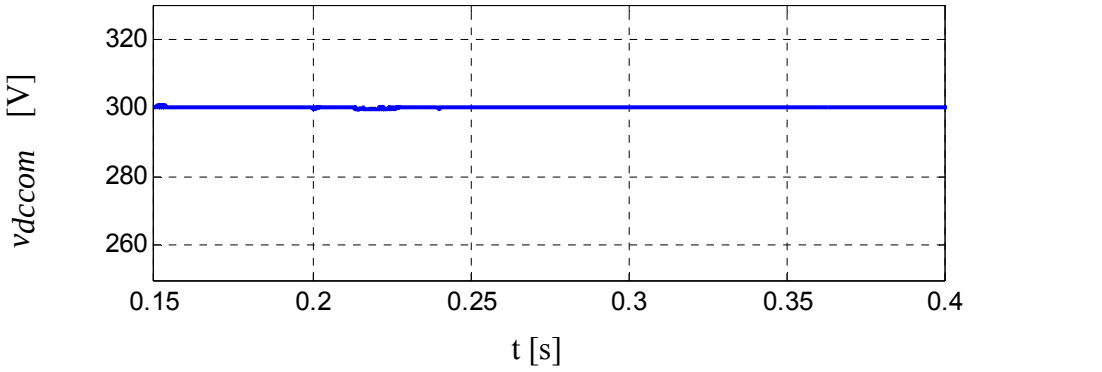

(c) floating capacitor voltage

Fig. 5.17 Series regulated CVVF system, simulation results, 34.5 Hz, 28% to 85%

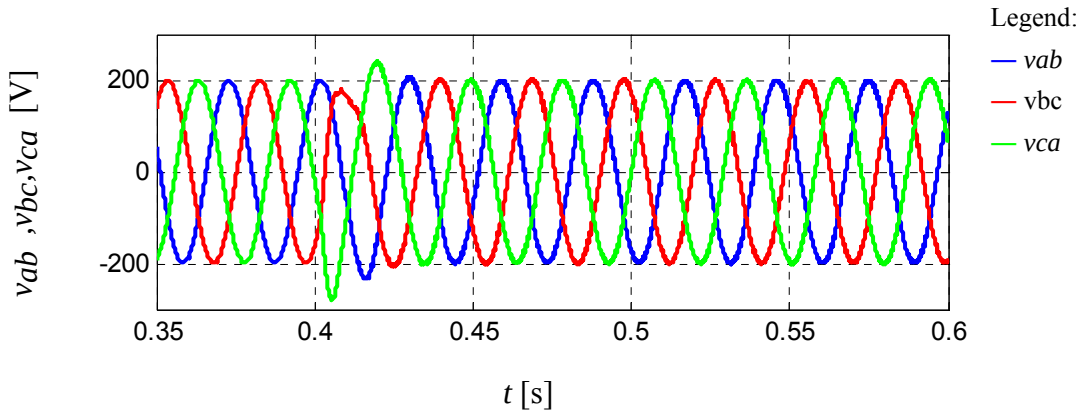

(a) line-to-line voltage

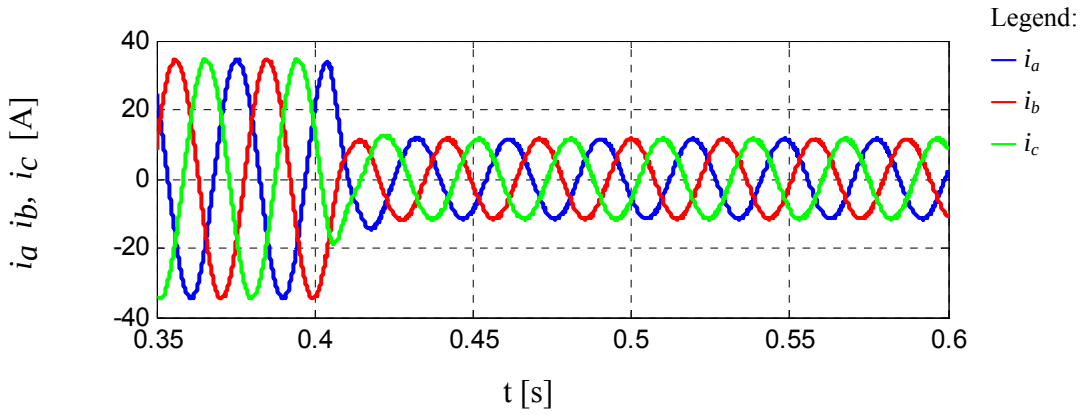

(b) generator current

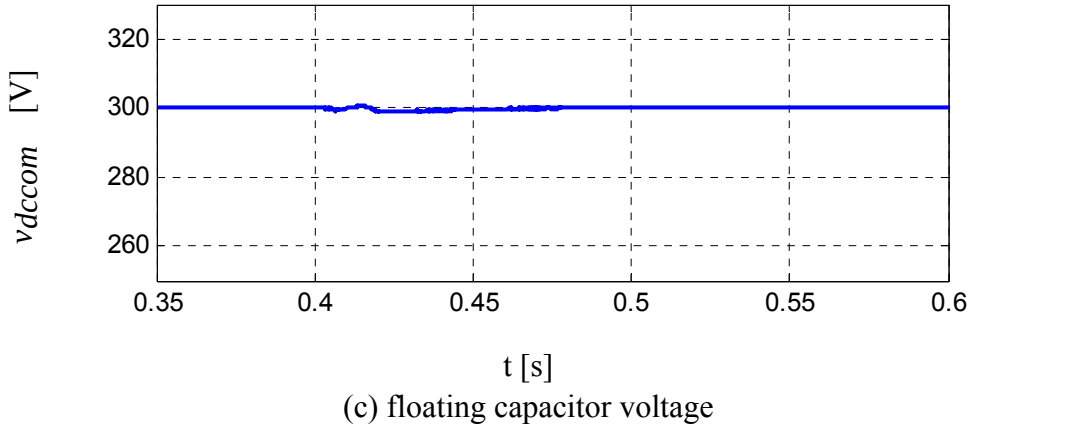

(c) floating capacitor voltage

Fig. 5.18 Series regulated CVVF system, simulation results, 34.5 Hz, 85% to 28%

(3) 48.8 Hz

The same load steps have been simulated at 48.8 Hz as well. This frequency corresponds to the highest speed of the generator. The controller does show some

limitation of performance at the highest generator speed. Although there is no steady state error shown in the load voltage, the over voltage is high when a large load step down is applied.

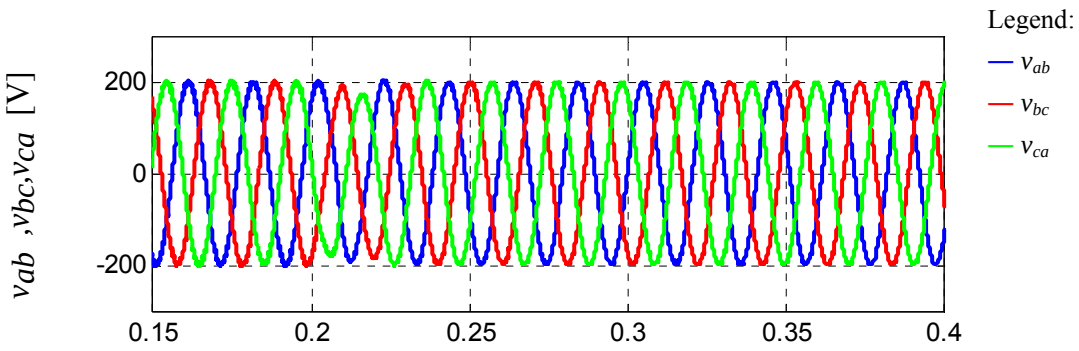

(a) line-to-line voltage

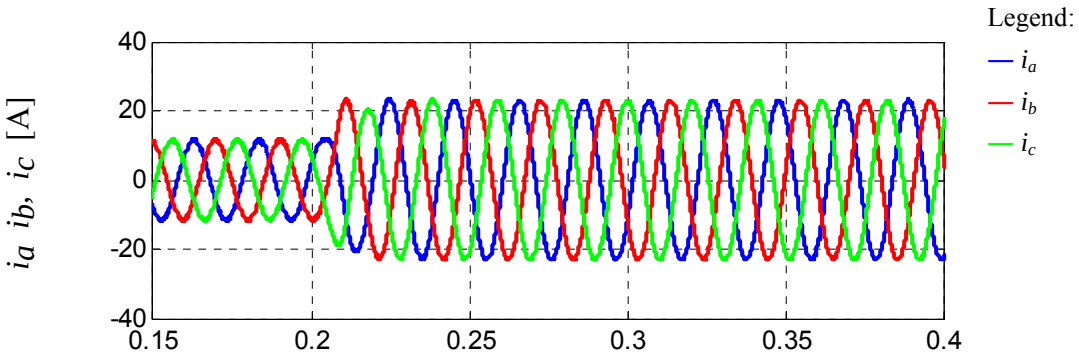

(b) generator current

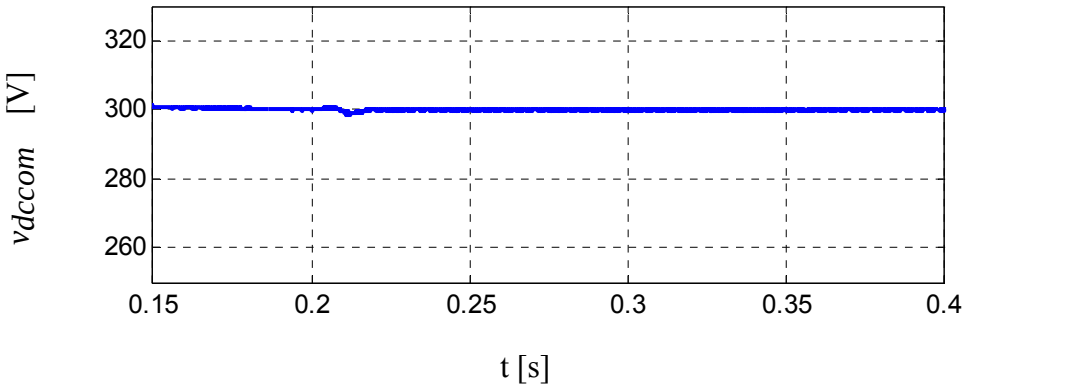

(c) floating capacitor voltage

Fig. 5.19 Series regulated CVVF system, simulation results, 48.8 Hz, 28% to 56%

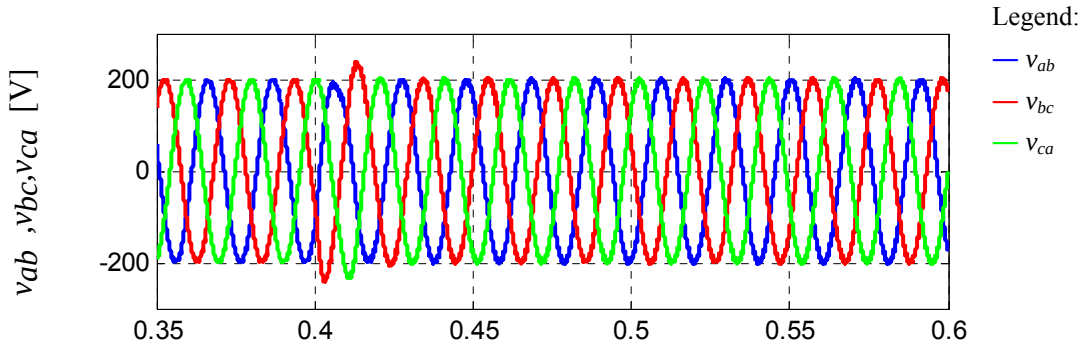

(a) line-to-line voltage

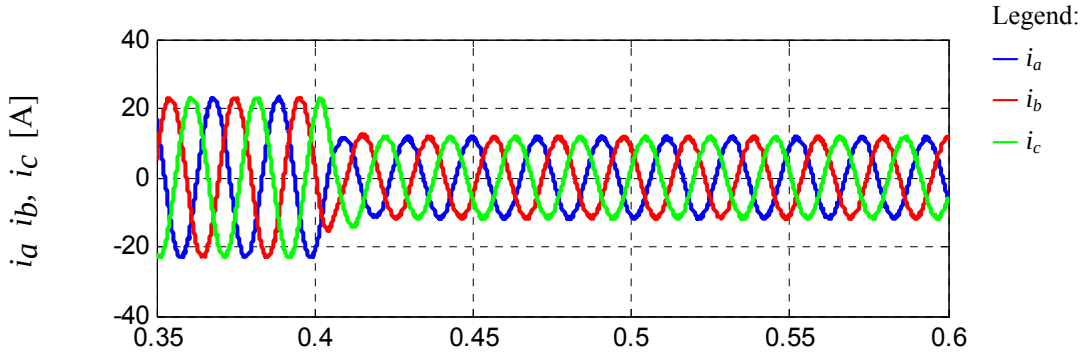

(b) generator current

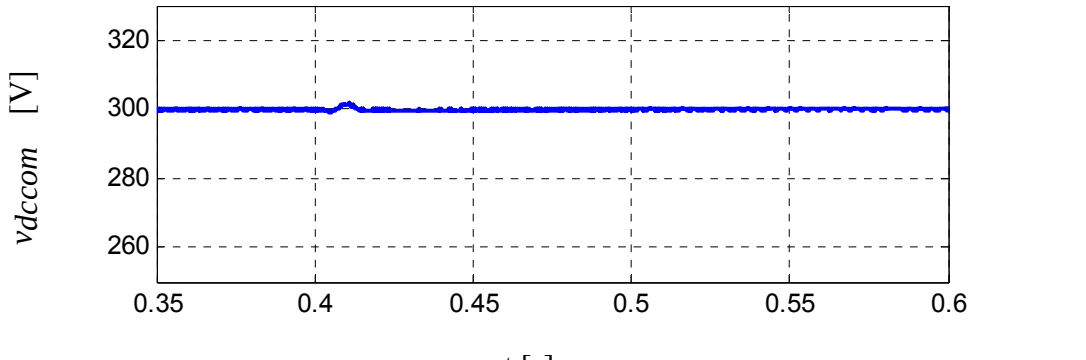

(c) floating capacitor voltage

Fig. 5.20 Series regulated CVVF system, simulation results, 48.8 Hz, 56% to 28%

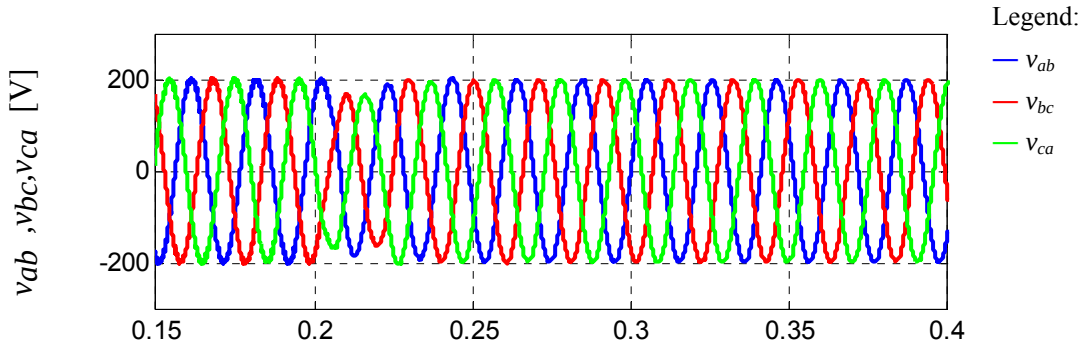

(a) line-to-line voltage

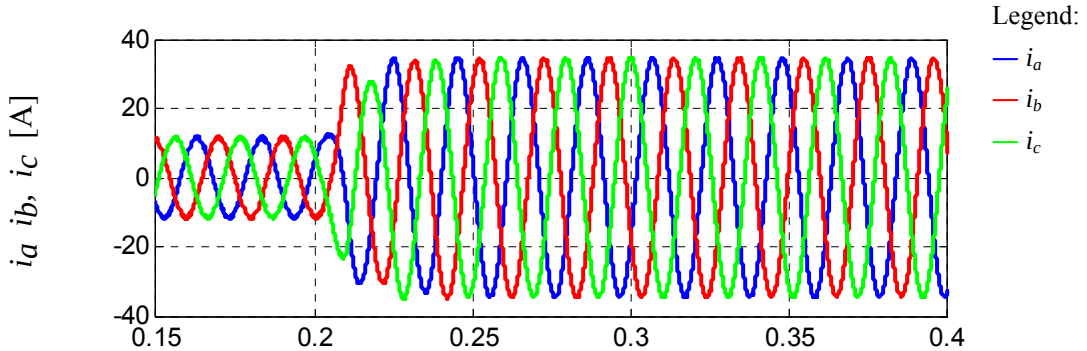

(b) generator current

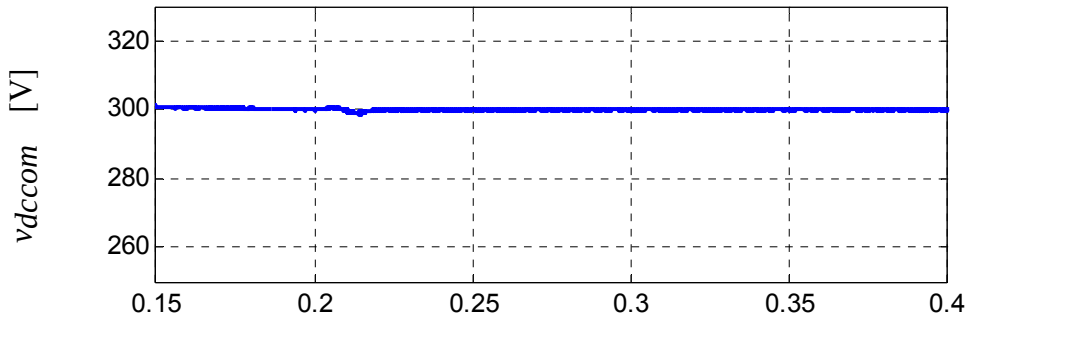

(c) floating capacitor voltage

Fig. 5.21 Series regulated CVVF system, simulation results, 48.8 Hz, 28% to 85%

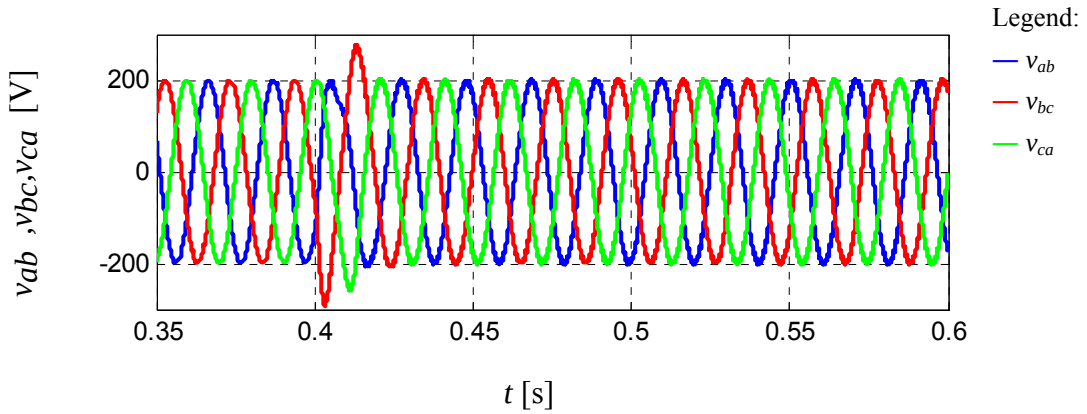

(a) line-to-line voltage

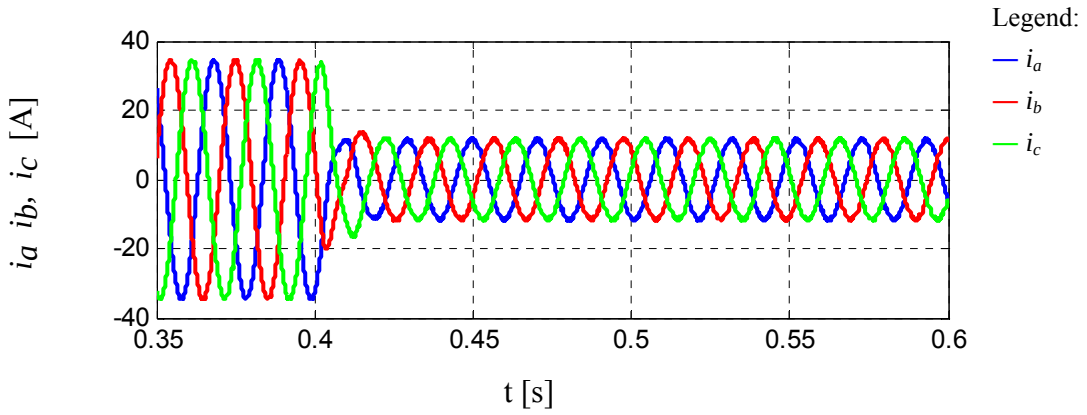

(b) generator current

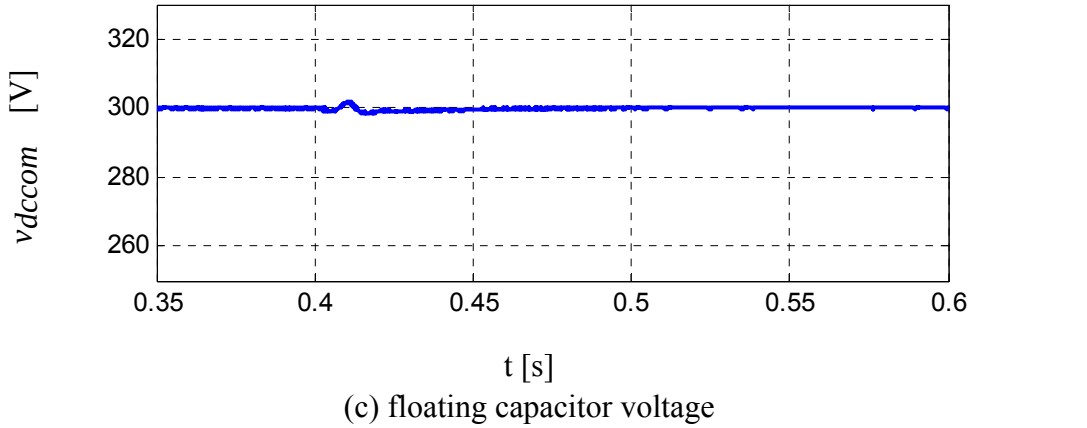

(c) floating capacitor voltage

Fig. 5.22 Series regulated CVVF system, simulation results, 48.8 Hz, 85% to 28%

The simulation results that have been presented show that the proposed series compensator is able to regulate the generator distribution side voltage at different speed and load levels. In steady state, the load voltage has the same amplitude before and

after the load change although the load current changes in a significant amount. The voltage is within the safe region during the transient. It also returns to its nominal value quickly after the load changes. The compensation DC bus voltage can also be well regulated during the transient at all three speeds.

5.5. Experimental Study

The experiment is carried out using the same PM machine and inverter system used in the previous chapters. A separate SCR inverter is build to control the load level. The details of the set up are described in the appendix.

(1) 24.4 Hz

The experimental results at 24.4 Hz is shown in Fig. 5.23 to 5.26. The same load levels used in the simulation are used in the experiment. When the load is changed between 28% and 56%, the voltage regulation effects are noticeable but very good. The floating capacitor voltage can be well regulated by the compensation inverter. The over voltage is more apparent when the load is changed from 85% to 28% as expected.

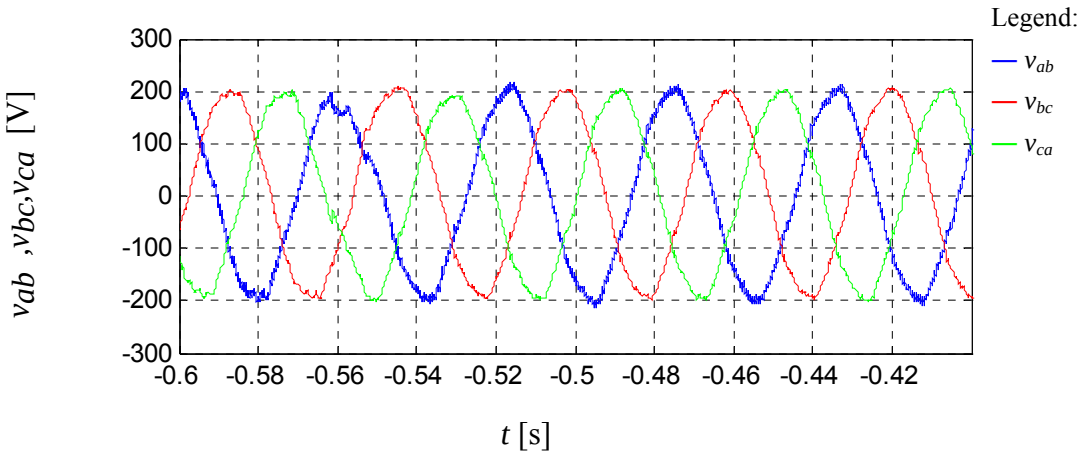

(a) line-to-line voltage

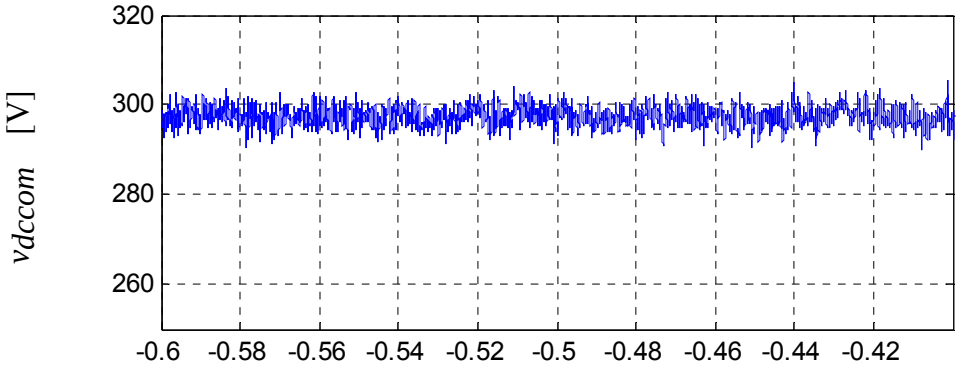

(b) floating capacitor voltage

Fig. 5.23 24.4 Hz, 28% to 56%

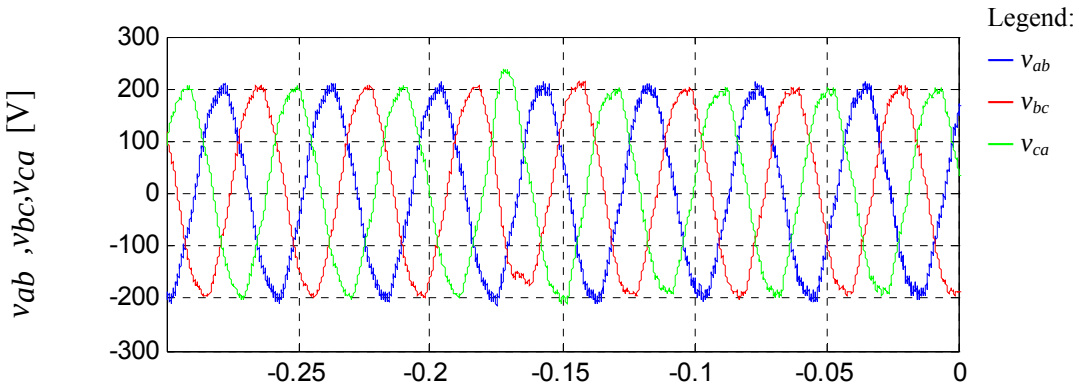

(a) line-to-line voltage

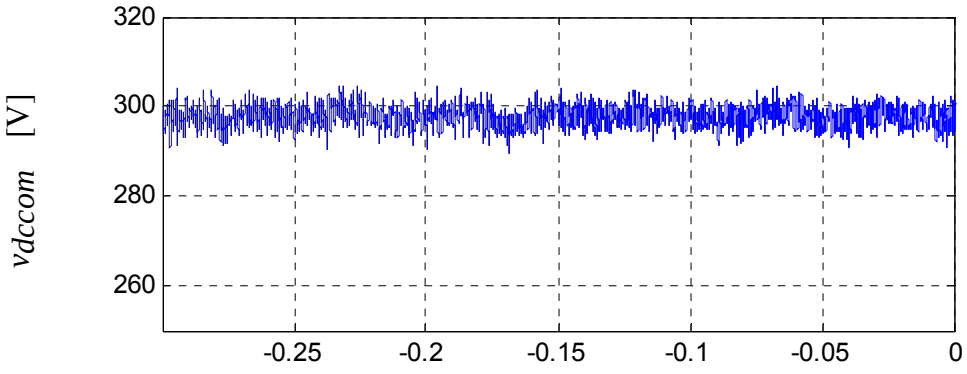

(b) floating capacitor voltage

Fig. 5.24 Series regulated CVVF system, experiment results, 24.4 Hz, 56% to 28%

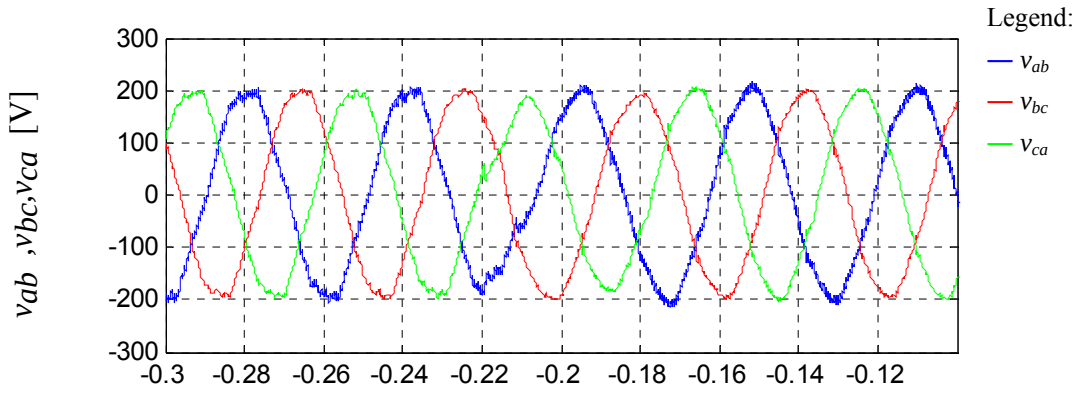

(a) line-to-line voltage

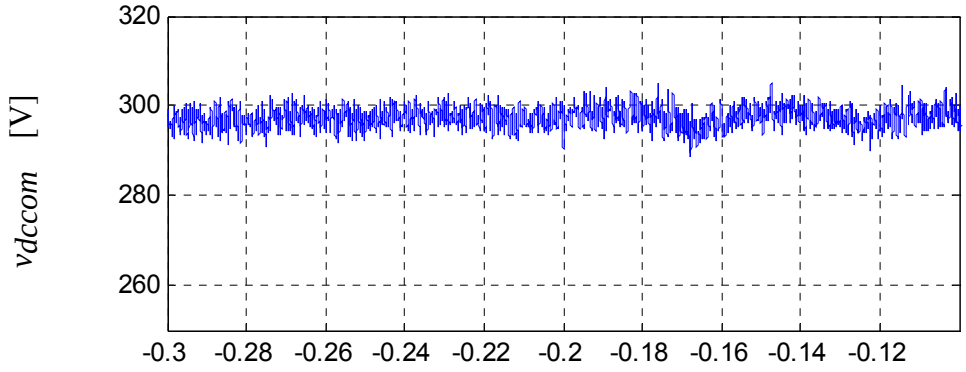

(b) floating capacitor voltage

Fig. 5.25 Series regulated CVVF system, experiment results,24.4 Hz, 28% to 85%

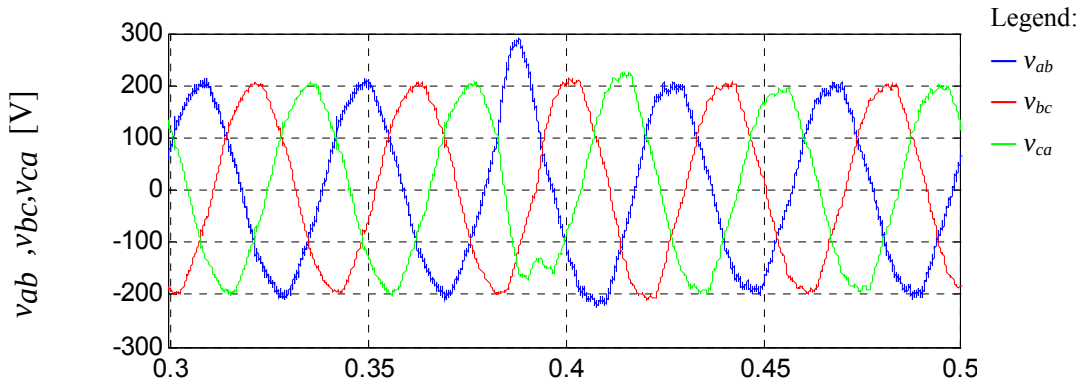

(a) line-to-line voltage

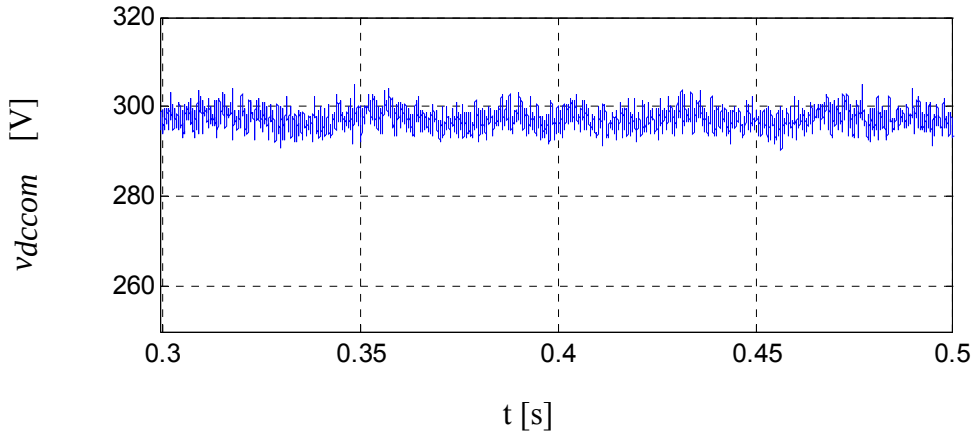

(b) floating capacitor voltage

Fig. 5.26 Series regulated CVVF system, experiment results,24.4 Hz, 85% to 28%

(2) 34.5 Hz

At 34.5 Hz, the voltage error during the transient is more apparent compared to that at 24.4 Hz. Similar phenomena was observed in the simulation results. The increased generator impedance is the reason for increased voltage transient.

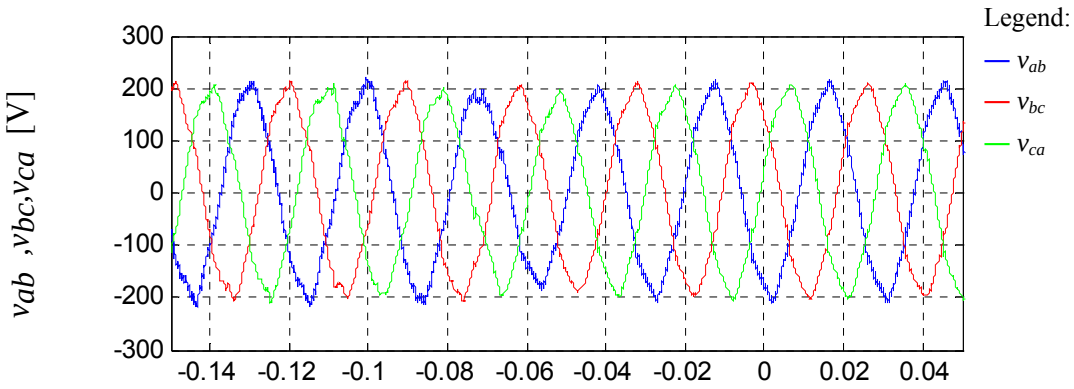

(a) line-to-line voltage

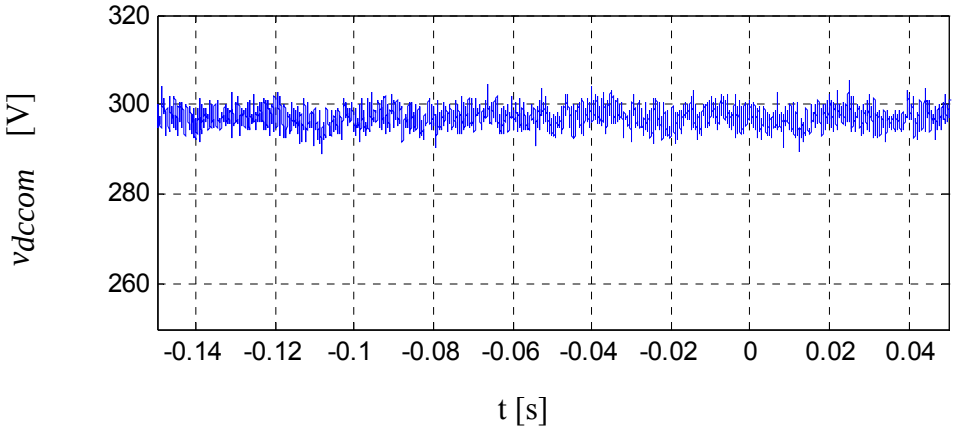

(b) floating capacitor voltage

Fig. 5. 27 Series regulated CVVF system, experiment results,34.5 Hz, 28% to 56%

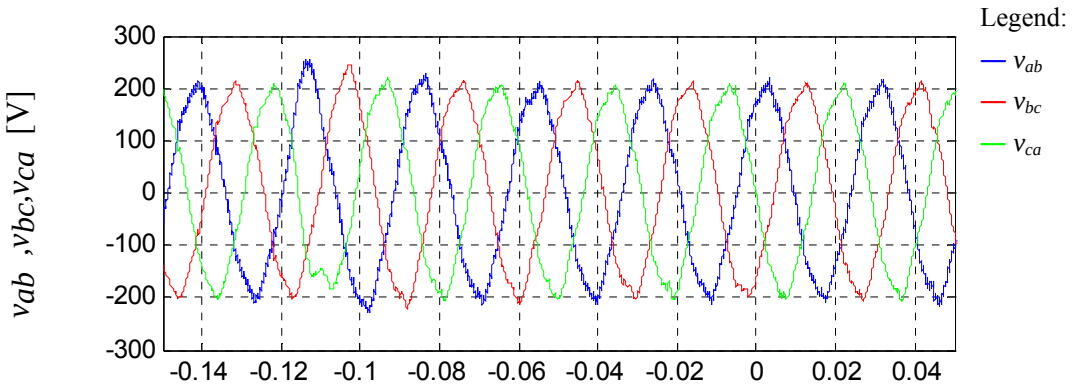

(a) line-to-line voltage

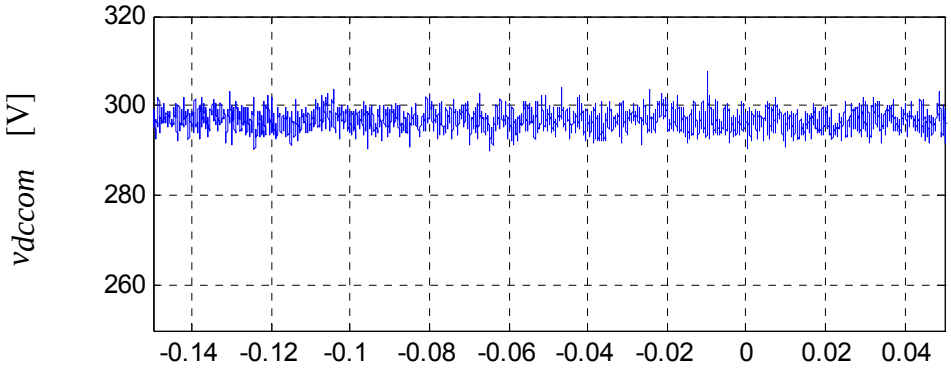

(b) floating capacitor voltage

Fig. 5.28 Series regulated CVVF system, experiment results,34.5 Hz, 56% to 28%

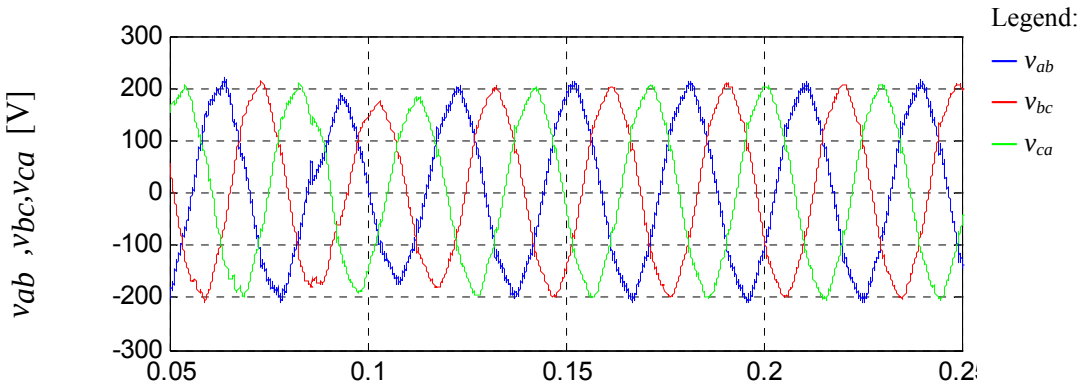

(a) line-to-line voltage

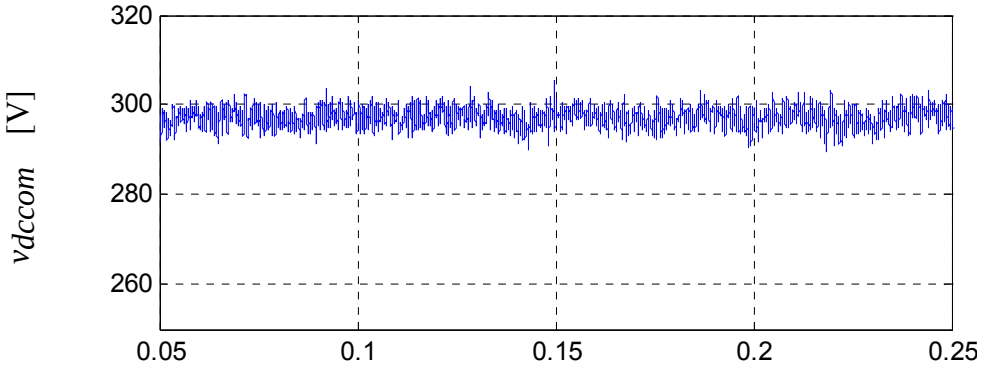

(b) floating capacitor voltage

Fig. 5. 29 Series regulated CVVF system, experiment results,34.5 Hz, 28% to 85%

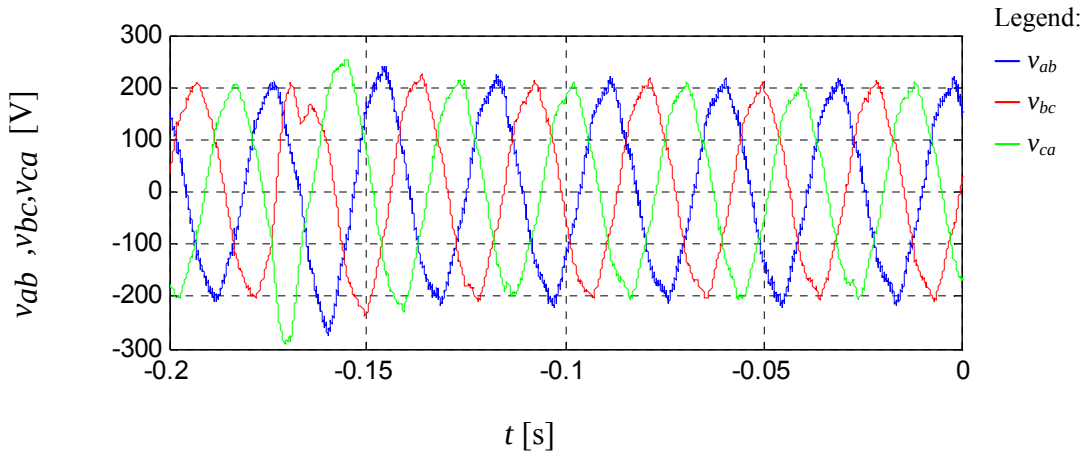

(a) line-to-line voltage

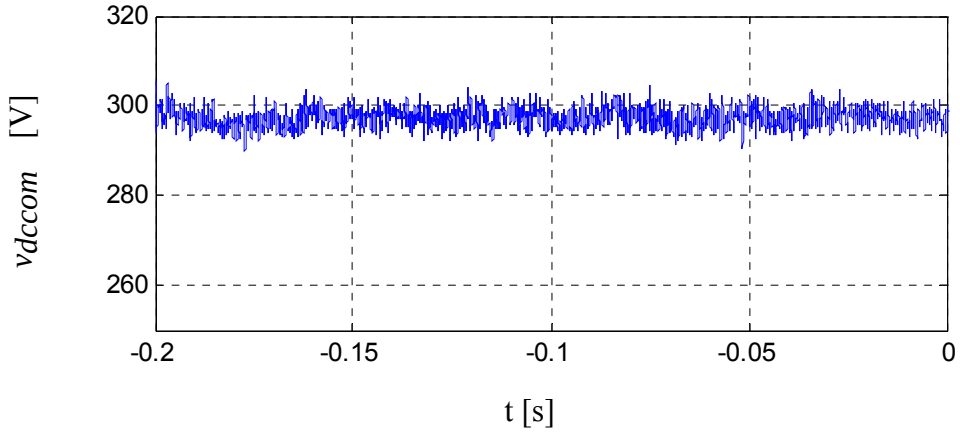

(b) floating capacitor voltage

Fig. 5. 30 Series regulated CVVF system, experiment results,34.5 Hz, 85% to 28%

(3) 48.8 Hz

The same step load test is performed at 48.8 Hz. The results are given in Fig. 31 to 34. As predicted by the simulation, the voltage transient is the worst at the top speed. However, in steady state, there is no error in the load voltage. The proposed system and control method is thus validated.

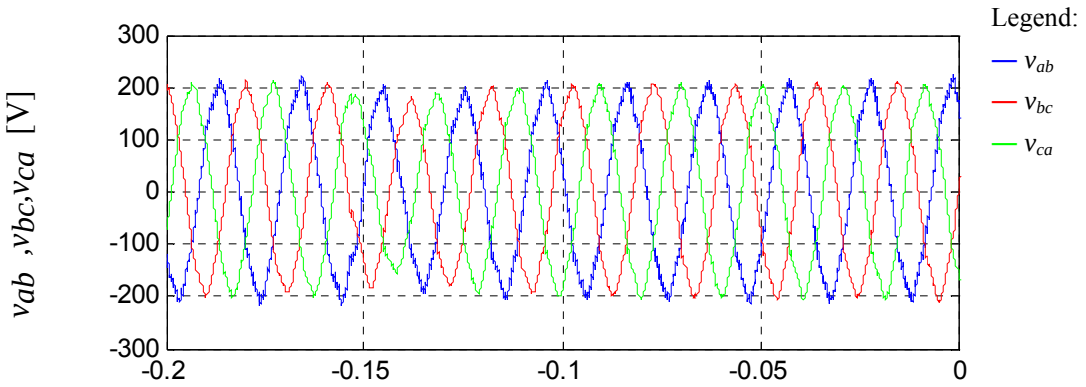

(a) line-to-line voltage

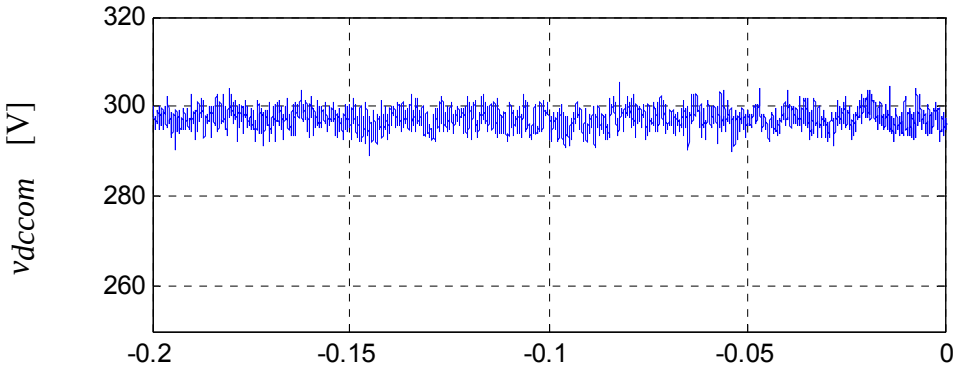

(b) floating capacitor voltage

Fig. 5.31 Series regulated CVVF system, experiment results,48.8 Hz, 28% to 56%

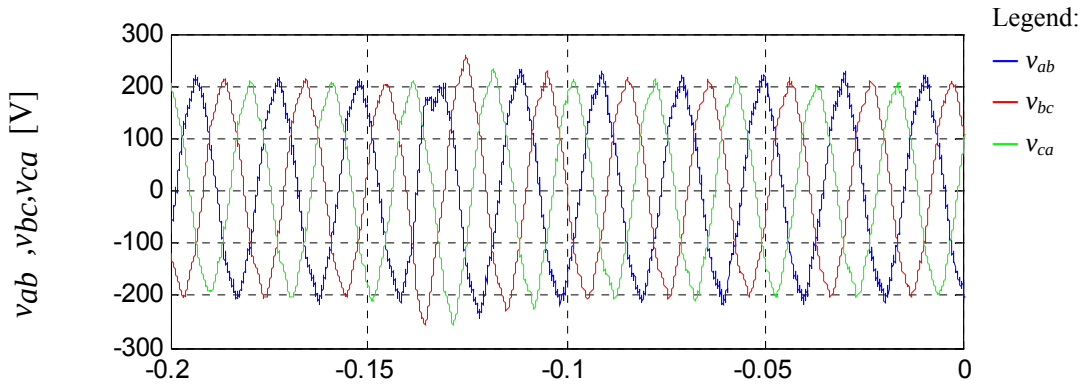

(a) line-to-line voltage

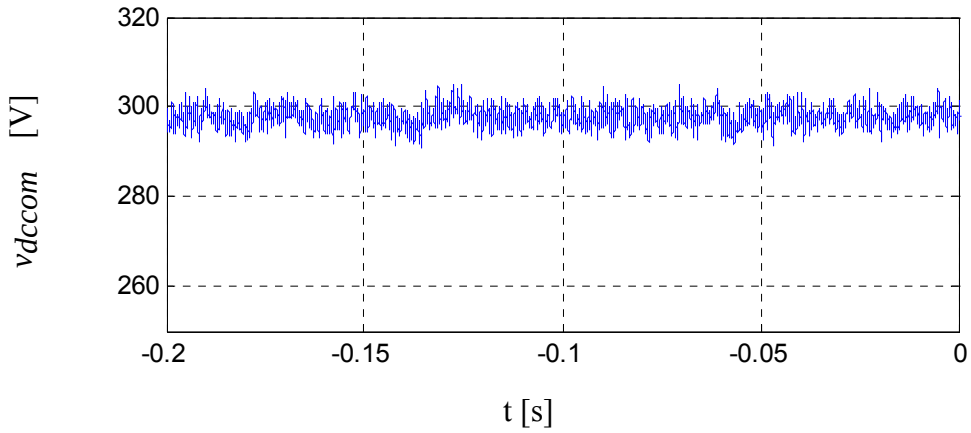

(b) floating capacitor voltage

Fig. 5.32 Series regulated CVVF system, experiment results,48.8 Hz, 56% to 28%

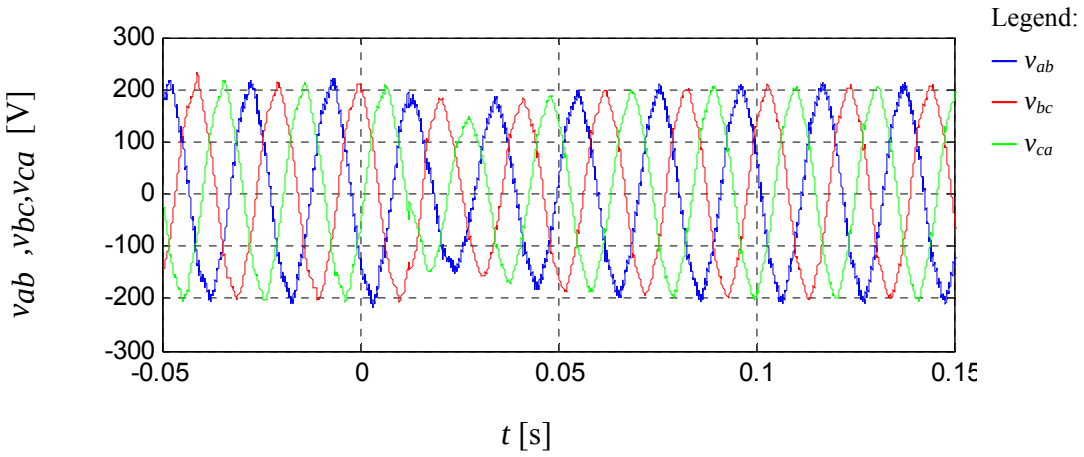

(a) line-to-line voltage

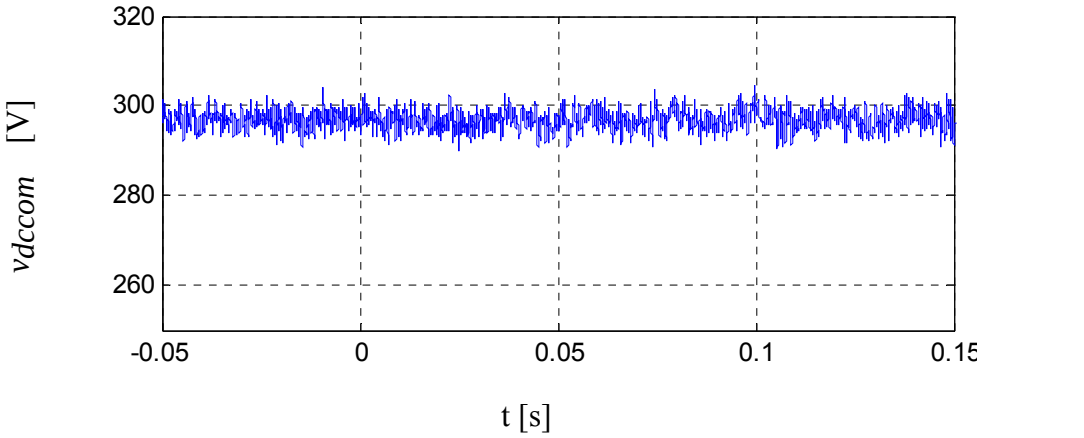

(b) floating capacitor voltage

Fig. 5.33 Series regulated CVVF system, experiment results,48.8 Hz, 28% to 85%

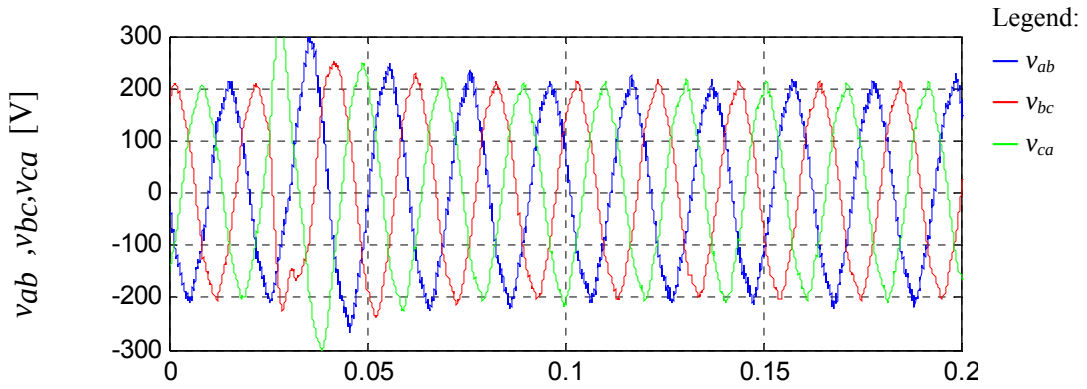

(a) line-to-line voltage

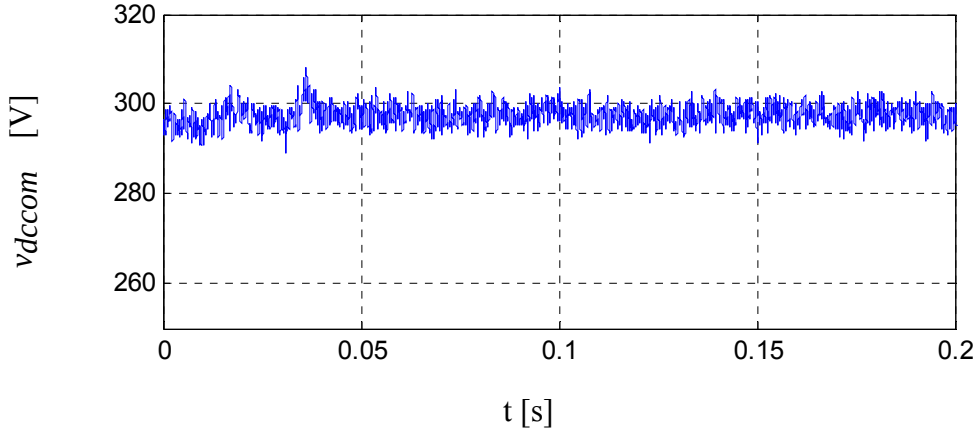

(b) floating capacitor voltage

Fig. 5.34 Series regulated CVVF system, experiment results,48.8 Hz, 85% to 28%

5.6. Practical Considerations

5.6.1. Load Protection under Faults

It has been mentioned that the generator in the proposed CVVF system has to be oversized in voltage rating. At the maximum operating speed, the back-emf would exceed the voltage rating at the load side. It is important that the loads are protected from over voltage damage under regulator shut down. If the circuit breakers at the load side can be open, the compensation inverter is only connected to one side of the generator windings. Ideally, there will be no over voltage seen by the compensation

inverter. In practice, a crowbar can be used at the load side for fast load over voltage protection. Fig. 5.35 shows the protection circuit. When an over voltage fault is detected and confirmed, the crowbar will be immediately fired. The generator will be shorted through the crowbar. The loads will not experience the over voltage because the generator is shorted through the crowbar. This would allow enough time for the circuit breaker to trip. However, in this case, the compensation converter and floating capacitor must be oversized so that they are able to withstand the peak value of the generator back-emf.

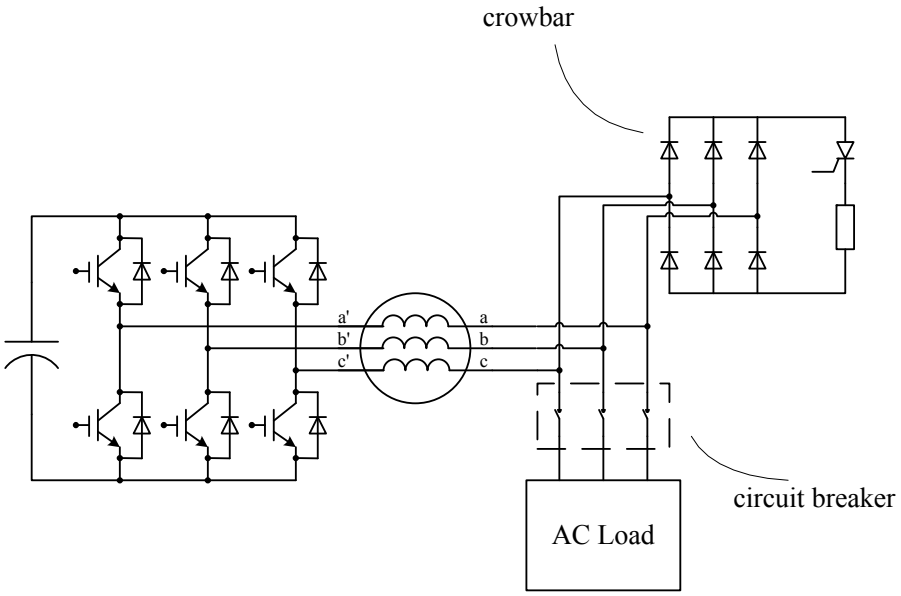

Fig. 5. 35 Protection of proposed CVVF system

Load short circuit protection is an embedded function that comes with the topology. When an over current is detected at the load side, the compensation inverter will be controlled as a large inductor to reduce the fault current. Considering the voltage rating of the compensation inverter is significant, the fault can be limited well below the rated current. Therefore, the circuit breakers at the load side have enough time to open.

5.6.2. Grounding of the System

In practical distribution systems, a floating subsystem is sometimes not desired for safety purposes. A ground may be needed for the series regulator. In practice, the compensation inverter can be grounded at the mid point of two split capacitors using high impedance. A circuit diagram is shown in Fig. 36. The high impedance would be sufficient to prevent a large amount of zero sequence current flowing in the system if the load is grounded. If the mid pint of the capacitors is hard grounded, additional measure must be taken to reduce the zero sequence current. For example, a common mode choke could be used to increase the zero sequence impedance. A modulation technique that ensures zero average zero sequence voltage will help to reduce the zero sequence current in the system as well. In short, if a ground point is required for the compensation inverter, there are several methods that can be used to limit the zero sequence current flow in the system.

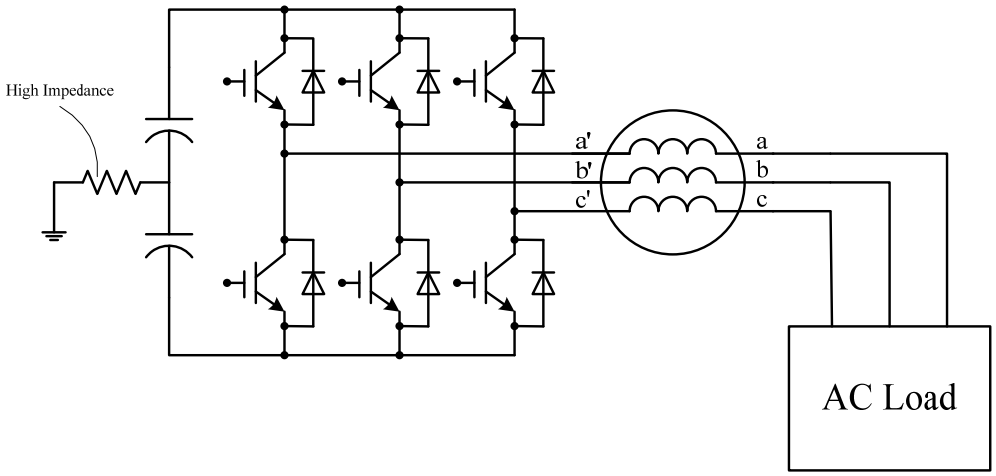

Fig. 5. 36 Grounding of compensation inverter

5.7. Summary

A small CVVF AC distribution system topology using open-winding PM generator was proposed in this chapter. A series connected inverter was used to regulate the load side voltage at different speed and load levels. The sizing of the compensation inverter is discussed. The impact of generator selection on inverter sizing was studied. The proposed topology was compared with its dual, the shunt regulator. Simulation and experimental results have been given to show the validity of the proposed system. The dynamic performance of the regulator is acceptable. Some of the practical issues are addressed at the end of the chapter.

Chapter 6

Conclusions, Contributions and Future Work

This thesis investigates series compensation of open-winding permanent magnet machines utilizing a voltage source inverter that is directly connected in series with the machine. The key conclusions, contributions and recommendation of future work are presented in this chapter.

6.1. Conclusions

This research focuses on the series compensation of open-winding PM machines by using a voltage source inverter as a controllable reactive power source. Some concepts from the FACTS literature have been adopted for several smaller single machine systems. Smaller size and variable frequency operation are two of the features that distinguish the considered systems from regular FACTS devices. Compared to more conventional series compensation methods, the proposed scheme has the benefits of lower cost, lighter weight, faster response and etc. Three different applications are used in this thesis to demonstrate the operation principle and benefits of the proposed compensation scheme. In the application examples discussed, the proposed series compensation scheme is applied to improve the performance and/or reduce the cost of the overall systems.

6.2. Contributions of this Work

6.2.1. Review of Existing Open-winding Machine Drives and FACTS Concepts in Small Systems

A thorough review of existing research on open-winding machines and drives has been presented in this thesis. Due to the different names and terminologies used by different authors, it has been very difficult to find open-winding machine drives related publications although significant amount of research efforts have been spent in this area. In Chapter 1, the review of open-winding machine drives covers a wide scope of this area, including high power motor drive applications, modulation techniques, variations of the basic topologies, EV/HEV applications, renewable power generation, microgrid applications, etc.

In addition, a review on the small single machine systems utilizing FACTS concepts is presented. The term FACTS is not mentioned in every cited literature. However, in the review, the covered publications all utilize some sort of power electronics devices combined with reactive elements for reactive power compensation. Three major areas are covered: generator voltage regulation, motor drive system, renewable power generation.

6.2.2. Series Compensation by Open-winding Machine Configuration

A series compensation scheme by open-winding machine configuration is proposed in this thesis. A voltage source inverter directly connected to the machine is used as the compensation device. The operating principle and control modes are discussed. Some of the concepts of the SSSC from the FACTS are directly applicable to the proposed compensation method. Impedance control, power flow control and voltage control are

possible by injecting reactive power into the machine from the inverter. It has also been identified the proposed compensation method is a preferred compensation method in smaller single machine systems compared to more conventional methods like the SSSC or the MERS due to the weight and cost reduction or performance improvement.

6.2.3. Extending the Operating Region of PM Motors by Series Compensation

A dual inverter open-winding PM machine drive is proposed in this work. Limited DC bus voltage can be better utilized at both low and high speed by controlling the compensation inverter to supply the reactive power required by the motor. The operating space of the motor can be extended considerably.

A large portion of the effort has been spent on investigating the advantages and disadvantages of the proposed topology:

(1) The sizing of the compensation inverter and floating capacitor base on the lab scale IPM machine is presented. The rating of the compensation inverter and floating capacitor can be determined from the operating space requirement;

(2) The proposed topology is compared with three more conventional topologies for the lab scale IPM machine. The comparison includes power capability, CSPR, inverter sizing, reactive elements and voltage waveform;

(3) The applicability of the proposed topology to other PMSM motors is investigated as well. The normalized machine parameter plane is used for the study. Several typical motors are used as example cases. It has been found that for motors that have limited flux weakening capability, the proposed topology is able to expand the CPSR considerably. In contrast, for motors that are designed for good flux weakening capability, the proposed topology is capable of postponing the start of flux weakening and having the motor delivering rated torque beyond rated speed.

The impact of the compensation inverter on the motor excitation voltage is also studied. It is found the improvement of harmonics in the proposed topology is not as good as more conventional open-winding motor drive with isolated voltage sources. For carrier based PWM, phase shift between carrier signals of the two inverters can be used to reduce the harmonics contents in the phase voltage waveform.

A control method based on widely used filed oriented controller is proposed in this thesis. The controller automatically switches between capacitive and inductive compensation and covers both low and high speed region of the lab scale IPM machine used.

An experimental setup has been built to study the proposed topology. The operating principle and the proposed control method have been successfully verified in tests.

6.2.4. Series Compensated Open-winding PM Generator System

A diode rectifier based wind power generation system utilizing the open-winding series compensation method is proposed in Chapter 4. The total active power electronics converter rating can be reduced in such a system compared to more conventional PM generator wind power systems.

With the compensation inverter providing the reactive power to the generator, the generator utilization can be improved in a diode rectifier based wind power generation system. Moreover, the generator power can be controlled without a full power rated converter.

The var requirement and inverter sizing are discussed in this thesis. The impact of generator parameters on inverter sizing is presented. The characteristic current and saliency ratio are used as the normalized parameters for the study.

The impact of compensation inverter on the generator excitation voltage and

current is studied. It is shown the fundamental excitation voltage is increased to higher than available voltage from the diode rectifier. With the added switching events and reduced discontinuity in the current waveform, the harmonics in the generator current can be reduced.

The control method of the proposed system under fixed or variable speed operation is proposed. The generator power is directly controlled by the compensation inverter. In addition, the proposed system can be operated without a position sensor installed.

Simulation model and experimental setup are built. The operating principle and proposed control method have been verified by both simulation and experiment.

6.2.5. Series Regulated PM Generator CVVF AC Distribution System

A series regulated CVVF AC distribution system is proposed in Chapter 5. The load voltage amplitude can be controlled to be constant as the generator speed and load level varies.

The proposed series regulator is compared with its parallel dual in the existing literature. The advantages and disadvantages of the two types of systems are presented. It is found generator has to be oversized in both types of systems due to the requirement of variable speed operation. For shunt regulated system, the generator is oversized for current rating. In contrast, the generator is oversized for voltage rating in a series regulated system.

Moreover, inverter sizing and generator considerations are presented in this thesis. Characteristic current and saliency ratio are used as the normalized parameters in the study to represent different designs of generators. Similar to a shunt regulated CVVF system, a high saliency ratio is preferred for minimizing the compensation inverter.

A control method for the series regulated CVVF system is proposed.

The validity of the proposed system and control method are verified by both simulation and experimental studies.

6.3. Future Work

This research has developed the basic concept and method of series compensation of PM machines using open-winding configuration. The functions of the series compensation have been demonstrated in three example systems. It becomes clear that some of the aspects of this work is worth further investigation. This section documents the suggestions of possible future work.

6.3.1. Advanced Control Methods for Open-winding Motor Drives

In this work, a basic variation of field orientated controller is used in the proposed motor drive system in Chapter 3. It can be expected that the transient performance of the proposed topology can be improved if more advanced control method is employed. For example, a deadbeat direct torque and flux control (DB-DTFC) of the proposed series compensated open-winding PM motor drive can be investigated. An extra degree of freedom of manipulating the volt-sec that can be applied to the motor is available in an open-winding motor drive. The controller can be optimized for losses or transient performance according to the requirements of the application. At the same time, when a floating capacitor is used at the auxiliary inverter DC bus, the amp-sec applied to the capacitor is another constrain that has to be taken into account.

Likewise, self-sensing control can be applied to the proposed topology to eliminate the position sensors in the drive for reduced cost or improved reliability. The frequency of the injected signal could potentially be increased because the effective switching frequency can be increased using proper PWM technique when a separate inverter is

available in the system.

A feedback style flux weakening control is used in the study. The dynamics of the flux weakening controller is shown to be limited during transient. New flux weakening control algorithms for series compensated open-winding PM motor drive can be developed to improve the dynamic performance of the system.

In this research, the floating capacitor voltage is controlled to be zero to reduce the switching losses at low speed. When needed, it is raised to the nominal value. It is possible to dynamically control this voltage to meet the power capability requirement and minimize the converter losses at the same time. A control algorithm needs to be developed to accurately estimate the required floating capacitor voltage on line.

The modulation technique of the proposed open-winding motor drive can be improved. Although the largest portion of publications on open-winding motor drives is on the modulation technique, none of the existing literature is focused on the operation when one of the inverter is used for pure reactive power compensation. The harmonic content can potentially be further reduced. Space vector modulation for compensation and harmonics reduction purpose could be one possible solution.

Furthermore, in this work, carrier based modulation with 3rd harmonic injection is used. The utilization of the DC bus voltage for both the inverters is still not maximized. Overmodulation techniques for an open-winding motor drive is another area worth investigation which will ultimately leads to six-step operation of both inverters. Another 10% of DC bus voltage is available for both of the inverters under six-step operation.

6.3.2. Advanced Control for Open-winding Generator Systems

In addition to the control of open-winding motor drives, the control of open-winding generator systems can also be improved. The compensation inverter used in this research is very similar to the SSSC and the DVR. Some of the more advanced

control algorithms have been developed for compensation control in the FACTS applications. Those control methods can be applied to the generation systems proposed in Chapter 4 and 5 with minimal modifications. For instance, generated power and voltage amplitude are the feedback signals chosen in this research. The time differential of power has been selected as feedback signal to improve load voltage control in some of the existing literature. It is possible that the performance of the controller can be improved considerably using more advanced controllers.

DVR control of small distribution system based on open-winding PM generator is possible when an energy storage element is attached to the compensation DC bus. Loads that are very sensitive can be protected if the compensation inverter is controlled as a DVR.

6.3.3. Variable DC Bus Voltage Series Compensated Open-winding PM Generator Wind Power System

Constant main DC bus voltage is assumed in Chapter 4 for the wind power system. There are certainly limitations imposed by this constraint. On the one hand, the real part of the generator terminal voltage is not adjustable. It is not possible to minimize the losses in the generator under some operating conditions. On the other hand, the diode rectifier will start to operate only when the peak value of the generator back-emf is higher than the DC bus voltage. The operating speed range is narrowed compared to a back-to-back PWM converter driven wind power system. These undesirable issues could potentially be solved by controlling the DC bus to be different value under different operating conditions using the grid side inverter.

Due to the natural property of the conventional voltage source inverter, the DC bus voltage has to be higher than the peak value of the grid side AC voltage. Therefore, the lower limit of the DC bus voltage is determined by the grid voltage. To allow low speed

operation, a boost type inverter can be used instead of the buck type inverter in the series compensated open-winding generator wind power system. A buck-boost type of inverter will allow even wider operation speed range.

Current source inverter can also be employed at the grid side. PWM type CSI would potentially result in wide operating speed range when a diode rectifier is used as the main power conversion device for the generator. The compensation inverter would improve the generator utilization the same as in a VSI based system. When a thyristor inverter is used, the total cost of the system can be further reduced compared to the proposed wind power system in Chapter 4.

6.3.4. Unbalance Operation of Series Regulated CVVF Distribution System

It was mentioned in Chapter 5 that the proposed series regulated CVVF system is not suitable for unbalance operation without any modifications. However, it is possible that the system would be capable of operating under unbalanced load when the inverter topology can be modified. For instance, a 4-leg inverter can be employed to allow zero sequence current to flow in the system. As a result, unbalanced load can be used to in the system.

6.3.5. Other Applications of Open-winding Compensation Configuration

This research proposes three applications using the open-winding compensation configuration. The potential of this compensation topology has certainly not been fully investigated yet. Some of the potential applications are given here.

First, energy storage can attached to the compensation inverter. It has been mentioned the compensation inverter can be used as an interface for the energy storage element. The benefits and control method when an extra degree of freedom added to the system can be explored. It is expected the overall system performance can be improved

for all proposed applications.

Second, the application of series compensated open-winding generator in microgrid can be explored. Diesel generator has been proposed as a back-up power source in microgrid. An open-winding generator could potentially replace the conventional Y connected generator. The compensation inverter can be controlled to regulate the voltage at the AC side and perform as a rectifier to supply any DC load in the microgrid. The control method needs to be modified to accommodate the plug-and-play concept of the microgrid.

Third, an open-winding generator can be used to power two separate DC loads. The voltage rating of the two DC loads can be different. For example, for HEV application, an IGBT rectifier can be used to power a 300 Volts DC bus for the traction motor while a MOSFET rectifier is connected to the other side of the generator can power a 24 V DC bus for the electronics devices on the vehicle.

In addition, the proposed open-winding compensation topology is not only for open-winding rotational machine. It is equally applicable to open-winding transformer. A voltage source inverter can be connected to an open-winding transformer for compensation and energy storage purposes.

6.3.6. Other FACTS Type of Devices in Smaller Systems

Applying FACTS concept in smaller systems is a relatively new concept. This research only focuses on one type of device. Other type of FACTS devices may have equal potentials when adopted by smaller systems. However, the benefits and control methods will surely vary from case to case. Some research efforts are needed to answers the questions of whether they are overall a better solution for certain applications.

Appendix

A.1 Experimental Setup

A.1.1 Open-winding PM Machine

The open-winding PM machine used in this project is modified from an IPM generator used by a previous project [66]. The generator is modified from a commercial generator from Reliance. Fig. A.1 is a picture of the generator.

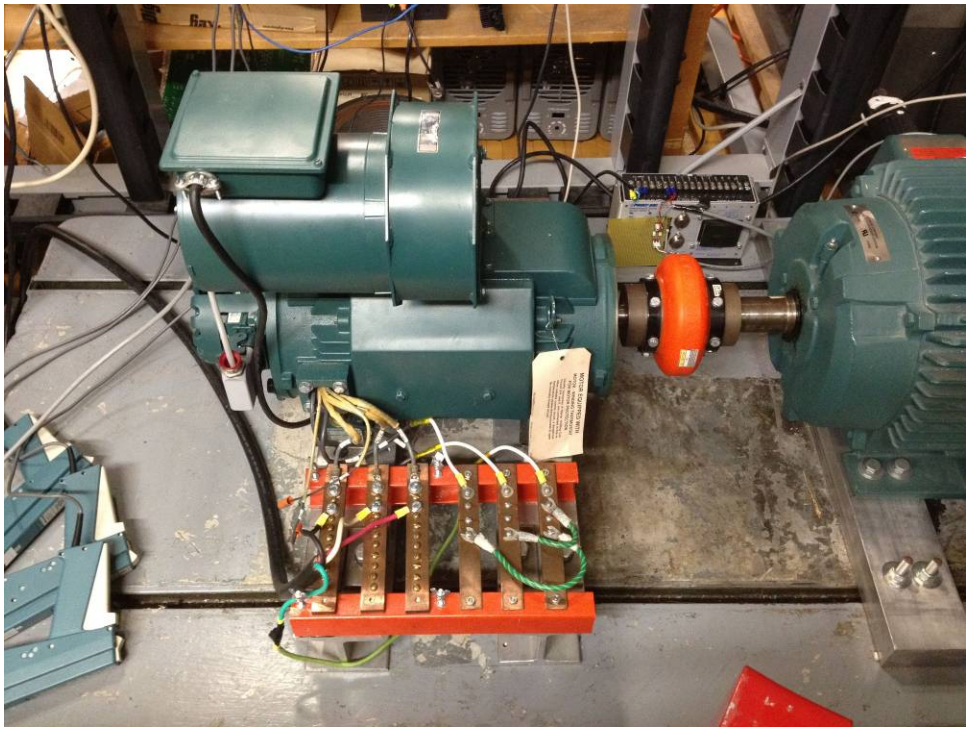

Fig. A.1 Open-winding IPM motor under test

The stator windings are rewound according to the requirement of the previous project. The parameters of the generator after the rewind are given in Table A.1.

Table A.1 Parameters of the original generator

Parameter	Symbol	Value
Rated power	P_r	10 kW
Rated voltage	V_r	115 Vrms
Rated current	I_r	29 Arms
Rated speed	n_r	1035 rpm
Base frequency	fb	34.5 Hz
Base radian speed	ω_{rb}	215.8 elec rad/s
Stator resistance	r_s	0.315 Ohm
d-axis inductance	L_d	16 mH
q-axis inductance	L_q	51 mH
PM flux linkage	λ_m	0.75 wb
Number of poles	P	4

The neutral connection of the machine is disconnected at a local winding shop. All six leads of the three-phase winding are taken out to the terminal.

It has been found in the test that the machine has significant of 17^{th} and 19^{th} harmonics. At high speed, the harmonics frequency could exceeds the bandwidth of the current regulator and induces undesirable harmonics in the machine current.

A.1.2 Dynamometer

A 30 kw reliance industrial induction motor is used as the dynamometer motor. The motor is powered from a Danfoss 5602 industrial drive. The motor is equipped with a 1000 line encoder for precise torque and speed control. The DC bus voltage of the dynamometer drive is different from the open-winding motor drive because it is powered from the 480 V power grid. Therefore, a back-to-back drive configuration is not possible to directly circulate power through the DC bus. Dynamic brake resistor bank is added to the system to dissipate the regenerated power from the induction motor.

A.1.3 Inverters

To simplify the design work, identical inverters are used for both main and compensation inverters. The inverter built for the study is shown in Fig. A.2. An IPM module 6MBP75RA120 from Fuji Electric is used for each inverter. The inverter board includes gate signal isolation circuit, current and voltage sensing and conditional circuit, hardware protection circuit, power supply for gate drives, interface circuit for CPLD, DSP and encoder. Each of the inverters has sensors and signal conditional circuits for three channels of phase current, two channels of AC voltage and one channel for the DC bus voltage. This allows the inverter to be used for multiple purposes including motor drive inverter and grid side inverter. The use of programmable logic devices Altera Max II enables the flexible protection which can be configured as either one-shot or pulse-by-pulse operations. The protection functions of the inverter board includes over current, over DC bus voltage, IPM module shoot through and over temperature. A single TI TMS320F28335 DSP is used to control both of the inverters. The evaluation board eZdsp F28335 is selected for use. The DSP board is equipped with serial communication interface to send stored internal control data to the monitoring PC. The Serial Peripheral Interface (SPI) is also available for use with the digital-to-analog converter built for the project.

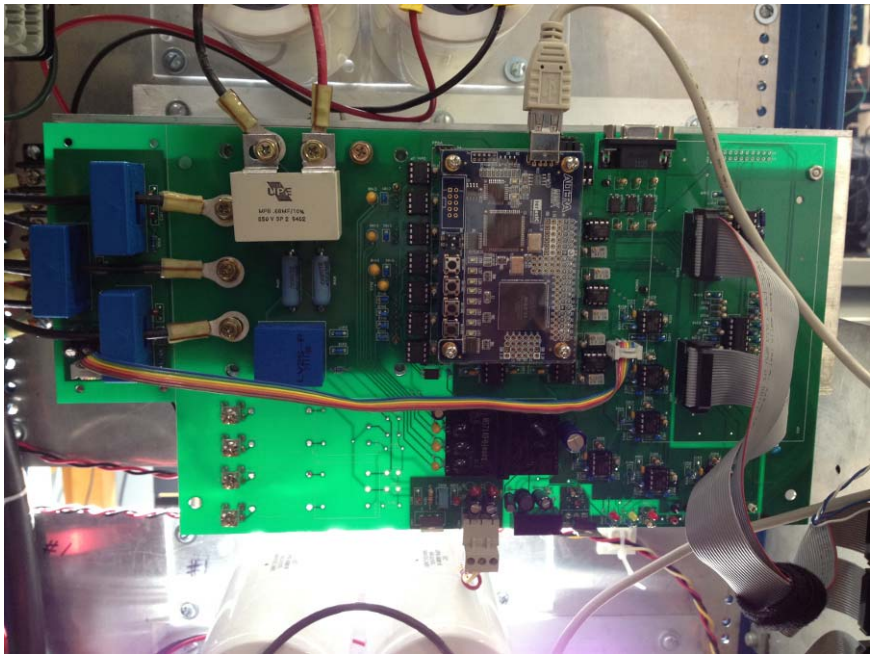

Fig. A.2 Inverter built for experiment study

A.1.4 Auxiliary Circuits

(1) SCR Interface Circuit

As mentioned in Chapter 5, SCR interface circuit is needed between the generator and passive loads due to the large generator inductance. The SCR interface circuit is built with integrated opto-triac IC as the isolation circuit. Moreover, zero-crossing detection function is integrated in the opto-triac chip MOC3061M used in the circuit. Fig. A.3 is a picture of the interface circuit.

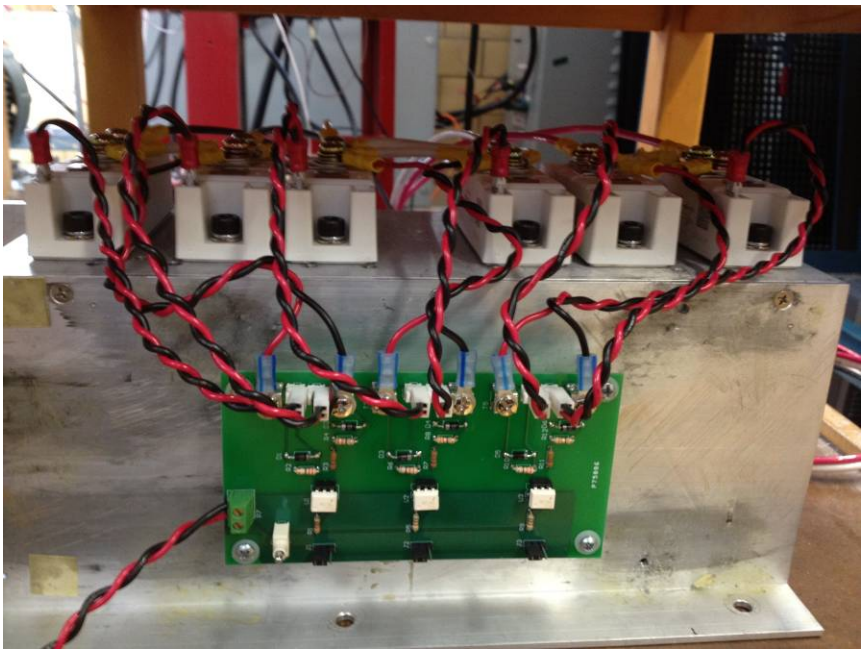

Fig. A.3 SCR interface circuit

(2) DAC Board

Digital-to-analog converter is an important tool for debugging the system. A DAC board with SPI interface is built for use in this project. The DAC chip used is 4-channel 12-bit DAC7715 from Texas Instrument. Fig. A.4 shows the DAC board built.

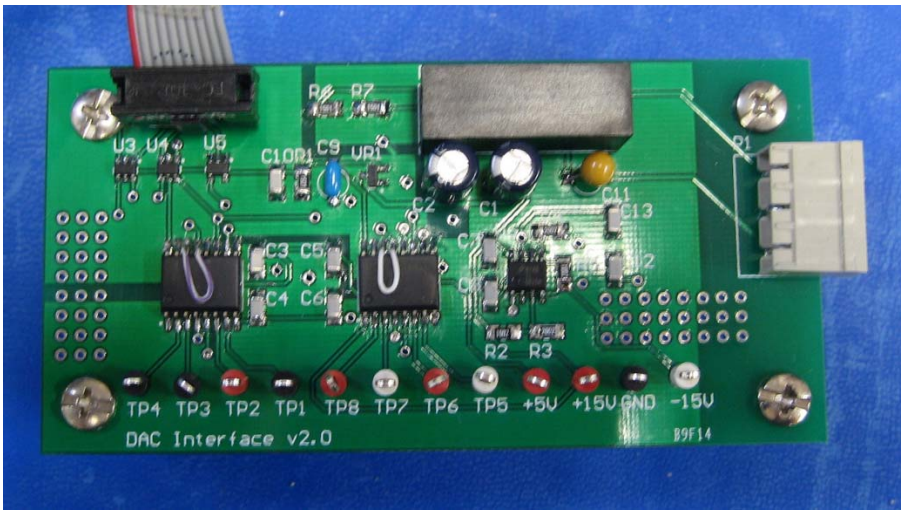

Fig. A.4 DAC board

(3) DSP Breakout Board

The inverter board is designed so that the DSP board can be directly stacked on the inverter board. With two inverters used in the system, a separate DSP interface board is built so that identical interface connectors can be used for both of the inverters. This breakout board also includes the SCI and SPI interface connector.

(4) Dynamic Break

Due to the lack of dynamic break switch in the IPM module used, a separate inverter is used as the dynamic break module. The lower switch of one inverter leg is used as the dynamic break switch. The CPLD software is changed accordingly to accommodate this function. The turn-on and turn-off voltage can be set manually by adjusting the potentiometer on the inverter board.

A.1.5 System Configurations

The inverters and auxiliary circuits presented above are the building blocks for the test setup. The system is configured differently for the three application examples. The configurations are given in this section.

(1) Open-winding PM Motor Drive

Fig. A.5 shows the system configuration for the experimental study in Chapter 3. The INV1 is powered from the 230 V power grid through a variac for adjustable main DC bus voltage. Both the main and the compensation inverters are controlled by the DSP board. A dynamic brake is connected to the main DC bus to dissipate the regenerated power during transient.

(2) Open-winding PM Generator Wind Power System

Fig. A.6 shows the system configuration for the series compensated open-winding generator wind power system proposed in Chapter 4. The main inverter is replaced by a diode rectifier. The dynamic brake is used to regulate the main DC bus voltage at its nominal value.

(3) Open-winding Generator CVVF System

Fig. A.7 is the block diagram for system configuration of the CVVF system proposed in Chapter 5. Passive loads are divided into two parts for step load transient test. One set of load is directly connected to the generator while the other set is connected to the generator through the SCR interface. A manual switch controls the load level during the test.

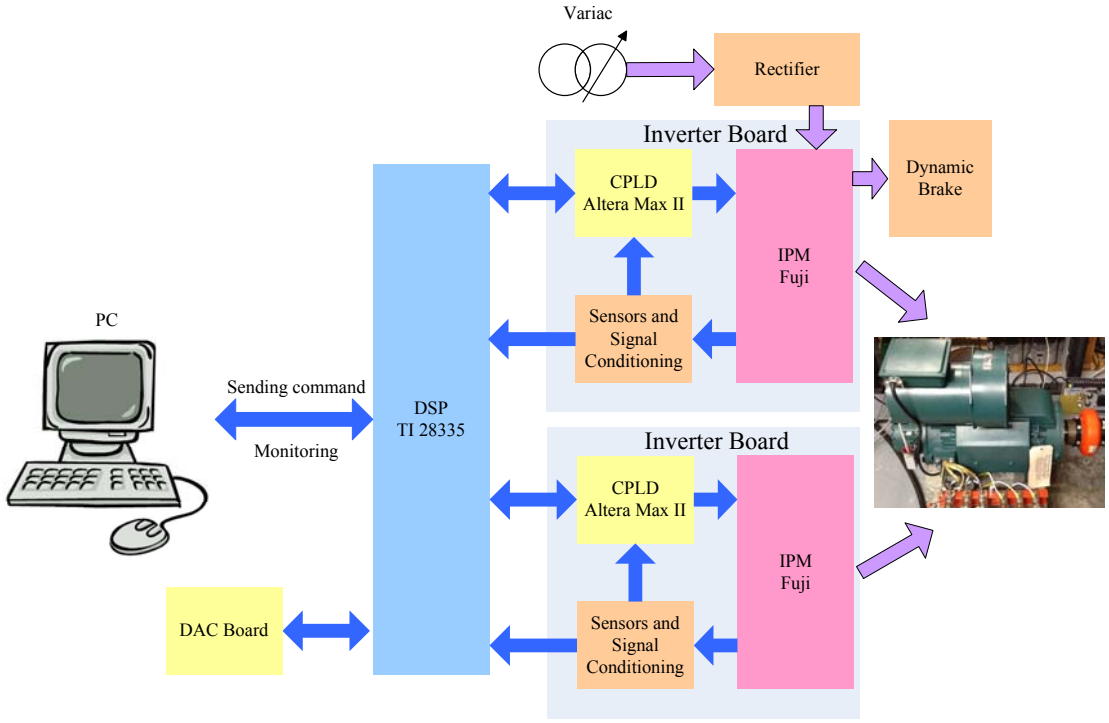

Fig. A.5 Test Setup configuration for open-winding motor drive in Chapter 3

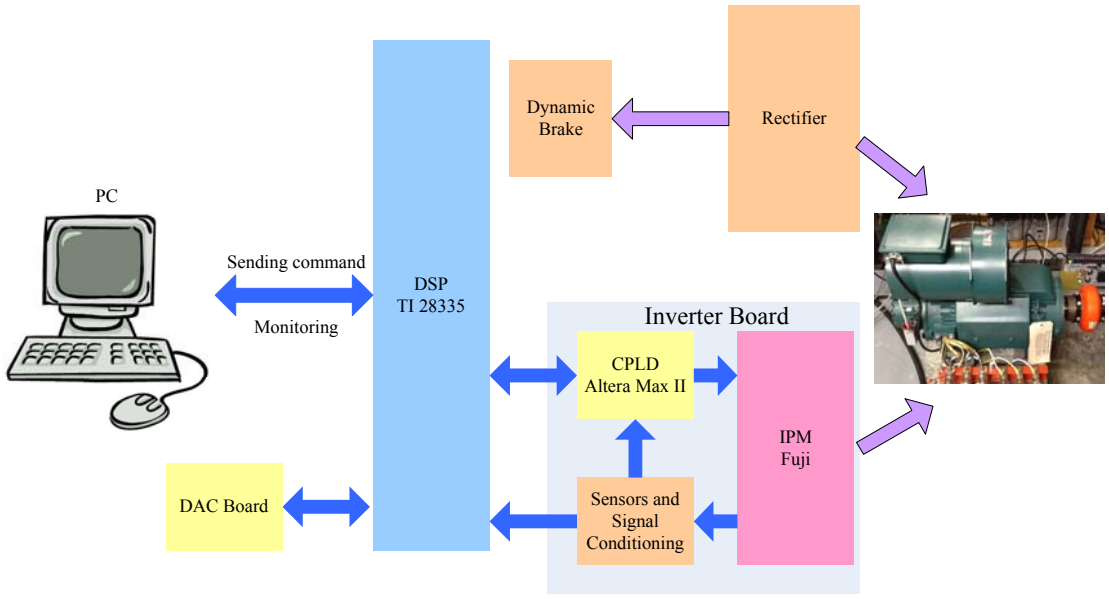

Fig. A.6 Test Setup configuration for open-winding wind power system in Chapter 4

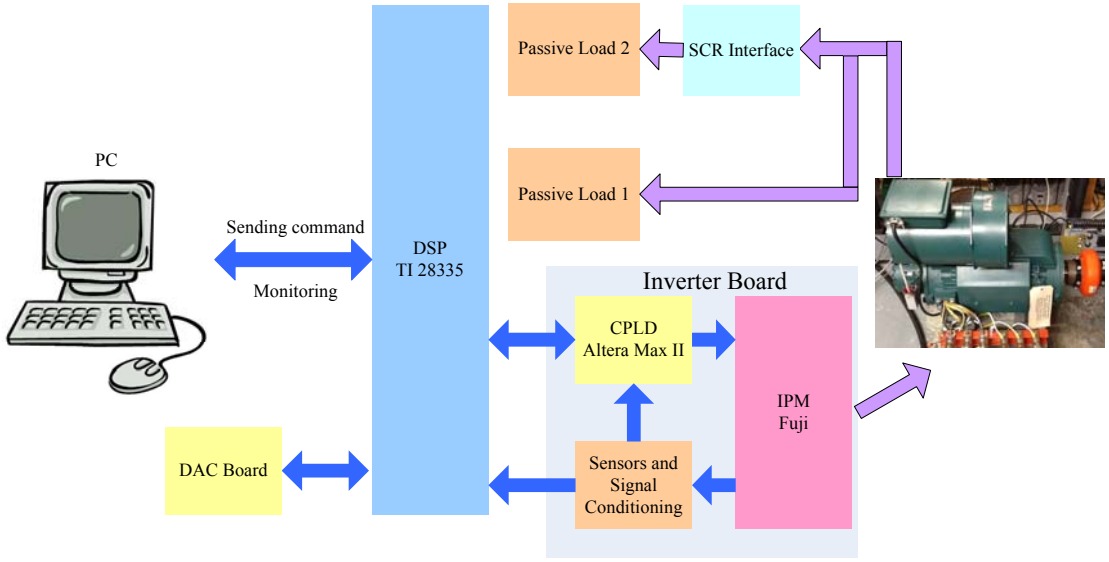

Fig. A.7 Test Setup configuration for open-winding generator CVVF system in Chapter 5

A.2 Definition of transformation

In most cases, it is easier to analyze and control an AC machine in a rotating reference frame. The reference transformation used through out this work is defined as below:

$$f_d = \frac{2}{3}\left[f_a \sin(\theta_{rf}) + f_b \sin(\theta_{rf} - \frac{2}{3}\pi) + f_c \sin(\theta_{rf} + \frac{2}{3}\pi)\right] \quad \text{(A.1)}$$

$$f_q = \frac{2}{3}\left[f_a \cos(\theta_{rf}) + f_b \cos(\theta_{rf} - \frac{2}{3}\pi) + f_c \cos(\theta_{rf} + \frac{2}{3}\pi)\right] \quad \text{(A.2)}$$

$$f_0 = \frac{1}{3}[f_a + f_b + f_c] \quad \text{(A.3)}$$

Where f represents any three phase quality, for example voltage and current, in abc or dq0 reference frame. The angle θ_{rf} is the angle of the reference frame in electrical rad/s. For PM machines, rotor reference frame is usually used. Therefore, the rotor angle in electrical rad/s is used as the reference frame angle in modeling the machine. In part of this work, current phase angle is selected as the reference angle for the controller. By using current phase angle, the q-axis is aligned with the peak of phase A current.

There are a variety of definitions of transformation. To be clear, the amplitude of vector variable in dq plane is defined to be the peak value of AC component of variables in abc reference frame.

The inverse reference transformation can be derived as:

$$f_a = f_d \sin(\theta_{rf}) + f_q \cos(\theta_{rf}) + f_0 \quad \text{(A.4)}$$

$$f_b = f_d \sin(\theta_{rf} - \frac{2\pi}{3}) + f_q \cos(\theta_{rf} - \frac{2\pi}{3}) + f_0 \quad \text{(A.5)}$$

$$f_c = f_d \sin(\theta_{rf} + \frac{2\pi}{3}) + f_q \cos(\theta_{rf} + \frac{2\pi}{3}) + f_0 \quad \text{(A.6)}$$

Bibliography

[1] B. K. Bose, Modern Power Electronics and AC Drives. Upper Saddle River, NJ: Prentice-Hall PTR, 2002.

[2] Jahns, T.M.; Owen, E.L.; , "AC adjustable-speed drives at the millennium: how did we get here? ," *Power Electronics, IEEE Transactions on* , vol.16, no.1, pp.17-25, Jan 2001

[3] D. W. Novotny and T. A. Lipo, Vector Control and Dynamics of AC Drives. New York: Oxford Univ. Press, 1996.

[4] N. Mohan, T. M. Undeland, and W. P. Robbins, *Power Electronics: Converters, Applications and Design*, Piscataway NJ: John Wiley, 1996.

[5] Wheeler, P.W.; Rodriguez, J.; Clare, J.C.; Empringham, L.; Weinstein, A.; , "Matrix converters: a technology review," *Industrial Electronics, IEEE Transactions on* , vol.49, no.2, pp.276-288, Apr 2002

[6]Wei, L.X; The Development of Matrix Converters with Reduced Number of Switches, PhD thesis, University of Wisconsin-Madison, 2002

[7] Bose, B.K.; , "Power electronics and motion control-technology status and recent trends," *Industry Applications, IEEE Transactions on* , vol.29, no.5, pp.902-909, Sep/Oct 1993

[8] Finch, J.W.; Giaouris, D.; , "Controlled AC Electrical Drives," *Industrial Electronics, IEEE Transactions on* , vol.55, no.2, pp.481-491, Feb. 2008

[9] Rodriguez, J.; Jih-Sheng Lai; Fang Zheng Peng; , "Multilevel inverters: a survey of topologies, controls, and applications," *Industrial Electronics, IEEE Transactions on* , vol.49, no.4, pp. 724- 738, Aug 2002

[10] Chenchen Wang; Yondong Li; , "A survey on topologies of multilevel converters

and study of two novel topologies," *Power Electronics and Motion Control Conference, 2009. IPEMC '09. IEEE 6th International* , vol., no., pp.860-865, 17-20 May 2009

[11] Hammond, P.W.; , "A new approach to enhance power quality for medium voltage AC drives," *Industry Applications, IEEE Transactions on* , vol.33, no.1, pp.202-208, Jan/Feb 1997

[12] Peng, Fang Zheng; , "A generalized multilevel inverter topology with self voltage balancing," *Industry Applications, IEEE Transactions on* , vol.37, no.2, pp.611-618, Mar/Apr 2001

[13] Barbosa, P.; Steimer, P.; Steinke, J.; Winkelnkemper, M.; Celanovic, N.; , "Active-neutral-point-clamped (ANPC) multilevel converter technology," *Power Electronics and Applications, 2005 European Conference on* , vol., no., pp.10 pp.-P.10, 0-0 0

[14] Pulikanti, S.R.; Agelidis, V.G.; , "Five-level active NPC converter topology: SHE-PWM control and operation principles," *Power Engineering Conference, 2007. AUPEC 2007. Australasian Universities* , vol., no., pp.1-5, 9-12 Dec. 2007

[15] Kieferndorf, F.; Basler, M.; Serpa, L.A.; Fabian, J.-H.; Coccia, A.; Scheuer, G.A.; , "A new medium voltage drive system based on ANPC-5L technology," *Industrial Technology (ICIT), 2010 IEEE International Conference on* , vol., no., pp.643-649, 14-17 March 2010

[16] Venkataramanan, G.; Bendre, A.; , "Reciprocity-transposition-based sinusoidal pulsewidth modulation for diode-clamped multilevel converters," *Industrial Electronics, IEEE Transactions on* , vol.49, no.5, pp. 1035- 1047, Oct 2002

[17] Bendre, A.; Venkataramanan, G.; , "Radial state space vector modulation-a new space vector technique for reducing DC link capacitor harmonic currents in three level converters," *Industry Applications Conference, 2003. 38th IAS Annual Meeting. Conference Record of the* , vol.1, no., pp. 684- 691 vol.1, 12-16 Oct. 2003

[18] Bendre, A.; Krstic, S.; Vander Meer, J.; Venkataramanan, G.; , "Comparative

evaluation of modulation algorithms for neutral-point-clamped converters," *Industry Applications, IEEE Transactions on* , vol.41, no.2, pp. 634- 643, March-April 2005

[19] Lezana, P.; Pou, J.; Meynard, T.A.; Rodriguez, J.; Ceballos, S.; Richardeau, F.; , "Survey on Fault Operation on Multilevel Inverters," *Industrial Electronics, IEEE Transactions on* , vol.57, no.7, pp.2207-2218, July 2010

[20] Fei Wang; Rixin Lai; Xibo Yuan; Fang Luo; Burgos, R.; Boroyevich, D.; , "Failure-Mode Analysis and Protection of Three-Level Neutral-Point-Clamped PWM Voltage Source Converters," *Industry Applications, IEEE Transactions on* , vol.46, no.2, pp.866-874, March-April 2010

[21] Levi, E.; , "Multiphase Electric Machines for Variable-Speed Applications," *Industrial Electronics, IEEE Transactions on* , vol.55, no.5, pp.1893-1909, May 2008

[22] Khan, K.S.; Arshad, W.M.; Kanerva, S.; , "On performance figures of multiphase machines," *Electrical Machines, 2008. ICEM 2008. 18th International Conference on* , vol., no., pp.1-5, 6-9 Sept. 2008

[23] T. A. Lipo "A d-q model for six-phase induction machines", *Proc. Int. Conf. Electrical Machines*, vol. 2, pp. 1980 .

[24] Yifan Zhao; Lipo, T.A.; , "Space vector PWM control of dual three-phase induction machine using vector space decomposition," *Industry Applications, IEEE Transactions on* , vol.31, no.5, pp.1100-1109, Sep/Oct 1995

[25] Zhao, Y.; Lipo, T.A.; , "Modeling and control of a multi-phase induction machine with structural unbalance," *Energy Conversion, IEEE Transactions on* , vol.11, no.3, pp.578-584, Sep 1996

[26] A.A. Rockhill, T.A. Lipo,"A Simplified Model of a Nine Phase Synchronous Machine Using Vector Space Decomposition," IEEE Conf. on Power Electronics and Machines for Wind Applications, Proceedings of, June 24-26, 2009, Lincoln, NE.

[27] Burzanowska, H.; Sario, P.; Stulz, Ch.; Joerg, P.; , "Redundant Drive with Direct Torque Control (DTC) and dual-star synchronous machine, simulations and

verification," *Power Electronics and Applications, 2007 European Conference on* , vol., no., pp.1-10, 2-5 Sept. 2007

[28] Mohapatra, K.K.; Kanchan, R.S.; Baiju, M.R.; Tekwani, P.N.; Gopakumar, K.; , "Independent field-oriented control of two split-phase induction motors from a single six-phase inverter," *Industrial Electronics, IEEE Transactions on* , vol.52, no.5, pp. 1372- 1382, Oct. 2005

[29] Yazdani, D.; Ali Khajehoddin, S.; Bakhshai, A.; Joos, G.; , "Full Utilization of the Inverter in Split-Phase Drives by Means of a Dual Three-Phase Space Vector Classification Algorithm," *Industrial Electronics, IEEE Transactions on* , vol.56, no.1, pp.120-129, Jan. 2009

[30] Levi, E.; Jones, M.; Vukosavic, S.N.; , "Even-phase multi-motor vector controlled drive with single inverter supply and series connection of stator windings," *Electric Power Applications, IEE Proceedings* - , vol.150, no.5, pp. 580- 590, 9 Sept. 2003

[31] Jahns, Thomas M.; , "Improved Reliability in Solid-State AC Drives by Means of Multiple Independent Phase Drive Units," *Industry Applications, IEEE Transactions on* , vol.IA-16, no.3, pp.321-331, May 1980

[32] Ouyang, Wen; Modular Permanent Magnet Machine Drive System with Fault Tolerant Capability, Ph.D. thesis, University of Wisconsin-Madison, Dec., 2007

[33] Eden, T. S.; , "Relative Merits of Y and Delta Connection for Alternators," *American Institute of Electrical Engineers, Transactions of the* , vol.XXXIII, no.1, pp.803-806, Jan. 1914

[34] Wauchope, G.A.; , "A recent development in squirrel-cage induction-motor starters," *Electrical Engineers - Part II: Power Engineering, Journal of the Institution of* , vol.91, no.20, pp.101-107, April 1944

[35] Elliott, Kenneth C.; Elliott, William M.; , "Open-Wye-Type Phase Conversion Systems," *Industry and General Applications, IEEE Transactions on* , vol.IGA-6, no.2, pp.146-148, March 1970

[36] Stemmler, H.; Guggenbach, P.; , "Configurations of high-power voltage source inverter drives," *Power Electronics and Applications, 1993., Fifth European Conference on* , vol., no., pp.7-14 vol.5, 13-16 Sep 1993

[37] Shivakumar, E.G.; Gopakumar, K.; Sinha, S.K.; Pittet, A.; Ranganathan, V.T.; , "Space vector PWM control of dual inverter fed open-end winding induction motor drive," *Applied Power Electronics Conference and Exposition, 2001. APEC 2001. Sixteenth Annual IEEE* , vol.1, no., pp.399-405 vol.1, 2001

[38] Shiny, G.; Baiju, M.R.; , "Space Vector PWM scheme without sector identification for an open-end winding induction motor based 3-level inverter," *Industrial Electronics, 2009. IECON '09. 35th Annual Conference of IEEE* , vol., no., pp.1310-1315, 3-5 Nov. 2009

[39] Somasekhar, V.T.; Srinivas, S.; Kumar, K.K.; , "Effect of Zero-Vector Placement in a Dual-Inverter Fed Open-End Winding Induction Motor Drive With Alternate Sub-Hexagonal Center PWM Switching Scheme," *Power Electronics, IEEE Transactions on* , vol.23, no.3, pp.1584-1591, May 2008

[40] Sivakumar, K.; Das, A.; Ramchand, R.; Patel, C.; Gopakumar, K.; , "A three level voltage space vector generation for open end winding IM using single voltage source driven dual two-level inverter," *TENCON 2009 - 2009 IEEE Region 10 Conference* , vol., no., pp.1-5, 23-26 Jan. 2009

[41] Welchko, B.A; Contributions to the Reduced Cost and Increased Reliability of Permanent Magnet Synchronous Machine Drives, Ph.D. thesis, University of Wisconsin-Madison, 2003

[42] Grandi, G.; Rossi, C.; Lega, A.; Casadei, D.; , "Multilevel Operation of a Dual Two-Level Inverter with Power Balancing Capability," *Industry Applications Conference, 2006. 41st IAS Annual Meeting. Conference Record of the 2006 IEEE* , vol.2, no., pp.603-610, 8-12 Oct. 2006

[43] Rossi, C.; Grandi, G.; Corbelli, P.; , "Series hybrid powertrain based on the dual

two-level inverter," *Optimization of Electrical and Electronic Equipment, 2008. OPTIM 2008. 11th International Conference on* , vol., no., pp.277-286, 22-24 May 2008

[44] Welchko, B.A.; , "A double-ended inverter system for the combined propulsion and energy management functions in hybrid vehicles with energy storage," *Industrial Electronics Society, 2005. IECON 2005. 31st Annual Conference of IEEE* , vol., no., pp.6 pp., 6-6 Nov. 2005

[45] Mu-Shin Kwak; Seung-Ki Sul; , "Flux Weakening Control of an Open Winding Machine with Isolated Dual Inverters," *Industry Applications Conference, 2007. 42nd IAS Annual Meeting. Conference Record of the 2007 IEEE* , vol., no., pp.251-255, 23-27 Sept. 2007

[46] Mu-Shin Kwak; Seung-Ki Sul; , "Control of an Open-Winding Machine in a Grid-Connected Distributed Generation System," *Industry Applications, IEEE Transactions on* , vol.44, no.4, pp.1259-1267, July-aug. 2008

[47] Klaus Habur and Donal O'Leary; FACTS-Flexible Alternating Current Transmission Systems For Cost Effective and Reliable Transmission of Electrical Energy - World Bank Homepage

[48] Gyugyi, L.; , "Power electronics in electric utilities: static VAR compensators ," *Proceedings of the IEEE* , vol.76, no.4, pp.483-494, Apr 1988

[49] Urbanek, J.; Piwko, R.J.; Larsen, E.V.; Damsky, B.L.; Furumasu, B.C.; Mittlestadt, W.; Eden, J.D.; , "Thyristor controlled series compensation prototype installation at the Slatt 500 kV substation," *Power Delivery, IEEE Transactions on* , vol.8, no.3, pp.1460-1469, Jul 1993

[50] Butler, J. W.; Concordia, C.; "Analysis of Series Capacitor Application Problems," *American Institute of Electrical Engineers, Transactions of the* , vol.56, no.8, pp.975-988, Aug. 1937

[51] Gyugyi, L.; Schauder, C.D.; Sen, K.K.; , "Static synchronous series compensator: a solid-state approach to the series compensation of transmission lines," *Power Delivery,*

IEEE Transactions on , vol.12, no.1, pp.406-417, Jan 1997

[52] Bingsen Wang; Venkataramanan, G.; , "Operation and Control of a Dynamic Voltage Restorer Realized Using Cascaded H-Bridge Converters," *Power Electronics Specialists Conference, 2005. PESC '05. IEEE 36th* , vol., no., pp.2222-2229, 16-16 June 2005

[53] Hyosung Kim; Seung-Ki Sul; , "Compensation voltage control in dynamic voltage restorers by use of feed forward and state feedback scheme," *Power Electronics, IEEE Transactions on* , vol.20, no.5, pp. 1169- 1177, Sept. 2005

[54] Wiik, J.A.; Wijaya, F.D.; Shimada, R.; , "Characteristics of the Magnetic Energy Recovery Switch (MERS) as a Series FACTS Controller," *Power Delivery, IEEE Transactions on* , vol.24, no.2, pp.828-836, April 2009

[55] Gyugyi, L.; Schauder, C.D.; Williams, S.L.; Rietman, T.R.; Torgerson, D.R.; Edris, A.; , "The unified power flow controller: a new approach to power transmission control," *Power Delivery, IEEE Transactions on* , vol.10, no.2, pp.1085-1097, Apr 1995

[56] Iravani, M.R.; Maratukulam, D.; , "Review of semiconductor-controlled (static) phase shifters for power systems applications," *Power Systems, IEEE Transactions on* , vol.9, no.4, pp.1833-1839, Nov 1994

[57] Venkataramanan, G.; Johnson, B.K.; , "Pulse width modulated series compensator," *Generation, Transmission and Distribution, IEE Proceedings-* , vol.149, no.1, pp. 71-75, Jan 2002

[58] Mancilla-David, F.; Venkataramanan, G.; , "A pulse width modulated AC link unified power flow controller," *Power Engineering Society General Meeting, 2005. IEEE* , vol., no., pp. 1314- 1321 Vol. 2, 12-16 June 2005

[59] Hunt, W.; Steady state performance of electronically self-excited induction machines, MS thesis; University of Wisconsin-Madison, 1984

[60] Al-Saffar, M.A.; Voltage Control of SEIG Using a Continuously Controlled Capacitor; PhD thesis; University of Wisconsin-Madison, 1997

[61] Muljadi, E.; Series Compensated PWM Inverter with Battery Supply Applied to an Isolated Induction Generator; PhD thesis, University of Wisconsin-Madison, 1987

[62] Muljadi, E.; Lipo, T.A.; , "Series compensated PWM inverter with battery supply applied to an isolated induction generator," *Industry Applications, IEEE Transactions on* , vol.30, no.4, pp.1073-1082, Jul/Aug 1994

[63] Naidu, M.; Walters, J.; , "A 4-kW 42-V induction-machine-based automotive power generation system with a diode bridge rectifier and a PWM inverter," *Industry Applications, IEEE Transactions on* , vol.39, no.5, pp. 1287- 1293, Sept.-Oct. 2003

[64] U. S. Patent No.: 6838860 POWER GENERATING SYSTEM INCLUDING PERMANENT MAGNET GENERATOR AND SHUNT AC REGULATOR

[65] Nishida, K.; Ahmed, T.; Nakaoka, M.; , "Advanced Active Power Filter Controlled permanent-magnet synchronous generator for Automotive Applications," *Power Electronics Specialists Conference, 2007. PESC 2007. IEEE* , vol., no., pp.1508-1514, 17-21 June 2007

[66] Clements, N; Stator Side Voltage Regulation of Permanent Magnet AC Generators, PhD thesis, University of Wisconsin-Madison, 2010

[67] Muljadi, E.; Zhao, Y.; Liu, T.-H.; Lipo, T.A.; , "Adjustable AC capacitor for a single-phase induction motor," *Industry Applications, IEEE Transactions on* , vol.29, no.3, pp.479-485, May/Jun 1993

[68] Muljadi, E.; Lipo, T.A.; Novotny, D.W.; , "Power factor enhancement of induction machines by means of solid-state excitation," *Power Electronics, IEEE Transactions on* , vol.4, no.4, pp.409-418, Oct 1989

[69] Ahmed, T.; Nishida, K.; Nakaoka, M.; Noro, O.; , "Self-excited induction generator with regulated dc voltage scheme for wind power applications," *Applied Power Electronics Conference and Exposition, 2005. APEC 2005. Twentieth Annual IEEE* , vol.3, no., pp.1831-1837 Vol. 3, 6-10 March 2005

[70] Kimura, N.; Hirao, M.; Morizane, T.; Taniguchi, K.; , "Wind Power Generation

System with Induction Machine and Diode Rectifier," *Power Electronics and Motion Control Conference, 2006. EPE-PEMC 2006. 12th International* , vol., no., pp.1580-1584, Aug. 30 2006-Sept. 1 2006

[71] Singer, A.; Hofmann, W.; , "Static synchronous series compensation applied to small wind energy conversion system," *Power Electronics and Applications, 2007 European Conference on* , vol., no., pp.1-9, 2-5 Sept. 2007

[72] Singer, A.; Hofmann, W.; , "Combined System of Static Synchronous Series Compensation and Passive Filter applied to Wind Energy Conversion System," *Power Electronics and Drive Systems, 2007. PEDS '07. 7th International Conference on* , vol., no., pp.576-582, 27-30 Nov. 2007

[73] Takaku, T.; Homma, G.; Isober, T.; Igarashi, S.; Uchida, Y.; Shimada, R.; , "Improved wind power conversion system using magnetic energy recovery switch (MERS)," *Industry Applications Conference, 2005. Fourtieth IAS Annual Meeting. Conference Record of the 2005* , vol.3, no., pp. 2007- 2012 Vol. 3, 2-6 Oct. 2005

[74] Wiik, J.A.; Kulka, A.; Isobe, T.; Usuki, K.; Molinas, M.; Takaku, T.; Undeland, T.; Shimada, R.; , "Control design and experimental verification of a series compensated 50 kW permanent magnet wind power generator," *Power Electronics Specialists Conference, 2008. PESC 2008. IEEE* , vol., no., pp.4525-4531, 15-19 June 2008

[75] Grabic, S.; Celanovic, N.; Katic, V.A.; , "Permanent Magnet Synchronous Generator Cascade for Wind Turbine Application," *Power Electronics, IEEE Transactions on* , vol.23, no.3, pp.1136-1142, May 2008

[76] Jahns, Thomas M.; Kliman, Gerald B.; Neumann, Thomas W.; , "Interior Permanent-Magnet Synchronous Motors for Adjustable-Speed Drives," *Industry Applications, IEEE Transactions on* , vol.IA-22, no.4, pp.738-747, July 1986

[77] Morimoto, S.; Hatanaka, K.; Tong, Y.; Takeda, Y.; Hirasa, T.; , "Servo drive system and control characteristics of salient pole permanent magnet synchronous motor," *Industry Applications, IEEE Transactions on* , vol.29, no.2, pp.338-343, Mar/Apr 1993

[78] Schiferl, R.F.; Lipo, T.A.; , "Power capability of salient pole permanent magnet synchronous motors in variable speed drive applications," *Industry Applications, IEEE Transactions on* , vol.26, no.1, pp.113-123, Jan/Feb 1990

[79] Jahns, Thomas M.; , "Flux-Weakening Regime Operation of an Interior Permanent-Magnet Synchronous Motor Drive," *Industry Applications, IEEE Transactions on* , vol.IA-23, no.4, pp.681-689, July 1987

[80] Morimoto, S.; Sanada, M.; Takeda, Y.; , "Wide-speed operation of interior permanent magnet synchronous motors with high-performance current regulator," *Industry Applications, IEEE Transactions on* , vol.30, no.4, pp.920-926, Jul/Aug 1994

[81] Morimoto, S.; Takeda, Y.; Hirasa, T.; Taniguchi, K.; , "Expansion of operating limits for permanent magnet motor by current vector control considering inverter capacity," *Industry Applications, IEEE Transactions on* , vol.26, no.5, pp.866-871, Sep/Oct 1990

[82] Jang-Mok Kim; Seung-Ki Sul; , "Speed control of interior permanent magnet synchronous motor drive for the flux weakening operation," *Industry Applications, IEEE Transactions on* , vol.33, no.1, pp.43-48, Jan/Feb 1997

[83] Jahns, Thomas M.; “Permanent Magnet Synchronous Machine Drive”, ECE504 Course Notes, University of Wisconsin-Madison

[84] High Speed Operation of Permanent Magnet Machines, Ph.D. thesis, University of Wisconsin-Madison, 2005

[85] Lawler, J.S.; Bailey, J.M.; McKeever, J.W.; Joao Pinto; , "Extending the constant power speed range of the brushless DC motor through dual-mode inverter control," *Power Electronics, IEEE Transactions on* , vol.19, no.3, pp. 783- 793, May 2004

[86] EL-Refaie, A.M.; Novotny, D.W.; Jahns, T.M.; , "A simple model for flux weakening in surface PM synchronous machines using back-to-back thyristors," *Power Electronics Letters, IEEE* , vol.2, no.2, pp. 54- 57, June 2004

[87] Soong, W.L.; Miller, T.J.E.; , "Field-weakening performance of brushless

synchronous AC motor drives," *Electric Power Applications, IEE Proceedings* - , vol.141, no.6, pp.331-340, Nov 1994

[88] Wikipedia; Wind power, http://en.wikipedia.org/wiki/Wind_power

[89] National Renewable Energy Laboratory; Wind Power Today 2010; http://www.nrel.gov/wind/pdfs/47531.pdf

[90] Hansen A.D., Hansen, L.H., Market penetration of wind turbine concepts over the years, RisØ National Laboratory, 2007

[91] Wu B.,Lang, Y, Zargari N, and Kouro, S., "Power Conversion and Control of Wind Energy Systems", Wiley-IEEE Press, Hoboken,New Jersey, 2011, 453 pages,ISBN-13: 978-0-470-59365-3.

[92] Zhe Chen; Guerrero, J.M.; Blaabjerg, F.; , "A Review of the State of the Art of Power Electronics for Wind Turbines," *Power Electronics, IEEE Transactions on* , vol.24, no.8, pp.1859-1875, Aug. 2009

[93] Avery, C.R.; Burrow, S.G.; Mellor, P.H.; , "Electrical generation and distribution for the more electric aircraft," Universities Power Engineering Conference, 2007. UPEC 2007. 42nd International , vol., no., pp.1007-1012, 4-6 Sept. 2007